# Cell-based phenotypic screens to identify modulators of sensitivity to *N*-methyl-*N*′-nitro-*N*-nitrosoguanidine




**Submitted by Mr Nicholas Pedley of Wolfson College**

**for the degree of D.Phil Radiobiology**

**during Trinity term, 2011**

**Supervised by Professor Thomas Helleday,**

**at the Gray Institute for Radiation Oncology & Biology, University of Oxford,**

**and funded by the Medical Research Council**

**ACKNOWLEDGEMENTS**

I would like to dedicate this work to my loving family, to whom I owe everything that I have achieved. In particular, I am grateful beyond words for the unwaivering support of my parents, Susan and John. It is because of your constant emotional and financial support that it has been possible for me to have made it this far. I would also like to dedicate this work to my beautiful girlfriend, Lisa, for having lived every part of the rollercoaster with me, and for sharing in my tears and my joy. I cannot thank you enough for your love and counsel, as well as your constant patience and encouragement. I truly could not have achieved this without you. Finally, I would like to dedicate this work to my grandparents Lily and Bill for the spirit and determination you instilled in me, and on which I have relied so much. I hope you would be proud.

I would like to thank the Medical Research Council for funding this work, and the University of Oxford, the Gray Institute for Radiation Oncology and Biology, and Cancer Research UK for supporting the project. May I also take this opportunity to thank my supervisors, Professor Thomas Helleday, Dr Tim Humphrey, and Dr Cecilia Lundin for their help, support and guidance.

**CONTENTS**

**LIST OF FIGURES**_7

**LIST OF TABLES**_8

**ABBREVIATIONS**_9

**ABTRACT**_12

**CHAPTER ONE: INTRODUCTION**_15

1.1 Mismatch repair

*1.1.1 Mismatch repair: an overview_16*

*1.1.2 Mechanistic understanding of mismatch repair from Escherichia coli_17*

*1.1.3 The MutS complex_18*

*1.1.4 Recognition of base-base mismatches by MutS_18*

*1.1.5 The MutL complex_20*

*1.1.6 Strand discrimination and bi-directionality_21*

*1.1.7 Reconstituted Human mismatch repair_22*

1.2 DNA glycosylase-mediated mismatch excision

*1.2.1 Overview of base excision repair_24*

*1.2.2 Thymine DNA glycosylase_25*

1.3 Mismatch repair and the DNA damage response

*1.3.1 MNNG: The prototypical alkylating agent_26*

*1.3.2 Direct repair: $O^6$-methylguanine-DNA-methyltransferase_27*

*1.3.3 Mismatch repair function and the response to DNA-damaging drugs_28*

*1.3.4 Mismatch repair dictates cellular fate following alkylation damage_29*

1.4 Mismatch repair and cancer

*1.4.1 Mismatch repair defects, genetic instability and microsatellite instability_31*

*1.4.2 Cancer as a multi-step evolutionary process_33*

*1.4.3 Mismatch repair and cancer: Lynch syndrome_35*

*1.4.4 Mismatch repair and cancer: sporadic tumours_36*

*1.4.5 Mismatch repair inactivation and cancer?_36*

1.5 Mismatch repair in cancer treatment and prognosis

*1.5.1 Toxicity limitations of classical cytotoxic chemotherapies_38*

*1.5.2 Mismatch repair status and prognosis_40*

1.6 Inhibitors of DNA repair pathways and modern cancer chemotherapeutics

*1.6.1 Defective DNA repair capacity and cancer_41*

*1.6.2 Synthetic lethal interactions_43*

*1.6.3 Exploiting synthetic lethalities to selectively target tumours_43*

1.7 Aims

*1.7.1 Project scope_45*

*1.7.2 Specific aims_45*

**CHAPTER TWO: MATERIALS & METHODS**_47

2.1 Chemicals and common buffers

*2.1.1 Chemical stocks_48*

*2.1.2 Common buffers_49*

2.2 Cell culture

*2.1.1 Mammalian cell culture*

2.1.1.1 Cell lines_49

2.1.1.2 Cell culture conditions_50
2.1.1.3 Thawing liquid nitrogen stocks_50
2.1.1.4 Freezing cell stocks_51
2.1.1.5 *Mycoplasma* testing_51
*2.1.2 Bacterial cell culture*
2.1.2.1 Cell lines_52
2.1.2.2 Preparation of selective LB agar plates_52
2.1.2.3 Thawing bacterial stocks_53
2.1.2.4 Transformation of competent cells_53
2.1.2.5 Freezing bacterial stocks_53
2.3 Cloning bacterial vectors
*2.1.3.1 Plasmid purification (miniprep)_54*
*2.1.3.2 Plasmid purification (maxiprep)_55*
*2.1.3.4 Agarose gel preparation_55*
*2.1.3.5 Electrophoresis and visualisation of agarose gels_56*
*2.1.3.6 Measurement of DNA concentration_56*
*2.1.3.7 DNA sequencing_56*
2.4 Transfection of mammalian cells with RNA- and DNA-based substrates
*2.4.1 Small interfering RNA_57*
*2.4.2 DNA_58*
2.5 Libraries
*2.5.1 Small molecule compound libraries_58*
*2.5.2 siRNA library_58*
2.6 Preparation and quantification of mammalian cell extracts
*2.6.1 Whole cell extracts_59*
*2.6.2 Bradford assay_59*
2.7 Visualisation of proteins by Western blotting and chemiluminescence
*2.7.1 Electrophoresis_60*
*2.7.2 Nitrocellulose transfer_61*
*2.7.3 Immunodetection_61*
*2.7.4 Chemiluminescence_62*
*2.7.5 Densitometry_63*
2.8 Cell-based assays
*2.8.1 Cell viability assay_63*
*2.8.2 Clonogenic survival assay_63*
*2.8.3 Flow cytometry: cell-cycle analysis_64*
*2.8.4 Immunocytochemistry_64*
2.9 Screening assays
*2.9.1 High-throughput screen for genes that determine MNNG sensitivity_65*
*2.9.2 High-throughput screen for small molecules that decrease MNNG sensitivity_66*
2.10 Data analysis_66

**CHAPTER THREE: RESULTS 1**_68
3.1 Introduction
*3.1.1 Advent of high-throughput screening as a drug discovery tool_69*
*3.1.2 Small molecules and diverse small molecule libraries_70*
*3.1.3 Mechanistic basis of RNA interference_70*
*3.1.4 Development of RNA interference as a research tool_72*
*3.1.5 Biochemical- versus cell-based screening methods_73*
*3.1.6 Aims_76*
3.2 Results
*3.2.1 Cell line characterisation_76*
*3.2.2 Mismatch repair status and response to DNA-damaging drugs_77*
*3.2.3 End-point optimisation_78*

*3.2.4 Optimisation of differential MNNG responses_79*
*3.2.5 Small molecule screen: control optimisation and experimental design_81*
*3.2.6 siRNA-based screen: optimisation and integration of gene silencing_85*
*3.2.7 Screen automation_88*
3.3 Discussion
*3.3.1 Summary_90*
*3.3.2 Potential sources of error*
3.3.2.1 Cell lines_91
3.3.2.2 MNNG stability_93
3.3.2.3 Edge-effects_95
3.3.2.4 Resazurin_96
3.3.2.5 Screening concentration and replication (small molecule screen)_97
*3.3.3 Small molecule screen*
3.3.3.1 Imatinib as a potential positive control_99
3.3.3.2 Cadmium chloride as a potential positive control_100
3.3.3.3 9,10-dimethylanthracene as a potential positive control_102
3.3.3.4 DMSO chemoprotection_102
*3.3.4 siRNA screen*
3.3.4.1 Limitations of siRNA_103
*3.3.5 Expected performance of the screens_105*

**CHAPTER FOUR: RESULTS 2**_107
4.1 Introduction
*4.4.1 Functional screens and the exploitation of synthetic lethal interactions_108*
*4.4.2 Outstanding issues in mismatch repair*
4.4.2.1 Origin of the strand discrimination signal_111
4.4.2.2 Stationary, translocation, and molecular switch models_113
4.4.2.3 Futile cycling and direct signaling models_115
4.4.2.4 Role of MutLβ_115
*4.4.3 Aims_115*
4.2 Results
*4.2.1 Screen results_116*
*4.2.2 TDG validation*
4.2.2.1 Rationale for selection of TDG for hit validation_123
4.2.2.2 siRNA deconvolution_124
4.2.2.3 siRNA vendor_125
4.2.2.4 siRNA concentration_126
4.2.2.5 Clonogenic survival assay_126
4.2.2.6 DNA double-strand break assay_127
4.3 Discussion
*4.3.1 Known mismatch repair components and MNNG sensitivity_128*
*4.3.2 Thymine DNA glycosylase function and MNNG sensitivity_130*
*4.3.3 Future work*
4.3.3.1 Validation of remaining hits_133
4.3.3.2 Methodological improvements_135
4.3.3.3 Future directions_137

**CHAPTER FIVE: RESULTS 3**_139
5.1 Introduction
5.1.1 Cytotoxic anti-cancer treatments and their limitations_140
5.1.2 Small molecule inhibitors and exploitation of synthetic lethal interactions_141
5.1.3 Antioxidants and chemoprevention of cancer_143
5.1.4 Aims_145
5.2 Results

*5.2.1 Screen results_146*
*5.2.2 NSC197049 validation_150*
*5.2.3 NSC197049 characterisation_152*
*5.2.4 Oltipraz_155*
*5.2.5 Antioxidants phenocopy the chemoprotective activity of NSC197049_156*
5.3 Discussion_158
*5.3.1 Chemoprotection through antioxidant activity_159*
*5.3.2 Chemoprotection through mismatch repair inhibition_163*
*5.3.3 Chemoprotection through inhibition of apoptosis_167*
*5.3.4 Chemoprotection through direct inactivation of MNNG_169*

**CHAPTER SIX: DISCUSSION**_170
6.1 Summary of findings_171
6.2 Key genetic determinants of the response to MNNG_172
6.3 Role of thymine DNA glycosylase in MNNG sensitivity_175
6.4 Role of DNA double-strand breaks in MNNG toxicity_177
6.5 NSC197049 as a chemoprotective agent_179
6.6 NSC197049 as a chemopreventive agent_181
6.7 Inhibitors of mismatch repair and chemoprotection_185
6.8 Significance of this study in terms of exploitation of synthetic lethal interactions in the specific targeting of cancer_187

**CHAPTER SEVEN: FIGURE LEGENDS**_190

**CHAPTER EIGHT: REFERENCES**_221

**CHAPTER NINE: APPENDIX**_294

**LIST OF FIGURES**

**CHAPTER THREE**

3.1 Cell line characterisation_191
3.2 Mismatch repair status and the response to cytotoxic drugs_193
3.3 End-point optimisation_195
3.4 Optimising the differential response of MMR-proficient and –deficient cells to MNNG_197
3.5 Optimisation of controls and design of the small molecule screen_199
3.6 Optimisation of siRNA-mediated knockdowns and design of the RNA interference screen_202
3.7 Screen automation_205

**CHAPTER FOUR**

4.1 High-throughput screen for the key genetic determinants of MNNG sensitivity_207
4.2 TDG validation data_209

**CHAPTER FIVE**

5.1 High-throughput screen for small molecule structures that decrease sensitivity to MNNG_211
5.2 Small molecule hit validation_213
5.3 Characterisation of NSC197049 chemoprotection_215
5.4 Effect of Oltipraz and antioxidants on MNNG sensitivity_217
5.5 Protection against $O^6$-methylguanine toxicity by antioxidants and NSC197049_219

**LIST OF TABLES**

**CHAPTER TWO**

Table 2.1 Chemical reagent information_48
Table 2.2 Common buffer information_49
Table 2.3 p95-1 sequencing primers_57
Table 2.4 Western blotting antibodies_62
Table 2.5 Immunocytochemistry secondary antibodies_65

**CHAPTER THREE**

Table 3.1 $IC_{50}$ values for indicated cytotoxic drugs and cell lines_78

**CHAPTER FOUR**

Table 4.1 Performance of small interfering RNA screen controls_117
Table 4.2 Correlation between replicate plates and screen repeats_120
Table 4.3 Small interfering RNA screen hits_121
Table 4.4 Summary of functions for hit genes_122

**CHAPTER FIVE**

Table 5.1 Performance of small molecule screen controls and correlation between replicates_147

**CHAPTER NINE**

Table A1 Table of genes targeted by the custom siRNA library_295

**ABBREVIATIONS**

| | |
|---|---|
| 53bp1 | p53 binding protein 1 |
| 5-HT3 | 5-hydroxytryptamine 3 receptor |
| 5FU | 5-fluorouracil |
| 5MeC | 5-methylcytosine |
| 6TG | 6-thioguanine |
| 8oxoG | 7,8-dihydro-8-oxoguanine |
| γ-H2AX | Phosphorylated histone H2AX |
| A | Adenine |
| Abl | Abelson |
| ADP | Adenosine diphosphate |
| ANI | 4-amino-1,8-napthalimide |
| AP | Apurinic/apyrimidinic |
| APE1 | Apurinic/apyrimidinic endonuclease 1 |
| ATM | Ataxia telangiectasia mutated |
| ATP | Adenosine triphosphate |
| ATR | Ataxia telangiectasia and Rad3 related |
| ATRIP | Ataxia telangiectasia and Rad3 related interacting protein |
| BCR-ABL | Breakpoint cluster region Abelson |
| BER | Base excision repair |
| BRCA1 | Breast cancer 1 early onset |
| BRCA2 | Breast cancer 2 early onset |
| BRD1 | Bromodomain containing 1 |
| C | Cytosine |
| c-Abl | Cytoplasmic Abelson |
| CMMR-D | Constitutional mismatch repair deficiency syndrome |
| CNS | Central nervous system |
| CRC | Colorectal cancer |
| CTL | Cytotoxic T lymphocytes |
| DMA | 9,10-dimethylanthracene |
| DMSO | Dimethyl sulfoxide |
| DNA | Deoxyribonucleic acid |
| dRP | 2'deoxyribo-5'-phosphate |
| DSB | Deoxyribonucleic acid double-strand break |
| dsRNA | Double-stranded ribonucleic acid |
| Exo1 | Exonuclease 1 |
| FEN1 | Flap endonuclease 1 |
| G | Guanine |
| GADD45α | Growth arrest and DNA damage 45 alpha |
| GFP | Green fluorescent protein |
| GST | Glutathione-S-transferase |
| HER2 | Human epidermal growth factor receptor 2 |
| HIF-1α | Hypoxia inducible factor 1 |
| HR | Homologous recombination |
| IDL | Insertion/deletion mutation |

| | |
|---|---|
| IEL | Intraepithelial lymphocyte |
| Keap1 | Kelch-like ECH-associated protein 1 |
| LS | Lynch syndrome |
| MBD4 | Methyl-CpG-binding domain protein 4 |
| MGMT | $O^6$-methylguanine deoxyribonucleic acid methyltransferase |
| miRNA | Micro-ribonucleic acid |
| MLH1 | MutL homolog 1 |
| MLH3 | MutL homolog 3 |
| MMR | Mismatch repair |
| MNNG | *N*-methyl-*N'*-nitro-*N*-nitrosoguanidine |
| MPG | Methylpurine glycosylase |
| mRNA | Messenger ribonucleic acid |
| MSH2 | MutS homolog 2 |
| MSH3 | MutS homolog 3 |
| MSH6 | MutS homolog 6 |
| MSI | Microsatellite instability |
| MSI-H | Microsatellite instability high |
| MSI-L | Microsatellite instability low |
| MSS | Microsatellite stable |
| MutYH | MutY homolog |
| NADH | Nicotinamide adenine dinucleotide |
| NADPH | Nicotinamide adenine dinucleotide phosphate |
| NCI | National cancer institute |
| Nrf2 | Nuclear factor erythroid 2-related factor 2 |
| O6BG | $O^6$-benzylguanine |
| O6MeG | $O^6$-methylguanine |
| p53 | Tumour protein 53 |
| PARP | Poly(adenine diphosphate-ribose) polymerase |
| PARP1 | Poly(adenine diphosphate-ribose) polymerase 1 |
| PARP2 | Poly(adenine diphosphate-ribose) polymerase 1 |
| PCNA | Proliferating cell nuclear antigen |
| PER1 | Period circadian protein homolog 1 |
| PI3K | Phosphoinositide 3-kinase |
| PINK1 | Phosphatase and tensin homolog-induced putative kinase 1 |
| PMS1 | Post-meiotic segregation increased 1 |
| PMS2 | Post-meiotic segregation increased 2 |
| Polα | Deoxyribonucleic acid polymerase alpha |
| Polβ | Deoxyribonucleic acid polymerase beta |
| Polδ | Deoxyribonucleic acid polymerase delta |
| Polε | Deoxyribonucleic acid polymerase epsilon |
| RAD51 | Radiation sensitivity abnormal 51 |
| RFC | Replication factor C |
| RISC | Ribonucleic acid-induced silencing complex |
| RNA | Ribonucleic acid |
| RNAi | Ribonucleic acid interference |
| RPA | Replication protein A |

| | |
|---|---|
| shRNA | Short hairpin ribonucleic acid |
| siRNA | Small interfering ribonucleic acid |
| SMUG1 | Single-strand selective monofunctional uracil deoxyribonucleic acid glycosylase |
| SN1 | Nucleophilic substitution 1 |
| SND1 | Staphylococcal nuclease and tudor domain containing 1 |
| SRB | Sulphorhodamine B |
| SSB | Deoxyribonucleic acid single-strand break |
| SSBP | Single-stranded binding protein |
| ssDNA | Single-stranded deoxyribonucleic acid |
| SSR1 | Signal sequence receptor 1 |
| SUMO1 | Small ubiquitin-like modifier 1 |
| SUMO2/3 | Small ubiquitin-like modifier 2/3 |
| T | Thymine |
| TDG | Thymine deoxyribonucleic acid glycosylase |
| TIL | Tumour infiltrating lymphocytes |
| U | Uracil |
| UNG | Uracil deoxyribonucleic acid glycosylase |
| XRCC1 | X-ray repair complementing defective repair 1 |

**ABSTRACT**

Defective DNA repair capacity has been shown to be a common feature of cancer, and loss of function mutations in 'stability' genes that normally maintain the integrity of the genome may prove a key rate-limiting step in carcinogenesis. Since even genetically unstable cells require some repair functionality to maintain viability, these cancers likely exhibit an over-reliance on other DNA repair pathways for survival. Therapeutically targeting backup repair processes in such tumours represents a novel means by which to achieve selective tumour toxicity. Full exploitation of these synthetic lethal interactions will require an in-depth knowledge of the genetic basis of DNA repair in combination with an armoury of small molecule inhibitors of cellular targets. To this end, we have designed, optimised and run two high-throughput cell-based screens to identify genes and small molecules that can modulate mismatch repair (MMR) activity. Key to these screening strategies are the resistance of cells with dysfunctional MMR to a range of cytotoxic drugs, including the alkylating agent *N*-methyl-*N'*-nitro-*N*-nitrosoguanidine (MNNG). By exploiting this MMR-dependent toxicity we have assayed for siRNA and small molecules that permit the survival of MNNG-treated MMR-proficient cells to levels comparable to MMR-deficient cells, and which therefore represent putative MMR modulating agents. A screen of 571 siRNA for gene depletions that reduce MNNG sensitivity by at least two population standard deviations identified 10 genes of potential interest, and included the four canonical MMR genes, *MSH2* (2.87 ± 0.28 (Z ± SE)), *MSH6* (4.87 ± 0.06), *MLH1* (3.42 ± 0.43) and *PMS2* (3.36 ± 0.44). TDG represented an unexpected hit that decreased MNNG sensitivity by 2.55 ± 0.04 population standard deviations. However, clonogenic survival experiments found TDG depletion to be

contextual synthetic lethal within an MMR-null background when treated with MNNG, reducing HCT116 clonogenicity by 37% ($p < 0.001$). Moreover, TDG knockdown increased the number of 53 binding protein 1 (53bp1) foci in MMR-proficient cells by 40% and MMR–deficient cells by 27% following MNNG exposure ($p < 0.001$). Combined with a failure to replicate the primary screen result, the role for TDG in the response to MNNG could be explained solely through its established role as a member of the base excision repair pathway. A second screen of the NCI Diversity I and II small molecule libraries (n=1786) was conducted to identify putative MMR inhibitors. Subsequent analysis revealed NSC197049 to increase cellular viability of MNNG treated cells by 3.60±0.32 population standard deviations and was successfully validated as a hit. Co-treatment of NSC197049 with MNNG conferred dose-dependent chemoprotection independently of MMR status and cell line, an effect that was lost if NSC197049 was pre- or post-treated. The protection was associated with a reduction in MNNG-dependent 53bp1 foci of 60% in MMR proficient cells and 15% in MMR deficient cells ($p < 0.001$), together with a marked reduction of >80% in subG1 content at 48 hours post-MNNG that was independent of MMR status. Interestingly, the characteristic G2/M arrest of MNNG-treated MMR-proficient cells remained intact (~40% arrested). Taken together, these observations are not consistent with NSC197049 acting as an inhibitor of MMR. Dithiolthiones have been described as chemoprotective agents that induce antioxidant defences, whilst we have found NSC197049 phenocopies known antioxidants ascorbic acid and glutathione in protecting against MNNG-induced toxicity. NSC197049 may therefore act by bolstering cellular antioxidant defences. The precise mechanism may be novel, since the proto-typical dithiolthione, Oltipraz, failed to be protective in this study.

In summary, we have confirmed that MMR is the primary determinant of MNNG sensitivity, and found that TDG is unlikely to be involved in MMR. We have also identified a novel chemoprotective small molecule that is unlikely to represent an MMR inhibitor, but that might be useful in cancer chemoprevention.

# CHAPTER ONE

*Introduction*

## 1.1 MISMATCH REPAIR

### 1.1.1 Mismatch repair: an overview

Mismatch repair (MMR) is a highly conserved and replication coupled deoxyribonucleic acid (DNA) repair pathway that functions to maintain genomic stability by increasing replication fidelity, suppressing inappropriate DNA metabolism, initiating DNA damage signalling, and eradicating cells that have suffered highly mutagenic insults (reviewed by Kunkel & Erie, 2005; Iyer *et al*., 2006; Jiricny, 2006; Hsieh & Yamane, 2008; Li, 2008). The classical function of MMR is the recognition and repair of misincorporated base pairs that arise during DNA replication, and nucleotide insertion/deletion loop (IDL) mutations that result from template slippage and escape polymerase proofreading. MMR also plays an important role in the DNA damage response, where its recognition and processing of certain DNA lesions triggers an apoptotic response that prevents inappropriate propagation of mutant DNA sequences. Given these functions, it is not surprising that loss of MMR results in a mutator phenotype characterised by an elevated mutation rate, increased cancer susceptibility, and altered cellular responses to some DNA-damaging drugs. Germ-line mutations in MMR genes give rise to Lynch Syndrome (LS), a hereditary cancer susceptibility syndrome that presents with a characteristic spectrum of tumours, particularly colorectal cancer (CRC). MMR is also known to possess a number of other functions, including regulating recombination between homologous sequences, as well as having a role in class-switch recombination and somatic hypermutation.

### 1.1.2 Mechanistic understanding of mismatch repair from *Escherichia coli*

Much of our mechanistic understanding of MMR stems from studies examining its function in bacteria (reviewed by Hsieh & Yamane, 2008). In *Escherichia coli*, the homodimeric mismatch recognition protein, MutS, is thought to be coupled to DNA replication via its interaction with the replication-associated β-sliding clamp (López de Saro & O'Donnell, 2001). MutS functions to recognise heteroduplex DNA that has escaped polymerase proofreading activities (Su & Modrich, 1986). MutS-mediated recognition of mismatched bases and IDL loops serves to act as a stimulus for the recruitment and activation of MutL to form a MutS/MutL complex (Hsieh & Yamane, 2008). From this perspective, MutL functions as a molecular matchmaker to recruit and activate MutH, a type II restriction endonuclease that incises the newly replicated strand either 5' or 3' to the mismatch. Following MutL-dependent loading and activation of DNA helicase II at the nicked site, the helicase unwinds the DNA helix past the mismatch to create a flapped region of single-stranded DNA (ssDNA) containing the misincorporated base (Dao & Modrich, 1998; Guarne *et al*., 2004). Single-stranded binding protein (SSBP) protects against double-stranded break (DSB) formation by coating and protecting the template strand from attack by cellular nucleases. When the MutH-mediated incision is orientated 5' to the mismatch, either exonuclease VII or RecJ 5'-3' exonucleases degrade the nicked strand up until and beyond the misincorporated base (Burdett *et al*., 2001). For 3' nick-directed MMR, the 3'-5' exonuclease I or exonuclease V perform this function. Following excision, repair synthesis of the resulting single-stranded gap is performed by DNA polymerase III, SSBP, and DNA ligase.

### 1.1.3 The MutS complex

Mismatch recognition is achieved in humans by homologues of the bacterial MutS protein; MutS homolog 2 (MSH2), MutS homolog 3 (MSH3), and MutS homolog 6 (MSH6). These interact to form two heterodimeric complexes that share a common MSH2 partner with either MSH6 (MutSα) or MSH3 (MutSβ) (Acharya *et al*., 1996). The steady-state level of MutSα has been shown to be 6- to 10-fold higher than MutSβ, and is therefore considered to be the 'primary' mismatch recognition complex (Drummond *et al.*, 1997; Genschel *et al*., 1998). There is partial redundancy in the functional specificities of the two species, with MutSα recognising base mismatches and IDLs involving 1 or 2 extra-helical bases, whilst MutSβ can detect longer IDLs ranging from 1 to 14 extra-helical bases. MutSβ has also been demonstrated to be capable of recognising some base mismatches that exhibit weak hydrogen bonding in *Saccharomyces cerevisiae*, although this additional role awaits investigation in mammalian cells (Harrington & Kolodner, 2007).

### 1.1.4 Recognition of base-base mismatches by MutS

Understanding the mechanism by which MutS complexes achieve mismatch recognition has required the concerted efforts of many research groups over a number of years. Early studies revealed purified MutS complexes to have low levels of ATPase activity (Haber & Walker, 1991; Chi & Kolodner, 1994) that was crucial for functional MMR, since disruption of conserved residues resulted in a mutator phenotype indicative of MMR deficiency (Harber & Walker, 1991; Wu & Marinus, 1994; Alani *et al*., 1997). MutS complexes are now known to possess high affinity binding sites for both ADP and

ATP (Martik *et al*., 2004), and differential binding by these substrates may allow MutS to function as a novel molecular switch (Gradia *et al*., 1997). In particular, MutS was demonstrated to be 'mismatch recognition competent' in its ADP bound form, with ADP-ATP exchange occurring following mismatch recognition. Hydrolysis of ATP to ADP was associated with a return to a 'mismatch recognition competent' state. In DNA-free solution, MutS assumes a configuration whereby the ADP binding sites are dimerised, whilst the finger domains form a disordered open structure, possibly caused by electrostatic repulsion of several basic residues (Jiricny, 2000; Lamers *et al*., 2000; Obmolova *et al*., 2000). In the presence of heteroduplex DNA, the finger domains form an ordered structure that encircles the DNA; a conformational change that could result from neutralisation of positively charged finger domains by non-specific interactions with the negatively charged DNA sugar-phosphate backbone. A phenylalanine amino acid residue from a characteristic phenylalanine-X-glutamate motif was observed to insert into the minor groove, bending the DNA and serving to 'lock' the complex on to the mismatched site. Post-mismatch recognition ADP to ATP exchange likely results in retraction of the phenylalanine residue, allowing the complex to dissociate from the mismatch and translocate as a sliding clamp (Gradia *et al*., 1997; Lamers *et al*., 2004). Given that the crystal structure data pointed toward a physical bending of the DNA by MutS, a seminal paper published in 2003 used atomic force microscopy to further elucidate the significance of such mechanics on mismatch recognition and specificity (Wang *et al*., 2003). They found that in the presence of homoduplex DNA, a single population of bent homoduplex DNA-MutS complexes existed, whereas when heteroduplex DNA was present, both bent and unbent heteroduplex DNA-MutS

populations were observed. This data is consistent with the aforementioned crystal structure data that observed DNA kinking at a mismatched site.

Taken together, this data is consistent with the notion that ADP-bound MutS interacts with homoduplex DNA via non-specific interactions that induce smooth bending of the DNA as MutS scans for mismatches. The inherently greater structural flexibility present at mismatched sites (Isaacs *et al*., 2002) would result in a sharper local kinking of the DNA as MutS arrives at a mismatch, and allows for the insertion of the phenylalanine residue to stabilise the recognition complex at the mismatched site. Following ADP to ATP exchange, MutS undergoes a conformational change that converts it into a sliding clamp that can translocate across the DNA without inducing any bending. Finally, upon completion of the role of MutS in signalling mismatch recognition, ATP hydrolysis through its inherent ATPase activity again returns MutS to its 'mismatch recognition competent' state, in which it bends and scans the DNA by non-specific interactions.

### 1.1.5 The MutL complex

Homologues of the bacterial MutL protein act to coordinate the response to mismatch recognition and to stimulate excision repair. The four homologues identified in humans include MutL homolog 1 (MLH1), MutL homolog 3 (MLH3), post-meiotic segregation increased 1 (PMS1), and post-meiotic segregation increased 2 (PMS2) (Nicolaides *et al*., 1994; Papadopoulos *et al*., 1994; Lipkin *et al*., 2000). These form heterodimeric complexes with MLH1 as the common partner with either PMS2 (MutLα), MLH3 (MutLβ), or PMS1 (MutLγ). All three partners interact with residues 492-742 of

MLH1 via a shared conserved region of 36 residues in their N-terminal regions (Kondo *et al*., 2001).

MutL only binds DNA substrates with low affinity via non-specific interactions (Drotschmann *et al*., 2002), and is instead thought to be primarily recruited to MMR substrates via its mismatch-dependent interaction with MutS. Mismatch recognition-induced conformational changes likely reveal conserved residues within domain II of MSH2, which have been demonstrated to permit docking and formation of the MutS-MutL tetramer (Mendillo *et al*., 2009). MutL complexes, and in particular, MLH1, are essential for MMR activity, although until recently their precise role has remained unclear. Due to its interactions with both MutS and downstream repair effectors such as replication factor C (RFC), proliferating cell nuclear antigen (PCNA), and exonuclease 1 (ExoI) (Cannavo *et al*., 2007), MutL has been recognised as a molecular bridge that couples mismatch recognition to excision repair. MutL has also been demonstrated to possess a latent endonuclease activity required for 3' nick-directed repair (Kadyrov *et al*., 2006), and to be important in the regulation of mismatch-provoked excision termination (Zhang *et al*., 2005).

### 1.1.6 Strand discrimination and bi-directionality

In order to avoid transition mutations, MMR must be able to discriminate between template and newly-synthesised DNA strands in order to ensure the misincorporated base is correctly excised. This is achieved in *E. coli* through the monitoring of adenine methylation within dGATC sequences, whereby newly synthesized DNA is transiently unmethylated and serves as the strand discrimination signal (Hare & Taylor, 1985; Li,

2008). Upon recruitment and activation in a manner dependent on MutS, MutL, ATP, and $Mg^{2+}$, MutH specifically cleaves the unmethylated strand at hemimethylated dGATC sites to provide an entry point from which an exonuclease can degrade past the mismatched base (Längle-Rouault *et al*., 1987; Au *et al*., 1992). A similar mechanism was originally proposed for mammalian MMR, since CpG sites were known to be transiently hemimethylated on the template strand following replication. However, this putative mechanism was later shown to fail to direct MMR to the newly synthesised strand (Drummond & Bellacosa, 2001). Nonetheless, human MMR is clearly nick-directed, and bi-directional in the sense that the nick can be either 5' or 3' to the mismatch (Wang & Hays, 2002; Dzantiev *et al*., 2004; Constantin *et al*., 2005; Zhang *et al*., 2005).

### 1.1.7 Reconstituted human mismatch repair

Our understanding of the MMR reaction was greatly aided by studies that focused on identifying the essential biochemical activities required to reconstitute MMR activity *in vitro*. A system comprising recombinant MutSα, MutLα, ExoI, replication protein A (RPA), RFC, and PCNA has been shown to be sufficient to support full 5' or 3' nick-directed bi-directional excision of heteroduplex substrates (Dzantiev *et al*., 2004), whereas complementation with DNA polymerase δ (Polδ) reconstituted the full repair activity of excised substrates (Constantin *et al*., 2005).

ExoI is an exonuclease with 5'-3' polarity, and thus it was surprising that a system containing only ExoI endonuclease activity could support both 5' and 3' nick-directed repair (Genschel *et al*, 2002). This oddity was later explained by the

demonstration that MutLα possesses a latent endonuclease activity that is activated in a mismatch-, MutSα-, RFC-, and PCNA-dependent manner, and that acts to introduce a nick 5' of the mismatch which serves as an entry point for ExoI (Kadyrov *et al*., 2006). This finding explained why bi-directional MMR activity is absolutely dependent on the presence of MutLα (Dzantiev *et al*., 2004), whereas in a partial reconstitution supporting only 5'-nick directed repair, the role of MutLα is limited to increasing the mismatch-dependence of ExoI-mediated excision (Genschel & Modrich, 2003).

RFC and PCNA are also crucial for bi-directional MMR, since systems lacking these components only support 5'-nicked substrates (Genschel & Modrich, 2003). RFC is thought to contribute to 3'-nick directed repair through a direct inhibition of inappropriate 5'-3' hydrolysis of 3' nicks by ExoI, in addition to an indirect role through its loading of PCNA onto DNA (Dzantiev *et al*., 2004; Kadyrov *et al*., 2006). RFC-loaded PCNA is absolutely required for activation of MutLα endonuclease activity, whilst the asymmetry of MutLα binding to PCNA appears to be important in directing strand incision 5' of the mismatch (Pluciennik *et al*., 2010).

The processivity of ExoI on nicked substrates is poor in the absence of MMR machinery, but highly stimulated in a mismatch- MutSα- and ATP-dependent manner (Genschel & Modrich, 2003); an effect thought to be mediated through physical interaction between ExoI and MSH2 (Schmutte *et al*., 1998). In contrast, RPA was found to negatively influence MutS-stimulated ExoI processivity, which suggests the accumulation of RPA-coated ssDNA behind the excision complex might be important in limiting the reaction from excessive hydrolysis and promoting turnover of excision complexes. ExoI activity was further suppressed in the absence of a mismatch in a

MutSα– and MutLα-dependent manner, which together with RPA serves to limit the extent of excision on nicked heteroduplexes and terminate excision activity once the mismatch has been removed. Repair synthesis of excised templates is completed in humans by the concerted action of Polδ and DNA Ligase I (Longley *et al*., 1997; Zhang *et al*., 2005).

## 1.2 DNA GLYCOSYLASE-MEDIATED MISMATCH EXCISION

### 1.2.1 Overview of base excision repair

The typical rate of spontaneous DNA damage in mammalian cells has been estimated to be in the order of several hundred to 1000 insults per cell per hour (Vilenchik & Knudson 2000). The base excision repair (BER) pathway plays a crucial role in recognising and excising a great deal of these, in addition to the many base modifications that arise from exposure to environmental toxins (Zharkov, 2008). BER reactions are initiated by DNA glycosylases, of which at least eleven different enzymes exist in humans, and are grouped by structure into the uracil-DNA glycosylase superfamily, the Nth superfamily, and the Fpg superfamily. Each glycosylase possesses a specific substrate repertoire and acts to catalyse the hydrolysis of the *N*-glycosidic bond in order to release a free base and generate an apurinic/apyrimidinic (AP) site. AP endonuclease 1 (APE1) represents the major AP endonuclease in humans, and flips the AP site extra-helically in order to cleave 5' of the AP site to create a free 3'-OH group to prime for repair synthesis (Mol *et al*., 2000). DNA polymerase beta (Polβ) is subsequently responsible for removing the residual 2'deoxyribo-5'-phosphate (dRP) moiety through its intrinsic dRP lyase activity, before continuing to fill the gap, and thus

permitting DNA ligation by DNA Ligase IIIα/X-ray repair complementing defective repair 1 (XRCC1) (Tomkinson *et al*., 2001; Prasad *et al*., 2005). This sequence of events is thus described as the 'short patch' pathway. If the 5' moiety cannot be successfully removed by the dRP lyase activity of Polβ, then 'long patch' BER is activated, whereby either Polβ, Polδ or DNA polymerase epsilon (Polε) mediate strand displacement synthesis to generate a long flap that is thought to be cleaved by flap endonulcease 1 (FEN1) (Stucki *et al*., 1998; Asagoshi *et al*., 2010a; Asagoshi *et al*., 2010b).

### 1.2.2 Thymine DNA glycosylase

An important class of spontaneous DNA damage that occurs in mammals is the deamination of cytosine and 5-methylcytosine (5MeC) to uracil and thymine, respectively (Duncan & Miller, 1980). These give rise to either G:U or G:T mismatches that, following DNA replication, result in 5MeC:G to T:A transition mutations. Elevated mutations rates are thus typical of sites containing 5MeC paired with guanine, and may be as much as 10-50-fold higher than other sites prone to transition mutations (Duncan & Miller, 1980; Hendrich *et al*, 1999). Consequently, a battery of DNA repair proteins exist that function to guard against transition mutations by recognising and excising uracil and thymine mispaired with guanine (Krokan *et al*., 1997). In mammalian cells, these proteins comprise the uracil DNA glycosylase superfamily, whose members include thymine DNA glycosylase (TDG), uracil DNA glycosylase (UNG), single-strand selective monofunctional uracil DNA glycosylase (SMUG1), and methyl-CpG-binding domain protein 4 (MBD4) (Neddermann & Jiricny, 1993; Slupphaug *et al*., 1995; Haushalter *et al*., 1999; Hendrich *et al*., 1999).

TDG is a 46 kDa nuclear localised DNA glycosylase with mismatch-restricted substrate specificity (Neddermann *et al*., 1996; Hardeland *et al*., 2001). Whilst the best recognised physiological role of TDG is its role in correcting G:T and G:U mismatches, substrate specificity has also been described for a wide variety of chemically modified bases (Cortázar *et al*., 2007). These include the 6-thioguanine (6TG) and $O^6$-methylguanine (O6MeG) base modifications, since TDG has been shown to be able to efficiently incise substrates containing mismatches involving these bases in cellular extracts (Griffin *et al*., 1994). Following TDG-mediated excision of the target base, the glycosylase remains bound and stabilises the AP site until APE1 can be recruited to mediate downstream base excision repair processes (Waters *et al*., 1999). The affinity of TDG for AP sites has been shown to be significantly decreased by non-covalent conjugation of TDG with small ubiquitin-like modifier 1 (SUMO-1) and small ubiquitin-like modifier 2/3 (SUMO2/3), and may facilitate turnover of TDG and transfer of the AP site to APE1 (Hardeland *et al*., 2002). TDG-mediated repair is not thought to be replication coupled, since it is degraded by the ubiquitin-proteasome system at the G1/S cell-cycle phase boundary and remains undetectable until entry into G2 (Hardeland *et al*., 2007).

## 1.3 MISMATCH REPAIR AND THE DNA DAMAGE RESPONSE

### 1.3.1 MNNG: The prototypical alkylating agent

*N*-methyl-*N'*-nitro-*N*-nitrosoguanidine (MNNG) is a direct-acting alkylating agent that, upon decomposition in aqueous solution, forms a methyl-diazonium cation that can methylate DNA (Galtress *et al*., 1992). MNNG produces a spectrum of DNA adducts in

characteristic frequency that reflects the electrostatic potentials of various nucleophilic sites within DNA. These adducts comprise $N^7$-methylguanine (67%), $N^3$-methyladenine (12%), $O^6$-methylguanine (7%), $N^3$-methylcytosine (2%), and $N^1$-methyladenine (1%) (Beranek, 1990). The most detrimental of these in a cellular setting is O6MeG; attributable to its mispairing with thymine during replication (Loechler *et al*., 1984) and induction of G>A transition mutations following subsequent rounds of replication. Unrepaired O6MeG lesions are not only highly mutagenic, but also one of the most cytotoxic lesions yet discovered (Bignami *et al*., 2000).

### 1.3.2 Direct repair: $O^6$-methylguanine-DNA-methyltransferase

A leading defence against O6MeG in mammalian cells is the direct repair enzyme, $O^6$-methylguanine DNA methyltransferase (MGMT). MGMT is translocated to and retained within the nucleus upon alkylation damage induction (Lim & Li, 1996). Direct transfer of the alkyl group from the $O^6$ position of guanine to cysteine 145 within its active site occurs concomitantly with repair of the O6MeG lesion and the protein's inactivation (Foote *et al*., 1980; Olsson & Lindahl, 1980; Ling-Ling *et al*., 1992). One molecule of MGMT is consumed for each O6MeG lesion repaired, and large or prolonged alkylation insults can result in MGMT depletion and failure to repair futher O6MeG lesions. Indeed, MGMT expression level has been demonstrated to be a critical determinant of sensitivity to alkylating agents such as temozolomide and MNNG (Middlemas *et al*., 2000; Yamada *et al*., 2001; Donson *et al*., 2007). The number of active MGMT molecules remaining following one insult therefore influences the sensitivity towards subsequent insults (Citti *et al*., 1998).

### 1.3.3 Mismatch repair function and the response to DNA-damaging drugs

The first steps towards identifying the role of MMR in the response to alkylation damage in human cells was taken when Goldmacher *et al*. isolated a TK6 cell line variant termed 'MT1' that was highly resistant to MNNG exposure, although at the cost of increased mutational burden (Goldmacher *et al*., 1986). The authors noticed that MT1 cells were tolerant, rather than resistant, to O6MeG. They also found MT1 to exhibit a 45-fold higher mutation rate compared with the parental cell line, and noted that an earlier study had demonstrated a mutator phenotype to be characteristic of MMR deficiency in bacteria (Glickman & Radman, 1980). They hypothesised that MT1 tolerates O6MeG-induced toxicity because of an acquired inactivating mutation in MMR, which would otherwise recognise and process O6MeG:T mispairs into a cytotoxic outcome. Indeed, the authors were correct in their hypothesis and MMR is now known to be a major determinant of sensitivity, not only to alkylating agents, but to many DNA-damaging drugs.

Following treatment with MNNG, a large Chk1- and Chk2-dependent G2/M arrest has been shown to be dependent on functional MMR activity (Adamson *et al*., 2005). Cells with compromised MMR activity exhibit elevated resistance, not only to nucleophilic substitution 1 ($S_N1$) alkylating agents such as MNNG (Aebi *et al*., 1997), but also antimetabolite drugs including 6-TG and 5-fluoruracil (5FU) (Carethers *et al*., 1999), platinum-containing compounds such as cisplatin and carboplatin (Fink *et al*., 1996), inhibitors of topoisomerases I (camptothecin, irinotecan, topotecan) and II (etoposide, doxorubicin, epirubicin, mitoxantrone) (Fedier *et al*., 2001), and some DNA minor groove binding drugs (Colella *et al*., 1999). More recent work utilised a strictly isogenic

system with inducible MLH1 expression to confirm that the sensitivity of cells toward MNNG and cisplatin are dependent upon functional MMR activity itself, rather than a secondary consequence of MMR inactivation (Papouli *et al*., 2004).

### 1.3.4 Mismatch repair dictates cellular fate following alkylation damage

Two models have been proposed to explain how MMR dictates the cellular response to DNA damaging drugs. The 'futile cycling' model is based on the observation in bacteria that MMR excision activity is restricted to the newly synthesised strand (Lu *et al*., 1983; Pukkila *et al*., 1983); a feature that is almost certainly conserved in humans, albeit via a different strand discrimination signal. The model postulates that MMR may recognise and attempt to process lesions such as O6MeG that reside on the parental strand, entering a futile cycle of abortive repair that ultimately results in induction of DNA damage signalling and cell death (Li, 1999). An alternative model proposes that MMR instead acts as a 'sensor' of DNA damage, and that upon recognition of lesions such as O6MeG will signal directly for activation of DNA damage and apoptotic responses.

A key piece of evidence supporting the futile cycling model used an *in vitro* mismatch repair assay to demonstrate that O6MeG could be efficiently removed by MMR when it was present on a discontinuous strand but was irreparable when present on the continuous strand (York & Modrich, 2006). This is significant because MMR strand discrimination is thought to be nick-directed in mammalian cells (Constantin *et al*., 2005), and these results imply that O6MeG can be efficiently repaired by MMR when present on the non-template strand but not when it resides on the template strand.

Moreover, York & Modrich were able to show that attempts to repair O6MeG on the continuous strand were iterative, and that in a small fraction of cases resulted in incision of the discontinuous strand. In 2004, a strictly isogenic system was used to demonstrate cells undergo an MMR-, ATR-, and Chk1-dependent G2/M arrest in the second cell-cycle following MNNG treatment that was associated with induction of phosphorylated histone H2AX (γ-H2AX) and RPA foci (Stojic *et al*., 2004). Collectively, the data largely supports a processing hypothesis, since O6MeG:T mispairs are generated during the first cell-cycle following MNNG treatment but do not elicit a G2/M arrest, as would be predicted by the direct signalling hypothesis. The additional presence of RPA also suggests some form of ongoing repair activity. Another publication has provided compelling evidence of MMR-dependent single-stranded gaps occurring in newly replicated DNA during the first S phase following MNNG treatment (Mojas *et al*., 2007). Progression into the second cell-cycle was found to require homologous recombination (HR) activity, whilst the subsequent G2/M arrest characteristic of the response to MNNG required the continued presence of O6MeG. The authors postulated that the continued presence of O6MeG and futile cycling activity might be required to prevent unscheduled repair synthesis and maintain the persistence of the single-stranded gaps until the cells enter the second round of replication. In such a model, SSBs entering the second round of replication would collapse replication forks and be converted into lethal one-ended DSB lesions.

The direct signalling hypothesis instead postulates that MutSα- and MutLα–mediated recognition of O6MeG leads to the recruitment and activation of ataxia telangiectasia mutated (ATM) or ataxia telangiectasia and Rad3 related (ATR)/ATR

interacting protein (ATRIP) and the cell-cycle checkpoint. Indeed, ATR/ATRIP have been found to form a complex together with MutSα and MutLα in a manner dependent on O6MeG, leading to ATR-dependent phosphorylation of Chk1 (Yoshioka *et al*., 2006). This work is supported by the findings of the aforementioned study carried out by Stojic *et al*. (2004), where ATR and Chk1 were found to be crucial for G2/M arrest following MNNG, and nuclear foci were observed for DNA damage signalling, including ATR and its substrates together with γ-H2AX. Perhaps the strongest evidence in favour of the signalling hypothesis are studies showing that separation of function mutations exist that inactivate the repair function of MMR whilst leaving the DNA damage-response intact (Lin *et al*., 2004).

## 1.4 MISMATCH REPAIR AND CANCER

### 1.4.1 Mismatch repair defects, genetic instability and microsatellite instability

An association between defects in MMR function and a mutator phenotype was first observed 30 years ago in *E. coli* (Glickman & Radman, 1980). When assessed at the *HPRT* locus, the mutation rates measured in a panel of cancer cell lines demonstrated MMR-deficient cells to have mutations rates 50 to 750-fold greater than MMR-proficient cells (Glaab & Tindall, 1997). In the same study, a pair of semi-isogenic cell lines was used to demonstrate the MMR-deficient partner to have a 12-fold elevated mutation rate. Interestingly, we now know that inactivation of different MMR proteins leads to different 'flavours' of genetic instability, characterised not only by different impacts on the overall mutation rate, but also in a different mutational spectra (Baranovskaya *et al*., 2001). Concomitant inactivation of *MSH6* and *MLH1* produced a higher mutation rate than that

seen when only *MLH1* was inactivated. The primary repair defects associated with *MLH1* inactivation were IDLs, whereas concomitant inactivation of *MSH6* caused an additional increase in transition and transversion mutations. This data suggests our mechanistic understanding of MMR as a binary on/off pathway whose status is determined by the presence of a full complement of MMR proteins is incorrect, and that instead multiple pathways may exist that require different combinations of MMR proteins to repair specific lesions.

Microsatellites refer to simple sequence repeats of 1-6 nucleotide iterations found distributed across the genome. Mutation rates are often demonstrably elevated at microsatellite regions owing to polymerase slippage (Boyer & Farber, 1998), which has been calculated to increase exponentially with increased numbers of repeats (Lai & Sun, 2003). The mutation rate at a $(CA)_{17}$ repeat in normal human fibroblasts has been calculated as being $7 \times 10^{-9}$ mutations/nucleotide/generation, compared against an overall mutation rate in diploid human cells of $1 \times 10^{-10}$ mutations/nucleotide/generation (Boyer & Farber, 1998). The authors ascribed the differential rates as accounting for the increased number of mutations observed at microsatellite sequences. A primary function of MMR is to correct insertion-deletion mutations that occur during DNA replication, and that often arise at microsatellite regions as a result of polymerase slippage (Boland & Goel, 2010). This relationship between MMR function and the stability of microsatellites was first reported in yeast, where inactivation of *MSH2*, *MLH1*, or *PMS1* was shown to lead to a 100 to 700-fold increase in microsatellite instability (MSI) (Strand *et al*., 1993). Correspondingly, the mutation rate of a $(CA)_{17}$ microsatellite was shown to be 340-fold and 16-fold higher in MMR-deficient LoVo (MSH2-) and H6 (MLH1-) cell lines,

respectively, than an MMR-proficient HT-1080 cell line (Hanford *et al*., 1998). MMR-deficient cells therefore exhibit MSI, whereby the number of repeats that comprise a given microsatellite becomes unstable and expands or contracts in size. The clinical assessment of MSI has been formalised so that a panel of two mononucleotide repeats (BAT25, BAT26) and three dinucleotide repeats (D2S123, D5S346, D17S250), termed the 'Bethesda panel', are examined (Boland *et al*., 1998). A MSI high (MSI-H) phenotype is called if 40% or more of the markers display instability, whereas MSI low (MSH-L) is called if fewer than 20% of the markers are unstable, and microsatellite stable (MSS) is called if all markers are stable.

### 1.4.2 Cancer as a multi-step evolutionary process

Cancer is a broad term that refers to a group of more than 100 diseases arising clonogenically from a genetically distinct cell that does not respond to normal homeostatic controls and can divide unchecked. Such tumourigenic-competent cells evolve from somatic cells in a multi-step manner via a complex evolutionary process. At the start of the millennium, Hanahan & Weinberg published their seminal paper, entitled, 'The Hallmarks of Cancer', which proposed that the genetic complexity seen both within and between different types of cancers could be understood by six underlying principles (Hanahan & Weinberg, 2000). They reasoned that any cancerous cell must acquire a number of functional capabilities that include; self-sufficiency in growth signals, insensitivity to anti-growth signals, limitless replicative potential, evasion of apoptosis, sustained angiogenesis, and tissue invasion & metastasis. Under this framework, the tens of thousands of genotypic changes associated with different cancers can all be understood

in terms of acquiring one of these functional capabilities, or as a consequence of it. In accordance with this notion, human cells have been demonstrated to require a number of mutations in order to achieve neoplastic transformation, the precise nature of which differing in a cell type-specific manner (Rangarajan *et al*., 2004). In particular, human fibroblasts were shown to require inactivation of p53, retinoblastoma protein, and some protein phosphatase 2 functions, as well as activation of telomerase with the presence of an oncogenic Ras allele. The downstream Ras effectors that were required to transform immortalised human fibroblasts were Raf and Ral-GEF, whereas human embryonic kidney cells required phosphoinositide 3-kinase (PI3K) and Ral-GEFs, and human mammary epithelial cells required Raf, PI3K, and Ral-GEFs. Thus, the precise combination of mutations that are sufficient for cellular transformation varies between cell types, and most likely reflects the diverse (epi)genetic patterns characteristic of their tissue of origin.

Although studies have shown that a relatively small number of mutations are sufficient for oncogenic transformation, Stoler *et al*. (1999) found as many as 11,000 genomic alterations in cells of a premalignant colorectal polyp. This surprising value can be understood when cancer is viewed not as a rationally-driven laboratory experiment, but as a real-world evolutionary process that evolves by a process of stochastic mutations and clonal selection (Merlo *et al*., 2006). An initiating mutation provides a growth advantage from which the cell's progeny are subject to further cycling of stochastic mutation and clonal selection. As with any evolutionary process, a heterogeneous population of cells with varying fitness results, containing clones of diversifying genotypes with numerous mutations that are either detrimental, neutral, or that provide a

growth advantage. That up to 11,000 genomic alterations have been observed in premalignant cells when less than 10 are necessary in principle, demonstrates the process of carcinogenesis to be a stochastic and chaotic process.

Once one or more cells have acquired tumourigenic potential a primary tumour will begin to grow, and typically follows an exponential Gompertzian model of growth (Demicheli *et al*., 1991). The process of mutation-driven variation and natural selection of clones continues, with tumours often acquiring the ability to metastasize away from the tissue of origin to form secondary tumours at other sites around the body.

### 1.4.3 Mismatch repair and cancer: Lynch syndrome

LS, formally known as 'hereditary non-polyposis colorectal cancer', is an autosomally dominant cancer predisposition syndrome and accounts for an estimated 2.8% of all CRCs (Hampel *et al*., 2008). The cardinal features of LS include earlier average age of CRC onset, a tendency to form proximal colonic tumours with accelerated rate of carcinogenesis from adenomas to carcinomas, high risk of secondary CRC and increased risk of extracolonic cancers, altered tumour histology and increased CRC survival rates (Reviewed by Lynch *et al*., 2009). Genome-wide linkage analysis studies have revealed two cancer susceptibility loci to be present on chromosome 2p (Peltomäki *et al*., 1993) and 3p (Lindblom *et al*., 1993), whilst other studies have demonstrated LS patients to exhibit an MSI phenotype (Aaltonen *et al*., 1993; Ionov *et al*., 1993). These data, combined with the knowledge that MMR deficiency causes MSI (Strand *et al*., 1993), helped lead researchers to the conclusion that mutations in MMR genes are responsible for LS. Loss of function mutations in *MLH1*, *MSH2*, *MSH6* and *PMS2* have

now all been demonstrated to be causative LS mutations (Fishel *et al*., 1993; Leach *et al*., 1993; Bronner *et al*., 1994; Nicolaides *et al*., 1994; Papadopoulos *et al*., 1994; Vogelstein & Kinzler, 1994; Hendriks *et al*., 2004).

### 1.4.4 Mismatch repair and cancer: sporadic tumours

MMR defects are not restricted to familial cases of CRC, since ~15-20% of sporadic colon cancers also exhibit an MMR-deficient and MSI-H phenotype. Unlike LS, however, where MMR inactivation usually occurs via germ-line mutation of an MMR gene, inactivation in sporadic CRC predominantly results from hypermethylation of the *MLH1* promoter and transcriptional silencing of both *MLH1* alleles (Kane *et al*., 1997; Cunningham *et al*., 1998). That said, there have been a very small minority of LS cases where epigenetic silencing of *MLH1* has been found, although these represent exceptions rather than the rule (Suter *et al*., 2004; Hitchins *et al*., 2005). With regard to cancers that are not part of the LS spectrum of tumours, MSI has been identified in prostate cancer and head and neck cancer, whilst alterations in MMR genes has been demonstrated in cancers of the breast, prostate, lung, bladder, oesophagus, and head and neck (Peltomäki, 2003).

### 1.4.5 Mismatch repair inactivation and cancer

The previously described 'Hallmarks of Cancer' by Hanahan & Weinberg has recently been expanded upon to include genetic instability (Negrini *et al*., 2010), in addition to evasion of immune surveillance, DNA damage and replication stress, oxidative stress, mitotic stress, proteotoxic stress, and metabolic stress (Luo *et al*.,

2009b). Whilst genetic instability is certainly widespread in cancer, there has been considerable debate in the literature as to its role in carcinogenesis. The basic tenet of the 'mutator hypothesis' is that physiological mutation rates are insufficient to generate the numbers of mutations required for carcinogenesis, and therefore, mutations in genes that maintain genomic stability are critical bottlenecks in the development of cancer (proposed by Loeb *et al*., 1974 and more recently reviewed by Loeb *et al*., 2003).

In support of the mutator hypothesis of carcinogenesis, mathematical modelling has shown a mutator phenotype to be a more efficient route to tumourigenesis than a non-mutator phenotype, and that mutator phenotype induction is more likely to occur early and when the number of oncogenic mutations required for transformation is higher (Beckman, 2009). The available laboratory data does indeed show genetic instability to be an early event (Stoler *et al*., 1999) and that human tumours require a higher number of oncogenic mutations than lower animals for cellular transformation (Rangarajan *et al*., 2004). Beckman's study also demonstrated that whilst mutator mutations were likely to occur in only a minority of premalignant cells, these were disproportionally likely to form subsequent malignant tumours.

The mutator phenotype hypothesis states that the mutation rate is the most significant check against carcinogenesis and places inactivation of MMR as a key mechanism by which genetic stability can be lifted to permit sufficient activating mutations in oncogenes and inactivating mutations in tumour suppressor genes to promote carcinogenesis. An alternative hypothesis instead focuses on the role of MMR in detecting, and eradicating by apoptosis, cells that have sustained significant or irrepairable genomic insults. In this scenario, the main check on carcinogenesis is not the

occurrence of oncogenic mutations, but their evasion from the cellular machinery and propagation into daughter cells. However, in the absence of separation of function mutations, the individual functions of MMR are not thought to be separated out *in vivo*; and thus the most likely scenario is that MMR defective cells benefit from both increased mutation rates and protection from some pro-apoptotic stimuli.

## 1.5 MISMATCH REPAIR IN CANCER TREATMENT AND PROGNOSIS

### 1.5.1 Toxicity limitations of classical cytotoxic chemotherapies

Classical cancer chemotherapies utilise cytotoxic drugs that kill or inhibit the growth of rapidly proliferating cells, often by inflicting some form of DNA damage. Such drugs are crude in the sense that they lack significant selectivity, and indiscriminately target all replicating cells, not only cancerous cells. Nonetheless, cytotoxic chemotherapeutic drugs remain in widespread use for treating a large range of cancers due to their efficacy (see Skeel, 2007 for a complete review of cancer chemotherapies and their contemporary use). They are, however, limited by their association with a range of undesirable side-effects and the emergence of drug-resistant tumour populations.

Of the most common chemotherapy-associated side-effects it is estimated that approximately 82-96% of cancer patients experience fatigue (Iop *et al*., 2004), and, despite the use of antiemetics, 60% experience nausea and 50% vomiting (Zachariae *et al*., 2007). Quality of life is a key factor in a patient's decision making process when considering beginning, continuing or completing chemotherapy regimes for the treatment of cancer. A study conducted in 1998 involving 86 women who had undergone systemic

adjuvant therapy for stage I-II breast carcinoma demonstrated this notion (Lindley *et al*., 1998). Of those patients that underwent chemotherapy but experienced little or no disruption to their normal life, 86% were willing to undergo further treatment, which contrasts with only 58% of patients who experienced disruption to their of lives. In agreement with this data, a second study found poor management of chemotherapy side-effects can lead to delayed or failure to complete treatment in 25-50% of patients (Schnell, 2003). A further study of 100 cancer patients looked at which side-effects were seen as the most severe from the patient's perspective (Carelle *et al*., 2002). Patients reported the psychosocial complaint of 'affects my family or partner' as the most severe, with alopecia ranking second, and fatigue third.

A two-fold increase in drug concentration has been shown in animal models to result in a 10-fold increase in tumour cell kill, although this is not usually possible because of the associated increase in drug toxicity (Malhotra & Perry, 2003). One can thus invoke the concept of a therapeutic window, whereby a drug concentration range exists that is sufficient to produce a therapeutic effect but not so large that drug toxicities undermine any such response. The optimal drug concentration for effective response to chemotherapy therefore represents a balance between these two variables.

Therapeutic strategies aimed at protecting non-cancerous cells from cell death during chemotherapy can be expected to reduce adverse side-effects and increase the number of patients accepting, continuing, and completing chemotherapy for cancer treatment. Not only would this lead to increased average life expectancies following diagnosis, but would also improve quality of life for both the patient and their families.

### 1.5.2 Mismatch repair status and prognosis

There has been significant interest over the past decade as to the value of the MSI phenotype as an independent prognostic marker for CRC. Popat *et al*. (2005) scanned the literature using strict inclusion criteria and identified 43 eligible studies examining this relationship (Popat *et al*., 2005). Ten studies were removed in order to avoid bias resulting from datasets that either overlapped or were superseded by subsequent studies, leaving 32 studies to be included in the meta-analysis. These studies represented a total of 7,642 cases of colorectal cancer, 1,277 of which were shown to exhibit MSI. The authors found that MSI was associated with a significantly improved prognosis compared with patients harbouring a MSS tumour, with a combined hazard ratio estimate of 0.65 (95% CI, 0.59-0.71).

The mechanism underlying this phenomenon is not clear, but it has been suggested that the frameshifted mutant proteins expressed by MMR-deficient cells might act as a novel source of tumour-specific antigens, and that this might propagate an immunological response against those tumours. Indeed, Linnebacher *et al*. (2001) generated cytotoxic T lymphocytes (CTLs) that could target and lyse cells exogenously loaded with frameshifted peptides, and further demonstrated a CTL culture raised against a -1 frameshift mutation in the transforming growth factor beta II receptor gene could lyse the CRC cell line, HCT116, which bears this frameshift mutation.

A number of other studies have also observed MMR-deficient tumours to be associated with higher numbers of tumour infiltrating lymphocytes (TILs) (Gafà *et al*., 2000; Alexander *et al*., 2001; Smyrk *et al*., 2001; Buckowitz *et al*., 2005; Meijer *et al*., 2009). In a study of 245 colorectal cancer patients, 43.1% were shown to be MSI-H, with

such tumours showing significantly higher numbers of activated cytotoxic intraepithelial lymphocytes (IELs) (Guidoboni *et al*., 2001). In agreement with the findings by Popat *et al*., the overall survival (72% versus 35%) and relapse-free rates (66% versus 39%) of MSI-H patients was significantly better than MSS/MSI-L patients. High numbers of activated cytotoxic IELs were also found to be associated with a lower risk of death in both MSS/MSI-L and MSI-H cases. Interestingly, the risk of death in the presence of both MSI-H and high activated IEL content was dramatically reduced compared to either MSI-H or high activated IEL alone. Indeed, the risk of death in MSI-H tumours with high activated IEL was reduced by ~90% compared with MSS/MSI-L with low activated IEL content.

Together, these data indicate that MSI-H patients have improved prognosis, and such tumours are often associated with high numbers of activated TILs. These can, at least in principle, become activated by the tumour-specific frameshifted peptides characteristic of MMR-deficient tumours, and result in specific tumour killing. These data are in turn consistent with the observation that high TIL content improves prognosis and is further enhanced if combined with MSI-H.

## 1.6 INHIBITORS OF DNA REPAIR PATHWAYS AND MODERN CANCER CHEMOTHERAPEUTICS

### 1.6.1 Defective DNA repair capacity and cancer

Disturbance of the normal cellular machinery that maintains genome integrity through regulation and initiation of DNA repair events are increasingly considered to be critical events in the development and progression of many tumours. Breast cancer 1

early onset (BRCA1) and breast cancer 2 early onset (BRCA2) are proteins that play vital roles in the repair of DNA DSBs via the error-free HR repair pathway (reviewed by Powell & Kachnic, 2003). Disrupting the function of either gene leads to a genetically unstable phenotype characterised by both numerical and structural chromosomal changes (Shen *et al*., 1998; Tutt *et al*., 1999). Moreover, germ-line mutations in *BRCA1* or *BRCA2* are strongly associated with a risk of developing hereditary breast cancers. *BRCA1* mutations have been shown to elevate the risk of developing breast cancer before 80 years of age from 6.8% to 73.5%, and to elevate the lifetime risk of ovarian cancer from 1.8% to 27.8% (Whittemore *et al*., 1997). In agreement with this data is another large study demonstrating carriers of *BRCA1* or *BRCA2* mutations to have a 82% lifetime risk of developing breast cancer, and for *BRCA1* or *BRCA2* mutation carriers to have 54% and 23% lifetime risks, respectively, of ovarian cancer (King *et al*., 2003). Indeed, a plethora of studies are now available to support the notion of *BRCA1* and *BRCA2* as key tumour suppressor genes (Reviewed by Fackenthal & Olopade, 2007). As discussed above, mutational inactivation of the MMR DNA repair pathway similarly results in genetic instability, albeit at the nucleotide rather than chromosome level (Strand *et al*., 1993; Hanford *et al*., 1998), and defects in these pathways are associated with hereditary and sporadic cancers. Such evidences have lent support to the modern notion that defective DNA repair capacity leads to genetic instability, and that this predisposes to cancer. The finding that DNA repair defects are common in many tumours has contributed towards making genetic instability a hallmark of cancer.

### 1.6.2 Synthetic lethal interactions

Synthetic lethality describes a genetic interaction that consists, in its simplest form, of two genes, that when inactivated together produces a cytotoxic phenotype that does not occur if one is inactivated in isolation (Guarente, 1993; Kaelin, 2005). Synthetic sick interactions similarly describe a situation whereby inactivation of two genes decreases the viability of the cell, compared to the effect of inactivating any of the genes alone. Although systematic screening of the human genome for synthetic lethal interactions has not yet been achieved, there is reason to believe that these interactions are not rare. A recent study in yeast crossed mutations in 132 query genes with ~4700 deletion mutants, and identified a large number of synthetic lethal interactions ranging from 1 to 146 interactions per query gene with an average of 34 per gene (Tong *et al*., 2004). The authors estimate that if the data is representative of the rest of the yeast genome, then as many as 100,000 synthetic lethal interactions may exist. Another study screened a similar number of yeast deletion mutations against 8 query genes, and identified 291 synthetic lethal interactions involving 204 genes (Tong *et al*., 2001).

### 1.6.3 Exploiting synthetic lethalities to selectively target tumours

The relevance of synthetic lethality to the treatment of cancer was brought to the fore after the publication of data demonstrating that *BRCA2*-deficient breast cancer cells could be selectively killed with small molecule inhibitors of poly(ADP-ribose) polymerase (PARP) (Bryant *et al*., 2005; Farmer *et al*., 2005). PARP1 is an important component of the BER pathway, which functions as the predominant pathway for repairing small base lesions and SSBs that result from oxidation and alkylation events

(reviewed by Almeida & Sobol, 2007). PARP1 plays structural and functional roles in the recruitment and formation of lesion-induced BER repair complexes, and its absence was shown by Bryant *et al*. (2005) to result in γ-H2AX and radiation sensitivity abnormal 51 (Rad51) foci induction. The authors proposed that spontaneous SSBs go unrepaired in PARP1-deficient cells, which subsequently collapse replication forks and trigger a rescue reaction by Rad51-dependent HR. Supporting this notion was the finding that PARP1 inhibition was selectively toxic to BRCA2-deficient cells, which are unable to utilise HR, and the finding that PARP1 is hyperactivated in HR defective cells (Bryant *et al*., 2005; Farmer *et al*., 2005; Gottipati *et al*., 2010). Bryant *et al*. (2005) were the first to demonstrate how a synthetic lethal interaction can be exploited to kill BRCA2-deficient tumour cells by therapeutic inhibition of PARP1, which is not toxic to cells with functional HR activity (i.e. non-tumour cells).

More recently, other researchers have identified new synthetic lethal interactions involving proteins involved in DNA metabolism, demonstrating that MSH2- or MLH1-defective cells are selectively sensitive to depletion of Polβ and Polγ, respectively (Martin *et al*., 2010). The authors noted elevated expression of the respective DNA polymerase in MSH2- or MLH1-deficient cells, a protective 'buffering effect' that appears to occur when only one partner in a synthetic lethal interaction is knocked out. The MSH2/Polβ interaction was observed to cause an accumulation of nuclear 7,8-dihydro-8-oxoguanine (8oxoG) lesions, while the MLH1/ Polγ interaction caused accumulation of mitochondrial 8oxoG. That 8oxoG can mispair with adenine during replication, and that knocking out MutY homolog (MutYH), the glycosylase that acts on such mispairs could rescue the observed synthetic lethalities, suggests that 8oxoG is

processed by MutYH into more cytotoxic lesions. Under the model suggested by Martin *et al*. (2010), the MSH2/Polβ and MLH1/Polγ synthetic lethalities serve to increase the number of 8oxoG lesions, which are subsequently processed by MutYH into lesions that prove toxic to the cells.

## 1.7 AIMS

### 1.7.1 Project scope

The key scope of this project is to support the development of the next generation of cancer therapeutics based on exploiting existing defects found in cancers to achieve selective tumour killing. To this end, the project focuses upon DNA repair as a key activity and potential drug target in oncology, and in particular on MMR. The MMR pathway has been heavily implicated in the development and progression of both sporadic and hereditary cancers, and shown to play important roles in shaping the cellular response to a number of chemotherapeutic drugs. A more complete understanding of DNA repair pathways such as MMR is expected to be vital if we are to fully delineate the mechanistic basis of the synthetic lethalities we discover, and in fully exploiting the therapeutic potential that these present. Moreover, identification of small molecule inhibitors of DNA repair processes will not only permit the translation of synthetic lethalities into preclinical trials, they may also be of use as novel chemoprotective agents.

### 1.7.2 Specific aims

The first aim of the project is to design, optimise and automate a high-throughput screening method that can be used to systemically screen both small interfering

ribonucleic acids (siRNA) and small molecules for those that increase the cellular tolerance or resistance to MNNG. Since MMR is a key determinant of MNNG sensitivity, this approach represents a novel approach through which to screen for genes and small molecules that modulate the cellular response to MNNG in MMR-dependent and –independent manners. This aspect of the project is described in chapter three.

The second aim is to apply the screening methods developed as the first part of this project to conduct a high-throughput screen of an siRNA library, in order to identify the key genetic players involved in the normal cytotoxic response to MNNG (chapter four).

The final aim of this study is to apply the methods developed in the third chapter to conduct a high-throughput screen of small molecule compounds for structures that increase cellular tolerance or resistance following MNNG exposure (chapter five). Such compounds might be expected to represent inhibitors of MMR.

# CHAPTER TWO

*Materials & Methods*

## 2.1 Chemicals & common buffers

### 2.1.1 Chemical stocks

**Table 2.1.** Chemical reagent information.

| Chemical | Supplier | Solvent | Stock concentration | Sterility | Storage temp | Storage duration |
|---|---|---|---|---|---|---|
| 5-Fluorouracil | Sigma-Aldrich | DMSO | 5 mM | Solvent sterile-filtered | -20°C | 1 year |
| 6-Thioguanine (6-TG) | Sigma-Aldrich | 1% NaCl (w/v) in 1x phosphate buffered saline (PBS) | 50 mM | 0.2 µM membrane | -20°C | 1 year |
| 9,10-dimethylanthracene (DMA) | Sigma-Aldrich | 100% DMSO (v/v) | 50 mM | Solvent sterile-filtered | RT | 1 week |
| Cadmium chloride | Fluka | 1x PBS | 50 mM | Solvent autoclaved | 4°C | 1 year |
| Cisplatin | Sigma-Aldrich | 1 % NaCl (w/v) in 1x PBS | 5 mM | Sterile-filtered (0.2 µM) | 4°C | 1 day |
| Dimethyl sulfoxide (DMSO) | Sigma-Aldrich | - | 100% | Sterile-filtered (0.2 µM) | RT | 1 year protected from light |
| Etoposide | Sigma-Aldrich | DMSO | 5 mM | | -20°C | 1 year |
| Irinotecan hydrochloride | Sigma-Aldrich | DMSO | 50 mM | Solvent sterile-filtered | -20°C | 1 year |
| *N*-Methyl-*N*'-nitro-*N*-nitrosoguanidine (MNNG) | TCI Europe | 100% DMSO (v/v) | 50 mM | Solvent sterile-filtered | -20°C | 1 year protected from light |
| Phosphate buffered saline (PBS) | Oxoid | Millipore $H_2O$ | 1x | Autoclaved | RT | >1 year |
| Resazurin sodium salt | Sigma-Aldrich | 1x PBS | 1 mg/ml | Sterile-filtered (0.2 µM) | -20°C | > 1 year |

Unless otherwise stated, all chemicals were obtained from Sigma-Aldrich, UK.

### 2.1.2 Common buffers

**Table 2.2.** Common buffer information.

| Chemical | Contents | Stock concentration | Sterility | Storage temp | Storage duration |
|---|---|---|---|---|---|
| Lysis buffer | 25 mM Tris (pH 7.6), 150 mM NaCl, 1% NP-40 (v/v), 1% sodium deoxycholate (v/v), 0.1% SDS, 10 mM NaF, 5 mM NaPPi, 1 mM $Na_3VO_4$, and 1x 'Complete-mini' protease inhibitor cocktail (Roche) | 1x | Non-sterile | 4°C | 1 day |
| TBE buffer | 108 g Tris base and 55 g boric acid dissolved in 980 ml deionised water and 20 ml 0.5 M EDTA (pH 8) | 10x | Non-sterile | RT | >1 year |
| TBS buffer | 61 g Trizma base and 90 g NaCl dissolved in 1 L deionised water. pH adjusted to pH 7.6 with addition of 1 M HCl | 10x | Non-sterile | RT | >1 year |
| TBS-T buffer | As TBS buffer but with addition of 10 ml Triton X-100 | 10x | Non-sterile | RT | >1 year |

## 2.2 Mammalian cell culture

### 2.2.1 Cell lines

HCT116 is a human colon carcinoma cell line that exhibits a DNA mismatch repair (MMR)-null phenotype attributable to its absence of *MLH1* expression (Koi *et al*., 1994). Similarly, HEC59 is a human endometrial carcinoma cell line that expresses a MMR-null phenotype owing to bi-allelic mutations within the *MSH2* and *MSH6* genes (Umar *et al*., 1997). Functional MMR activity has been restored in the semi-isogenic HCT116+Ch3 and HEC59+Ch2 sub-lineages by micro-injection of chromosome 3 or chromosome 2, respectively, that restores wild-type expression of their defective proteins. Selection of these phenotype rescuing chromosomes was maintained by

supplementation of media with 0.4 mg/ml G418 (Invitrogen, UK). The cell lines used in this study have not been authenticated.

### 2.2.2 Cell culture conditions

All cells were maintained in T175 flasks (Corning) with 20 ml Dulbecco's modified minimal essential medium (DMEM) (Gibco, Invitrogen) supplemented with 10% foetal bovine serum (Gibco, Invitrogen), 1x non-essential amino acids solution, 100 U penicillin, and 0.1 mg/ml streptomycin (termed here, 'complete media'). Cells were split every 2-4 days (at approximately 80% confluency) at a ratio of 1:10 (HCT116, HEC59) and 2:10 (HCT116+Ch3, HEC59+Ch2). They were split by aspirating the existing media and washing the flask twice with 10 ml warm 1x phosphate buffered saline (PBS) and once with 5 ml warm 1x trypsin-EDTA solution. Following 5 minutes incubation at 37°C, the cells were re-suspended in complete media and transferred into a sterile 50 ml tube (Corning). Vigorous pipetting was used to ensure a single-cell suspension before cells were diluted by the appropriate ratio in fresh complete media and returned to the flask. All cell cultures were incubated at 37°C in a humidified atmosphere containing 5% $CO_2$.

### 2.2.3 Thawing liquid nitrogen stocks

Liquid nitrogen stocks were rapidly thawed at 37°C for 2 minutes, and the cell suspension diluted in a drop-wise fashion with 10 ml complete media. The cells were spun into a pellet by centrifugation at 800 rpm for 5 minutes, the DMSO-containing media aspirated off, and the cells re-suspended with 10 ml fresh complete media. The

cell suspension was then transferred to a T75 flask (Corning) and cells allowed to revive for 3 passages before they were used for experimentation. If the cell line required selective antibiotics, these were re-introduced between the first and second passages.

### 2.2.4 Freezing cell stocks

Early passage cell lines to be frozen were grown to 80% confluency in T175 flasks (Corning) and trypsinised as described above. The cells were re-suspended in 10 ml complete DMEM containing 10% Hybrid-max sterile-filtered DMSO (v/v) and a single-cell suspension obtained. 1 ml aliquots were prepared in cyrotubes and placed directly into -80°C overnight before being transferred into liquid nitrogen. These 'primary' stocks were subsequently tested for *Mycoplasma* infection and used to create 'secondary' frozen stocks from which cells could be obtained for experimentation. The primary stocks were thus kept to replenish secondary stocks with early passage cells as needed.

### 2.2.5 *Mycoplasma* testing

Liquid nitrogen stocks of all cell lines used were shown to be *Mycoplasma* negative, and thawed cultures were maintained for a maximum of one month before being discarded and replaced. Growing cultures were subjected to periodic *Mycoplasma* testing, which involved seeding a 96-well plate at a density of 4,000 cells per well and allowing the cells to grow in antibiotic-free but otherwise complete media for 48 hours. The media was then replaced with 100 µl PBS containing 70% methanol (v/v), and incubated at room temperature for 20 minutes, before staining the DNA in a similar

incubation with 100 µl PBS containing 1 µg/ml DAPI for 5 minutes. This solution was then replaced with 100 µl PBS and the cells imaged under 20x magnification using an InCell Analyser (GE Healthcare, UK). *Mycoplasma*-infected cultures were identified by the presence of a halo and/or shading around the outside of the nucleus and within the cytoplasm. Cellular morphology was also checked daily and if any significant changes were detected the culture was discarded.

## 2.3 Bacterial cell culture

### 2.3.1 Cell lines

The chemically competent *E. coli* bacterial cell line, DH5α (Invitrogen, UK), was used for all bacterial work described in this study. Following transformation, selection of vector-carrying clones was achieved by addition of 100 ng/ml ampicillin to all media. Aseptic technique was used throughout all steps involving bacterial cell culture.

### 2.3.2 Preparation of selective Luria broth agar plates

A 1L volume of Luria broth agar (LB agar) was prepared by dissolving 25 g of luria broth powder and 8 g of agar powder in 1L of deionised water, and autoclaved to sterilise. Once the solution was sufficiently cool to handle, 100 µl of a 100 mg/ml ampicillin stock was added to create media selective (100 ng/ml ampicillin) for the vectors used in this study. 10 ml aliquots were poured into sets of sterile Petri dishes and allowed to cool and set in a sterile cabinet. Plates were stored for up to 1 month at 4°C before use.

### 2.3.3 Thawing bacterial stocks

Bacterial stocks were stored at -80C until use. An aliquot was thawed on the bench and a sterile loop used to streak a selective LB agar plate so as to obtain single colonies. The bacterial stock was returned to the freezer and streaked plate incubated at 37C for 24 hours. Liquid cultures were obtained by picking a single colony from the streak plate and inoculating a 5 ml volume of LB containing the selective antibiotic within a 50 ml sterile tube. The inoculated tube was incubated on a 250 rpm shaking rack at 37C for 24 hours. Streak plates containing viable colonies were stored at 4C for up 1 week.

### 2.3.4 Transformation of competent cells

Bacterial transformations were carried out in DH5α competent cells according to the manufacturer's instructions (Invitrogen). Briefly, DH5α were thawed on ice and 1-10 ng DNA added to 50 µl aliquots. After a 30 minute incubation on ice, the cells were heat-shocked at 42°C for 20 seconds, and then returned to ice for a further 2 minutes. 950 µl pre-warmed LB media was added to each tube and incubated at 37°C for 1 hour at 225 rpm. 20 µl and 200 µl aliquots were spread on pre-warmed selective plates and incubated at 37°C overnight. Individual colonies were then selected for downstream applications.

### 2.3.5 Freezing bacterial stocks

A liquid culture of 5 ml of selective LB was inoculated with a single colony and incubated overnight at 37°C with 250 rpm shaking. 0.5 ml aliquots of liquid culture were

transferred into 1.5 ml cryotubes (Thermo Scientific, UK) and diluted with 0.5 ml sterile 87% glycerol (v/v). Each aliquot was adequately mixed and transferred to the -80°C freezer for long-term storage.

### 2.3.6 Plasmid purification (miniprep)

Plasmid purification from bacterial cultures was performed using Qiagen QIAprep spin miniprep kits according to the manufacturer's instructions. Briefly, a culture of 5 ml of selective LB was inoculated with a single colony and incubated overnight at 37°C with 250 rpm shaking. Bacterial cells were harvested at room temperature by 3 minute centrifugation at 13,000 rpm. The pellet was re-suspended in 250 µl buffer P1 and vortexed, and cells subsequently lysed by addition of 250 µl buffer P2 with thorough but gentle mixing. Genomic DNA was precipitated from solution by addition and mixing in of 350 µl buffer P3, and the resulting suspension centrifuged at 13,000 rpm for 10 minutes at room temperature. The supernatant was pipetted into a QIAprep spin column and the genomic DNA pellet discarded. The QIAprep column was centrifuged for 1 minute at maximum speed and the flow-through discarded. The column was next washed with 0.5 ml buffer PB, and then 0.75 ml buffer PE. The column was finally dried by a further centrifugation for 1 minute at maximum speed, and plasmid DNA eluted by incubating 50 µl buffer EB on the column for 1 minute before spinning the buffer through the column into a collection tube.

### 2.3.7 Plasmid purification (maxiprep)

Plasmid purification from bacterial cultures was performed using Qiagen QIAprep Spin Maxiprep kits according to the manufacturer's instructions. Briefly, a starter culture of 5 ml of selective LB was inoculated with a single colony and incubated overnight at 37°C with 250 rpm shaking. 200 ml of selective LB was subsequently inoculated with 1 ml of starter culture and again similarly incubated overnight. Bacterial cells were harvested by centrifugation at 6000 g for 15 minutes at 4°C, and the pellet re-suspended in 10 ml buffer P1. 10 ml buffer P2 was added and mixed, and incubated at room temperature for 5 minutes. Finally, 10 ml chilled buffer P3 was added and mixed, and incubated on ice for 20 minutes. Precipitated material was excluded by two centrifugation steps at 20,000 g and 4°C for 30 minutes and 15 minutes, respectively, and the supernatant applied to a QIAGEN-tip 500 equilibrated with Buffer QBT. The tip was washed twice with 30 ml Buffer QC and eluted with 15 ml Buffer QF. The DNA was finally concentrated by isopropanol precipitation, washed with 70% ethanol, and the dried pellet redissolved in 10 mM Tris-Cl (pH 8.5).

### 2.3.8 Agarose gel preparation

Agarose gels were prepared on the day of use by dissolving 1% (w/v) Ultrapure agarose (Invitrogen) in 1x TBE buffer (89 mM Tris, 89 mM boric acid, 2 mM EDTA pH 8) and briefly boiling to aid solubilisation. 1x Gel Red (Biotium) was added and mixed once the solution had cooled to 50-60°C, before pouring into a casting tray equipped with appropriate comb. Once set, the comb was removed and the gel stored at 4°C for at least an hour before use.

### 2.3.9 Electrophoresis and visualisation of agarose gels

Gels were submersed in tanks (Bio-Rad Laboratories) containing 1x TBE and orientated so that DNA samples move down the gel toward the positive electrode. Samples were diluted in 1x loading buffer (Qiagen) before loading together with an appropriately sized Hyperladder (Bioline). The gel was run at 50 V for 3-5 hours at room temperature, before visualisation using a UV transilluminator equipped with overhead camera (Nikon, UK) and Quantity One Gel Doc software (Version 4, Bio-Rad Laboratories). The Quantity One software was also used for densitometric quantification.

### 2.3.10 Measurement of DNA concentration

DNA concentration was measured using a Nanodrop 1000 (Thermo-Scientific) according to the manufacturer's instructions. Briefly, 2 µl of the DNA sample was pipetted onto the Nanodrop optical pedestal and the absorbance of the sample measured at 230 nm, 260 nm and 280 nm. The DNA concentration was calculated based on A260, an extinction coefficient of 50, and a path length of 1 mm. A260/A280 and A260/A230 ratios were also calculated as an indication of DNA purity, with values of >2.0 and >1.8, respectively, considered to be pure.

### 2.3.11 DNA sequencing

DNA sequencing was performed by Source BioScience Geneservice (http://www.geneservice.co.uk) using Illumina Genome Analyzer technology. For each sequencing reaction, 1 µg (100 ng/µl) of the purified DNA template was provided along with the appropriate forward and reverse primer sequences (table 2.3). The data was

analysed and sequence information extracted using FinchTV (Geospiza, USA), and comparison with the expected sequence completed using the Basic Local Alignment Search Tool (http://blast.ncbi.nlm.nih.gov/Blast.cgi).

**Table 2.3** p95-1 sequencing primers.

| Primer | Sequence (5'-3') |
|---|---|
| p95-1 Forward | CTGGTCGAGCTGGACGGCGACG |
| p95-1 Reverse | CATGGTCCTGCTGGAGTTCGTG |

## 2.4 Transfection of mammalian cells with RNA- and DNA-based substrates

### 2.4.1 Small interfering RNA

Reverse transfections were performed in 96-well format (Costar, Corning), and unless otherwise stated, used Qiagen siRNA and Qiagen HiPerFect transfection reagent, at final concentrations of 2 nM and 0.75% (v/v), respectively. 10 µl volumes of serum/antibiotic/non-essential amino acids-free DMEM containing 20 nM siRNA were added to wells and incubated at room temperature for 5 minutes. Similarly, DMEM containing 7.5% HiPerFect (v/v) was incubated at room temperature for 5 minutes before addition of 10 µl volumes to the siRNA. The transfection complexes were allowed to self-assemble over the next 20 minutes with occasional gentle swirling of the plate to mix. 80 µl aliquots of cell suspension (75,000 cells /well) in complete DMEM was next added to the transfection complexes and the plate incubated at 37°C for 24 hours before the transfection media was replaced. An additional 24 hour incubation was then permitted to allow optimal gene depletion to occur prior to beginning further experimentation.

### 2.4.2 DNA

Cells were seeded in 100 µl volumes of complete DMEM (120,000 cells /ml) on 96-well plates and permitted to attach overnight. 110 µl volumes of transfection mix were next formulated on separate conical-bottomed 96-well plates in serum/antibiotic/non-essential amino acids-free DMEM. Aliquots of 55 µl polyethylenimine (15 ng/µl) and 55 µl DNA (2.5 ng/µl) were first incubated at room temperature for 5 minutes, and then mixed together and similarly incubated for 20 minutes. Media was subsequently aspirated from the experimental cell plates and replaced with 100 µl transfection mix for a 4 hour incubation, after which, it was replaced with complete DMEM and cells incubated for a further 20 hours before downstream applications were performed.

## 2.5 Libraries

### 2.5.1 Small molecule compound libraries

Chemical libraries were kindly received from the Developmental Therapeutics Program at the National Cancer Institute (Bethesda, MD, USA), comprising the 'Diversity I Set' (1990 compounds, 10 mM), and 'Diversity 2 Set' (1364 compounds, 10 mM). Additional vialed samples of hit compounds and related structures were also generously provided upon individual request. All compounds were dissolved in 100% DMSO and stored in 96-well plate format at -80°C.

### 2.5.2 siRNA library

A custom made siRNA library targeting 579 genes known to be involved in DNA metabolism and cell-cycle function was supplied by Qiagen. The complete list of siRNA that comprises the library can be found in the appendix (table A1).

## 2.6 Preparation and quantification of mammalian cell extracts

### 2.6.1 Whole cell extracts

Unless otherwise stated, whole cell extracts were prepared from cells growing in 96-well plates. Lysis buffer was prepared on the day of use. Cells were washed once with 200 µl aliquots of warm 1x PBS before 10 µl aliquots of 1x lysis solution were incubated on the cells for 5 minutes on ice, with occasional swirling of the plate to ensure equal coverage. Pipette tips were used to scrape the wells and collect the lysate, which was subsequently incubated in an ice-cold sonicating water bath for 15 minutes, prior to centrifugation at 14,000 g for 15 minutes to pellet cellular debris. The supernatant was collected, protein concentration estimated by Bradford assay, and aliquots stored at -20°C.

### 2.6.2 Bradford assay

Bradford assays were carried out in 96-well plate format. A protein standard consisting of 0, 10, 20, 30, 40, 50, 60, 70, 80, 90, and 100 µg/ml bovine serum albumin was first created, and duplicate 5 µl aliquots transferred to a 96-well plate. The experimental sample was next diluted 1:10 by adding 1 µl sample to 9 µl 1x PBS, and 5 µl aliquots of the diluted sample added to the 96-well plate. 250 µl aliquots of shaken

Coomassie Plus protein assay reagent (Thermo Scientific) was transferred to each well and the plate incubated in the dark at room temperature for 10 minutes, before reading the absorbance of each well at 595 nm using an Envision 2103 multi-label plate reader (Perkin Elmer). To obtain an estimate of protein concentration from the data, the blank control was first subtracted from all wells, and a standard curve of BSA concentration against absorbance was plotted. A linear regression was performed and the equation, y = slopex + intercept, solved. Each experimental sample value was subtracted from the intercept and divided by the slope, before dividing by 10 to account for the dilution factor, and finally dividing by 1000 to give a protein concentration estimate in µg/ µl.

## 2.7 Visualisation of proteins by Western Blotting and chemiluminescent detection

### 2.7.1 Electrophoresis

Pre-cast 4-12% graduated Bis-Tris gels (Invitrogen) were prepared by removal of the comb and non-conducting strip, and rinsing the wells with Millipore $H_2O$ ($mH_2O$) to remove air bubbles. These were loaded into tanks and both chambers filled with 1x NuPAGE MOPS SDS running buffer (Invitrogen). 500 µl antioxidant (Invitrogen) was added to the inner chamber. 10 µg protein was diluted in 1x LDS sample buffer (Invitrogen) and 1x reducing agent (Invitrogen), and the proteins denatured by incubation at 70°C for 10 minutes. Samples were subseqeuently loaded onto the gel, alongside a Seagate Blue Plus (Invitrogen) ladder. The gel was run at 180 V for one hour.

### 2.7.2 Nitrocellulose transfer

The gel was removed from its casing, rinsed with m$H_2O$, and the leading edge cut away and discarded. A transfer 'sandwich' was created by overlaying a 1x transfer buffer soaked sponge, with 3 similarly soaked pieces of Whatman paper, which were rolled smooth to ensure a flat surface for even protein transfer. The gel was next placed onto the sandwich, and covered with a nitrocellulose membrane on which the orientation had been marked. The sandwich was completed by an additional 3 pieces of Whatman paper and second sponge. The whole apparatus was inserted into a transfer tank containing 1x transfer buffer and ice block, and ran at 100 V for 1 hour. The nitrocellulose membrane was subsequently rinsed in 1x TBS-T, and non-specific binding blocked by overnight incubation at 4°C in 1x TBS-T containing 5% skimmed milk (w/v, Fluka).

### 2.7.3 Immunodetection

The nitrocellulose membrane was incubated at room temperature on a shaking board in 1x TBS-T containing 5 % milk (w/v) and an appropriate dilution of primary antibody (table 2.4) for 1 hour. After three 10 minute washes with 1x TBS-T, the membrane was similarly incubated in 1x TBS-T containing 5 % milk (w/v) and a 10,000x dilution of either mouse, rabbit, or goat secondary antibody (table 2.4). The membrane was again washed three times with 1x TBS-T for 10 minutes.

**Table 2.4.** Western blotting antibodies.

| Antibody | Supplier | Stock concentration | Dilution | Secondary |
|---|---|---|---|---|
| Mouse antiactin | Abcam | Not determined | 1:10,000 | Mouse |
| Mouse antiMLH1 | BD Pharmingen (Clone G168-15) | 0.5 mg/ml | 1:100 | Mouse |
| Rabbit antiPARP2 | | | 1:5000 | Rabbit |
| Goat antiTDG | Santa-Cruz Biotechnology | 0.2 mg/ml | 1:200 | Goat |
| Mouse antiTubulin | Abcam | 1 mg/ml | 1:5,000 | Mouse |
| Rabbit antiRAD51 | Abcam | 1.12 mg/ml | 1:1000 | Rabbit |
| Mouse secondary | Abcam | 1 mg/ml | 1:10,000 | - |
| Rabbit secondary | Abcam | 1 mg/ml | 1:10,000 | - |
| Goat secondary | Abcam | 1 mg/ml | 1:10,000 | - |

### 2.7.4 Chemiluminescence

Protein chemiluminescence was achieved using the BM Chemiluminescence ELISA Substrate kit (Roche) according to the manufacturer's instructions. Briefly, 100 µl starting reagent B (stabilized $H_2O_2$) was added to 10 ml substrate reagent A (buffered solution containing Horseradish peroxidase, luminol and 4-iodophenol) and mixed, immediately before use. The nitrocellulose membrane was coated with the mixed solution and incubated at room temperature for 1 minute, before blotting off the excess fluid. Under dark room conditions, the membrane was transferred into a Hypercassette (Amersham Biosciences) and overlaid with X ray film (Fujifilm). The X ray film was exposed for between 1-10 minutes and subsequently fixed using a film processor (Konica Minolta SRX-101A, USA). Quantification of protein expression was completed using Quantity One software (Version 4, Bio-Rad Laboratories).

### 2.7.5 Densitometry

Fixed X-ray films were digitally scanned in greyscale using a HP ScanJet 2400 scanner and analysed using ImageJ graphical software. The relative densities of each sample was measured and expressed relative to the density of the loading control.

## 2.8 Cell-based assays

### 2.8.1 Cell viability assay

Cell viability was estimated following a 1 hour incubation of adherent cells with 10 μg/ml resazurin sodium salt dissolved in fresh complete DMEM. Fluorometric analysis was subsequently performed at $Ex_{530}$ $Em_{590}$ using a Perkin Elmer Envision plate reader. Unless otherwise stated, blank controls were subtracted and viability expressed as a fraction of the matched untreated control.

### 2.8.2 Clonogenic survival assay

10 cm tissue culture dishes (Corning) were seeded at a density of 100 cells /ml (10 ml per dish) and incubated overnight to allow cells to attach. The media was next supplemented with the indicated treatment and incubated for a further 24 hours, prior to removal of the treatment and incubation of the cells in fresh complete DMEM for 14 days to allow colony outgrowth. Colonies were fixed and stained by replacing media with a solution of 70% methanol (v/v) and 0.5% methylene blue (w/v) for 1 hour. Plates were then rinsed with tap water and allowed to dry overnight. Colonies were counted and plating efficiency calculated from the untreated controls. Clonogenic survival was expressed as a fraction of the untreated control.

### 2.8.3 Flow Cytometry: Cell-cycle analysis

$1x10^6$ cells were fixed in 70% ethanol at -20°C overnight and subsequently rehydrated in PBS, before re-suspension in 0.1 mg/ml propidium iodide and 8 µg/ml RNase A solution (Invitrogen). Samples were subjected to fluorocytometric analysis using a CyAn FACS machine (Dako North America, Carpinteria, CA) and data analysed using CellQuest software (BD Biosciences).

### 2.8.4 Immunocytochemistry

Adherent cells grown in 96-well plates were washed once with 200 µl room temperature PBS and fixed in 50 µl 4% paraformaldehyde (w/v) dissolved in PBS for 15 minutes. Cells were subsequently washed twice with 200 µl PBS and once with 200 µl PBS containing 0.1% Triton X-100 to permeabilise the cell membrane. Non-specific binding was blocked by a 40 minute room temperature incubation with 3% BSA (w/v) dissolved in PBS. The cells were stained with 50 µl primary antibody diluted in 3% BSA (dissolved in PBS) overnight at 4°C. Following three 200 µl PBS washes to remove unbound primary antibody, the appropriate secondary Alexa antibody (table 2.5) was diluted 1:500 in 3% BSA and 35 µl aliquots added to each well for a 1 hour room temperature incubation. Unbound secondary antibody was similarly washed off, and the nucleus stained with DAPI diluted 1:1000 in PBS. After a 5 minute incubation, DAPI was removed and 100 µl aliquots of PBS added to each well. Cells were imaged and quantified under 20x magnification using an InCell Analyser (GE Healthcare, UK) equiped with the appropriate filters.

**Table 2.5.** Immunocytochemistry secondary antibodies.

| Antibody | Supplier | Species | Dilution |
|---|---|---|---|
| Alexa Fluor 488 | Invitrogen | Mouse | 1:500 |
| Alexa Fluor 555 | Invitrogen | Rabbit | 1:500 |

## 2.9 Screening assays

### 2.9.1 High-throughput screen for genes that determine MNNG sensitivity

10 µl aliquots of OptiMEM containing 20 nM siRNA was added to each well of a sterile RNase-free 96-well plate, and gently mixed with the addition of 10 µl aliquots of OptiMEM containing 4.5 % (v/v) Qiagen HiPerFect. Negative control wells containing plain OptiMEM or OptiMEM containing only HiPerFect were included, alongside positive controls targeting MSH2 and MLH1 expression. The mixtures were incubated at room temperature for 20 minutes to allow the transfection complexes to form. 80 µl aliquots of a cell suspension containing 75,000 cells/ml was next pipetted onto the transfection mixture to yield a cell density of 6,000 cells/well with final concentrations of 2 nM siRNA and 0.45% HiPerFect (v/v). Transfected cells were incubated at 37°C 5% $CO_2$ for 24 hours before replacing the transfection mixture with 200 µl complete media. After a further 24 hours (48 hours post transfection) media was removed from all wells and replaced with 50 µl fresh complete media. A two-fold dilution with 50 µl complete media containing 10 µM MNNG was performed shielded from light, to give a final concentration of 5 µM MNNG. This treatment was removed 24 hours later when 200 µl complete media was added, and cells incubated for a further 120 hours before assessment of cellular viability. Media was refreshed 48 hours prior to estimation of viability.

### 2.9.2 High-throughput screen for small molecules that decrease MNNG sensitivity

96-well plates were seeded with 200 µl volumes of a HCT116+Ch3 cell suspension (60,000 cells / ml). HCT116 were similarly seeded as a positive control. The cells were incubated at 37°C 5% $CO_2$ and allowed to attach for 24 hours. Media was subsequently aspirated and replaced with 50 µl fresh media containing 20 µM small molecule test compounds and 1% DMSO (v/v). Equivalent concentrations of PBS or DMSO were also added to control wells. After approximately 6 hours, each well was diluted two-fold with 50 µl media containing 10 µM MNNG, to give a final concentration of 5 µM MNNG, 0.5% DMSO, and 10 µM small molecules. Untreated control wells were diluted two-fold with complete media alone. Due to the photo-sensitivity of MNNG, it is important to shield the plates from light during the 6 hour incubation. 200 µl fresh complete media was used to replace existing media in each well following a subsequent 18 hour incubation, and again 72 hours thereafter. A final 48 hour incubation was completed prior to assessing cellular viability.

## 2.10 Data analysis

Unless otherwise stated, error represents standard error calculated from nine measurements conducted in three independent experiments. 2-sample T-tests were used to generate statistical significance. Where more than three conditions were analysed, one-way analysis of variance with Tukey's test for pairwise comparisons was used to generate statistical significance. All statistical calculations were performed using Minitab (Version 15, Minitab, U.S.A.). One star refers to a p value of $<0.05$, two stars

<0.01, and three stars <0.001, whereas the abbreviation 'NS' means 'not significantly different'.

High-throughput screening strategies were evaluated and compared by calculating their Z-factor (Zhang *et al*., 1999). Simply described, the Z-factor relates to the probability that a given screening strategy will successfully identify positive samples, assuming sufficient throughput. A value of 0 represents a futile strategy, values >0 and <0.5 have marginal chances of success, whereas those scoring ≥0.5 are deemed excellent assays with high chances of success.

Screen results were ranked by Z-score, calculated by subtracting the sample measurement from the plate mean, and dividing this by the standard deviation of the plate (Brideau *et al*., 2003). Z-scores that were two or more standard deviations away from the population mean were deemed significant.

# CHAPTER THREE

*Results*

## 3.1 INTRODUCTION

### 3.1.1 Advent of high-throughput screening as a drug discovery tool

High-throughput screening refers to an approach that began in the early 1990s, whereby the miniaturisation of assays together with advances in automation permitted the systematic testing of large numbers of chemical species for those that possessed interesting biological activities (Mayr & Bojanic, 2009). The National Cancer Institute (NCI) in the United States were early pioneers, who in the late 1980s changed the emphasis of drug discovery away from murine models of leukaemia towards human cell line models of solid tumours (Shoemaker, 2006). They assembled a panel of 60 neoplastic cell lines that represented human tumours originating from the blood, colon, lung, central nervous system (CNS), renal system, skin, ovaries, breast, and prostate. The cell lines were grown on 96-well plates, and systematically exposed to increasing concentrations of test compounds. The impact of each compound on the phenotype was assessed using a sulphorhodamine B (SRB) method that permitted measurement of inhibition of growth and cellular toxicity (Voigt, 2005). SRB binds basic amino acid residues of proteins to produce a stable colourimetric end-point that is sufficiently sensitive to detect 1000-2000 cells per well. One of the first class of compound to be identified with selective anti-tumour activity were the ellipticinium derivatives (Acton *et al*., 1994). These compounds were demonstrated to undergo selective uptake and processing by CNS-derived tumours (Vistica *et al*., 1996), and were shown to be capable of inhibiting the growth of subcutaneous and orthotopic glioblastoma xenografts (Shoemaker *et al*., 1995). Whilst preclinical trials of ellipticines did not reflect their early

promise (Arguello *et al*., 1998), a very large number of novel drugs with anti-cancer specificities have since been identified from the NCI screen (Monks *et al*., 1997).

### 3.1.2 Small molecules and diverse small molecule libraries

The term 'small molecule' refers to a non-polymerised organic compound with a molecular weight less than 800 daltons (Nelson & Cox, 2004). The majority of currently approved drugs are small molecules, and so drug discovery through the screening of novel small molecule structures is of interest within the pharmaceutical industry. Modern chemical techniques permit the design and synthesis of large-scale libraries of diverse small molecule structures for use in high-throughput screening studies (Thompson & Ellman, 1996). A common source of small molecules published within the academic literature is the NCI's 'open chemical repository collection' (accessible via http://dtp.cancer.gov), which contains more than 200,000 compounds. The NCI libraries used in these studies were the 'Diversity I', and 'Diversity II' sets, which contain compounds selected to represent the structural diversity present within the larger collection.

### 3.1.3 Mechanistic basis of RNA interference

RNA interference (RNAi) refers to an evolutionarily conserved mechanism whereby double-stranded RNA (dsRNA) directs sequence-specific post-transcriptional gene silencing (Fire *et al*., 1998; Hamilton & Baulcombe, 1999; Elbashir *et al*., 2001). The initiation step of RNAi is mediated by dicer, an RNase III endonuclease that cleaves dsRNA into shorter 21-25 guide RNAs with a two nucleotide 3' overhang (Bernstein *et*

*al*., 2001). These 'small interfering' RNA determine the sequence-specificity of gene silencing when one strand is incorporated into the 'RNA-induced silencing complex' (RISC) (Hammond *et al*., 2000; Martinez *et al*., 2002). RISC mediates the recruitment of mRNA molecules complementary to the siRNA antisense strand, and the mRNA is subsequently cleaved by the argonaute 2 endonuclease subunit (Liu *et al*., 2004; Meister *et al*., 2004). The stability of specific mRNA transcripts can thus be controlled through siRNA-guided mRNA degradation by RISC. siRNA targeted to promoter regions of genes have also been shown to modulate gene expression at the transcriptional level (Kawasaki & Taira, 2004; Kawasaki *et al*., 2005). For instance, targeting of the E-cadherin promoter was found to result in methylation of both DNA and histone H3 lysine 9, and repressed E-cadherin expression at the transcriptional level.

An important evolutionary role of RNAi is thought to be in providing protection against viral gene expression, whereby viral dsRNA is cleaved by dicer into siRNA, and the antisense strand used as a guide by RISC to mediate degradation of viral RNA transcripts (Ding & Voinnet, 2007). RNAi also forms a crucial component in the normal post-transcriptional control of gene expression. Expression of more than 1000 microRNAs (miRNA) is thought to regulate the expression of ~30% of genes within the human genome (Pillai *et al*., 2007). Primary-miRNA are long nuclear-encoded molecules transcribed by RNA polymerase II, and are cleaved into ~70 nucleotide pre-miRNAs following processing by the microprocessor complex, consisting of the Drosha RNase III endonuclease (Lee *et al*., 2003) and the dsRNA binding domain protein (Gregory *et al*., 2004). Upon transportation into the cytoplasm, pre-miRNA are cleaved by dicer into final 22 nucleotide miRNA molecules that associate with RISC and guide

mRNA degradation (Hutvágner *et al*., 2001; Gregory *et al*., 2005). There is therefore some overlap in the molecular machinery that executes the siRNA and miRNA pathways of gene silencing. Whilst miRNA can regulate the silencing of multiple genes because the guide strand base pairs imperfectly with target mRNA within RISC, the siRNA guide strand base pairs perfectly with target mRNA and hence mediates more specific silencing of individual genes (Pillai *et al*., 2007).

### 3.1.4 Development of RNA interference as a research tool

The discovery of RNAi has provided researchers with a powerful new tool with which to perform novel functional studies (Lord *et al*., 2009). The introduction of synthetic siRNA into cultured cells permits the selective depletion of genes in order to observe their contribution to the phenotype. Yeast deletion mutants had previously permitted the systematic investigation of gene function in lower eukaryotes, and now RNAi has allowed the systematic depletion of genes in human cells for the first time (Tong *et al*., 2001; Lord *et al*., 2009).

Whilst the initial impetus in siRNA design was centred on developing sequence algorithms that maximised knockdown of the target protein (Reynolds *et al*., 2004), little was known about methods of improving siRNA knockdown specificity. It is therefore unsurprising that despite its early potential, genome-wide expression profiling studies found siRNA off-target effects to be a serious problem, with individual gene depletions resulting in 1.5-3.0-fold changes in expression of multiple non-target genes (Jackson *et al*., 2003). These effects were not considered to represent a non-specific interferon response to RNA, since the off-target profiles were sequence-dependent. Around the

same time, an siRNA-based screen for novel modulators of the hypoxia inducible factor 1 alpha (HIF-1α) pathway found the top three hits to be false positives resulting from off-target depletion of HIF-1α (Lin *et al*., 2005).

It is perhaps because of the enormous potential of RNAi to functional genetic studies that the concerted effort of researchers across the world has hugely improved the specificity of modern siRNA designs. An important advance was the observation that off-target effects are concentration-driven, and thus strategies that attain gene depletion at low siRNA concentrations will significantly reduce off-target effects (Jackson *et al*., 2003; Semizarov *et al*., 2003). This was achieved by adoption of a 'pooling' strategy by siRNA vendors, whereby two or more siRNA containing distinct sequences targeting the same gene are pooled together. Pooling therefore permits the concentration of each siRNA type to be reduced by at least 50% whilst maintaining gene depletion efficacy. Specific chemical modifications of the sense and antisense strands have also been identified that can further increase siRNA specificity, eliminating as much as 80% of off-target effects (Jackson *et al*., 2006). Finally, advances in bioinformatics have improved the specificity of siRNA design. Particularly useful was the finding that off-targeting is strongly associated with one or more matches between 3' untranslated regions and nucleotides 2-8 of the antisense strand of siRNA (Lin *et al*., 2005; Birmingham *et al*., 2006).

### 3.1.5 Biochemical- versus cell-based screening methods

Traditionally, pharmaceutical companies have preferred a cell-free approach to high-throughput screening (personal communication, Helleday, T., 2010). This approach

involves the purification of the intended protein drug target and biochemical monitoring of its activity following systematic exposure to potential chemical inhibitors. The major advantage of biochemical screening is that the drug target is automatically known, and since it involves directly analysing the interaction between small molecule and drug target, it is more amenable to drug optimisation through structure-activity relationship studies than cell-based approaches. Biochemical screening also has the added advantage of being more rapid and better suited to automation. However, a prior knowledge of the biological system to be targeted is required for biochemical screening, as is the ability to purify the drug target. Moreover, positive hits generated from biochemical screens tend to be significantly less potent when applied in a cellular setting; their biochemical characteristics may prevent entry into the cell or appropriate cellular compartment, the drug-target interaction may be disrupted by endogenous binding partners, or the drug may be metabolised into an inactive product. Similarly, many hit compounds are promiscuous, and inhibit multiple cellular targets that either antagonise their clinical utility or prove toxic to the cell.

An alternative and increasingly utilised approach to drug discovery is cell-based screening, also referred to as 'phenotypic screening'. Whereas biochemical screening requires the rational selection of a drug target that is believed *a priori* will produce a clinically desirable phenotype, a phenotypic approach instead directly screens small molecules for those that induce that phenotype in a cellular setting. By definition, hit compounds arising from phenotypic screens therefore possess the elementary pharmacokinetics to reach and impact upon their drug targets, and do not possess promiscuous activity that disrupts the desired phenotype or necessitates a hit toxicity

screen. A further advantage is that a prior knowledge of the target biological system is not required, which permits researchers to identify novel pharmaceuticals for diseases irrespective of our understanding of the underlying biology. A phenotypic approach combined with a sufficiently large chemical library allows 'nature' to select the best targets or combination of targets to produce the desired phenotype, which is likely to be more efficacious than individual drug targets manually selected in a biochemical approach on the basis of an incomplete understanding of a disease. The major drawback of this approach is that the identity of the drug target(s) is not initially known and must be elucidated in downstream assays. Moreover, metabolism of small molecules during a phenotypic screen might result in the active chemical structure not reflecting the initial structure. This, together with a lack of knowledge concerning the drug target, complicates traditional structure-activity studies and the prediction of risk when escalating candidate drugs into preclinical and clinical trials.

The wider availability of automated techniques and screening expertise within the research community, together with the development of RNAi into a mature research tool, has opened many new avenues of research and catalysed an explosion of high-throughput screening studies. Such studies have proved fruitful in uncovering new drug targets (Turner *et al*., 2008; Arora *et al*., 2010), small molecule drug candidates (Duan *et al*., 2009), and in undertaking functional genetic studies that shed new insights into the mechanistic basis of many processes (Berns *et al*., 2004).

### 3.1.6 Aims

The aim of this chapter was to design and optimise a cell-based assay that was appropriate to phenotypically screen small molecule and siRNA libraries for those agents that significantly increase cellular viability following exposure to MNNG. As MMR is a major determinant of MNNG sensitivity, the assay had to be able to discriminate between MMR-deficient-like and MMR-proficient-like phenotypes. The first objective was therefore to define a cellular system, characterise its response to DNA damaging drugs, and to optimise the assay parameters to achieve maximal differential survival between MMR-deficient and -proficient cells. Subsequent objectives were to integrate the MNNG assay into two screening approaches in the context of appropriate controls and experimental design. The resulting screening assays needed to be sufficient to query small molecule and siRNA libraries for agents that increase tolerance or resistance to MNNG. Once completed, the screening assays had to be automated to permit high-throughput screening capacity for both studies.

## 3.2 RESULTS

### 3.2.1 Cell line characterisation

HCT116 is a human colon carcinoma cell line that exhibits a MMR-deficient phenotype ($p < 0.001$) (fig 3.1b) attributable to its absence of MLH1 expression (fig 3.1a). In contrast, its chromosome 3-complemented counterpart expresses normal levels of MLH1 and is proficient in MMR (Koi *et al*., 1994). Study of the growth kinetics of these cell lines indicated HCT116 to have a slight proliferative advantage, with a doubling time

of 15.98 ± 0.55 hours compared with 18.4 ± 0.04 hours for HCT116+Ch3 ($p < 0.001$) (fig 3.1c).

### 3.2.2 Mismatch repair status and response to DNA damaging drugs

In agreement with the literature (Fink *et al*., 1996; Aebi *et al*., 1997; Fedier *et al*., 2001), we found the MMR-deficient HCT116 cell line to be significantly more resistant than MMR-proficient HCT116+Ch3 to the $S_N1$ alkylating agent, MNNG, the antimetabolities 6TG and 5FU, and the topoisomerase poisons irinotecan and etoposide ($p < 0.001$) (fig 3.2a-e). $IC_{50}$ values for these compounds are shown in table 3.1. Such effects can be attributed to MMR status because siRNA-mediated depletion of MLH1 in HCT116+Ch3 increases its resistance to MNNG to levels comparable with HCT116 ($p < 0.001$) (fig 3.2f). Moreover, the MMR-deficient HCT116+Ch2 control cell line exhibits similar MNNG resistance to HCT116, demonstrating the MNNG sensitivity of HCT116+Ch3 not to be an artifact of chromosome micro-injection and subsequent selection (Koi *et al*., 1994). Finally, an experiment was performed to check whether the difference in MNNG sensitivity between HCT116 and HCT116+Ch3 could be explained in terms of differential expression of MGMT (fig 3.2g). $O^6$-benzylguanine (O6BG) is a potent inhibitor of MGMT (Dolan *et al*., 1991), and was therefore co-treated with MNNG in order to test this possibility. As expected, O6BG treatment decreased the viability of both MNNG-treated cell lines, although it did not alter the relative resistance of HCT116 over HCT116+Ch3. This data therefore supports the notion that MGMT activity in both cell lines is similar, and that the difference in response to MNNG is attributable to MMR status rather than MGMT expression.

**Table 3.1.** $IC_{50}$ values for indicated cytotoxic drugs and cell lines.

| Compound | HCT116 (μM) | HCT116+Ch3 (μM) |
|---|---|---|
| MNNG | 10.82 ± 0.32 | 6.43 ± 0.46 |
| 5-Fluorouracil | 18.44 ± 0.80 | 14.22 ± 0.53 |
| 6-Thioguanine | 22.03 ± 1.25 | 2.66 ± 0.42 |
| Irinotecan | 20.47 ± 1.11 | 5.00 ± 0.83 |
| Etoposide | 6.88 ± 0.77 | 2.34 ± 0.91 |

### 3.2.3 End-point optimisation

Resazurin is a non-fluorescent dye that can be converted, upon reduction by NADH or NADPH, to a highly fluorescent red compound named resorufin. Resazurin can therefore serve as an indicator of cellular metabolic activity, and has been demonstrated to not only compare favorably with more established methods such as [3H]thymidine incorporation, but to be sufficiently sensitive to detect as few as 40 cells (Ahmed *et al*., 1994). Cell viability estimated by metabolic reduction of resazurin was therefore chosen as the major end-point to optimise for these studies.

We first examined the stability of resazurin when dissolved in cell culture medium under both ambient light and darkened conditions (fig 3.3a). This was important in order to determine whether light shielding had to be employed to avoid invoking unnecessary false positive and false negative errors that might result from differential light exposure across and between plates. Spectrophotometric measurement of cell culture medium containing 10 μg/ml resazurin at 37°C under lit conditions revealed the compound to degrade at a linear rate of 0.022 μg/ml per minute, with the loss of 13.2% per hour. In contrast, resazurin was completely stable over the time period measured when incubated under similar conditions but protected from light ($p < 0.001$). Tin-foil was employed in subsequent experiments to shield plates from light and protect against photo-degradation of the dye.

We next checked that the resorufin signal resulting from cellular metabolism was directly proportional to the number of cells present in the sample (fig 3.3b). Increasing numbers of cells were therefore seeded across a number of plates and the resulting resorufin signal measured. A near-perfect correlation was observed between cell density and signal intensity, with an $R^2$ value of 0.999.

Another variable to optimise was the length of time to co-incubate the resazurin solution and cells before analysis of viability. One hour incubation increments from one to five hours were tested and the strength of the fluorescent signal recorded (fig 3.3c). There was no significant difference in signal strength observed between one to five hours. A one hour incubation time was therefore selected for use in subsequent assays.

Finally, since resazurin is marketed as being non-toxic, we examined whether it could be used to measure cell viability at multiple time points during the same experiment without adverse effects on cellular growth (fig 3.3d). We therefore measured the cell viability of the same set of plates every 24 hours for four time points, and compared the viability to plates that were only measured once at the equivalent time point. No significant difference in viability was measured at any of the time points, confirming that repeated resazurin measurements do not interfere with cellular growth under our assay conditions.

### 3.2.4 Optimisation of differential MNNG responses

Key to any successful screen is the optimisation of experimental conditions to maximise the statistical parameter 'R', defined by Zhang *et al.,* as the difference between the positive and negative controls. In this study, this amounts to maximising the

differential viability of MMR-proficient and –deficient cells following MNNG treatment. Initial experiments revealed MNNG to be exquisitely light sensitive (fig 3.4a). A 1 mM solution of MNNG solution dissolved in cell culture medium was observed to completely degrade within 15 minutes when exposed to light. The rate of degradation could be significantly decreased, but not abolished, by addition of light shielding ($p < 0.001$). The failure to achieve a stable solution even in darkened conditions might in part be explained by the fact that spectrophotometric measurements necessitate periodic exposure to light.

A dose-response experiment was next performed to identify the MNNG concentration that best discriminates between cells of opposing MMR function (fig 3.4b). There was a clear MMR-dependent concentration range where MMR-proficient HCT116+Ch3 cells are selectively killed, with the optimal differential killing occurring at ~7.5 μM ($p < 0.001$). The cellular response to MNNG appears to be independent of MMR status at high MNNG doses, since HCT116 became sensitised to MNNG at 15 μM and the differential viability compared with HCT116+Ch3 was lost. This feature is consistent with MNNG inducing a spectrum of lesions in addition to MMR-dependent O6MeG (Wyatt & Pittman, 2006) that can be repaired by MMR-deficient cells at low doses but that saturate these processes and become toxic at higher doses.

Also important to optimise was the length of MNNG treatment and subsequent drug-free incubation period required before measurement of the end-point. Consistent with our earlier observations concerning poor MNNG stability, a 3 hour exposure produced an equivalent response to a 24 hour period and was therefore chosen as optimal (fig 3.4c). Drug-free incubations following drug treatments were necessary to allow the cells time to respond to the treatment condition. We therefore examined the cell viability

that resulted following MNNG treatment under the optimised conditions at 24-120 hour time points post treatment (fig 3.4d). A small but significant difference of 0.06 in the viable fraction was observed between the two cell lines 24 hours post-treatment ($p < 0.01$), and continued to increase to 0.32 at 120 hours post-treatment ($p < 0.001$). A clear biphasic response was observed in HCT116+Ch3 viability, with a fast reduction in viability from 48-72 hours post-treatment, and a slower reduction from 72-120 hours. A drug-free incubation of 120 hours was chosen as optimal.

The final parameter to optimise was the initial density at which cells were seeded onto the plates (fig 3.4e). Cell seeding densities between 4,000 and 14,000 cells/well were investigated, all of which produced a significant difference in HCT116 and HCT116+Ch3 viability following MNNG treatment ($p < 0.001$). The maximal differential viability was observed at cell densities above 12,000 cells/well. Since MNNG is a replication-dependent drug, 12,000 cells/well was chosen as being optimal over 14,000 cells/well, since this would leave more space in the well and help prevent contact-inhibition of growth during the later stages of the assay.

### 3.2.5 Small molecule screen: control optimisation and experimental design.

Since DMSO is the solvent typically used in small molecule libraries, it was important to determine what concentrations of this vehicle were well tolerated by HCT116 and HCT116+Ch3, and to check whether the vehicle itself impacts upon their response to MNNG (fig 3.5a). Doses of DMSO up to 1% (v/v) were found to produce a dose-dependent increase in the viable fraction of HCT116+Ch3 following MNNG treatment. Addition of 1% DMSO was found to increase the viable fraction of MNNG-

treated HCT116+Ch3 cells from 0.43±0.04, to 0.79±0.01 ($p < 0.001$), a level which is comparable to the HCT116 viability of 0.84±0.01 at 0% added DMSO. No additional increase in HCT116+Ch3 viability was seen above 1.5% DMSO. It was therefore clear that DMSO concentrations should be maintained as low as possible in order to maintain a large dynamic range between the positive and negative controls, and to ensure differential killing is attributable to MNNG- rather than DMSO-mediated effects.

Although HCT116 acts as a semi-isogenic MMR-deficient positive control, it was desirable to identify a small molecule positive control to include in the screen. Abelson (Abl) tyrosine kinase has been described as acting downstream of MMR-dependent processing of O6MeG lesions following MNNG treatment (Li *et al*., 2008). Specifically, c-Abl kinase was shown to act within a MLH1/c-Abl/p73α pathway that is required for apoptosis, but not G2/M arrest, following MNNG treatment. A similar MLH1/c-Abl/growth arrest and DNA damage 45 alpha (GADD45α) pathway was necessary for both G2/M arrest and apoptotic responses. Imatinib is a rationally designed and specific inhibitor of c-Abl kinase (reviewed by Capdeville *et al*., 2002). It has been shown to protect against MMR-dependent MNNG-induced G2/M arrest and apoptosis, and consequently increase the clonogenic survival of MMR-proficient cells to levels comparable to MMR-deficient cells (Li *et al*., 2008; Wagner *et al*., 2008). We therefore investigated using Imatinib as a small molecule positive control under the assay conditions optimised in figure 3.4. Three dose-response experiments were conducted, beginning Imatinib exposure either 3 hours prior to the addition of MNNG, at the same time as the MNNG, or 3 hours after the addition of MNNG. Surprisingly, none of the three treatment regimes conferred protection of MMR-proficient cells against MNNG-

induced toxicity. Representative Imatinib pre-treatment data is shown in figure 3.5b, whereby increasing Imatinib concentrations further sensitised rather than protected HCT116+Ch3 to MNNG ($p < 0.001$), and was toxic regardless of MMR status or MNNG treatment at concentrations above 25 μM. Imatinib was therefore ruled out as a suitable positive control.

Cadmium chloride has been demonstrated to inhibit DNA mismatch repair in both yeast and mammalian cells (Jin *et al*., 2003), and is thought to disrupt the mismatch recognition step through its non-specific binding to MutS complexes (Wieland *et al*., 2009). 9,10-dimethylanthracene (DMA) is one of a number of anthracene derivatives that have been named as 'chemical inhibitors of DNA mismatch repair' on a US patent (Nicolaides *et al*., 2006). These compounds were therefore examined as additional small molecule positive controls by exposing MNNG-treated MMR-proficient and –deficient cells with increasing doses (fig 3.5cd). Neither compound conferred any level of protection for HCT116+Ch3 against MNNG-induced toxicity. Whilst DMA appeared to have little impact on the MNNG sensitivity of either cell line, cadmium chloride instead acted to sensitise MMR-deficient cells to MNNG in a dose-dependent manner, with 40 μM $CdCl_2$ reducing the viability of HCT116 so that there was no significant difference between it and similarly treated HCT116+Ch3 cells. Both compounds were therefore ruled out as suitable positive controls.

Since the screening assay had been developed and optimised with semi-isogenic cell lines in the absence of a small molecule control, it is possible that the differential response observed following MNNG treatment is attributable to a genetic difference not related to MMR function. Not only has HCT116+Ch3 been growing apart from its

parental line for a number of passages, but the micro-injection of an additional copy of chromosome 3 also disturbs the copy number of various genes (Koi *et al*., 1994). The phenotypic effects of such differences are hard to predict, and it is thus vital for the screening assay to be tested for its capacity to detect agents that disrupt MMR. In the absence of a suitable small molecule, siRNA technology was employed to specifically deplete the MLH1 protein in HCT116+Ch3, and the screening assay performed to test for sensitivity to MNNG (fig 3.5e). As expected, vehicle-transfected HCT116 were significantly more resistant to MNNG than similarly-treated HCT116+Ch3 ($p < 0.001$). Transfection of siRNA containing a 'non-targeting' sequence had no impact on the HCT116+Ch3 response and therefore controlled against sequence-independent effects of RNA on MNNG response. siRNA targeting the HR protein, Rad51, further increased the sensitivity of HCT116+Ch3 cells to MNNG compared with vehicle or non-targeting control transfected cells ($p < 0.001$), which is consistent with previous reports that HR can partially rescue MNNG toxicity (Cejka *et al*., 2005; Tsaryk *et al*., 2006; Roos *et al*., 2009). In contrast, transfection of a pool of four siRNA with MLH1-silencing sequences significantly increased the resistance of HCT116+Ch3 cells to MNNG ($p < 0.001$). In order to demonstrate that the pool was 'on-target', four individual MLH1-silencing RNA were also used to successfully reproduce the phenotype observed with the pooled siRNA. Western blots confirmed that MLH1 was successfully depleted by the pooled and individual siRNA, but not the non-targeting siRNA (fig 3.5e).

These data demonstrate the screening assay to be capable to detecting agents that disrupt MMR activity. The optimised experimental design and plate formats for the

screen are shown schematically in figure 3.5f, and described in detail in the methods chapter.

### 3.2.6 siRNA-based screen: optimisation and integration of gene silencing

The second screen to be developed is closely related to the small molecule screen described above, and was intended to detect genes that are required for the normal cellular response to MNNG. Key to the success of such a screen was optimisation of the siRNA transfection method to maximise gene silencing, and to integrate it with the method developed in figure 3.4 that uses MNNG response to discriminate between MMR-proficient and –deficient cells.

The two most important parameters to optimise for efficient gene silencing were the concentrations of transfection reagent and siRNA. We therefore first sought to determine the siRNA concentration ranges that could be used without inducing significant toxicity (fig 3.6a). Transfection of 0-16 nM non-targeting siRNA had no observable impact upon the cellular viability of vehicle- or MNNG-treated HCT116 and HCT116+Ch3. The effect on HCT116+Ch3 cell viability of a 24 hour treatment with HiPerFect and DharmaFECT transfection reagents was assessed after 48 hours of subsequent growth, and included the manufacturer's recommended starting concentrations of 0.75% and 0.1%, respectively (fig 3.6b). DharmaFECT was significantly more toxic than HiPerFect at all the concentrations tested ($p < 0.001$), whilst HiPerFect had minimal effect on cell viability at concentrations ranging up to 0.9%. HiPerFect was therefore selected for further optimisation.

As one of the positive controls for the screen, the siRNA and transfection reagent concentrations were optimised to efficiently silence the *MLH1* gene (fig 3.6c). No dose-dependent increase in gene silencing was observed when transfecting either 2 nM or 10 nM siMLH1; and thus 2 nM was chosen as optimal in order to minimise any concentration-driven off-target effects. HiPerFect concentration appeared to be the main determinant of gene silencing efficiency, with 0.45% concentrations resulting in >90% silencing of MLH1.

Cell seeding density was also found to have a large impact on gene silencing, with an inversely proportional relationship between cell seeding density and silencing efficiency (fig 3.6d). Whilst a density of 2,000 cells per well achieved the most efficient depletions, we knew from the data collected in figure 3.4e that high seeding densities maximise the differential response of HCT116 and HCT116+Ch3 to MNNG. Since this is the main end-point for this screen, we therefore opted for a cell seeding density of 6,000 cells per well, which represents a compromise between efficient gene depletion and a large differential MNNG response.

Using the complete set of optimised conditions, it was possible to achieve a knockdown efficiency of ~87%, 48 hours post-transfection (fig 3.6e). MLH1 re-expression occurs gradually thereafter, with gene silencing decreasing to ~70% 72 hours post-transfection, and to ~50% at 96 and 120 hours (fig 3.6f).

In order to ensure that the parameters optimised above are indeed optimal with respect to differential response to MNNG, we next sought to test different transfection lengths and drug-free growth periods (fig 3.6g). A 48 hour transfection interval was

found to be optimal, with 120 hours of drug-free growth producing the large differential response expected from our earlier optimisations.

Since siRNA off-target effects are largely concentration driven, steps were taken to use the minimum RNA concentration possible to achieve target gene silencing. siRNA pools permit the use of lower RNA concentrations whilst maintaining high silencing efficiency when compared with individual siRNA, and have been shown by others to produce stronger phenotypes more suited to high-throughput approaches (Parsons *et al*., 2009). The siRNA library utilised here hence consisted of pools of four siRNA targeting each gene. The optimal siRNA concentration of 2 nM described here therefore refers to the collective RNA concentration, with each individual siRNA being present at 0.5 nM. Transfection with only 1 nM siMLH1 did significantly increase viability following MNNG ($p < 0.001$), but not to the level seen in the *MLH1*-null HCT116 cell line, whereas 2 nM transfections produced an equivalent phenotype to the knockout cell line (fig 3.6h). Surprisingly, we found a 10 nM siMLH1 transfection to be toxic to MNNG-treated HCT116 cells, which do not express the target gene ($p < 0.001$). Since higher concentrations of non-targeting siRNA were not found to be cytotoxic (fig 3.6a), this clearly demonstrates off-target effects occurring at 10 nM siMLH1, and indicates 2 nM represents a good balance between maximal knockdown efficiency and minimisation of off-target effects.

The final optimised experimental design is shown schematically in figure 3.6i. Each plate of the screen will contain 16 control wells consisting of four positive and four negative controls treated with and without MNNG, and 80 experimental wells (fig 3.6j). Each plate was run in duplicate, and the entire screen repeated twice.

A final test experiment was performed under the complete set of optimised conditions in order to assess whether the screen would perform as expected (fig 3.6k). Indeed, the viability of MNNG-treated MMR-proficient HCT116+Ch3 cells transfected with vehicle or non-targeting siRNA was significantly lower than similarly treated MMR-deficient HCT116 cells ($p < 0.001$). Moreover, this difference could be abbrogated by inactivating mismatch repair in HCT116+Ch3 cells through silencing of either MSH2 or MLH1.

### 3.2.7 Screen automation

The PerkinElmer Janus Automated Workstation was used to automate the screening assays. In brief, the workstation is enclosed within a tissue culture cabinet, and consists of three main components; the 'Flexdrop', which is an automated cell seeding device with connected plate stacks, the 'Verispan', which is an eight tip liquid dispensing arm with connected plate stackers, and the 'MDT', which is a 96 pin liquid dispensing arm. An overview of the workstation setup is shown schematically in figure 3.7a.

Cell seeding was achieved using the Flexdrop, which can retrieve 96-well plates from the stack, aliquot defined volumes of a cell suspension into the appropriate wells, and return the plate to the stack. Four separate bottles could be connected (labeled A-D), with each bottle being linked by hose to a 'bank' of eight fixed valves. The 96-well plate was moved by conveyer belt horizontally under the valves, seeding one column per dispense. It was important to eliminate any sources of error at this stage, since small errors in cell seeding are amplified as the cells divide throughout the duration of the

assay. The dispense volume obtained by each valve of every bank was therefore assessed gravimetrically in order to determine the dispense error (fig 3.7b). Using the default valve mapping, relatively large dispense errors were identified for each bank. The mean error for banks A, B, and D were 1.5% (range 8.83%), -0.74% (range 6.40%), and -3.24% (range 10.25%), respectively. Calibration curves were produced (data not shown) and the valve mappings optimised. This reduced the dispense errors for banks A, B, and D to 0.24% (range 3.40%), -0.08% (range 0.96%), and 0.56% (range 2.59%), respectively.

The Verispan eight tip arm has 'liquid-level sensing' technology that allows the machine to verify that the pipette tip picked up and dispensed a given sample. The Verispan was therefore used for addition of small molecules and siRNA to the experimental plates, since this feature would flag up any wells in which there may have been a problem adding the reagent. Although it was not possible to optimise the dispense accuracy of the Verispan, we found that both manual multi-channel and Veripsan pipetting were largely comparable in terms of dispense error (fig 3.7c).

Whilst the Verispan was used for more critical pipetting steps such as the addition of siRNA, the MDT's 96 pin head was used for bulk liquid dispensing operations, such as for whole plate media changes and the addition of resazurin. As before, it is not possible to optimise the dispense accuracy of the MDT, but a comparison against manual multi-channel pipetting revealed the MDT to be more accurate (fig 3.7d).

The Janus workstation possesses two gripper arms that are capable of de-lidding a 96-well plate at any part of the protocol, although we found this process to be time consuming and error prone. We therefore investigated whether the entire screening assay could be conducted without plate lids, or whether the higher rates of evaporation around

the plate edges would adversely affect cell viability (fig 3.7e). In order to assess these 'edge-effects', we measured the viability of three lidded and three de-lidded plates after 120 hours growth. After averaging of replicates, we took the mean value for each row and column of the lidded and de-lidded plates, and performed a t-test to examine whether there were any significant differences between the two conditions. Indeed we found pronounced row and column effects, with the de-lidded plates having significantly higher viability in all rows except 2 and 4, and in all columns except 2, 3, 5, and 8 ($p < 0.05$). This would be consistent with the de-lidded plates experiencing higher rates of evaporation and therefore subjecting the cells to hypertonic stress, which is known to induce a proliferative response (Dmitrieva & Burg, 2005). We therefore opted to compromise and re-lid the plates manually after each Janus operation was completed.

## 3.3 DISCUSSION

### 3.3.1 Summary

The two screening assays developed in this chapter were designed to detect agents that modify the normal cellular response to MNNG, and to be sufficient to discriminate between agents that modify the response in an MMR-dependent- or MMR–independent-like manner. Application of these methods in the context siRNA- and small molecule-based high-throughput screens may yield new insights into the major genes involved in MMR-dependent and –independent MNNG toxicity, and reveal novel chemical inhibitors with potential utility in both research and the clinic. Whilst no methodology is devoid of weaknesses, the most useful are those that have been carefully designed with steps taken to control against them in order to obtain data from which useful conclusions can be

drawn. In some cases this might include addition of internal controls and procedures to reduce error and aid interpretation of results. Other cases might instead include the use of different methods in downstream validation steps to remove artificial results. Here we highlight the inherent strengths and weaknesses of the screening methods developed in this chapter, and discuss the measures taken to ensure these assays produce high quality data that is of sufficient quality to meet the aims of this study.

### 3.3.2 Potential sources of error

#### 3.3.2.1 Cell lines

293T is a human embryonic kidney cell line that exhibits a MMR null phenotype due to epigenetic silencing of the *MLH1* gene (Trojan *et al*., 2002). In 2003, Cejka *et al*. (2003) generated a 293T Lα clone that expressed a vector encoding *MLH1* under the control of a 'Tet-Off' control element. 293T Lα therefore expresses MLH1 and is MMR competent under normal cell culture conditions, but when grown in the presence of doxycycline MLH1 expression is silenced to confer an MMR-deficient phenotype (Cejka *et al*., 2003). Whilst a strictly isogenic system such as this would have been a technically superior cellular model for use in these studies, we found the cell line to be slow growing and poorly adherent, with an unpredictable tendency to detach during media changes (data not shown). The adherence of the cell line was so problematic that we were not able to complete an entire run of the screening protocol, despite numerous attempts using conditioned media and coated plasticware. 293T Lα cells were therefore not suited to the high-throughput assays used here. The semi-isogenic human colon carcinoma cell lines, HCT116 and HCT116+Ch3, were instead selected for use in these studies. The use of

human cell lines not only increases the relevance of our findings in oncology, it also allows for the straightforward and meaningful interpretation of results in relation to the literature. The HCT lineage also represents a well studied and characterised cell line with respect to their origin, DNA repair capability, and response to anti-cancer drugs (Koi *et al*., 1994; Aebi *et al*., 1997; Lei *et al*., 2004).

Whilst HCT116 and HCT116+Ch3 have been widely used as a model to test the phenotypic consequences of MMR deficiency, it should be noted that a number of additional genetic differences exist between the cell lines. In particular, the precise size of the chromosome 3 portion cloned into the cell line has not been defined, and it is anticipated that HCT116+Ch3 will possess increased copy numbers of a number of genes flanking the *MLH1* region (Koi *et al*., 1994). Moreover, tumour cells are known to harbour large numbers of mutations, with 5,272 mutated genes having been described from ~40 tumour types (Baudot *et al*., 2010), and thus it is likely that the fibroblastic chromosome 3 portion micro-injected into HCT116 possesses a different mutational spectra from the endogenous sequence. Combined with the fact that DNA methylation patterns are known to vary in a cell line specific manner (Paz *et al*., 2003), it is likely that HCT116+Ch3 expresses an altered proteome with respect to HCT116. It was important to be aware of such differences, and not simply infer that an assay that discriminates between HCT116 and HCT116+Ch3 does so on the basis of differential MMR status. We therefore demonstrated that inactivation of MMR function in MNNG-treated HCT116+Ch3 by siRNA-mediated silencing of MSH2 or MLH1 was sufficient to increase viability to levels similar to those seen in MMR-deficient HCT116.

#### 3.3.2.2 MNNG stability

A notable potential weakness of the approach used here is the inherent photo-instability of MNNG (Mikuni & Tatsuta, 1994). Although these problems could be overcome by insertion of a manual MNNG addition step into the automated procedure, this solution introduced an increased risk of false positive errors. Attempting to manually add MNNG as quickly as possible under darkened conditions in order to minimise light exposure makes it more likely that one or more pipetting errors may occur over a large batch. This would result in a small number of wells escaping MNNG treatment and presenting as false positives. A further concern with using such an exquisitely light sensitive compound is whether small differences in timings and light levels during the manual treatment step significantly influences the equal exposure of cells both within plates and between plates. Since it is not possible to treat all wells of a single plate or multiple plates simultaneously, one must accept there will be small differences in the stability of the stock MNNG solution between the first and last wells and plates, in addition to small differences in the total length of MNNG exposure for each plate.

A number of steps were taken to minimise the potential errors associated with using MNNG. A single stock of MNNG was initially prepared, before being aliquoted and stored at -20°C protected from light. By frequently using a fresh aliquot of MNNG, it was possible to avoid a progressive degradation in the potency of the MNNG stock solution in between batches. Variation in MNNG exposure across a plate was minimised by use of a multi-channel repeater pipette, which took up sufficient MNNG into the tips to treat the entire plate and thus allowed a plate to be treated in less than 10 seconds. Plates were treated in small batches of five in order to reduce inter-plate variation, and

the MNNG stock replaced every four batches. Although it is impossible to eliminate manual pipetting errors, we found that using cell culture media excluding phenol red for the MNNG stock but not for the existing media in the well, made it easier to identify errors, since the wells that avoided addition of clear MNNG appeared a deeper red colour. This, together with extensive practice, made the occurrence of false positives from manual pipetting relatively less common. False positive errors can be further decreased in the small molecule screen by the use of duplicate measurements. Each member of a duplicate set of plates were separated so to ensure that they are treated with MNNG in different batches and further decrease the possibility of systematic error. Due to the additional sources of error that are present when siRNA rather than small molecules are used, the siRNA screen will be performed in triplicate, with each triplicate plate treated with MNNG in separate batches, and the entire siRNA screen repeated in duplicate.

Whilst an obvious solution might have been to use a compound other than MNNG, its use did convey numerous advantages. Not only was it one of the most effective compounds tested at discriminating between cells based on their MMR status, its poor stability also meant it did not need to be removed at the end of the treatment period, thus helping to minimise the number of liquid handling steps. It also simplified the process for disposal of waste liquid generated by the screen. When the steps taken to reduce potential error are considered, the use of MNNG was more beneficial than detrimental.

#### 3.3.2.3 Edge-effects

A well documented phenomenon with the use of microtitre plates in high-throughput screening is that of the 'edge-effect', which refers to a systematic spatial gradient within plates whereby exogenous environmental factors negatively affect the performance of the assay (Burt *et al*., 1979; Kricka *et al*., 1980; Oliver *et al*., 1981). In terms of cell culture, the outer wells of a plate are thought to experience more intense thermal gradients and higher rates of evaporation. These factors cause an uneven distribution of cells in the outer wells during cell seeding that influences growth kinetics, in addition to generating hypertonic stress, which has been demonstrated to cause changes in cell-cycle progression and gene expression (Pellicciari *et al*., 1995). Others have found that the distribution of adherent cells following cell seeding can be normalised in outer wells by introducing a 60 minute room temperature pre-incubation following cell seeding and prior to incubation at 37°C (Lundholt *et al*., 2003). This technique was therefore employed in these studies. Despite this inclusion, significant edge-effects were observed on un-lidded plates that, if unchecked, would complicate the interpretation of results. This could particularly cause problems in a screening study, where control wells are traditionally situated on the outer two columns of the plate (Malo *et al*., 2006). Due to the throughput requirements of this study, it was not practical to simply exclude the outer wells, as has been done in some studies (Turner *et al*., 1998). Instead, 'low-evaporation lids' were applied to each plate during all incubation steps, and was found to significantly decrease the observed edge-effects.

#### 3.3.2.4 Resazurin

Metabolic reduction of resazurin to the red fluorescent dye resorufin was chosen as a suitable estimate of cellular viability and end-point for these screening studies. An important consideration was therefore whether the small molecules or gene depletions used in these screens could interfere with the redox reactions that generate the cell viability signal. Small molecules were extremely unlikely to interfere with the end-point since there was a large temporal separation of 144 hours between their additions. Moreover, the small molecules were only present from 24 to 48 hours post cell seeding, after which they were removed and the cells washed a further two times with 200 µl of cell culture media over the next 120 hours before addition of resazurin. Similarly, gene depletions that positively affect cellular metabolism could have potentially resulted in increased resazurin reduction and the generation of a false positive result. However, we have shown that re-expression of target proteins is well advanced by 144 hours post-transfection, whereas the resazurin treatment does not occur until 192 hours post-transfection. It is therefore unlikely that gene depletions would have directly influenced resazurin redox reactions independently of their effect on cellular viability.

Although cellular viability has been shown to be a good surrogate for survival (Ahmed *et al*., 1994), it can only discriminate between dead and alive cells, not between damaged and healthy cells. It may therefore be possible for an agent that sufficiently prolongs the processing of methylation damage or apoptotic response to allow a damaged cell to survive long enough to register as a 'viable' cell following resazurin measurement. This is one of the reasons why the screening protocol allows for a period of growth post-treatment, in order to give the cells time to respond to their treatments and execute

apoptotic pathways where appropriate. Moreover, any positive results obtained from the screens will ultimately be validated with the use of clonogenic survival assays, which measure the clonogenicity of individual cells following the treatment (Plumb, 2004). Any artificial results that do arise will therefore be filtered out by downstream validation assays that utilise different methods to estimate cytotoxicity.

#### 3.3.2.5 Screening concentration and replication (small molecule screen)

Biological systems interact with drug-like molecules via a dose-response relationship. Although the mathematical nature of the relationship varies depending on the precise nature of the interaction, concentration thresholds typically exist, below which there is insufficient compound to produce a phenotype, and above which a non-specific cytotoxic response results (Calabrese, 1994). Between these points, increasing concentrations of biologically active small molecules typically correlate with an increased phenotype. It is this concentration range that should ideally be targeted in high-throughput screening in order to identify molecules with the desired biological activity. However, since high-throughput screening involves screening libraries of diverse small molecules, no single optimal concentration exists. The optimal concentration for compound A may represent a toxic concentration for compound B, and an insufficient concentration for compound C. Whilst a logical approach might involve screening a low concentration on the basis that the screen will be selective for compounds with high target affinities, one should remember a small molecule library consists of diverse structures that may serve only as starting points for pharmacological optimisation. The most suitable drug candidate is therefore not always the most potent hit identified in

the initial screen. Large screening enterprises have side-stepped such issues by screening each compound at multiple concentrations in order to search for dose-response relationships. The most successful example of this is the NCI anti-cancer drug screen, which in the 1990s screened 10,000 compounds a year in triplicate at five concentrations (Shoemaker, 2006). Due to resource constraints, screening multiple concentrations is not a viable approach in this study, and thus a single small molecule concentration of 10 μM was chosen for screening of the NCI libraries, since this is the concentration recommended by the NCI. Whilst a single concentration approach increases the chances that potentially interesting compounds will be missed, when resources are limited it has to be balanced against achieving sufficiently high throughput.

Each plate of the small molecule library will be screened in duplicate, which will help compensate for errors in cell seeding, addition of small molecules, MNNG exposure, and end-point measurements. It should be noted that due to practical considerations the duplicates are not completely independent, since both duplicate plates are processed in the same screening experiment. This type of replication would therefore be vulnerable to some types of systematic errors, such as being insufficient to compensate for a faulty tip on the robotic platform, for example.

The approach of screening a single concentration in non-independent duplicate replicates therefore represents a compromise between an optimal setup and resource limitations. Whilst this approach may yield a relatively higher number of false positive results in the initial screen, the relatively high capacity of the method permits rapid re-screening of these hits to improve the specificity of the screen. On the other hand, it should be noted that the use of small molecule libraries with diverse structures does

amplify the impact of false negative results. Whereas a given structural backbone may be represented by two or more chemical analogues in a larger commercial library, the small molecule libraries used here contain structurally diverse compounds. Whilst this allows one to more quickly identify key structures with interesting activity, it also means that the structure is more likely to be missed in the case of a false negative. In contrast, the backbone structure may still be detected in a larger commercial library by one of the chemical analogues that would also have been screened. The approach used in this study will therefore permit the screening of a relatively large number of structural classes for the resources used, but at the increased risk of missing potentially interesting compounds.

### 3.3.3 Small molecule screen

#### 3.3.3.1 Imatinib as a potential positive control

c-Abl kinase has been proposed to be necessary for MMR-dependent G2/M checkpoint and apoptotic responses that occur following treatment with MNNG (Shan Li *et al*., 2008; Wagner *et al*., 2008). Consequently, either pharmaceutical inhibition of c-Abl kinase by Imatinib or shRNA-mediated c-Abl depletion increased the clonogenicity of MMR-proficient RKO7 cells to levels comparable with MMR-deficient RKO6 cells. Although it is difficult to directly compare the viability assays used in this study and clonogenic survival assay data published by Wagner *et al*. (2008), it was surprising to find that Imatinib did not produce a similar protective effect here. This is despite our performing a 24 hour pre-treatment at comparable Imatinib concentrations to their 1 hour pre-treatment. Both studies also treated Imatinib and MNNG concomitantly and additionally included a significant period of growth post-treatment. The reason for the

failure of Imatinib to protect against MNNG-induced toxicity is therefore not immediately apparent. It is interesting to note that alternative splicing produces two isoforms of c-Abl termed, 1a and 1b, and that these differ in their intracellular localisation, post-translational modifications, and cellular functions (Kharbanda *et al*., 1997). Moreover, murine data suggests that their expression level may vary between different tissue and cell types (Renshaw *et al*., 1988). It is therefore possible that Imatinib does protect against MNNG-induced toxicity in RKO7 but not HCT116 cells because of cell type specific differences in c-Abl isoform expression.

#### 3.3.3.2 Cadmium chloride as a potential positive control

A large body of evidence has now been demonstrated to support the notion that cadmium can inhibit both the repair and DNA damage response functions of MMR. $CdCl_2$ treatment increases the overall mutation rate and the number of point mutations in yeast, inhibits repair of IDLs in human extracts, and suppresses the MMR-dependent G2/M cell-cycle arrest usually seen following MNNG treatment in human cells (Jin *et al*., 2004; Lützen *et al*., 2004). $CdCl_2$ has since been shown to decrease, but not abolish, the binding affinity of MutSα for mismatched substrates, and to block its ATPase activity (Clark & Kunkel, 2004; Banerjee & Flores-Rozas, 2005). This inhibition occurs in the low micromolar range and results from non-specific binding of cadmium to MutSα in yeast, with ~100 cadmium ions being sufficient to inactivate MutSα (Wieland *et al*., 2009). $CdCl_2$ has also been shown to inhibit yeast replication factor C (RFC), and both the MutS and MutL complexes in *Escherichia coli*, all of which are critical MMR factors in humans (Constantin *et al*., 2005).

The data presented by Jin *et al*. (2004) suggests the highest dose of $CdCl_2$ used in this study (40 μM) might be expected to inhibit MMR activity by 61-82%, while it has been shown elsewhere that the MMR-dependent response to MNNG requires a full complement of MLH1 protein (Cejka *et al*., 2003). Other studies have demonstrated low expression levels of MSH2 (~10%) and MSH6 (~20%) were sufficient to repair a G:T mismatch but otherwise induced an MMR-deficient MNNG-tolerant phenotype (Lettieri *et al*., 1999; Claij & Te Riele, 2002). Moreover, Lützen *et al.* were able to abolish the MMR-dependent G2/M arrest response following MNNG treatment with only 5 μM $CdCl_2$, which fell within the concentration range tested here. When taken together, it is therefore surprising that no $CdCl_2$ concentration within a range of 5-40 μM increased the tolerance of HCT116+Ch3 cells to MNNG. The treatment regime used in this study involved pre-treating cells with $CdCl_2$ for approximately 4 hours prior to the co-treatment with MNNG for a further 24 hours. This differs from that used by Lützen *et al*., 2004, who pre-treated with $CdCl_2$ for 24 hours prior to a 1 hour co-treatment with $CdCl_2$ and MNNG, and followed by a 48 hour $CdCl_2$ post-treatment. The different experimental conditions may account for the failure of cadmium to protect against MNNG-induced toxicity in our system. However, $CdCl_2$ is not a specific MMR inhibitor, and impairs a wide range of cellular targets either directly by substitution of zinc in zinc finger motif containing proteins (reviewed by Witkiewicz-Kucharczyk & Bal, 2006), or indirectly by non-specific binding to protein targets (Wieland *et al*., 2009). Consequently, $CdCl_2$ has been shown to disrupt other DNA repair systems including BER and nucleotide excision repair (reviewed by Giaginis *et al*., 2006), in addition to damage response proteins such as p53 (Méplan *et al*., 1999). $CdCl_2$ also disrupts calcium transport and signaling (Peng

*et al*., 1999; Misra *et al*., 2002), and can modulate cell adherence molecules (Prozialeck *et al*., 2003). The promiscuous activity of $CdCl_2$ together with our observation that it decreased the resistance of MMR-deficient HCT116 cells to MNNG in a dose-dependent manner suggests that, at least in our system, $CdCl_2$ mediates other effects besides inhibiting MMR, and that these antagonise the resistance that would normally be conferred against MNNG by inhibition of MMR.

#### 3.3.3.3 9,10-dimethylanthracene as a potential positive control

Although we were unable to find any research articles to support the claim, we did identify a US patent describing DMA as a chemical inhibitor of MMR (Nicolaides *et al*., 2006). However, the compound was not found to affect the viability of MNNG-treated MMR-proficient cells, even at concentrations in excess of 50 μM. It should be noted, however, that DMA was only one of ten compounds listed on the patent, and that the others were not tested in our system. Moreover, the patent described these structures as having utility for inhibiting MMR in yeast or plants. We therefore cannot rule out the possibility that DMA inhibits yeast or plant, but not human MMR, or that one of the other structures not tested would have induced a MMR inhibitor-like phenotype in our system.

#### 3.3.3.4 DMSO chemoprotection

We were initially surprised to find that the DMSO vehicle was able to protect HCT116+Ch3 cells from MNNG toxicity in a dose-dependent manner. However, this phenomenon is most likely attributable to the finding by others that DMSO can act as an antioxidant (Sanmartin-Suárez *et al*., 2010). It is known that MNNG undergoes photo-

decomposition to yield oxidising species such as the hydroxyl radical (Mikuni & Tatsuta, 1994), and that antioxidants such as ascorbate can protect against MNNG-induced DNA damage, mutagenicity and carcinogenesis (Galloway & Painter, 1979; Vojteková & Miertus, 1986; Foltínová *et al*., 1994; Biasiak *et al*., 2002). It is therefore possible that DMSO protects against MNNG-induced toxicity in our system by quenching the free radical species that mediate the cytotoxic effects of MNNG. This notion is supported by the findings of others that low concentrations of DMSO can inhibit peroxynitrite-induced hydroxyl radical formation (Jia *et al*., 2010). Nonetheless, characterisation of the impact of DMSO concentration on MNNG toxicity permitted adaptation of the screening assay so as to maintain dynamic range of the assay.

### 3.3.4 siRNA screen

#### 3.3.4.1 Limitations of siRNA

Whilst RNAi-based technology has reinvigorated functional genetic studies, there are a number of limitations that must be considered when interpreting the data produced in such experiments. It is important to distinguish between the digital binary nature of gene knockouts and the continuous analog nature of gene depletion. Whereas a gene knockout completely abolishes expression of the target protein at all time points, the level of expression in gene depletions can vary on a continuous spectrum over time. The observed phenotype resulting from gene depletion depends upon the extent, the timing, and the duration of the maximum knockdown, in addition to the kinetics of gene depletion and subsequent re-expression. To further complicate matters, these variables are difficult to control across a screening experiment, since the kinetics of gene depletion

and re-expression are not only determined by experimental conditions but by intrinsic factors such as the abundance and half-life of each protein target.

Interpretation of siRNA data is further complicated by the fact that the protein dose required for optimal function varies from protein to protein. Some phenotypes are exquisitely sensitive to small changes in a protein's concentration, whereas others do not become apparent until the protein is almost completely depleted. MLH1 is one such example, whereby only a modest reduction in protein level functionally inactivates its role in DNA damage signaling, but leaves its DNA repair function intact (Cejka *et al*., 2003). Incomplete knockdowns can therefore potentially uncouple protein functions and further complicate interpretation. It is therefore crucial that siRNA screens can be shown to be sufficiently sensitive and specific to detect the desired phenotype, with a large number of strong controls to permit a rational assessment of the screen performance. Importantly, the MNNG-based assay described in this study was developed to be capable of discriminating between the differential MMR status of a pair of semi-isogenic cell lines. That siRNA-mediated depletion of MLH1 in HCT116+Ch3 produced an equivalent MNNG resistant phenotype to that observed in HCT116 demonstrates this approach is specific to agents that disrupt MMR activity, and sensitive enough to detect gene depletions in addition to gene knockouts. Mock-transfected HCT116 and HCT116+Ch3 cells were included on all screening plates as positive and negative controls, respectively. In addition to these genetic controls, two siRNA positive controls were included that targeted MSH2 and MLH1 expression, and two negative controls that included non-targeting siRNA and siRNA targeting Rad51 expression. Reassuringly, MSH2 depletion was sufficient to induce a 'MLH1-like' phenotype, whereas non-

targeting siRNA had no effect compared to mock-transfected controls, and Rad51 depletion sensitised cells to MNNG treatment, as has been previously described (Cejka *et al*., 2005; Tsaryk *et al*., 2006). The fact that every screening plate contained 16 optimised controls, that each plate was ran in triplicate, and that the entire screen was repeated twice independently, lends a great deal of confidence that the resulting data will be of a high quality.

### 3.3.5 Expected performance of the screens

A report was published in 1999 that introduced a statistical parameter that formalised the process of assessing the quality of a screening assay as to whether it is suitable for generating statistically valid data (Zhang *et al*., 1999). The parameter integrates the dynamic range and variation of an assay, and returns a statistical score termed the 'Z-factor', which reflects the ability of the assay to produce a statistically valid positive hit. As defined by Zhang *et al*. (1999), a Z-factor of 1.0 reflects an 'ideal assay', 0.5-1.0 an excellent assay with large separation of positive and negative controls, 0.0-0.5 a marginal assay with small separation, whilst Z-factors less than 0.0 mean there is overlap between positive and negative controls that makes screening essentially impossible. Test experiments were performed of the small molecule and siRNA screens in order to obtain estimates of the Z-factor (data not shown). The small molecule assay test involved screening five plates in duplicate and yielded a Z-factor of 0.54, whilst the siRNA assay test involved screening five plates in triplicate, and gave a Z-factor of 0.63. Both of these Z-factors correspond to 'excellent' assays that show a large separation

between the positive and negative controls, with no overlap and little variation, and that are therefore capable of producing statistically valid positive hits.

# CHAPTER FOUR

*Results*

## 4.1 INTRODUCTION

### 4.1.1 Functional screens and the exploitation of synthetic lethal interactions

The notion that DNA repair defects are common in many cancers, and that this Achilles' heal can be exploited through therapeutic inhibition of synthetic lethal partners, is now well established (Kaelin, 2005). The approach has the advantage of targeting the 'backup' pathways on which the tumour relies in order to achieve specific killing, whilst having minimal effects on non-cancerous cells that possess functional 'primary' pathways. Since the discovery that *BRCA2*-deficient tumours can be selectively targeted by synthetic lethal inhibition of PARP (Bryant *et al*., 2005; Farmer *et al*., 2005), the focus within oncology research has been on the identification of additional interactions with which to target other tumour types (Nijman, 2010). Numerous synthetic lethal screens have since been conducted to identify novel interactions involving genes commonly mutated in cancer, including Rad51 (van Haaften *et al*., 2004), PARP (Turner *et al*., 2008), Ras (Luo *et al*., 2009a), and epidermal growth factor receptor (Astsaturov *et al*., 2010). However, in order to fully exploit the new synthetic lethal interactions such efforts will discover, it is important that we possess a sound mechanistic understanding of the underlying biology. Whilst knowledge that gene A is mutated in cancer and synthetic lethal with gene B presents an opportunity to therapeutically target gene B, a more detailed knowledge of the pathways and processes within which gene A and B function might reveal additional clinical utility. It is this premise that will be further discussed below.

Using the BRCA2-PARP interaction as an example, if we were to lack any functional understanding of these proteins or their respective pathways, the therapeutic

options available would be fairly limited. Not only would we miss the opportunity to exploit an underlying concept to treat cancers that do not possess *BRCA* mutations, it would also make it difficult to effectively anticipate and combat drug resistance. It is because we understand that PARP functions in BER to correct SSBs and that BRCA2 functions in HR to repair DSBs, that it is possible to form the mechanistic basis of the synthetic lethality. Namely, that in the absence of PARP, SSBs go unrepaired and collapse DNA replication forks into lethal DSBs, a phenomenon that can be rescued by HR. This functional explanation reveals it is not the proteins *per se* that are synthetic lethal, but rather the repair functions of their respective pathways. This realisation reveals a host of potential targets within these pathways, which not only permits the rational selection of optimal drug targets based on their intrinsic drugability, but could provide opportunities to target a sub-pathway that exploits the synthetic lethal interaction whilst leaving other functions of the repair pathway intact, thus minimising drug toxicity in non-cancerous tissues. Understanding synthetic lethalities at the pathway level also allows one to search for other cancers that may harbour mutations in those pathways, and that might be targeted with equal efficacy through the same mechanism. Indeed, 'BRCAness' refers to a concept whereby tumours that do not possess mutations in *BRCA* genes themselves, but nonetheless display a *BRCA* mutated-like phenotype (Turner *et al*., 2004). This phenotypic mimicry results from mutations in other genes that functionally interact with *BRCA* and are critical for successful DSB repair and replication fork restart by HR. The concept therefore increases the number of tumours that are treatable with PARP inhibitors from the relatively small proportion of breast cancers that possess *BRCA*

mutations to an estimated 25% of sporadic breast cancers that express a BRCA-like phenotype (Turner *et al*., 2004).

Despite their initial sensitivity, *BRCA2*-defective cells often acquire resistance to inhibition of PARP1 via an intragenic *BRCA2* deletion that partially restores HR activity (Edwards *et al*., 2008). However, because we understand that a failure to repair SSBs in PARP-deficient cells creates an absolute requirement for HR activity to rescue collapsed replication forks, it was possible to for researchers to anticipate how resistance to PARP inhibitor resistance might be overcome. Issaeva *et al*. (2010) hypothesised that the partial restoration of HR in PARP inhibitor resistant cells may be insufficient to protect them against drugs that induce a different spectrum of SSB lesions to PARP inhibitors, and found such cells were hypersensitive to the base analogue, 6TG. 6TG generates single-stranded gaps in DNA, in addition to other recombogenic lesions that are unable to be repaired by the partial HR activity in PARP inhibitor resistant cells. 6TG was therefore identified by rational reasoning based on our accrued knowledge of the BRCA2-PARP interaction as a drug that could be used to combat and overcome resistance to PARP inhibitors.

Finally, a complete understanding of the pathways and processes to be therapeutically manipulated is critical in the accurate estimation of risk in clinical trials. The consequences of getting this wrong is no more clearly demonstrated than in a phase 1 study of TGN1412, a CD28 agonist, where all six volunteers receiving the drug developed systemic inflammatory response syndrome and multiple organ dysfunction syndrome (Suntharalingam *et al*., 2006).

Synthetic lethal screens are clearly important in identifying the initial Achilles heal of a tumour, and represents a novel and exciting prospect for the future of anti-cancer drug development. However, functional studies of the implicated proteins and the pathways they participate in are equally important if we are to fully exploit these weaknesses. It is therefore the combination of these approaches that will dictate the success of using synthetic lethal interactions to selectively target cancer.

### 4.1.2 Outstanding issues in mismatch repair

MMR has been heavily implicated in the development and progression of both sporadic and hereditary cancers, plays important roles in shaping the cellular response to a number of chemotherapeutic drugs, and has been demonstrated to be synthetic lethal with multiple cellular targets (Cunningham *et al*., 1998; Popat *et al*., 2005; Hampel *et al*., 2008; Martin *et al*., 2010). MMR is therefore of great clinical importance in elucidating the biology of cancer, the response of tumours to current anti-cancer treatments, and in fully exploiting the next generation of cancer chemotherapeutics. Despite the enormous progress that has been made since MMR was discovered in bacteria over 30 years ago, a large number of fundamental questions still remain, some of which are highlighted below.

#### 4.1.2.1 Origin of the strand discrimination signal

It has been known for some time that during DNA replication, bacterial MutH directs MMR to the newly synthesised strand by utilising the transient hemi-methylation of dGATC sequences to identify and cleave the newly synthesised strand (Hare & Taylor,

1985; Li, 2008). However, unlike MutS and MutL, no homolog of the MutH endonuclease has been identified in humans (Li, 2008). Whilst it has been established that human MMR is also nick-directed, our understanding of how this strand discrimination signal is generated remains lacking (Wang & Hays, 2002; Dzantiev *et al*., 2004; Constantin *et al*., 2005; Zhang *et al*., 2005).

One hypothesis states that the strand discrimination signals may arise from DNA replication itself (Wagner & Meselson, 1976; Crouse, 2010). Replication in eukaryotes is mostly catalysed through the activity of Polα/primase, Polδ, and Polε (Hübscher *et al*., 2002). Polα/primase is required for the synthesis of short 10 RNA nucleotide primers to form double-stranded RNA/DNA hybrids that serve as substrates upon which to load the main replicative polymerases. DNA replication occurs at replication forks whereby the antisense helical structure is progressively unwound to yield individual stands of opposing polarity (Waga & Stillman, 1998). Since the replicative DNA polymerases are restricted to a 5'-3' polarity, the 'leading strand' with 5'-3' polarity can be synthesised 'continuously' by Polε in long stretches of several thousand nucleotides. However, the 'lagging strand' requires synthesis by Polδ in a series of small ~200 nucleotide fragments, termed 'Okazaki' fragments that each require Polα-mediated priming. RNA primer sites undergo a maturation process whereby the RNA is removed by either a polymerase strand displacement/flap trimming/ligation mechanism or through the action of a nucleolytic helicase with subsequent polymerase gap filling and ligation (Burgers, 2009). A possible source of the strand discrimination signals are therefore the single-stranded gaps that occur intrinsically to the replication process. This notion is supported by the finding that mutation rates in yeast are lower on the lagging strand than the leading

strand, and that this strand bias is ablated in MMR-deficient strains (Pavlov *et al*., 2003). This is consistent with the lagging strand having a higher density of strand gaps than the leading strand to act as strand discrimination signals. Another study has demonstrated that the efficiency of MMR repair is higher for mismatches generated by Polα than by Polδ (Nick McElhinny *et al*., 2010). This data makes sense, since mismatches generated by Polα will always be closer to the 5' end of Okazaki fragments than mismatches generated by Polδ. The work of Pavlov *et al*. (2003) and Nick McElhinny *et al*. (2010) therefore goes some way to building a sensible framework for how strand discrimination may be achieved in eukaryotic MMR, although further work is required to show this is definitively the case.

#### 4.1.2.2 Stationary, translocation, and molecular switch models

A further cause of debate is how communication occurs between the strand discrimination signal and the mismatched site, which can be separated by several hundred nucleotides and yet still successfully mediate MMR reactions (Fang & Modrich, 1993). Three models have been devised to propose how this may occur (Li, 2008). The 'stationary' model proposes that MMR proteins induce DNA bending to bring the two sites into contact. The 'translocation' model states that mismatch-activated MutS complexes may act like an ATP-driven molecular ratchet that feeds the helix through itself to form a loop that brings both sites into contact. Finally, the 'molecular switch' model posits that mismatch-activated MutS forms a sliding clamp that freely diffuses along the DNA to the strand discrimination site where it forms a nick-directed repairosome.

The two key pieces of evidence cited as support for the stationary model are the finding that a mismatched site could stimulate the MutH-mediated cleavage of a dGATC site located on a second mismatch-free DNA molecule (Junop *et al*., 2001), and that insertion of a biotin-streptavidin blockade between a mismatch and strand discrimination signal did not block repair of the mismatch (Wang & Hays, 2004). However, other researchers have published data that shows protein blockades or DSBs between the two sites are sufficient to inhibit repair of the mismatch (Pluciennik & Modrich, 2007). Moreover, whilst direct visualisation of homoduplex and heteroduplex DNA in the presence of MutS has revealed MutS to bend DNA, the angle was insufficient to bring disparate sites into contact, and there was no evidence of loop structures in heteroduplex DNA (Wang *et al*., 2003). Such data is therefore inconsistent with a stationary or translocation model but favours the molecular switch model. The discovery that mismatch binding and dissociation by MutS is regulated by ADP and ATP binding, respectively, provided strong additional support for the molecular switch model whereby ADP-ATP exchange occurs following mismatch recognition and permits MutS to dissociate and act as a sliding clamp (Gradia *et al*., 1997). That streptavidin blockage of both termini of a DNA substrate could prevent dissociation of MutSα complexes from heteroduplex but not homoduplex molecules, supports this notion of a non-stationary model with MutSα as a sliding clamp (Blackwell *et al*., 1998). Whilst the weight of the evidence appears to favour a moving model over a stationary model, there remains debate as to the exact mechanism by how translocation of MutSα mediates communication between the mismatch and strand discrimination sites.

#### 4.1.2.3 Futile cycling and direct signalling models

The respective evidence supporting the futile cycling and direct signalling models of MMR-dependent toxicity are discussed in detail within section 1.3.4.

#### 4.1.2.4 Role of MutLβ

Whilst the roles of MutSα, MutSβ, and MutLα have been relatively well defined, much less is known about MutLβ. The MLH1-PMS1 heterodimer was not found to be sufficient to complement an *in vitro* MMR system deficient in MLH1 or PMS2 activity, and was unable to rescue the repair of substrates containing either a G:T mismatch, or a 1-, 2-, or 4-nucleotide IDL, irrespective of whether the nick was 5' or 3' to the lesion (Räschle *et al*., 1999). It was therefore surprising that PMS1 knockout mice were found to display instability at mononucleotide microsatellites, as this implies a role in the repair of insertion-deletion errors (Prolla *et al*., 1998). Moreover, the observation by Prolla *et al*. (1998) that PMS2 knockout mice exhibit a different spectra of cancers to MLH1 knockout mice suggests the existence of other MLH1 partners that function in MMR. Thus whilst it seems like that MutLβ has some role in MMR, the exact nature of this remains unclear.

### 4.1.3 Aims

The focus of this chapter was to examine what genes are required for the normal cytotoxic response to alkylating agents. Since MMR is a key determinant of the DNA damage response following exposure to alkylating agents, this represents a novel approach with which to systematically test what genes are involved in this aspect of

MMR function. Whilst reconstitution studies have revealed the minimal set of MMR components required to provide full MMR repair functionality, the components and mechanistic basis for the DNA damage response functions of MMR are less clear. The approach taken in this study may shed some light on these matters, which might become particularly important when considering targeting synthetic lethal interactions involving MMR components. For example, if a synthetic lethality involving the DNA damage response function of MMR was to be targeted, it would be advantageous to be able to target this function whilst sparing the repair activity, since this would avoid unnecessarily raising the mutation rate in the patient's cells. Equally, without a complete understanding of these processes, it is possible synthetic lethal interactions will be identified in genes that are not yet classified as MMR genes, which may influence our interpretation of the mechanism or compromise our ability to fully exploit the interaction in therapeutic terms.

The specific aims of this chapter are to utilise the automated siRNA screening method developed in chapter three to screen a custom library for siRNA that increase the resistance or tolerance of MNNG-treated MMR-proficient HCT116+Ch3 cells to levels comparable with MMR-deficient HCT116. The screen data will be assessed to determine whether it yields statistically valid data, and one hit gene rationally selected in order to validate its role in modulating the response to MNNG.

## 4.2 RESULTS

### 4.2.1 Screen results

A library of 571 siRNA targeting genes known to be involved in DNA metabolism, the DNA damage response or cell-cycle control were screened in duplicate

to identify those gene depletions that increased the tolerance or resistance of a MMR-proficient cell line to MNNG. The screening data was first assessed in order to determine its quality, which comprised checking the internal controls performed within expected parameters and that the plate replicates and screen repeats correlated. The data was normalised on a per-plate basis against the untreated control and plotted as a histogram (fig 4.1a). The data was found to follow a bell-shaped normal distribution. Z-scores were calculated on a per-plate basis, and each plate assessed against a panel of inclusion criteria to identify those that did not produce robust data with a wide separation between negative, non-targeting, and positive controls. In order to avoid exclusion from subsequent analysis, a plate needed to have at least three population standard deviations between the non-targeting control and one of the two positive controls, and at least four standard deviations between the negative control and one of the positive controls. This equates to a 99.9936% probability that the negative and positive controls are not separated by chance, and a 99.73% chance that the positive control is not separated from the non-targeting control by chance. On this basis, one replicate of plate 3 and 4 and both replicates of plate 8 were excluded from the first screen repeat, together with one replicate of plate 1, 7, and 8 of the second screen repeat (fig 4.1b; table 4.1).

**Table 4.1.** Performance of small interfering RNA screen controls. Number of population standard deviations (Z) that separate the positive and negative controls on the replicates of each library plate. Data for both repeats of the screen are shown. Figures highlighted in red do not meet the minimal requirements for inclusion in the study that there must be at least three population standard deviations between the non-targeting

control and one of the two positive controls, and at least four standard deviations between the negative control and one of the positive controls. Negative controls were non-targeting siRNA (siNONT) and siRNA targeting Rad51 expression, whilst positive controls targeted MSH2 and MLH1 expression.

| **Screen Repeat** | **Plate (replicate)** | **siNONT - siMSH2 (Z)** | **siNONT – siMLH1 (Z)** | **siRad51 – siMSH2 (Z)** | **siRad51 – siMLH1 (Z)** |
|---|---|---|---|---|---|
| 1 | P1 (1) | 2.86 | 3.30 | 5.01 | 5.44 |
| 1 | P1 (2) | 4.26 | 4.20 | 7.33 | 7.27 |
| 1 | P2 (1) | 3.92 | 3.49 | 5.82 | 5.40 |
| 1 | P2 (2) | 3.76 | 3.41 | 5.68 | 5.34 |
| 1 | P3 (1) | 3.11 | 3.92 | 5.24 | 6.05 |
| 1 | P3 (2) | 0.52 | 0.89 | 2.72 | 3.09 |
| 1 | P4 (1) | 3.10 | 3.09 | 6.18 | 6.18 |
| 1 | P4 (2) | 1.17 | 0.84 | 4.22 | 3.89 |
| 1 | P5 (1) | 4.92 | 5.31 | 8.07 | 8.46 |
| 1 | P5 (2) | 3.59 | 3.98 | 5.59 | 5.98 |
| 1 | P6 (1) | 4.62 | 4.51 | 6.94 | 6.84 |
| 1 | P6 (2) | 4.52 | 4.52 | 6.56 | 6.55 |
| 1 | P7 (1) | 6.98 | 5.51 | 9.93 | 8.46 |
| 1 | P7 (2) | 7.70 | 5.33 | 10.78 | 8.41 |
| 1 | P8 (1) | 1.14 | 0.73 | 4.60 | 4.18 |
| 1 | P8 (2) | 0.62 | 0.21 | 3.75 | 3.35 |
| 2 | P1 (1) | 3.57 | 6.58 | 5.86 | 4.79 |
| 2 | P1 (2) | 0.24 | 2.65 | 4.39 | 1.15 |
| 2 | P2 (1) | 3.00 | 5.40 | 5.15 | 3.81 |
| 2 | P2 (2) | 5.06 | 6.95 | 6.79 | 5.45 |

| | | | | | |
|---|---|---|---|---|---|
| 2 | P3 (1) | 2.70 | 4.39 | 3.40 | 4.51 |
| 2 | P3 (2) | 2.38 | 5.58 | 2.75 | 6.11 |
| 2 | P4 (1) | 5.57 | 8.87 | 8.33 | 6.47 |
| 2 | P4 (2) | 2.80 | 7.33 | 5.82 | 5.43 |
| 2 | P5 (1) | 3.25 | 5.58 | 5.27 | 5.14 |
| 2 | P5 (2) | 4.33 | 6.58 | 6.40 | 5.83 |
| 2 | P6 (1) | 5.57 | 8.35 | 8.31 | 5.69 |
| 2 | P6 (2) | 3.62 | 9.15 | 6.96 | 6.93 |
| 2 | P7 (1) | 2.47 | 5.80 | 4.73 | 3.66 |
| 2 | P7 (2) | 4.99 | 6.69 | 7.77 | 5.72 |
| 2 | P8 (1) | 2.94 | 4.90 | 4.71 | 3.51 |
| 2 | P8 (2) | 3.80 | 6.46 | 5.50 | 4.82 |

In order to assess the level of correlation between replicates, the Z score data from each plate replicate was plotted against one another and the $R^2$ values derived (table 4.2). Similarly, $R^2$ values were derived from plotting the mean values of each screen repeat against one another (fig 4.1c; table 4.2). An $R^2$ cut-off of 0.5 was set as being the minimal level of correlation required for those data to be admitted for subsequent analysis. The data demonstrates an excellent overall level of correlation, suggesting the data is high quality and reproducible. Only the $R^2$ value for plate 7 fell below the threshold of 0.5, both in terms of correlation between plate replicates and screen repeats. All plate 7 data was therefore excluded from subsequent analysis.

**Table 4.2.** Correlation between replicate plates and screen repeats. Table showing the $R^2$ values derived between individual plate replicates in each repeat of the screen, as well as those for the two repeats of the screen themselves. Those plates that did not meet the minimal $R^2$ of 0.5 are highlighted in red and were excluded from the study.

| **Plate** | **Repeat 1 ($R^2$)** | **Repeat 2 ($R^2$)** | **Repeat 1 versus Repeat 2 ($R^2$)** |
|---|---|---|---|
| 1 | 0.85 | 0.59 | 0.70 |
| 2 | 0.88 | 0.57 | 0.69 |
| 3 | 0.78 | 0.83 | 0.79 |
| 4 | 0.74 | 0.64 | 0.50 |
| 5 | 0.76 | 0.65 | 0.65 |
| 6 | 0.73 | 0.71 | 0.74 |
| 7 | 0.40 | 0.40 | 0.46 |
| 8 | 0.78 | 0.50 | 0.79 |

Following the strict application of inclusion criteria to ensure we were analysing high quality data, the remaining data was ranked in order so that those gene depletions that increased the tolerance or resistance of MNNG-treated HCT116+Ch3 cells by the most population standard deviations were ranked the highest (fig 4.1d; table 4.3). *MSH6*, *MLH1*, and *PMS2* were the top three ranking gene depletions, and decreased the sensitivity of HCT116+Ch3 cells to MNNG by 4.87 ± 0.06, 3.42 ± 0.43, and 3.36 ± 0.44 population standard deviations, respectively. *MSH2*, the remaining canonical MMR gene was ranked sixth, whose depletion decreased sensitivity to MNNG by 2.87 ± 0.28 population standard deviations. In contrast, *MSH3* (-0.47 ± 0.21), *PMS1* (0.18 ± 0.83), *MLH3* (0.87 ± 0.54), and *EXO1* (0.27 ± 0.59) were not found to significantly alter

MNNG sensitivity. Using a threshold of two standard deviations to define a hit, 10 gene depletions were identified as being of potential interest, representing a 2% hit rate (table 4.3).

**Table 4.3.** Small interfering RNA screen hits. Table showing all gene depletions that increased the viability of MNNG treated HCT116+Ch3 cells by at least two population standard deviations (Z). Standard deviation (SD) and standard error (SE) are also shown.

| Rank | Plate (well) | Gene | Z | SD | SE |
|---|---|---|---|---|---|
| 1 | 1 (F11) | MSH6 | 4.87 | 0.08 | 0.06 |
| 2 | 2 (A08) | MLH1 | 3.42 | 0.61 | 0.43 |
| 3 | 3 (C3) | PMS2 | 3.36 | 0.63 | 0.44 |
| 4 | 8 (A3) | FLJ35220 | 3.34 | - | - |
| 5 | 4 (A2) | SSR1 | 2.94 | 0.36 | 0.26 |
| 6 | 2 (C9) | MSH2 | 2.87 | 0.39 | 0.28 |
| 7 | 6 (A3) | BRD1 | 2.67 | 0.19 | 0.14 |
| 8 | 4 (A3) | TDG | 2.55 | 0.06 | 0.04 |
| 9 | 6 (A4) | SND1 | 2.40 | 0.04 | 0.03 |
| 10 | 3 (A2) | PER1 | 2.17 | 0.72 | 0.51 |

**Table 4.4.** Summary of gene functions for those genes whose siRNA depletion increased MNNG resistance by greater than two population standard deviations. Information was obtained from the National Center for Biotechnology Information (http://www.ncbi.nlm.nih.gov/gene, accessed 26-07-2011).

| **Gene** | **Function** |
|---|---|
| MSH6 | MutS homolog 6<br>Component of DNA mismatch repair. Forms the MutSα heterodimer with MSH2 and plays a role in the recognition of mismatched nucleotides and small insertion-deletion loops. Mutation in this gene disrupts mismatch repair activity, causes microsatellite instability, and predisposes to a number of sporadic cancers. Mutations in *MSH6* have been associated with hereditary nonpolyposis colon cancer. |
| MLH1 | MutL homolog 1<br>Component of DNA mismatch repair. MLH1 can partner with PMS2, PMS1, or MLH3 to form the MutLα, MutLβ, or MutLγ heterodimers, respectively. Mutation in this gene disrupts mismatch repair activity, causes microsatellite instability, predisposes to a number of sporadic cancers, and disrupts meiotic recombination. Mutations in *MLH1* have been associated with hereditary nonpolyposis colon cancer. |
| PMS2 | Post-meiotic segregation increased 2<br>Component of DNA mismatch repair. PMS2 can partner with MLH1 to form the MutLα heterodimer. Mutation in this gene disrupts mismatch repair activity, causes microsatellite instability, predisposes to a number of sporadic cancers, and disrupts meiotic recombination. Mutations in *PMS2* have been associated with hereditary nonpolyposis colon cancer. |
| FLJ35220 | Hypothetical protein. |
| SSR1 | Signal sequence receptor 1<br>Encodes the 34 kD glycoprotein subunit of the signal sequence receptor, a glycosylated endoplasmic reticulum (ER) membrane receptor associated with protein translocation across the ER membrane. |
| MSH2 | MutS homolog 2<br>Component of DNA mismatch repair. Forms the MutSα or MutSβ heterodimers with MSH6 or MSH3, respectively, and plays a role in the recognition of mismatched nucleotides and insertion-deletion loops. Mutation in this gene disrupts mismatch repair activity, causes microsatellite instability, and predisposes to a number of sporadic cancers. Mutations in *MSH2* have been associated with hereditary nonpolyposis colon cancer. |
| BRD1 | Bromodomain containing 1<br>Encodes a protein of unknown function. The protein contains a bromodomain, a sequence motif often found in transcriptional coactivators, and colocalises to the nucleus in testis and several other cell types. |
| TDG | Thymine DNA glycosylase<br>Removes thymine moieties from G:T mismatches by hydrolysing the carbon-nitrogen bond between the sugar-phosphate backbone of DNA and mispaired thymine. With lower activity, the enzyme removes thymine from C:T and T:T mispairings. TDG can also remove uracil and 5-bromouracil from mispairings with guanine. The enzyme plays a central role in cellular defence against genetic mutation caused by spontaneous deamination of 5-methylcytosine and cytosine. |
| SND1 | Staphylococcal nuclease and tudor domain containing 1<br>Functions as a bridging factor between STAT6 and the basal transcription factor. It |

| | |
|---|---|
| | plays a role in Pim-1 kinase regulation of v-myb myeloblastosis viral oncogene homolog activity, and functions as a transcriptional coactivator for the Epstein-Barr virus nuclear antigen 2. |
| PER1 | Period homolog 1<br>The specific function of PER1 is not known. The period family of genes are expressed in a circadian pattern in the suprachiasmatic nucleus, the primary circadian pacemaker in the mammalian brain. They encode components of the circadian rhythms of locomotor activity, metabolism, and behaviour. |

### 4.2.2 TDG validation

#### 4.2.2.1 Rationale for selection of thymine DNA glycosylase for hit validation

The primary screen data demonstrates the extent to which TDG depletion protected against MNNG-induced toxicity to be comparable to other known mismatch repair genes. The cellular viability of TDG-depleted MNNG-treated cells increased by 2.55 ± 0.04 population standard deviations, compared against MSH2 depletion which increased viability by 2.87±0.28 population standard deviations. Moreover, western blot analysis of whole cell extracts of vehicle-transfected or siTDG-transfected HCT116+Ch3 cells confirm that siTDG was successfully depleted during these experiments (fig 4.2a). The primary screen data was therefore consistent with an important role for TDG in the cellular response to MNNG. Indeed, it was possible to envisage a model that might explain its contribution to the MMR-dependent toxicity of MNNG. MNNG treatment has been shown elsewhere to result in the generation of persistent single-stranded gaps in newly replicated DNA, and these are thought to be converted into lethal DSBs following subsequent rounds of replication (Mojas *et al*., 2007). O6MeG:T mispairs that form following replication of MNNG-treated cells are known TDG substrates, whilst TDG has been demonstrated to enhance incision of a DNA molecule containing O6MeG:T mismatches in human nuclear extracts (Griffin *et al*., 1994; Lari *et al*., 2001). One hypothesis might therefore involve the TDG-dependent conversion of O6MeG:T mispairs

into AP sites following the first round of replication. Such lesions would be vulnerable to AP lyase attack and may form a mechanistic explanation for the generation of single-stranded gaps that occurs following MNNG treatment. Failed attempts by MMR to repair O6MeG:T mispairs would result in the MMR-dependent recruitment of TDG to excise O6MeG and generate an AP site. Under this hypothesis, the cell switches to TDG-initiated BER following failed attempts by MMR to excise O6MeG. However, BER might be expected to become rapidly saturated, and hence to result in unrepaired AP sites entering the second round of replication. AP sites would thus be prone to AP lyase attack to generate SSBs that can collaspe replication forks. TDG therefore represents a rational gene selection for further validation and investigation.

#### 4.2.2.2 siRNA deconvolution

A common method for validating an siRNA hit as being 'on-target' is to reproduce the observed phenotype with the individual siRNA oligonucleotides that comprised the pool used in the screen. If the phenotype is attributable to silencing of the target protein, the majority of individual siRNA oligonucleotides should deplete the target and be sufficient to reproduce the phenotype. For 'off-target' effects, it is likely that only the siRNA oligonucleotide containing the promiscuous sequence would reproduce the effect. Previous studies have classified a hit to be on-target when more than 50% of the individual siRNA successfully reproduce the observed phenotype (Turner *et al*., 2008). We therefore performed an experiment whereby the phenotypes produced by TDG depletion with pooled and individual siRNA were compared (fig 4.2b). siRNA targeting MLH1 was included as a positive control and non-targeting siRNA as a

negative control. MNNG treatment resulted in the normal differential viability seen in cells with differential MMR status, such that the vehicle transfected HCT116 cell line and siMLH1-depleted HCT116+Ch3 cell line had significantly increased viability compared to the vehicle transfected HCT116+Ch3 cell line and non-targeting siRNA-depleted HCT116+Ch3 cell line ($p < 0.001$). That vehicle and non-targeting siRNA-transfected HCT116+Ch3 were equally sensitive to MNNG confirms siRNA itself did not influence MNNG-sensitivity independently of sequence context. Surprisingly, we found that neither pooled nor individual siRNA targeting TDG significantly increased the cellular viability of HCT116+Ch3 compared with non-targeting siRNA-transfected cells. Thus, under the conditions of this experiment, we were unable to reproduce the phenotype produced by TDG-depletion in the primary screen.

#### 4.2.2.3 siRNA vendor

A second siRNA screen validation technique often used in the literature is to reproduce the observed phenotype with siRNA obtained from a different vendor. The rationale being that each vendor uses their own proprietary sequences to target a given protein, and switching the vendor acts to control against sequence-specific off-target effects. We therefore performed an experiment using pooled siRNA obtained from Dharmacon rather than Qiagen. MNNG-treated HCT116 and HCT116+Ch3 cells were transfected with Dharmacon siRNA targeting the four canonical MMR genes, *MSH2*, *MSH6*, *MLH1*, and *PMS2*, together with siRNA targeting *TDG* and non-targeting siRNA (fig 4.2c). However, we again found that the data did not support a role for TDG in MNNG-induced toxicity. Whilst siRNA targeting the four established MMR genes

significantly increased the cellular viability of MNNG-treated HCT116+Ch3 compared to vehicle and non-targeting siRNA (siNONT) transfected cells ($p < 0.001$), depletion of TDG did not. Indeed, the viability of siTDG-transfected HCT116+Ch3 following MNNG treatment was not significantly different from the vehicle or siNONT controls.

#### 4.2.2.4 siRNA concentration

Since the validation experiments described above used separately purchased stocks of siRNA rather than library stocks, we wondered whether differences in the siRNA concentration might exist between them as a result differences in their age and number of freeze/thaw cycles. Data from chapter three highlighted the sensitivity of this assay to siRNA concentrations, with too high a level producing toxic off-target effects and too little achieving insufficient gene depletion. An experiment was therefore setup to investigate this possibility, whereby siTDG was titrated so as to produce a range of siTDG transfection conditions ranging from 0.2-20 nM prior to MNNG exposure (fig 4.2d). As expected, MNNG treatment was selectively toxic to MLH1-expressing cells ($p < 0.001$), and could be protected against by siMLH1-mediated silencing of MLH1 expression. However, none of the siTDG transfection conditions was found to significantly increase cellular viability following MNNG treatment, which remained at levels comparable to the siNONT control.

#### 4.2.2.5 Clonogenic survival assay

In order to exclude the possibility of problems with the method itself, we next sought to use the clonogenic survival assay rather than resazurin assay to assess the

survival of TDG-silenced cells following treatment with MNNG. Cell populations were thus transfected in 6 well plates with either transfection vehicle alone, or siRNA targeting MSH6 or TDG. After 24 hours, the cells from each condition were trypsinised, counted, and re-seeded onto 10 cm dishes in triplicate. After a further 24 hours, the cells were treated with increasing concentrations of MNNG or vehicle, and allowed to grow out for 14 days, at which point colonies were visualised and counted. Cells that were transfected with siMSH6 formed significantly higher numbers of colonies than both siNONT- and siTDG-transfected cells at both 2.5 μM and 5 μM MNNG ($p<0.001$) (fig 4.2e). However, there was no significant difference between the clonogenicity of cells transfected with siTDG and the siNONT control.

#### 4.2.2.6 DNA double-strand break assay

53bp1 is known to be critical component of DSB repair, and can be used as an immunocytochemical marker of DSBs, forming discrete nuclear foci that can be quantified (Schultz *et al*., 2000). A final validation experiment was therefore performed whereby 53bp1 foci were measured to assess the impact of depletion of MLH1 or TDG on the formation of DNA DSBs following MNNG treatment at both early (upper panel) and late (lower panel) time points (fig 4.2f). An MNNG-dependent increase in 53bp1 foci was observed in both MMR-proficient and –deficient cells at 24 hours. By 72 hours, 53bp1 foci had mostly dissipated in MLH1-deficient and MLH1-depleted cells but persisted unchanged in vehicle-transfected and MLH1-proficient cells ($p <0.001$). In contrast, TDG-depletion did not protect HCT116+Ch3 cells against DSB formation following MNNG treatment, but rather sensitised cells to DSB formation at the 24 hour

timepoint ($p < 0.001$). By 72 hours, TDG-depleted cells continued to harbour an equivalent number of 53bp1 foci to the other MMR-proficient controls. TDG therefore does not appear to protect against the lethal persistent DNA DSBs that are formed in response to MNNG.

## 4.3 DISCUSSION

### 4.3.1 Known mismatch repair components and MNNG sensitivity

Of the ten identified genes that increased cellular viability of MNNG-treated HCT116+Ch3 by at least two standard deviations, all four canonical genes were represented, with MSH6, MLH1, and PMS2 as the top three hits. This result validates our approach, since these genes encode the proteins that comprise the primary MMR complexes, MutSα and MutLα, and whose role in dictating the cellular response to MNNG has been well established in the literature. Further supporting the quality of the screen results is our finding that MSH3, PMS1, and MLH3 were not found to influence sensitivity to MNNG, as will be discussed in more detail below.

Depletion of MSH3 by other researchers has demonstrated that the protein does not modulate the cellular response to alkylating agents such as MNNG in model organisms such as yeast or Chinese hamsters (Hinz & Meuth, 1999; Cejka *et al*., 2005). Whilst MSH3 over-expression has been associated with methotrexate resistance, this was found to be a consequence of its sequesteration of MSH2 preventing the formation of MutSα, which in turn leads to proteolytic degradation of MSH6 (Drummond *et al*., 1997; Marra *et al*., 1998). Since MutSβ represents the minor heterodimer present under normal steady-state conditions and it is MutSα that primarily determines sensitivity to MMR-

dependent drugs, it is unlikely that MSH3 depletion could alter MNNG sensitivity through a similar mechanism.

With regards to PMS1, its potential role in MMR function remains puzzling, for it does not appear to play an essential role in repair of MMR substrates, nor does it increase cancer susceptibility in knockout mice (Prolla *et al*., 1998; Räschle *et al*., 1999). Our finding that PMS1 depletion did not increase resistance to MNNG is therefore consistent with current data that suggests PMS1 is not important for normal MMR function.

MLH3 binding with MLH1 forms the MutLγ heterodimeric complex that is thought to be primarily involved in meiotic recombination, particularly in establishing and maintaining crossover intermediates (Svetlanov & Cohen, 2004). A role for MLH3 (and hence MutLβ) in repair of insertion-deletion mutations has been described in yeast, although even after 13 years has not been reported in humans (Flores-Rozas & Kolodner, 1998). Nonetheless, it is possible that MLH3 functions similarly in humans, repairing a small subset of IDL mutations in a manner akin to MutSβ. In such an eventuality, the finding that both MSH3 or MLH3 were not identified as hits in this screen is consistent with the notion that they play minor roles restricted to suppression of frameshift mutations.

Depletion of the ExoI was not found in these studies to increase resistance to MNNG. However, reconstitution studies have shown that Exo1 is sufficient to mediate both 5'-3' and 3'-5' excision of mismatched substrates (Dzantiev *et al*., 2004; Constantin *et al*., 2005), a finding that has been confirmed *in vivo* by study of *EXO1* -/- mice (Wei *et al*., 2003). Moreover, such mice exhibit elevated mutation rates and MSI, in addition to being cancer prone and sterile. A further study has shown *EXO1* -/- mice display similar

levels of resistance to alkylating agent-induced O6MeG as *MSH6* -/- mice (Klapacz *et al*., 2009). Taken on face value, such findings are inconsistent with our data that did not identify Exo1 as a protein that plays a role in determining sensitivity to MNNG. However, the *EXO1* -/- mice studied by Wei *et al*. (2003) were not deficient in repair of IDLs involving greater than one nucleotide, only exhibited MSI at monosatellite repeats, displayed only a weak mutator phenotype, and were not prone to gastrointestinal tumours as is the case with MSH2 or MLH1 mutants (Jiricny, 2006). Moreover, Klapacz *et al*. (2009) found the alkylation resistant phenotype of *EXO1* null mice to be variable and tissue specific, unlike *MSH6* null mice which exhibited a fully resistant phenotype. Thus while the available data establishes a firm and important role for Exo1 in MMR function, the picture is clearly more complicated than for canonical proteins such as MSH2 and MLH1. An explanation consistent with the results reported in this study would be that Exo1 is not important in determining MNNG sensitivity in the gastrointestinal origins of the cell lines used here. Our data is also in agreement with that published by Cejka & Jiricny (2008) who conducted a screen of 4644 *Saccharomyces cerevisiae* mutants for those that decreased sensitivity to MNNG. The authors found mutations in MutSα and MutLα components primarily determined MNNG sensitivity but did not identify a similar role for Exo1 (Cejka & Jiricny, 2008).

### 4.3.2 Thymine DNA glycosylase function and MNNG sensitivity

Of the six screen hits that were not already established MMR proteins, TDG was considered to be a promising finding, since its depletion resulted in a large reduction in MNNG sensitivity that was comparable to depletion of known MMR genes. This finding

was extremely reproducible across both repeats of the screen and between each of the triplicate measurements contained therein. Adding to our interest in TDG was formulation of a possible model with which to explain the role of TDG in the MMR-dependent response to alkylation damage (section 4.2.2.1). It was therefore surprising to find that despite extensive efforts, all subsequent attempts to validate TDG outside of the primary screen failed. Despite its early promise, the validation data instructs us to conclude that TDG represented a false positive result. Some of the potential explanations for how this may have arisen are discussed below.

A major source of variability in cell-based assays is the condition of the cell lines used, which can be influenced by the time they have been growing, how often they have been passaged, and by the presence of any contaminating organisms or infection. However, the cells for both screen and validation attempts originated from the same batch, were freshly thawed, grown under the same conditions, and were demonstrated to be free from *Mycoplasma* infection. Whilst it is in principle possible that phenotypic differences may have been accrued in the one week period between cell thawing and the start of an experiment, it is highly unlikely since the cell handling in the post-thaw period was standardised to ensure the cells were always subjected to the same culture stresses. Moreover, that both the effect observed in the screen and the lack of effect in validation experiments was so reproducible argues against an idiosyncratic cause.

An interesting trend that was identified from the screen results was that of the seven hits that were not known MMR genes, all were located in wells on the outside of the plate. Of these, six of the seven hits were located in either well position A2, A3, or A4; an area of the plate particularly prone to edge-effects (fig 3.7e). One possible explanation

for the failure of TDG to validate outside of the screen is therefore that of a systematic edge-effect resulting in a false positive result. Indeed, whilst the screen controlled for inter-plate variation by inclusion of triplicate measurements and two independent repeats of the screen, it did not control for intra-plate variation. The explanation of a systematic edge-effect is therefore certainly possible. Another variable that existed between the screening and validation experiments was that of automation, since validation experiments were performed manually. Whilst the performance of liquid handling operations was assessed as part of the method development, any problems that arose thereafter would not have been detected and in principle may have affected the screen data results.

A major drawback of siRNA technology is that it is difficult to definitively attribute a phenotype to depletion of a specific protein. Even well designed and optimised siRNA experiments that utilise the latest siRNA design features to improve specificity are subject to off-target effects (Birmingham *et al*., 2007; Vankoningsloo *et al*., 2008). Interestingly, Vankoningsloo *et al*. (2008) has shown that experimental variables such as the duration of siRNA transfection and post-transfection incubation time can result in different patterns of off-target expression. If the resistant phenotype mediated by siTDG in the screen was driven by off-target effects, this could, in principle, provide an explanation for the failure to validate TDG in subsequent experiments. It is inevitable that small differences in timing and other variables will result between a large-scale automated screen and a small-scale manual validation experiment, despite the best attempts to minmise them. The data published by Vankoningsloo *et al*. (2008) illustrates the possibility that such differences may have altered gene expression patterns, perhaps

sufficiently to loose the resistant phenotype observed during the screen. Equally, if the quality and timecourse of TDG depletion by siRNA were sensitive to small changes in experimental parameters between the screen and validation experiments, it is possible that TDG represents a true hit that failed to validate due to technical difficulties of siRNA. Without resort to a strictly isogenic knockout model, it is not possible to definitively determine between these two possibilities. However, the finding that TDG depletion increased 53bp1 foci formation above control levels 24 hours post-MNNG treatment, demonstrates that TDG was depleted sufficiently to produce a phenotype in validation experiments. This data therefore supports the notion that TDG failed to validate because it represents a false positive result that arose from systematic error during the primary screen.

It was interesting to note that MLH1-depleted cells had comparable numbers of 53bp1 foci to vehicle-treated MLH1-expressing cells 24 hours post-MNNG, and which were lower than the number of 53bp1 foci seen in TDG-depleted cells. This data supports a notion whereby TDG plays a protective role against MNNG-induced DSBs, perhaps through its role as a component of BER (Liu *et al*., 1999).

### 4.3.3 Future work

#### 4.3.3.1 Validation of remaining hits

Z scores represent a useful tool that is widely used within high-throughput screening literature to order large datasets according to the number of standard deviations the data-point varies from the population mean (Zhang *et al*., 1999; Malo *et al*., 2006). Significant data-points are most often considered to be those that are placed at least two

standard deviations from the population mean, which corresponds to the 95% level in a normally distributed population. Such cut-offs are often viewed in a simplistic binary manner, whereby two data-points that straddle the cut-off and that are not significantly different from each other being classified as differentially significant. Whilst cut-offs are useful in bringing the most likely hits of interest into focus, it is important to remember here that gene depletion efficacy will vary across the library, and thus a borderline hit where only 50% gene depletion efficacy was achieved may become highly significant if the transfection is optimised for that gene. Rather than applying strict mathematical rigor to the classification of hits, it therefore makes sense to also consider those borderline data-points in light of the literature and to judge whether there is a rationale for checking whether an incomplete depletion is generating a partial phenotype. Future work might therefore consider both the remaining hits that were not further investigated in this study and the borderline hits, and seek to validate those with promise.

For those hits whereby the phenotype observed in the screen can be reproduced in deconvolution validation experiments, it will be important to include a non-siRNA based method in order to demonstrate the phenotype is specifically linked to the absence of that gene product. A strict isogenic model, whereby a cell line deficient in the target gene is transfected with a vector that expresses that gene under the influence of a tetracycline-responsive element, represents an excellent system in which to conduct such experiments (Nishijima *et al*., 2009).

#### 4.3.3.2 Methodological improvements

In light of the finding in this study that apparently false positive results arose from systematic plate effects, future screening studies are recommended to implement a number of methodological improvements. One approach taken by others to combat the issue of edge-effects is to exclude the outer wells of each plate from the experiment (Turner *et al*., 2008). Whilst this can have an unacceptable impact on throughput in larger screens, this strategy would be realistic for functional studies that screen targeted libraries of up to ~500 siRNA. Where throughput remains an issue, miniaturisation of the assay to 384 well plates might provide the opportunity to exclude outer wells whilst maintaining capacity. Little additional benefit is gained from excluding more than the outermost wells (Wiles *et al*., 2008), and thus applying this strategy to 384 well plates leaves ~80% of wells available for screening, compared with only ~63% of a 96-well plate. The authors also found that plates located on the top of a stack were most prone to edge-effects, which could be avoided by addition of a plate containing only water in these positions (Wiles *et al*., 2008).

An alternative approach to reducing edge-effects is to decrease the impact that they have on the quality of screening data, and could be achieved by varying the location of siRNA on each replicate plate and screen repeat. Modulation of the plate layout in such a manner could act to dilute out the proliferative effect that occurs in the outside wells and result in a replicate mean that more closely reflects the true mean. Modern automated equipment makes this a realistic option, although extensive testing would be required to ensure the system operates as programmed and avoid introduction of error. However, it would be important to consider an appropriate logarithm to ensure bias is not introduced

by disproportionally exposing a particular siRNA to edge-effects. This strategy could be extended to monitoring the incubation location of each plate to ensure replicates are not clustered, whereby local environmental factors could influence them all to the same extent.

A final strategy that could be used to reduce the impact of edge-effects is to employ mathematical correction. The B-score is a statistical tool that performs a two-way median polish to identify systematic row and column effects within the dataset, and then divides the resulting residuals by the median absolute deviation of each condition to generate a normalised B score (Brideau *et al*., 2003; Malo *et al*., 2006). Mathematical corrections such as these are effective in removing systematic error, but should be used with caution, since the occurrence of multiple hits in the same row or column will be interpreted as a systematic error. The B score should therefore not be used with small targeted libraries where a high hit rate is expected, or where siRNA or small molecules are not randomly distributed across the library plates, but grouped by function or structure.

It is recommended that future screens exclude the outer wells from the assay if possible, use water-filled plates on top of each stack, and vary the plate layouts between replicates and/or repeats. In addition to the measures used in this study, including the use of low evaporation lids and allowing freshly seeded cells to cool to ambient temperature before incubation (Lundholt *et al*., 2003), these recommendations should minimise the occurrence of systematic errors leading to false positive results.

#### 4.3.3.3 Future directions

The use of custom siRNA libraries targeted at genes involved in specific cellular processes represents a means to conduct rapid and cost-effective screens with a higher likelihood of generating hits that can be more easily interpreted than a hit gene involved in a disparate process for which there is no obvious link. Subsequent to our screen of a custom library targeting genes known to be involved in DNA metabolism and cell-cycle progression, it would interesting to screen a library for genes that are involved in post-translational regulation of MMR. This might include libraries of siRNA that target known kinase and phosphatase proteins, for example. Whilst much work has focused on the actual mechanisms of DNA repair processes, less attention has been placed on regulation of DNA repair activities, and how the activities of different repair pathways might be fine tuned to orchestrate cellular responses to diverse insults. In combination with synthetic lethal data, a deeper understanding of the regulatory interactions that occur between DNA repair pathways would allow us to build models to help understand how tumours evolve, and how they respond to and form resistance to different therapeutic drugs.

Whilst this study has focused on screening for genes that are involved in the DNA damage response functions of MMR, additional screens that examine the repair function would be of equal value. Whilst the minimal set of components required for MMR has been identified in a reconstituted biochemical setting (Constantin *et al*., 2005), this might not necessarily reflect the true picture *in vivo*. That Exo1 is sufficient for full bi-directional repair of mismatch substrates in biochemical studies is inconsistent with the findings of Wei *et al*. (2003), that report *EXO1* null mice only a weak phenotype

compared with mice deficient in other more established MMR proteins. In 2004, Lei *et al*. published a novel method that permits the measurement of MMR activity in live cells, which in combination with siRNA technology could be used to screen directly for genes required for MMR activity *in vivo*. Briefly, the authors have described a vector that encodes green fluorescent protein (GFP) wherein the start codon is disrupted by a G:T mismatch. Upon transfection into live cells, successful repair of the mismatch restores a functional start codon and is detected by increased expression of GFP, which can be measured by flow cytometry. Thus, a screen that is based on this assay could first simply deplete genes of interest and then assess their impact on repair of the mismatch, as assessed by high-throughput flow cytometry. Other researchers have reported methods that make the large scale production of mismatched substrates possible, hence making the assay described by Lei *et al*. (2004) suitable for high-throughput studies (Wang & Hays, 2000).

The methods described here and elsewhere mean it is now possible to build a complete picture of the MMR pathway in terms of both its repair and DNA damage response functions. One can envisage a Venn diagram whereby sets of genes are specifically required for either the repair or DNA damage response, in addition to core genes that are critical to both of these functions. Repair functions might be further sub-divided into genes that function to repair particular types of lesions, and DNA response functions into those genes that mediate the response to particular types of DNA damaging agents. Such information would help us understand the role that MMR plays in carcinogenesis and progression, how it shapes the response to anti-cancer treatments, and how it may be best exploited in the development of novel cancer therapies.

# CHAPTER FIVE

*Results*

## 5.1 INTRODUCTION

### 5.1.1 Cytotoxic anti-cancer treatments and their limitations

The focus of anti-cancer pharmaceutical development has undergone a large shift away from grossly cytotoxic agents that target rapidly dividing cells, toward rationally designed and highly specific monotherapies that exploit defects existing only within the tumour (Kaelin, 2005). Classical cytotoxic treatments possess low therapeutic indices because they often act through induction of replication-dependent cytotoxic damage, thus targeting all proliferative tissues (Remvikos *et al*., 1989). Despite this limitation, cytotoxic chemotherapy represented a large step forward that has been the mainstay of cancer therapy for the past 50-60 years. Using breast cancer as an example, metastatic breast cancer was found during the 1950s and 1960s to be sensitive to a range of cytotoxic agents, including alkylating agents, antimetabolities, anti-tumour antibiotics, and vinca alkaloids (Hortobagyi, 2000). Development of combination regimens of cytotoxic chemotherapies during the late 1960s and 1970s demonstrated yet greater anti-tumour efficacies, and have been under constant refinement ever since. Despite these successes, toxicity continues to limit the potential of cytotoxic drugs, so much so that the majority of chemotherapeutic agents are administered at their maximally tolerated dose (Hortobagyi, 2000). Common dose-limiting side-effects of chemotherapy include (depending on the agent used), nausea and vomiting, diarrhoea or constipation, anaemia, malnutrition, memory loss, immunosuppression, haemorrhage, cardiotoxicity, hepatotoxicity, nephrotoxicity, ototoxicity, post-chemotherapy cognitive impairment, and death.

The severity of chemotherapy-associated side-effects largely influences the acceptance and completion of a chemotherapy regimen, and on the willingness of the patient to undergo subsequent treatments (Lindley *et al*., 1998; Schnell, 2003). Interventions that minimise adverse effects are therefore of central importance, both in terms of quality of life and in ensuring tumours are optimally treated to achieve the best clinical outcome. Progress has been made in some areas, such as with chemotherapy-associated nausea and vomiting, which affects 60% and 50% of patients, respectively (Zachariae *et al*., 2007), and has been reported to be the most distressing side-effect of chemotherapy (Coates *et al*., 1983). Antiemetic medications such as 5-hydroxytryptamine 3 receptor (5-HT3) antagonists combined with corticosteroids such as dexamethasone reduces emesis in 65-80% of patients (Walton, 2000). More recent 5-HT3 antagonists such as palonosetron can further reduce the number of acute and chronic episodes of chemotherapy-associated nausea and vomiting (Clark *et al*., 2009). Research is ongoing to develop more efficacious strategies with which to manage the adverse effects of cytotoxic anti-cancer chemotherapy (Sharma *et al*., 2005).

### 5.1.2 Small molecule inhibitors & exploitation of synthetic lethal interactions

As our understanding of the underlying biology of cancer has improved, numerous cellular components have been identified that are crucial for tumour progression and survival. This has lead to exciting breakthroughs in developing novel therapeutic approaches that are highly specific with substantially reduced toxicity. A large step forward in breast cancer treatment came with the finding that aberrant signaling through the human epidermal growth factor receptor 2 (HER2) is associated

with risk of relapse and poor survival (Slamon *et al*., 1987; Harris *et al*., 1989; Pierce *et al*., 1991). Subsequent clinical trials found monoclonal antibodies that block HER-2 activation could induce complete or partial remission in a subset of patients that had already undergone extensive chemotherapy regimens (Baselga *et al*., 1996; Cobleigh *et al*., 1999). Such studies were instrumental in demonstrating the cancers possess Achilles' heals that can be specifically targeted to bring about tumour destruction without the severe toxicity associated with traditional anti-cancer chemotherapy. The potential of this concept was dramatically demonstrated by the finding that breast tumours with loss of function *BRCA2* mutations are exquisitely sensitive to small molecule inhibitors of PARP (Bryant *et al*., 2005; Farmer *et al*., 2005; Gottipati *et al*., 2010). These exciting early findings have lead to the maturation of synthetic lethality, synthetic sickness, and contextual synthetic lethality as vital tools with which to specifically target tumours with minimal toxicity (Kaelin, 2005). Those genes implicated in DNA repair have been cited as particularly useful synthetic lethal targets (Helleday *et al*., 2008), and an impressive number of potential therapeutic targets have been identified to date. A brief survey of the recent literature reveals silencing of PTEN-induced putative kinase 1 (PINK1) is synthetic lethal with MSH2, MSH6, or MLH1 deficiency (Martin *et al*., 2011), Polβ and Polγ are synthetic lethal with MSH2 or MLH1, respectively (Martin *et al*., 2010), Rad52 is synthetic lethal with BRCA2 (Feng *et al*., 2011), and ATR, WT1, or Cdk4 are synthetic lethal with oncogenic Ras (Gilad *et al*., 2010; Licciulli & Kissil, 2010; Puyol *et al*., 2010). Our list of potential therapeutic targets has thus undergone an unprecedented expansion since the identification of the BRCA2-PARP1 synthetic lethality (Bryant *et al.,*

2005; Farmer *et al*., 2005). A likely future bottleneck will therefore not be identification of suitable targets, but the availability of small molecule inhibitors of those targets.

### 5.1.3 Antioxidants and chemoprevention of cancer

Tumours are thought to form through an evolutionary process of random mutation accelerated by genetic instability to generate a heterogenous population of mutant clones, from which natural selection can favour those with the highest propensity to escape cellular control mechanisms to grow and survive in that particular micro-environmental niche (Merlo *et al*., 2006). Viewed at this level, administration of an anti-cancer therapy creates an artificial selection pressure for clones that possess inherent resistance to that therapy, and that can subsequently repopulate the tumour to cause a relapse at a later date. Tumours seem equally capable of utilising this mechanism to generate resistance to both crude cytotoxic DNA damaging agents and highly specific targeted therapies. For instance, resistance to the non-specific DNA damaging agents 5FU and methotrexate can arise from amplification of the thymidine synthase (Wang *et al*., 2004) and dihydrofolate reductase/*MSH3* genes (Drummond *et al*., 1997), respectively. Point mutation in the breakpoint cluster region-Abl (*BCR-ABL*) gene similarly confers resistance to imatinib, a rationally designed and highly specific drug used to treat chronic myeloid leukaemia (Gorre *et al*., 2001). Cancer treatments are therefore expected to be most effective when the tumour is detected early, when the genetic heterogeneity of the tumour is relatively low (Merlo *et al*., 2006). Similarly, combinations of drugs that target a single protein through different mechanisms or that target diverse processes decreases the likelihood

that the tumour will possess a clone that is resistant to all the drugs in that combination (Daub *et al*., 2004).

It is because of the inherent difficulties with treating cancer that increasing emphasis has been placed on pharmacological prevention of carcinogenesis. MNNG is a common dietary carcinogen that is sufficient to initiate and promote carcinogenesis in a number of animal models in an oxidative stress-dependent manner (Ketkar *et al*., 1978; O'Connell *et al*., 1987). It was first demonstrated in 1985 that reaction of MNNG and $H_2O_2$ leads to the production of the hydroxyl free radical (OH•), as assessed by electron spin resonance and the OH• spin trapping agent 5,5-dimethyl-1-pyrroline-1-oxide (Mikuni *et al*., 1985). The authors noted that OH• production only occurred in the presence of light. More recently, the same authors put forward a reaction scheme whereby the nitric oxide group of MNNG undergoes nucleophilic attack by $H_2O_2$ to form 1-methyl-3-nitroguanidine and peroxynitric acid (ONOOH). The subsequent splitting of ONOOH produces OH• and nitrogen dioxide (Mikuni & Tatsuta, 2002). MNNG has also been shown to yield OH• in an $H_2O_2$- and $O_2^{-\bullet}$- independent but light-dependent manner (Mikuni & Tatsuta, 1994). Thus MNNG can produce free radicals in principle, although it should be noted that the concentrations of MNNG and $H_2O_2$ used in those studies are much higher than would be expected in a physiological setting. However, a plethora of studies have demonstrated that antioxidants can protect against the mutagenesis and carcinogenesis of MNNG, and thus supports the notion that the biological activities of MNNG depend on the formation of free radicals. For instance, researchers have used various biological assays to demonstrate ascorbate can decrease the mutagenicity of MNNG (Vojteková & Miertus, 1986; Jain *et al*., 1989; Foltínová *et al*., 1994), whilst others have used comet assays to

show ascorbate decreases MNNG-induced DNA damage (Galloway & Painter, 1979; Biasiak *et al*., 2002). Equally, ascorbate (Jain *et al*., 1989) and a wide range of other molecules with antioxidant properties including (-)-epigallocatechin gallate (Yamane *et al*., 1995), polyphenon-B (Murugan *et al*., 2007), ginkgo biloba extract (Jiang *et al*., 2009), s-allylcysteine and lycopene (Velmurugan & Nagini, 2005), neem leaf extracts (Subapriya & Nagini, 2003), selenomethionine (Mukherjee *et al*., 2001), naringenin (Ekambaram *et al*., 2008), azadirachta indica and ocimum sanctum (Manikandan *et al*., 2008) can decrease the MNNG-induced gastric carcinogenesis in rats.

### 5.1.4 Aims

The primary aim of this chapter was to conduct a high-throughput screen of small molecule libraries in order to identify those chemical structures that increase the tolerance or resistance of cells following treatment with MNNG. Such compounds might be expected to act via one of a number of mechanisms, such as through inhibition of MMR or through increasing cellular antioxidant defences. Studies that identify novel inhibitors of cellular targets, particularly those implicated in DNA repair processes such as MMR, will be required in order to permit rapid progression from the identification of a synthetic lethal interaction to preclinical trials, and as a research tool with which to identify novel therapeutic targets. The PARP inhibitor, 4-amino-1,8-napthalimide (ANI) is a classic example of this, since it was discovered and characterised in 1999, only to be instrumental 6 years later in identification of the BRCA2-PARP1 interaction (Schlicker *et al*., 1999; Bryant *et al*., 2005). Moreover, the selective application of MMR inhibitors may also be of interest in terms of chemoprotection of non-cancerous tissues against

toxicity induced by cytotoxic chemotherapies that are dependent on function MMR. Finally, molecules with novel antioxidant activities may possess clinical activity in terms of the chemoprevention of cancer.

## 5.2 RESULTS

### 5.2.1 Screen results

The NCI Diversity 1 and Diversity 2 small molecule libraries comprised a total of 3354 compounds, and were screened in duplicate for those structures that increased the tolerance of resistance of MMR-proficient cells to MNNG. The resulting data was normalised on a per-plate basis against the untreated control, and expressed as a histogram to examine its distribution (fig 5.1a). The data was found not to be normally distributed, and comprised two or more overlapping distributions. Whilst it is equally valid to use Z-score analysis to rank data that is not normally distributed, it is important to note that the percentage of data within a particular number of standard deviations from the mean will differ from a normal distribution.

In order to assess data quality, the performance of the internal controls on each plate was checked to ensure that the assay had operated within the expected parameters. We first analysed the number of population standard deviations that separated the untreated HCT116+Ch3 DMSO control and the MNNG-treated HCT116+Ch3 DMSO negative control to determine whether the toxic response to MNNG was intact. Secondly, we analysed the number of population standard deviations that separated the MNNG-treated HCT116+Ch3 DMSO negative control and the MNNG-treated HCT116 DMSO positive control, so as to ensure that the resistant response seen in MMR-deficient

cells was intact. The data relating to these analyses are displayed in table 5.1. A threshold of at least two population standard deviations from the mean was required for inclusion in subsequent analysis, which corresponds in this distribution to a 2% chance that the data point occurred by chance. On this basis, 16 plates were excluded from the study due to inadequate performance of the screening assay. Correlation between replicate plates was next assessed in order to assess the reproducibility of the screening data (table 5.1). An $R^2$ threshold of 0.5 was assigned as being the minimum level of correlation required to be included in the study, and on this basis a further 3 plates were excluded from subsequent analysis.

In general, the correlation between replicates was found to be excellent, with an overall $R^2$ value of 0.76 (fig 5.1b), although there was significant variation in assay performance across the screen (table 5.1). Following application of inclusion criteria to the data, a total of 19 plates were excluded from subsequent analysis, which corresponded to the exclusion of 1568 compounds (46.8%). Whilst it was not ideal to exclude this proportion of compounds, the strategy ensures that the data relating to the remaining 1786 compounds is of high quality, thereby reducing the number of false positives and helping to focus the available resources on the hits most likely to reflect the true positives.

**Table 5.1.** Performance of small molecule screen controls and correlation between replicates. Data relating to the screen of NCI Diversity Set I (NDS1) and 2 (NDS2) libraries, showing the correlation between replicates ($R^2$) and the number of population standard deviations that separate the untreated (HCT116+Ch3 DMSO control), negative

(HCT116+Ch3 MNNG control), and positive (HCT116 DMSO control) controls. Figures highlighted in red do not meet the inclusion criteria stipulated in this study, that each plate should have an $R^2$ of at least 0.5, with a separation between controls of at least two population standard deviations.

| **Library** | **Plate** | **$R^2$** | **Untreated – Negative control (Z)** | **Positive – Negative control (Z)** |
|---|---|---|---|---|
| NDS1 | 4231 | 0.18 | 16.08 | 17.85 |
| NDS1 | 4232 | 0.52 | 15.85 | 13.62 |
| NDS1 | 4233 | 0.66 | 10.72 | 8.33 |
| NDS1 | 4234 | 0.61 | 9.13 | 9.30 |
| NDS1 | 4235 | 0.48 | 12.93 | 8.86 |
| NDS1 | 4236 | 0.42 | 9.36 | 8.75 |
| NDS1 | 4237 | 0.74 | 5.81 | 4.16 |
| NDS1 | 4238 | 0.77 | 5.93 | 4.45 |
| NDS1 | 4239 | 0.81 | 5.84 | 4.92 |
| NDS1 | 4240 | 0.76 | 3.29 | 1.77 |
| NDS1 | 4241 | 0.82 | 2.81 | 2.20 |
| NDS1 | 4242 | 0.86 | 3.17 | 2.32 |
| NDS1 | 4243 | 0.91 | 3.33 | 2.56 |
| NDS1 | 4244 | 0.86 | 2.69 | 2.06 |
| NDS1 | 4245 | 0.93 | 3.00 | 2.32 |
| NDS1 | 4246 | 0.86 | 2.96 | 1.80 |
| NDS1 | 4247 | 0.89 | 3.05 | 1.33 |
| NDS2 | 4531 | - | 14.07 | 4.15 |
| NDS2 | 4532 | - | 5.72 | 1.10 |

| | | | | |
|---|---|---|---|---|
| NDS2 | 4533 | - | 5.94 | 1.63 |
| NDS2 | 4534 | 0.46 | 5.81 | 1.66 |
| NDS2 | 4535 | 0.32 | 4.03 | 0.64 |
| NDS2 | 4536 | 0.60 | 4.07 | 2.00 |
| NDS2 | 4537 | 0.89 | 5.29 | 1.71 |
| NDS2 | 4538 | 0.87 | 4.50 | 1.82 |
| NDS2 | 4539 | 0.93 | 3.56 | 1.10 |
| NDS2 | 4540 | 0.89 | 4.81 | 2.04 |
| NDS2 | 4541 | 0.93 | 2.69 | 1.63 |
| NDS2 | 4542 | 0.88 | 2.36 | 1.13 |
| NDS2 | 4543 | 0.82 | 3.58 | 1.28 |
| NDS2 | 4544 | 0.93 | 3.11 | 1.84 |
| NDS2 | 4545 | 0.80 | 3.41 | 2.02 |
| NDS2 | 4546 | 0.86 | 5.06 | 1.00 |
| NDS2 | 4547 | 0.83 | 4.38 | 0.42 |
| NDS2 | 4548 | 0.69 | 4.73 | 2.10 |

The remaining data was ranked by Z score so that those compounds that increased cellular viability of MNNG-treated HCT116+Ch3 by the most population standard deviations were ranked highest (fig 5.1c). Using a hit threshold of two population standard deviations, three compounds were identified, corresponding to a hit rate of 0.19%. These hit compounds were NSC197049, NSC52343, and NSC173723, and increased cellular viability by 3.60±0.32, 3.14±0.34, and 3.06±0.05 population standard deviations, respectively. In order to verify these results, the three hit compounds were included in a repeat of the screening assay (fig 5.1d). Consistent with the primary screen data, NSC197049 increased the cellular viability of MNNG-treated HCT116+Ch3 from

41±0.05% to 58±0.05% of the untreated control, whereas NSC52343 (42±0.02%) and NSC173723 (41±3%) did not affect the HCT116+Ch3 viability. NSC197049 did not increase the viability of MNNG-treated HCT116+Ch3 cells to the same extent as similarly treated HCT116 cells (0.73±0.03), but certainly appeared to confer some level of chemoprotection. NSC197049 was therefore selected for further validation and investigation.

### 5.2.2 NSC197049 validation

An important step in the validation of small molecules is to conduct a dose-response experiment to demonstrate a causal relationship between the concentration and the phenotype observed in the primary screen. HCT116 and HCT116+Ch3 were co-treated for 24 hours with 7.5 μM MNNG together with increasing concentrations of either DMSO vehicle or NSC197049 (fig 5.2a). Whilst vehicle alone did not alter the differential viability of either cell line to MNNG, a clear dose-dependent relationship between NSC197049 concentration and HCT116+Ch3 viability was observed. Treatment with 10-20 μM NSC197049 significantly increased the viability of HCT116+Ch3 cells compared with vehicle-treated controls ($p < 0.001$), while concentrations above 15 μM increased viability to levels that exceeded MMR-deficient HCT116 ($p < 0.001$). In order to ensure that the aliquots present within our library was actually NSC197049, a new aliqouot of the original stock (note not a resynthesis) was obtained from the NCI and the experiment repeated (fig 5.2b). A similar pattern of activity was observed as with the original stocks, with NSC197049 treatment protecting against MNNG-toxicity in a dose-dependent manner ($p < 0.001$). Interestingly,

NSC197049 was found to increase the viability of MNNG-treated cells irrespective of MMR status, which suggests the molecule does not act via a mechanism that involves inhibition of MMR. That the potency of new NSC197049 stocks was greater than original stock suggests the library stocks may have been subject degradation during their storage and use.

We next investigated whether the chemoprotective activity of NSC197049 is an effect specific to the HCT lineage or a more general activity. A similar dose-response experiment was therefore conducted as before, but using a different pair of semi-isogenic cell lines. HEC59 is a human endometrial tumour cell line that exhibits a MMR-deficient phenotype attributable to bi-allelic mutations in *MSH2* and *MSH6* (Umar *et al*., 1997). In contrast, the HEC59+Ch2 cell line expresses a MMR-proficient phenotype that results from expression of wild-type MSH2 and MSH6 from the introduction of an additional copy of chromosome 2. Correspondingly, the HEC59 cell line was significantly more resistant than the HEC59+Ch2 cell line to increasing doses of MNNG ($p < 0.001$) (fig 5.2c). HEC59/Ch2 cells required higher doses of MNNG to produce the equivalent differential viability seen in HCT116/Ch3 cells; a phenomenon that is likely attributable to their five-fold higher level of MGMT expression (Adamson *et al*., 2005). HEC59 and HEC59+Ch2 cells were thus co-treated with 20 μM MNNG and increasing concentrations of NSC197049 (fig 5.2d). Consistent with the HCT116/Ch3 data, NSC197049 protected HEC59+Ch2 cells from MNNG-induced toxicity in a dose-dependent manner ($p < 0.001$). This activity was apparently independent of MMR status since NSC197049 also increased the viability of MNNG-treated MMR-proficient HEC59+Ch2 cells to levels exceeding similarly treated and MMR-deficient HEC59 cells

($p < 0.001$). The compound also increased MNNG-treated HEC59 viability to levels comparable with the untreated control.

The clonogenic survival assay is considered by the research community to be the 'gold standard' assay of choice when determining the toxicity of a given treatment (Plumb, 2004). We therefore sought to reproduce the differential outcome expected of HCT116 and HCT116+Ch3 following MNNG exposure, and to examine whether the chemoprotective activity of NSC197049 increases clonogenicity following such treatments (fig 5.2e). In agreement with the viability data, we observed NSC197049 to produce a dose-dependent increase in HCT116+Ch3 clonogenicity after treatment with 1.25 μM and 2.5 μM MNNG ($p < 0.001$).

Taken together, these data demonstrate NSC197049 to be an efficient and cell line-independent chemoprotectant molecule that protects against the reduction in cellular viability and clonogenicity normally associated with MNNG-treatment. The observed increase in viability of MNNG-treated MMR-deficient cell lines also suggests the protective activity of NSC197049 may act independently of MMR status.

### 5.2.3 NSC197049 Characterisation

NSC197049 is a dithioethione compound with the chemical structure shown in figure 5.3a. In order to further characterise the effect of the molecule in the absence of other treatments, we first exposed HCT116+Ch3 cells to increasing doses of NSC197049 or DMSO vehicle for 24 hours, and after permitting 120 hours of drug-free growth, measured its effect on cellular viability (fig 5.3b). NSC197049 was found to produce

neither a toxic nor proliferative response when compared to the DMSO vehicle-treated control.

The O6MeG-mediated toxicity elicited by MNNG has been demonstrated to be strictly dependent on cell-cycle progression and proliferation (Roos *et al*., 2004). We reasoned that any agent that protects against MNNG-induced toxicity may thus act by inhibiting DNA replication, either directly or through modulation of cell-cycle control. We therefore examined the cell-cycle profiles of HCT116 and HCT116+Ch3 cells that result from 24 hour and 48 hour treatments with 10 μM NSC197049, and compared this against 5μM aphidicolin and DMSO vehicle-treated controls (fig 5.3c). Aphidicolin is a selective inhibitor of Polα that induces a G1/early S phase arrest and was included as a positive control (Ikegami *et al*., 1978; Pedrali-Noy *et al*., 1980). No observable differences in cell-cycle distribution were found between DMSO vehicle-treated or NSC197049 treated populations at either time point. In contrast, aphidicolin treatment resulted in a subG1 population of ~15% at 24 hours that persisted through to 48 hours, and was accompanied by a time-dependent increase in the population of S phase cells, indicative of the S phase arrest described above. NSC197049 therefore appears not to indirectly protect cells from MNNG by disrupting DNA replication, since such events might be expected to produce a similar S phase arrest as was seen with aphidicolin. Equally, NSC197049 was not found to prevent entry into S phase by modulating other phases of cell-cycle. This data therefore supports the notion that the mechanism of NSC197049 does not involve modulation of cell-cycle progression.

We next sought to identify the time point at which NSC197049 acts during the assay, since such information may be informative in elucidating its mechanism of action.

A comparison of HCT116 and HCT116+Ch3 cells treated with 10 μM NSC197049 for 3 hours either prior (pre-treatment), during (co-treatment), or after (post-treatment) MNNG treatment was therefore conducted (fig 5.3d). NSC197049 did not exert any chemoprotective activity when pre-treated or post-treated, but provided complete protection against MNNG-induced toxicity only when it was co-treated together with the MNNG.

We also examined the G2/M arrest that occurs following MNNG alone or in combination with a protective dose of NSC197049. As expected, an MMR-dependent G2/M arrest following MNNG treatment was observed at both 24 hour and 48 hour time points (fig 5.3e). Similarly, there was a large and sustained induction of subG1 cells that was dependent on functional MMR. Interestingly, co-treatment of MNNG and NSC197049 did not abrogate the G2/M arrest response, which appeared completely intact at 24 hours and only marginally decreased at 48 hours. NSC197049 did, however, completely abolish the large induction of subG1 cells at 24 hours post MNNG treatment, and largely reduced it at 48 hours. This is consistent with the data showing NSC197049 treated cells have increased viability and clonogenicity following MNNG treatment. It thus appears that NSC197049 might uncouple the G2/M arrest from apoptosis following MNNG treatment.

A key question that arose from the above findings was whether NSC197049 protects against or permits tolerance to the lethal DNA DSBs that arise from MNNG treatment. We therefore sought to examine the effect of NSC197049 on 53bp1 foci formation following a 24 hour 7.5 μM MNNG treatment (fig 5.3f). HCT116+Ch3 formed a significantly higher number of 12.15 ± 0.07 53bp1 foci per cell when compared

with 3.67 ± 0.53 foci per cell seen in HCT116 ($p < 0.001$). 10 μM and 20 μM doses of NSC197049 reduced 53bp1 foci induction in HCT116+Ch3 to 4.22 ± 0.05 and 2.99 ± 0.20, respectively, and in HCT116 from 3.67 ± 0.53 to 2.45 ± 0.29 and 1.63 ± 0.29, respectively ($p < 0.001$). Importantly, all NSC197049 treatments decreased 53bp1 foci significantly more than their corresponding vehicle controls ($p < 0.001$). NSC197049 therefore appears to protect cells from MNNG-induced toxicity by preventing the formation of damage-induced DSBs, as measured by 53bp1 foci formation, and to do so independently of MMR status.

Given the above findings, we were interested to find if NSC197049 is also able to protect HCT116 cells from the effects of MNNG treatment (fig 5.3g). As expected, HCT116 cells had a significantly higher clonogenic survival than HCT116+Ch3 at both 1.25 μM and 2.5 μM MNNG ($p < 0.001$). Co-treatment with 2.5-10 μM NSC197049 increased HCT116 clonogenicity in a dose-dependent manner ($p < 0.001$). In summary, NSC197049 has been found to protect against MNNG toxicity independently of MMR status, and may do so by disrupting the process that leads to MNNG-induced DSB formation.

### 5.2.4 Oltipraz

A search of the literature for chemical analogues of NSC197049 revealed that 3*H*-1,2-dithiole-3-thiones are a class of compounds with ascribed chemoprotective action. In particular, a compound named 'Oltipraz' (5-(2-pyrazinyl)-4-methyl-1,2-dithiol-3-thione), whose structure is shown in figure 5.4a, has been extensively studied and demonstrated to have protected against carcinogenesis resulting from carcinogen exposure in a number of

animal models (reviewed by Zhang & Munday, 2008). Oltipraz's mechanism of action has largely been ascribed to its role as an NF-E2-related factor 2 (Nrf2) activator and subsequent activation of detoxification genes including those controlled by antioxidant response elements.

We first sought to reproduce with Oltipraz the chemoprotection conferred by NSC197049 against MNNG. MNNG-treated HCT116 and HCT116+Ch3 cells were exposed to increasing doses of Oltipraz, and the outcome monitored via measurement of cellular viability (fig 5.4b upper panel). Surprisingly, Oltipraz failed to confer any protection against MNNG-induced toxicity, even at concentrations of 50 μM, which approaches the compound's solubility limit. This contrasts with NSC197049, which is able to completely abolish MNNG-toxicity under similar treatment conditions (fig 5.2b). Since Oltipraz is known to act by modulation of gene expression, we reasoned that a pre-treatment period might be necessary for Oltipraz to be effective. We therefore performed a 24 hour pre-treatment with increasing Oltipraz concentrations before co-treating with Oltipraz and MNNG for a following 24 hours (fig 5.4b lower panel). Despite these efforts we failed to observe Oltipraz-mediated protection against MNNG-induced toxicity.

### 5.2.5 Antioxidants phenocopy the chemoprotective activity of NSC197049

Although it was unexpected for Oltipraz to be ineffective in our system, the compound has been very successfully demonstrated to protect against MNNG-induced glandular stomach carcinogenesis in a rat model (Nishikawa *et al*., 1998). Moreover, it has been known for some time that antioxidants can also protect against MNNG-induced

stomach carcinogenesis in rats (Balansky *et al*., 1986). We were therefore interested in the possibility that NSC197049 might also act to protect against MNNG by inducing, either directly or indirectly, some form of antioxidant activity. In order to assess this possibility, we tested whether antioxidants could phenocopy NSC197049 and protect against MNNG toxicity in our system. MNNG- and vehicle-treated HCT116/Ch3 (fig 5.4c) or HEC59/Ch2 (fig 5.4d) cells were exposed to increasing concentrations of an antioxidant mix containing ascorbic acid and glutathione, and viability measured as the end-point. For both pairs of cell lines, we observed the expected differential survival between MMR-proficient and –deficient cell lines following MNNG treatment and a dose-dependent protection by the antioxidant mixture of all MNNG-treated cell lines ($p < 0.001$). At the highest antioxidant concentrations of 2.5 mM, HCT116+Ch3 and HEC59+Ch2 viability was restored to levels reaching that of the untreated controls. Although antioxidants could also protect HCT116 and HEC59 to a reasonable extent, it is not clear from the data whether they can completely abolish MNNG-induced toxicity.

Since O6MeG is the primary toxic lesion generated by MNNG, we were interested in testing whether NSC197049 could specifically protect against this lesion, and whether antioxidants could phenocopy the effect. O6BG was therefore used for its ability to inhibit the O6MeG-repair enzyme, MGMT, and examine whether this is the case. An experiment was conducted whereby differential killing was elicited in HCT116 and HCT116+Ch3 cells by treatment with 7.5 μM MNNG, and increasing concentrations of either NSC197049 or antioxidant mixture used until MNNG-induced toxicity in HCT116+Ch3 was completely abolished relative to the MMR-deficient control (fig 5.5a). A comparable set of conditions were also included but with the extra addition of 20 μM

O6BG to inhibit MGMT activity. Whilst O6BG addition was found to reduce the chemoprotective activity of NSC197049 or antioxidants ($p < 0.001$), this reduction was incomplete. Moreover, a dose-dependent protection of MNNG/O6BG-treated cells was observed with increasing doses of NSC197049 or antioxidants ($p < 0.001$). Together, these data demonstrate that antioxidants and NSC197049 can protect against O6MeG-associated toxicity, and whilst the level of protection was not complete under the experimental conditions used here, the data suggests that this might be achieved at sufficiently high doses.

## 5.3 DISCUSSION

The aim of this chapter was to screen for novel small molecule structures that increase resistance to MNNG, since compounds with such activity might be expected to represent useful new drugs for the prevention and treatment of cancer. As a result, we can report the identification of NSC197049 as a novel molecule that protects against MNNG-induced DNA damage and cytotoxicity in a dose-dependent and cell line-independent manner, as assessed by 53bp1 foci, cellular viability and clonogenicity. Molecules with such traits may be expected to act via one of a number of mechanisms, such as by increasing antioxidant defence, modulating DNA repair systems such as the MMR pathway, or by inhibiting downstream apoptotic processes. Discussed here is the evidence provided in this study and elsewhere in order to evaluate the likelihood that NSC197049 acts by any such mechanism.

### 5.3.1 Chemoprotection through antioxidant activity

That antioxidants can protect against MNNG is interesting when one considers that NSC197049 belongs to a relatively well defined class of molecules known as dithiolethiones. In 1983, dithiolethiones were shown to be able to protect against hepatotoxicity in mice following administration of paracetemol and carbon tetrachloride (Ansher *et al*., 1983). Not only was mortality reduced, the authors demonstrated dithiolethiones prevented liver glutathione depletion, induced glutathione-S-transferase (GST) activity, and prevented liver damage. Other studies demonstrated the prototypical dithiolethione, Oltipraz, could protect against the formation of carcinogenic DNA adducts induced by aflatoxin B1 in rats (Kensler *et al*., 1985), and protect against carcinogenesis induced by benzo[a]pyrene, diethylnitrosamine, and uracil mustard in mice (Wattenberg & Bueding, 1986). It was recognised at the time that Oltipraz increased glutathione production and had complex effects on the expression of numerous detoxification enzymes (Ansher *et al*., 1986). It is now known that Oltipraz modulates gene expression by activating a major cellular defence pathway that protects against oxidative and xenobiotic stress (Lida *et al*., 2004; Motohashi & Yamamoto, 2004). Nrf2 is a transcriptional activator that is normally bound and negatively regulated by Kelch-like ECH-associated protein 1 (Keap1), which results in ubiquitin-proteosome-mediated degradation of Nrf2 (Itoh *et al*., 1999). Oltipraz-mediated disruption of the negative regulation of Nrf2 by Keap1 is thought to allow translocation of Nrf2 to the nucleus where it activates antioxidant or electrophile responsive elements that increase expression of phase II detoxification and antioxidant genes (Petzer *et al*., 2003). Thus, unlike wild-type mice, *NRF2*-null mutants are not protected against carcinogenesis by Oltipraz

(Ramos-Gomez *et al*., 2001). Oltipraz has been demonstrated to induce expression in rats of some phase I enzymes such as P450 1A2, P450 3A2, and P450 2B2, in addition to phase II enzymes inducing several GST subunits, NAD(P)H:quinone oxidoreductase 1, glutamate cysteine synthetase, epoxide hydrolase and uridine 5'-diphospho-glucuronosyltransferase (Buetler *et al*., 1995).

Consistent with the notion that dithiolthiones are chemoprotectants, we found NSC197049 efficiently protects against the DSBs, and reductions in cellular viability and clonogenicity normally associated with MNNG treatment. We were therefore surprised to find that despite the efficacy of NSC197049, Oltipraz did not provide any level of chemoprotection against MNNG-induced toxicity in our system. Certainly, the HCT lineage should be responsive to Oltipraz, since nitric oxide has been shown to activate Nrf2-mediated oxidative defences in this system (Li, 2009). Moreover, studies examining the structure activity relationship of dithiolthione analogs support the notion that the 1,2-dithiolthione ring represents the chemoprotective pharmacore (Kensler *et al*., 1987). An unsubstituted 1,2-dithiolthione ring compound was found to be the most potent structure with regard to reducing hepatic aflatoxin DNA adducts in rats by over 90%, whilst substitution of the sulphur atom at position 3 with an oxygen atom to produce 1,2-dithiol-3-one resulted in a ~3-fold reduction in activity. That said, the 2-pyrazinyl moiety at position 5 and methyl group at position 4 of Oltipraz was also shown to decrease the activity of the molecule when compared to the unsubstituted pharmacore, with Oltipraz treatment resulting in a less efficient reduction in DNA adducts of ~40%. Indeed, the addition of any bulky moiety to the unsubstituted ring reduced the activity of the molecule. Thus it might be hypothesised that Oltipraz would be expected to be less

potent than NSC197049, which lacks such moieties. Moreover, the ethyl ester moiety at position 4 of NSC197049 might be expected to be metabolised to a free carboxylic acid by intracellular esterases, thus preventing NSC197049 from diffusing out of the cell (Kerns & Di, 2008). The ethyl ester moiety might therefore cause NSC197049 to be sequestered intracellularly, increasing its effective concentration, when compared to Oltipraz which lacks this moiety. However, it remains surprising that no chemoprotection activity was observed by Oltipraz even at concentrations approaching its previously reported solubility limit (Petzer *et al*., 2003). This is especially the case when one considers other studies that show Oltipraz to be capable of protecting against other agents such as $H_2O_2$ at a ten times lower dose (Konwinski *et al*., 2004).

An interesting finding in this study was that NSC197049 protected against MNNG-induced toxicity only if co-treated with the alkylating agent, but not if pre- or post-treated. This binary effect and the small time differences between a pre-treatment, co-treatment, and post-treatment, argue against an Oltipraz-like mechanism of action involving NSC197049-mediated modulation of gene expression. Indeed, other well established direct antioxidants such as ascorbate can protect against DNA damage when treated simultaneously with MNNG, but a delay of 40 minutes before addition of ascorbate prevents any level of protection (Galloway & Painter, 1979). In contrast, a 24 hour Oltipraz pre-treatment was shown to protect against $H_2O_2$-induced toxicity, and this protection did not require Oltipraz to be present during the $H_2O_2$ exposure itself (Konwinski *et al*., 2004). This data supports the notion that Oltipraz acts via an indirect mechanism such as modulation of gene expression, and contrasts with NSC197049 which appears to act more directly. That NSC197049 is effective when co-treated with MNNG

but ineffective when post-treated also suggests that NSC197049 acts to prevent induction of DNA damage rather than by promoting its repair or by affecting the apoptotic response to DNA damage. The data is therefore consistent with a model where NSC197049 acts as a direct antioxidant. An alternative possibility is an indirect activation of existing antioxidant machinery by post-translational modification. Nonetheless, it appears that NSC197049 acts via a mechanism distinct from that of Oltipraz. Interestingly, Oltipraz has been demonstrated to generate superoxide radicals in a concentration and time-dependent manner, and this is considered a potential mechanism by which Oltipraz activates antioxidant response elements (Velayutham *et al*., 2005). It would therefore be useful for future studies to examine this property of Oltipraz and to compare it against NSC197049 in order to ascertain how far their structural similarity reflects their similarity in biological activity.

The focus of future experiments should be to elucidate the mechanism by which NSC197049 protects against MNNG-associated toxicity. It is interesting to note that others have shown a cell-free pre-incubation of MNNG with ascorbate to inactivate MNNG and render it non-mutagenic upon subsequent exposure to cells (Galloway & Painter, 1979). It is known that MNNG undergoes a decomposition process to form a methyl-diazonium cation species that subsequently methylates DNA, and that oxidative species are involved in this process (Galtress *et al*., 1992). It is therefore possible that antioxidants disrupt the normal process of MNNG decomposition and prevents formation of the mutagenic methylating species. Future experiments that address this possibility might apply similar methods to those used by Mikuni *et al*. (1985), and utilise electron spin resonance and the OH• spin trapping agent 5,5-dimethyl-1-pyrroline-1-oxide to

examine whether NSC197049 interferes with MNNG decomposition in a cell-free system. It is also possible to measure oxidative stress in cell-based systems through use of the non-discriminate free radical sensor, dichlorofluorescin diacetate (Wang & Joseph, 1999). Dichlorofluorescin diacetate is thought to enter cells via passive diffusion, and following deacetylation by intracellular esterases becomes trapped within the cell. Subsequent oxidation events form a highly fluorescent dichlorofluorescin derivative that can be detected by a fluorescence microplate reader and used as a marker for oxidative stress. Such methods would therefore allow for the investigation of whether NSC197049 might protect cells directly against MNNG-induced oxidative damage or indirectly by modulation of cellular defenses.

### 5.3.2 Chemoprotection through MMR inhibition

The hypothesis that NSC197049 exerts its chemoprotective activity through inhibition of MMR produces a number of testable predictions. A specific MMR inhibitor would be expected to, 1) protect MMR-proficient but not MMR-deficient cells against MNNG and other MMR-dependent cytotoxic drugs, 2) increase the resistance of MMR-proficient cells to such drugs to levels matching but not exceeding that seen in MMR-deficient cells, 3) abolish the G2/M arrest that occurs following treatment with MNNG or other MMR-dependent drugs, 4) inhibit the repair of base mismatches and IDLs in DNA, 5) and induce a mutator phenotype characterised by MSI.

Our data provides a number of lines of evidence that relate to these predictions and suggest it is unlikely that NSC197049 acts by inhibiting MMR. Importantly, NSC197049 protected the clonogenicity of MNNG-treated cells in dose-dependent

manner independently of MMR status. This was consistent with the finding that NSC197049 also reduced the population of subG1 DNA content HCT116 cells by 3.7-fold 48 hours post-MNNG treatment. Similarly, when one considers the percentage reduction in 53bp1 foci mediated by NSC197049 following MNNG, it becomes apparent that NSC197049 not only reduced HCT116+Ch3 53bp1 foci by ~56%, but also HCT116 53bp1 foci by ~22%. These data therefore demonstrate that NSC197049 does not comply with the first prediction that it should specifically protect MMR-proficient but not deficient cells against MNNG toxicity.

In terms of the second prediction, NSC197049 was observed to increase the cellular viability of MMR-proficient HCT116+Ch3 and HEC59+Ch2 cells to levels that exceeded their MNNG-treated MMR-deficient counterparts. It thus appears as though NSC197049 also violates the second prediction, since specific MMR inhibitors would phenocopy and not exceed the level of tolerance seen of MMR-deficient cells towards MNNG. However, it should be noted that this was not the case with the clonogenicity data, where NSC197049 did not significantly protect MMR-deficient HCT116 against MNNG.

Protective concentrations of NSC197049 also failed to abolish the G2/M arrest in HCT116+Ch3 cells following MNNG, apparently uncoupling DNA damage and apoptotic responses. That the G2/M arrest has been shown to be dependent on functional MMR activity suggests that NSC197049 also violates the third prediction and does not act by inhibiting MMR (Adamson *et al*., 2005).

The uncoupling of DNA damage and apoptotic responses to MNNG has previously been reported in p73α-shRNA depleted cells where an intact G2/M checkpoint response was observed (Wagner *et al*., 2008) despite an increase in clonogenicity and decrease in

apoptosis following MNNG treatment (Shan Li *et al*., 2008). These studies might be used to argue that NSC197049 could represent an inhibitor of p73α. However, although p73α depletion did not disrupt the G2/M checkpoint response, the margin by which it increased clonogenicity and decreased apoptosis was small, and only at doses of MNNG significantly higher than those used in this study. In contrast, Shan Li and colleagues did not find p73α-depletion to increase clonogenicity at MNNG concentrations more comparable to those used here. We would thus argue against p73α inhibition as a possible mechanism by which NSC197049 might protect against MNNG.

A number of studies have shown the steady state levels of MMR proteins required for the repair and DNA damage response functions of MMR are quite different. A full complement of MLH1 protein is required to elicit the characteristic G2/M arrest to MNNG, whereas less than 10% MLH1 sufficed to repair mismatched substrates (Cejka *et al*., 2003). A mouse embryonic stem cell line expressing 10% of control MSH2 levels was similarly MMR-proficient, as judged by their antimutagenic and antirecombinogenic phenotype and lack of MSI, but retained tolerance to methylating agents and consequently displayed increased clonogenicity following MNNG treatment, compared with cells with 100% MSH2 levels (Claij & Te Riele, 2002). These studies suggest that altering the relative activity of different MMR proteins can uncouple certain aspects of MMR function. This is further demonstrated by the finding that ~20% MSH6 expression in HCT15 cells produces a G2/M arrest proficient but MNNG-resistant phenotype (Lettieri *et al*., 1999), thus demonstrating the kind of DNA damage response uncoupling seen with NSC197049. It might therefore be argued that NSC197049 does represent a MMR inhibitor, but that the concentration used in this study only inhibited a proportion

of target protein, leaving an intermediate amount of active target that may have been sufficient to elicit a G2/M arrest but not to actually induce lethality following MNNG treatment. This hypothesis would therefore predict that a more 'MMR-like' phenotype should become apparent at higher NSC197049 concentrations.

Taken together, the evidence discussed here does not support a mechanism of action that involves NSC197049 acting as an MMR inhibitor, although the need to definitively rule the possibility out remains. This could be achieved in future studies by measuring the effect of NSC197049 on the repair function of MMR, the mutation rate, and the stability of microsatellites. Two established methods exist that measure the repair of a G:T mismatch in nuclear extracts (Thomas *et al*., 1991) and live cells (Lei *et al*., 2004). Comparing the effect of NSC197049 on MMR activity in both nuclear extracts and live cells is useful, since this would allow one to discern whether any inhibitory activity occurs via a direct mechanism or through modulation of gene expression. In terms of testing whether NSC197049 induces a MMR-null-like mutator phenotype, a method has been previously described that measures the mutation rate at the *HPRT* locus in cultured cells, and could be employed in future studies (Glaab & Tindall, 1997). MSI is a hallmark of MMR deficiency, and it would therefore be interesting to determine whether NSC197049 treatment alone can induce this phenotype. Microsatellites might be assessed by either the traditional manner (Boland *et al*., 1998) or by use of a plasmid-based frameshift-reversion assay that allows the stability of a range of microsatellite classes to be assessed by scoring for frameshift-mediated restoration of geneticin resistance (Hatch & Farber, 2004).

Since O6MeG has been shown to be subject to iterative processing attempts by MMR, one might expect functional MMR activity to disturb the replication dynamics of MNNG-treated cells (York & York, 2006). It would therefore be interesting to study the effect of MMR-dependent processing of MNNG lesions on the dynamics of DNA replication, and to compare this phenotype to the one elicited by NSC197049 treatment. The DNA combing technique can directly measure the speed of replication forks, the occurrence of replication fork stalling, and the firing of new replication origins (Lebofsky, 2003). Future studies might therefore also seek to utilise DNA combing to examine whether NSC197049 alters the replication dynamics of MMR-proficient MNNG-treated cells in a manner that phenocopies MMR-deficient cells.

### 5.3.3 Chemoprotection through inhibition of apoptosis

Cellular processes such as apoptosis are thought to represent key pathways through which the complexity of diverse genomic insults can be funnelled to effect a common apoptotic response. In support of this notion, cells with defective apoptotic responses are resistant to a wide range of DNA-damaging agents (Lowe *et al*., 1993; Los *et al*., 1997). Similarly, therapeutic restoration of the apoptotic response restores sensitivity to multi-drug resistant tumours (Soengas *et al*., 2001) whilst small molecule drugs that disrupt apoptosis have been shown to protect mice from the side-effects of DNA-damaging anti-cancer drugs (Komarov *et al*., 1999). The possibility therefore exists that NSC197049 may protect against MNNG, at least in part, through inhibition of one or more elements of the apoptotic machinery.

MNNG treatment has been shown to result in a large G2/M arrest that is dependent on MMR and the cell-cycle checkpoint kinases Chk1 and Chk2, and that precedes an apoptotic response (Adamson *et al*., 2005). Our finding that cells exposed to MNNG underwent an MMR-dependent G2/M arrest by 24 hours that continued to persist at 48 hours is consistent with the literature. Intriguingly, a protective concentration of NSC197049 did not prevent G2/M arrest, but did appear to inhibit the apoptotic response associated with MNNG exposure, as assessed by cellular viability, clonogenicity, and subG1 content. The data therefore suggests the G2/M arrest itself is not required for MNNG-induced toxicity, which is a notion that is supported by previous studies that show siRNA-mediated depletion of GADD45α can uncouple the G2/M arrest and apoptotic responses (Li *et al*., 2008). Moreover, this finding would be consistent with NSC197049 as a late-acting chemoprotectant that inhibits apoptosis. However, this should be counterbalanced against the finding that NSC197049 was only protective if co-treated with MNNG, and not immediately prior to or post MNNG exposure. Thus a mechanism of action involving inhibition of apoptosis appears less likely when considered in the full context of our findings.

In order to definitely assess the impact of NSC197049 on apoptosis, future studies might employ the annexin V method, which measures the characteristic flipping of phosphatidylserine from the inner to the outer side of the plasma membrane that occurs early in the apoptotic response (Vermes *et al*., 1995). Simultaneous immunostaining of cells with annexin V and propidium iodide permits the identification and discrimination of necrotic, apoptotic, and viable cells, which can be quantified by flow cytometry. This

method therefore allows one to analyse the capacity of NSC197049 to reduce the apoptotic response that occurs in response to pro-apoptotic stimuli such as Fas ligand.

### 5.3.4 Chemoprotection through direct inactivation of MNNG

That NSC197049 does not prevent MNNG-induced G2/M arrest strongly suggests that NSC197049 does not directly chemically inactivate MNNG. More likely is the possibility that NSC197049 either bolsters cellular antioxidant defences or acts directly by activating or inhibiting cellular targets that result in MNNG resistance. It is known that MNNG produces a wide spectrum of DNA lesions that are processed by multiple DNA repair pathways (Olsson & Lindahl, 1980; Beranek, 1990; Ye *et al*., 1998; Li, 1999). That sufficiently high NSC197049 concentrations can completely abolish MNNG-associated cytotoxicity therefore suggests that NSC197049 likely does not act by targeting specific repair processes, but instead acts via a more global mechanism. This is consistent with our finding that NSC197049 can equally protect MMR-proficient and deficient cells from MNNG-associated DSBs and cytotoxicity. A model whereby NSC197049 either acts early to decrease the amount of MNNG-induced damage elicited to DNA or acts late to inhibit apoptotic processes downstream of processing by DNA repair systems, therefore fit the observed data more comfortably. Moreover, since NSC197049 was only found to be protective when co-treated directly with MNNG, supports the model whereby NSC197049 acts early to limit the damage elicited by MNNG.

# CHAPTER SIX

*Discussion*

## 6.1 Summary of findings

We have designed, optimised, and conducted two high-throughput screens with the aim of identifying the key genetic players that determine cellular fate following exposure to MNNG, and small molecule structures that modify this response to confer a tolerant or resistant phenotype. MMR is a key DNA repair pathway heavily implicated in cancer but that remains incompletely understood. Studies that investigate these gaps in our knowledge may shed light on the role of MMR in carcinogenesis, tumour progression, prognosis, and response to therapy. Importantly, such knowledge may also help us exploit MMR to target cancers via synthetic lethal interactions. Having systematically depleted 571 genes known to be involved in DNA metabolism and cell-cycle control, we found 10 gene depletions increased tolerance or resistance to MNNG by at least two standard deviations from the population mean. Of these, the four canonical MMR genes were identified as key determinants of response to MNNG and thus validates our approach. TDG was selected for validation as an unexpected but robust hit on the basis of a model that was conceived to explain its role. Despite a comprehensive effort, TDG could not be validated as a true hit, and systematic error was assigned the most likely explanation for its appearance as a hit in the primary screen. The second part of this study probed for small molecules that conferred an MNNG tolerant or resistant phenotype. Such molecules might be expected to act as inhibitors of MMR, and would thus be of interest in manipulating MMR activity to achieve our therapeutic goals, such as by exploiting a synthetic lethality to selectively target cancer, for example. Moreover, modulators of the cellular response to cytotoxic drugs may have additional utility, regardless of their mechanism of action, in terms of chemoprotection or

chemoprevention. NSC197049 is a dithiolthione that was identified from these efforts, and was found to exhibit low micromolar activity that protected against MNNG-induced toxicity. The protective activity of NSC197049 was associated with a reduction in the number of MNNG-induced DSBs, was found to occur regardless of MMR status, and was dose-dependent and cell line independent. Moreover, NSC197049 appeared to act early, since it was only protective when co-treated alongside MNNG. The compound prevented the normal MNNG-induced accumulation of subG1 content cells but not the characteristic G2/M arrest following MNNG treatment. NSC197049 was shown to be capable of protecting against O6MeG lesions, and appeared to phenocopy antioxidants in their capacity to protect against MNNG toxicity. Collectively, the data do not support the notion that NSC197049 is an inhibitor of MMR, nor that it directly inhibits MNNG. More likely is the possibility that NSC197049 acts early and directly via a mechanism that does not involve changes in gene expression, to limit the damage done by MNNG, perhaps in a manner akin to that seen with direct-acting antioxidants. Whilst its precise mechanism requires further elucidation, the ascribed properties of NSC197049 make it an interesting candidate for chemoprevention studies.

## 6.2 Key genetic determinants of the response to MNNG

A key limitation of siRNA-based approaches is that it is not possible to exclude genes from a process on the basis that they did not produce the phenotype under study. Equally, it has been proposed that the majority of positive hits arising from siRNA-based screens are false positives (Mattila & Puig, 2010). It is therefore vital that positive hits undergo thorough validation experiments in order to exclude the possibilities of

systematic error, non-specific responses to dsRNA and off-target effects. Similarly, negative hits cannot be definitely excluded from the investigation without additional validation experiments.

Evidence from other studies suggests that there may be a number of genes in addition to those identified here that are key players in the response to MNNG. Several studies have examined the cell signalling machinery required to elicit the characteristic G2/M arrest response following treatment with MNNG, implicating ATM, ATR, and the serine/threonine-protein kinases Chk1, and Chk2 (Stojic *et al*., 2004; Adamson *et al*., 2005; Beardsley *et al*., 2005). Although there were some disagreements between the studies concerning the necessity of ATM and Chk2 for G2/M arrest response, all three agreed that ATR and Chk1 were absolutely required. Whilst the G2/M arrest was considered to be a pivotal component of MNNG-induced toxicity when these studies were published, it should be noted that it has been found here and elsewhere that the G2/M arrest can be uncoupled from apoptosis, and is not strictly necessary for MNNG-induced toxicity in some cell models (Li *et al*., 2008).

One previous study analysed the gene expression profiles from 24 MNNG-treated lymphoblastoid cell lines and identified a panel of 48 genes whose expression could be used to predict the response to MNNG with a sensitivity of 94% (Fry *et al*., 2008). Expression of MutYH was found to have the strongest positive association with MNNG sensitivity, with cells expressing high levels of MutYH being the most sensitive to MNNG. Whilst the authors noted that MutYH can interact with MutSα (Gu *et al*., 2002), they did not speculate on a mechanistic model. Given this data and that siRNA targeting MutYH were part of the library screened here, it is surprising that MutYH was not also

identified in this study. However, it should be noted that Fry *et al*. (2008) did not identify any of the MMR proteins that are well established determinants of MNNG sensitivity. That both studies identified different sets of genes might be explained through the realisation that Fry *et al*. (2008) only treated cells with 3.3 μM MNNG, which might be sufficiently low to be outside of the window of MMR-dependent toxicity.

It has been shown in human lymphoblastoid cells and peripheral lymphocytes that following MNNG exposure, an MMR-dependent stabilisation of p53 occurs that eradicates the cell by apoptosis through an extrinsic Fas receptor driven pathway (Dunkern *et al*., 2003; Roos *et al*., 2004). Contradicting such data is the earlier finding that induction of apoptosis in MNNG-treated CHO cell lines is independent of p53 and Fas receptor/ligand, but instead mediated by the intrinsic apoptotic pathway involving decreases in B cell lymphoma 2, cytochrome C release, and activation of caspase 9 and caspase 3 (Ochs & Kaina, 2000). It is thus possible that a common pathway of MMR-dependent induction of DSBs following MNNG exposure recruits and activates different subsets of apoptotic machinery in different cellular backgrounds to execute apoptosis. Whilst the majority of apoptotic apparatus was not included in the library, the diversity of downstream execution pathways between cell lines might provide an explanation for why genes such as p53 were not identified in this study. Certainly, p53 is phosphorylated in an MLH1-dependent manner by HCT116+Ch3 cells within 4 hours of exposure to alkylating agents (Yanamadala & Ljungman, 2003). However, that p53 phosphorylation is induced within 4 hours of drug exposure but do not become apoptotic for a further two cell-cycles suggests that p53 does not play an important role in MNNG-induced toxicity. This is supported by previous studies that confirm that p53 is induced in an MMR-

dependent manner following MNNG treatment, but that apoptosis can be executed in a p53-independent manner, and thus p53 is not required for the normal phenotypic response to MNNG (Hickman & Samson, 1999). These data further validate our screening approach, since p53 was not identified as a gene that influences this response.

### 6.3 Role of TDG in MNNG sensitivity

Whilst a role for TDG in MMR-dependent induction of MNNG toxicity was not established here, we did find that its knockdown increased the number 53bp1 foci in MNNG-treated cells. In contrast to MMR, this data indicates that TDG may play a protective role against MNNG-induced DSBs, and would support our finding that TDG failed to validate as a hit in the primary screen for mediators of MNNG toxicity. Moreover, co-depletion of TDG and MSH6 was able to inhibit the MNNG-resistant phenotype conferred by MSH6 depletion alone. However, it should be noted that due to the high sensitivity of vehicle-transfected cells, it was not possible to determine whether TDG knockdown further sensitised MMR-proficient cells to MNNG. These findings make sense in the context of the literature, since TDG is an established component of BER; the primary pathway through which the majority of MNNG-induced lesions are repaired (Liu *et al*., 1999). It is therefore not surprising that cells with defective BER functionality are highly sensitive to methylating agent toxicity, irrespective of MMR status (Sobol *et al*., 1996; Liu *et al*., 1999; Curtin *et al*., 2004). However, of the known substrate specificities of TDG, thymine mispaired with O6MeG is the only MNNG-induced lesion that is likely to be targeted by TDG (Griffin *et al*., 1994; Lari *et al*., 2001). In contrast, $N^7$-methylguanine and $N^3$-methyladenine are repaired by methylpurine

glycosylase (MPG) (Engelward *et al*., 1993), whilst $N^3$-methylcytosine and $N^1$-methyladenine are directly demethylated by the alkB alkylation repair homolog 2 and 3 dioxygenases (Falnes *et al*., 2002; Trewick *et al*., 2002). Existing data would therefore indicate that the protective role of TDG is likely mediated through its recognition and excision of O6MeG:T mispairs. Of course, this notion presents the apparent paradox whereby TDG protects against MNNG independently of MMR status, whereas the lesion it excises is the MMR-dependent O6MeG. This can be resolved through the realisation that whilst MMR-deficient cells escape MMR-dependent processing of O6MeG into lethal DSBs, they still ultimately require other repair processes to remove the highly mutagenic lesions O6MeG. Indeed, MGMT expression level is highly correlated with resistance to nitrosourea alkylating agents, its pharmacological inactivation sensitises cells to such agents, and this occurs independently of MMR status (Gerson *et al*., 1992). Thus it is possible that the protective effect of TDG against MNNG toxicity is mediated through its activity at O6MeG:T mispairs. However, it is surprising that upon recognition of a G:T or O6MeG:T mispair, TDG catalyses the removal of thymine rather than the guanine or O6MeG (Lari *et al*., 2001). This poses the question of how TDG might protect against O6MeG-induced DNA damage and toxicity when it is not sufficient to remove the lesion. TDG has been shown to operate via distinct ATP-dependent and –independent modes, the former being important for repair of (O6Me)G:T mispairs and the latter being implicated in repair of G:U mispairs (Lari *et al*., 2002). The authors additionally identified evidence that supports the involvement of other repair proteins in ATP-dependent repair, since A1235-MR4 extracts are deficient in the ATP-dependent activities of TDG, even after addition of wild-type TDG. This data supported the notion

that TDG acts in concert with ATP and other repair processes to successfully repair O6MeG:T lesions. Combined with the finding that TDG can tightly bind and stabilise AP sites involving O6MeG (Waters *et al*., 1999), this lead Lari *et al*. (2002) to propose that TDG acts on O6MeG:T mispairs to excise the thymine, stabilise the resulting AP site, and act to recruit additional repair factors. Thus whilst TDG cannot directly excise O6MeG, it is possible that it elicits a repair response that ultimately results in its removal.

## 6.4 Role of DNA double-strand breaks in MNNG toxicity

Studies that have shown that MNNG toxicity can be rescued by efficient HR have been suggestive of the notion that MNNG toxicity ultimately arises from the generation of DSBs (Cejka *et al*., 2005; Mojas *et al*., 2007; Roos *et al*., 2009). It has recently been shown in MNNG-treated *E. coli* that DSBs form in a dose- and MMR-dependent manner, with the majority being dependent on DNA replication and a smaller subset requiring active replication (Nowosielska & Marinus, 2008). The authors propose that replication-independent DSBs form overlapping MMR and BER repair tracts on opposing strands, whereas replication-dependent DSBs form through the collapse of replication forks encountering the persistent single-stranded gaps that have been observed to occur in an MMR-dependent manner (Mojas *et al*., 2007). Owing to their finding that MNNG toxicity correlates with doubling time, Nowosielska & Marinus (2008) hypothesised that the replication-dependent DSBs are the primary contributors to MMR-dependent cell death. Consistent with the literature, we found that human cells treated with MNNG also generate DSBs. However, a large subset of MNNG-induced DSBs produced by 24 hours was found to occur irrespective of MMR status, with a smaller subset of ~30%

developing in a manner dependent on functional MMR. Because we did not analyse DSB in non-replicating cells, it is not possible to determine what proportion, if any, of the MMR-independent or –dependent DSB required active DNA replication. However, by 72 hours, MMR-deficient cells were found to have repaired ~60% of their DSBs, compared with only ~1% of MMR-deficient cells. It thus appears as though functional MMR may not only generate an MMR-dependent subset of DSBs, but also interferes with the subsequent DSB repair, perhaps of both MMR-dependent and –independent DSBs. Certainly, data such as those discussed here are consistent with a futile processing model, whereby MMR actively generates repair intermediates that are converted into DSBs. However, it should be pointed out that this does not rule out an additional signalling role for MMR in the DNA damage response. Some key questions that can be posed from these data are whether MMR-dependent DSBs are somehow more toxic than MMR-independent DSBs, and whether it is the generation of MMR-dependent DSBs or the inhibition of their repair in cells with functional MMR that generates a lethal phenotype. Our finding that co-treatment of MNNG-treated cells with NSC197049 reduces the toxicity of MNNG in both MMR-proficient and deficient cells supports a model whereby the additional sensitivity of MMR-proficient cells can be explained through their generation of higher numbers of DSBs that are not repaired. Whilst we did not differentiate between toxicity arising from the induction of DSBs or the failure to repair them, this will be of interest in future studies. The finding that DSBs are not repaired in MMR-proficient cells but are in MMR-deficient cells cannot be used as evidence supporting the idea that MMR-dependent DSBs are ‘more lethal’, since MMR-

proficient cells are unable to repair any of their DSBs, even those that did not form in an MMR-dependent manner.

## 6.5 NSC197049 as a chemoprotective agent

Compounds that mitigate the carcinogenic and/or toxic effects of therapeutic agents may be of use in reducing the side-effects associated with the use of cytotoxic drugs. Since NSC197049 has been shown here to effectively protect against MNNG-induced DSBs and cytotoxicity, it is relevant to ask whether the molecule might have utility as a novel chemoprotective agent. It is important for any chemoprotective agent employed during cancer chemotherapy to possess some form of selectivity in favour of non-cancerous tissues, so that protection is not conferred to the tumour. For instance, nutlin-3 is a non-genotoxic activator of p53 that may be of use as a chemoprotective agent for patients with p53 null tumours (Kranz & Dobbelstein, 2006; Tokalov & Abolmaali, 2010). Nutlin-3 activation of p53 in non-cancerous tissues has been shown to induce S-phase arrest and provide protection against the replication-dependent cytotoxic drugs, whilst p53 null tumours remain insensitive to nutlin-3 and remain vulnerable. Other approaches to achieving selectivity include scalp cooling, which restricts blood flow to the scalp during chemotherapy and hence reduces chemotherapy-associated alopecia (Grevelman & Breed, 2005). In order to assess the clinical utility of NSC197049, it will therefore be necessary to study its biodistribution following various routes of administration. In theory, NSC197049 may be of use as a chemoprotectant if it is not distributed to tissues in which the tumour is located. Equally, if NSC197049 were to modulate cellular targets that have acquired loss of function mutations in particular

tumours, then NSC197049 would be naturally suited to chemoprotection in such patients. Alternatively, depending on the non-cancerous tissues to be targeted, it may be possible to combine routes of administration with medicinal chemistry to restrict the biodistribution of a chemoprotectant. The effect of physico-chemical and structural drug properties and their preparations on the biodistribution of topically applied drugs are well characterised (Nino *et al*., 2010), and thus it may be possible to restrict the biodistribution of a topically applied drug to the scalp, for example, in order to protect against chemotherapy-associated alopecia.

It is important to note that there is considerable debate in the literature as to whether systemic administration of antioxidants protects against chemotherapy-associated toxicity without affecting tumour control (Lawenda *et al*., 2008). Certainly, numerous studies have shown antioxidant supplements such as beta-carotene, vitamins E, C, *N*-acetylcysteine, ellagic acid, melatonin, glutathione to protect against different chemotherapy-associated toxicities, including alopecia, emesis, oral muscositis, diarrhoea, cardiotoxicity and neuropathy (Mills, 1988; Wadleigh *et al*., 1992; Cascinu *et al*., 1995; Wagdi *et al*., 1996; Smyth *et al*., 1997; Lissoni *et al*., 1999; Cascinu *et al*., 2002; Cerea *et al*., 2003; Falsaperta *et al*., 2005). However, Lawenda *et al*. (2008) noted that whilst the majority of these studies did not find antioxidant supplements to affect the tumour response or survival rates, the studies lacked sufficient statistical power to legitimately assess those end-points. Moreover, the large variety in experimental design amongst such studies makes it difficult to pool these data and perform a meta-analysis. It is therefore unclear whether systemic antioxidants inappropriately confer protection to the tumour, and this has lead to recommendations against use of antioxidants in

chemoprotection until larger studies have been completed (D'Andrea, 2005; Lawenda *et al*., 2008). Although the mechanism by which NSC197049 works remains incompletely understood, dithiolthiones are known to up-regulate antioxidant defences, and we have observed it to phenocopy the chemoprotective activity of established antioxidants. We must therefore recommend that NSC197049 is not utilised as a chemoprotective drug unless it can be definitely shown that either the tumour is insensitive to the drug or that its biodistribution prevents it from conferring protection to the tumour.

### 6.6 NSC197049 as a chemopreventive agent

Oltipraz is the best studied dithiolthione, and has been shown to protect against carcinogenesis in the kidney and liver of aflatoxin B1-treated rats (Kensler *et al*., 1985; Roebuck *et al*., 1991; Bolton *et al*., 1993), glandular stomach cancer in MNNG-treated rats (Nishikawa *et al*., 1998), forestomach and lung cancers in benzo[a]pyrene treated mice (Fahey *et al*., 2002; Sharma *et al*., 2006), lung and pancreatic cancers in *N*-nitrosobis(2-oxopropyl) amine-treated hamsters (Clapper *et al*., 1995; Son *et al*., 2000), and colon cancer in azoxymethane-treated rats (Liu *et al*., 1995; Wargovich *et al*., 1996). On the basis of this weight of evidence, Oltipraz has entered human trials, and is currently undergoing intensive study in a region of China called Qidong, where dietary contamination with aflatoxins results in a high incidence of hepatocellular carcinoma. The carcinogenicity of alfatoxin B1 depends on its metabolism to aflatoxin exo-8,0-epoxide by the cytochrome P450 enzymes 3A4 and 1A2, which subsequently rearranges in aqueous solution to the highly carcinogenic aflatoxin B1 exo-8,9-epoxide (Guengerich *et al*., 1998). Weekly administration of 500 mg Oltipraz for one month was found to

decrease a urinary phase 1 metabolite of aflatoxin by 51%, suggesting that Oltipraz may be sufficient to decrease aflatoxin B1 metabolism *in vivo* (Wang *et al*., 1999). Daily administration of 125 mg Oltipraz increased by 2.6 fold the urinary excretion of aflatoxin-mercapturic acid, a phase 2 metabolite that is generated from conjugation of carcinogenic aflatoxin B1 exo-8,9-epoxide with glutathione. The data therefore supported the findings of preclinical studies that Oltipraz protects against carcinogenesis, being sufficient at intermittent high doses to inhibit aflatoxin B1 activation and at low continual doses to promote excretion of its carcinogenic metabolite. However, subsequent studies within the same population and using the same Oltipraz treatment regime found Oltipraz did not decrease oxidative DNA adducts (Glintborg *et al*., 2006). Another study that examined whether 200 or 400 mg weekly administration of Oltipraz or placebo could decrease tobacco smoke-associated DNA adducts did not find any significant differences between the two arms (Kelley *et al*., 2005). Further studies will therefore be required to characterise the range of carcinogens against which Oltipraz may offer protection, and to examine the efficacy to which this is achieved. Our finding that NSC197049 can protect against MNNG-induced toxicity suggests that this structural analog may also have utility as a chemopreventive agent. Whilst Oltipraz's mechanism of action has been well studied, our data suggests NSC197049 may act via a distinct but related mechanism, and therefore warrants further study.

Whilst we have shown NSC197049 protects against the induction of DSBs, reduced clonogenicity and reduced cell viability by MNNG, we did not examine its intrinsic toxicity or the extent to which it limits genotoxic damage and carcinogenicity. Such factors will be critically important in determining its potential clinical usefulness in

chemoprevention. The comet assay is a well established technique that can be adapted to detect either SSBs or DSBs, and is frequently used to assess the genotoxicity of novel compounds (Collins, 2004). Future studies might therefore use the comet assay to assess whether NSC197049 monotherapy is non-genotoxic in this regard, and to confirm and extend the work begun here to examine whether it protects against both SSBs and DSBs induced by MNNG. It is likely that NSC197049 does protect against MNNG-induced SSBs, since current models suggest it is these that collapse into one-ended DSBs at replication forks (Mojas *et al*., 2007), and we have shown NSC197049 can prevent DSB induction independently of grossly altering DNA replication dynamics. Further studies might also examine the effect of NSC197049 monotherapy on the spontaneous mutation rate, and to test whether it can temper the elevation in mutation rates induced by MNNG. Existing methods such as analysis of the mutation rate at the *HPRT* locus would be suitable for such purposes (Glaab & Tindall, 1997). The demonstration that NSC197049 monotherapy does not elicit SSB or DSB, and that it does not increase the spontaneous mutation rate would provide strong evidence that the compound is not genotoxic, and would support our findings that the compound does not alter cellular viability or clonogenicity. Moreover, that NSC197049 did not alter cell-cycle progression in this study adds further weight to this idea, since genotoxic stresses are known to activate cell-cycle checkpoints and halt cell-cycle progression (Shackelford *et al*., 1999). If NSC197049 was also found to reduce the mutation rate in MNNG-treated cells, this would be highly suggestive of a mechanism of action that involves inhibition of base methylation events by MNNG. Ultimately, the use of animal models will be required to generate the rationale for further investigation of NSC197049 in humans, in particular to

demonstrate that NSC197049 is both non-carcinogenic as a monotherapy and chemoprotective *in vivo*.

A major disadvantage of a phenotypic screening approach is that the cellular target(s) modulated by a hit compound are not known, therefore making it more difficult to identify the mechanism of action or other potential therapeutic uses, and to appropriately assign risk in preclinical and clinical trials. Whilst it is the case that well characterised Oltipraz targets such as Nrf2 represent potential NSC197049 targets, the failure of these two compounds to phenocopy one another in this study suggests NSC197049 may act via one or more novel cellular targets. Two main approaches exist to identify drug targets following phenotypic screening. The target can be directly identified through affinity purification, expression cloning, three-hybrid systems, or through probing protein microarrays, or indirectly through comparison of the phenotype produced by the compound with that by other compounds with known targets (Hart, 2005). Whilst each approach and associated techniques have their own strengths and weaknesses, potentially the most efficient route with which to identify the target of NSC197049 is through an indirect bioinformatic means. As a component of an NCI public access library, NSC197049 has been screened within the NCI60 anti-cancer drug screen (Shoemaker, 2006). Data therefore exists that shows the growth inhibitory 50 ($GI_{50}$) values for five concentrations of NSC197049 against the panel of 60 cell lines. In order to assist with target identification, the NCI have developed the 'COMPARE' algorithm, which examines the $GI_{50}$ pattern produced by the compound of interest, and screens the database for other compounds that produced a similar pattern of phenotypic responses. The rationale for this approach is that compounds which modulate common

cellular targets would produce similar $GI_{50}$ panel responses, and thus by identifying compounds with known targets that phenocopy the query compound, it is possible to identify likely targets. This approach was first successfully used to identify tubulin as the target of halichondrin B (Bai *et al*., 1991). A priority for future studies will therefore to identify the target of NSC197049, first through the COMPARE algorithm, and if necessary, by use of more direct techniques.

## 6.7 Inhibitors of MMR and chemoprotection

One of the rationales for screening for small molecule modulators of the response to MNNG was that if inhibitors of MMR were identified, these may have some utility as novel chemoprotective agents. Whilst therapeutically inhibiting MMR in non-cancerous tissues represents a novel means by which to protect against MMR-dependent cytotoxic chemotherapy, MMR deficiency is known to be associated with a mutator phenotype, and thus raises ethical issues over its safety. However, evidence exists that does not support such concerns over the use of MMR inhibitors in clinical practice. The repair and damage response function of MMR has been shown to require different steady state levels of MLH1 (Cejka *et al*., 2003). The repair of mismatched substrates within *in vitro* repair assays remained intact even at 10% of wild-type MLH1 expression, and was found to be sufficient *in vivo* to suppress the MSI phenotype associated with MLH1 deficiency. In contrast, MNNG-treated cells expressing 10% MLH1 failed to activate the DNA damage signalling or G2/M checkpoint typical of MNNG-treated cells expressing wild-type MLH1 levels. These data demonstrate, that at least in the case of an MLH1 inhibitor, dose optimisation might permit the functional uncoupling of the repair and

DNA damage response of MMR. This might permit the inhibition of the MMR-dependent DNA damage response to induce tolerance to MNNG in non-cancerous tissues, whilst avoiding inducing a mutator phenotype and unduly increasing the mutation rate. Constitutional MMR deficiency syndrome (CMMR-D) is a rare disease associated with bi-allelic inactivation of one of the four canonical MMR genes, leading to a complete deficiency in MMR and resulting in a number of early onset malignancies (Wimmer & Etzler, 2008). CMMR-D therefore models the effect of long-term MMR inhibition, and in this regard it is interesting that the mean age of onset of cancer in these patients is 5.5 years. In contrast, MMR inhibitors might only be used in a transitory manner, being applied for a short period prior to administration of cytotoxic chemotherapy, and thus MMR inhibiton would be measured in days rather than years. Furthermore, that CMMR-D patients with bi-allelic mutations in *MSH2* or *MLH1* have an earlier tumour onset of 3.5 years compared with mutations in *MSH6* or *PMS2*, suggests that specific inhibitors of MSH6 or PMS2 would further maximise the safety of MMR inhibitors (Wimmer & Etzler, 2008). However, it is important to note that induction of tolerance in non-cancerous tissues during chemotherapy does permit the survival of cells that have been subjected to genotoxic insults, and that failure to eradicate them may increase the risk of secondary cancers. In this respect, activators of p53 represent a better chemoprotection strategy, since induction of a p53-dependent cell-cycle arrest prevents non-cancerous cells from generating replication-dependent DNA damage during chemotherapy regimes (Kranz & Dobbelstein, 2006; Tokalov & Abolmaali, 2010). Instead, arrested cells have time to recruit repair processes that can directly reverse such damage and thus avoid increasing the mutational burden of the cell. However, it will be

important to weigh the disadvantages of any chemoprotection strategy against the risk of non-uptake or continuance of potentially life-saving treatment (Lindley *et al*., 1998; Schnell, 2003), and to consider it in the context of the patient's life expectancy, in which quality of life may outweigh the risk of secondary cancers.

## 6.8 Significance of this study in terms of exploitation of synthetic lethal interactions in the specific targeting of cancer

Our finding that the four canonical MMR genes are the primary determinants of sensitivity to MNNG is in agreement with those previously reported in yeast (Cejka & Jiricny, 2008). Synthetic lethalities that implicate the MMR-dependent DNA damage response are therefore most likely to be effectively targeted through inhibition of MSH2, MSH6, MLH1, or PMS2. Whilst a number of cancers are known to inactivate MMR during carcinogenesis as a means of elevating the mutation rate and avoiding DNA damage surveillance-induced apoptosis, it is interesting to note that some cancers only rarely inactivate MMR (Peltomäki, 2003). Using MSI as a marker of MMR functionality, sporadic tumours of the LS spectrum frequently inactivate MMR, which is much less commonly seen in tumours originating from the breast or bladder, for example. Whilst this molecular diversity might be explained through the different barriers to tumourigenesis imposed between distinct anatomical sites, it would be interesting to examine whether MMR functionality is required in some tumours due to the existence of one or more synthetic lethalities. Where this requirement involves the non-repair functions of MMR, our data suggests inhibition of MSH6 or PMS2 would be as effective as MSH2 or MLH1. This is particularly relevant with respect to the aforementioned

studies that indicate MSH6 or PMS2 inhibition might be safer than MSH2 or MLH1 in terms of their carcinogenic potential (Wimmer & Etzler, 2008).

Inhibition of TDG would likely be ineffective in targeting a synthetic lethality involving the DNA damage response functions of MMR, since it appeared to work antagonistically against the MMR-dependent and –independent cytotoxicity of MNNG. However, our finding that TDG protects against alkylation damage suggests that its therapeutic inhibition may be effective in the sensitisation of tumour cells to alkylating agents. This approach has been shown to be the case for other components of the BER pathway, including MPG and APE1 (Adhikari *et al*., 2008).

Understanding the potential utility of NSC197049 for exploiting synthetic lethal interactions would require a more detailed knowledge of its mechanism of action, including identification of its cellular targets as discussed. Other dithiolthiones such as Oltipraz are known to activate rather than suppress gene expression, and thus if NSC197049 works through similar mechanisms, any use in exploiting synthetic lethalities might involve activation of one or more genes that prove to be toxic in that genetic background. It is interesting to note that p53 activation by nutlin-3 has been shown to be sufficient to specifically induce p53-dependent apoptosis in some human tumours (Miyachi *et al*., 2009). Rhabdomyosarcoma is a paediatric cancer in which 70-80% express wild-type p53, and in a proportion of which p53 is functionally inactivated by over-expression of murine double minute 2, a negative regulator of p53. Therapeutic p53 activation in such cells appears to re-activate p53-dependent DNA damage signalling in rhabdomyosarcoma cells, leading to cell-cycle arrest and apoptosis. Thus whilst NSC197049 awaits more detailed characterisation, a mechanism of action involving

either inhibition or activation of cellular targets may be of interest in terms of exploiting synthetic lethalities.

# CHAPTER SEVEN

*Figures*

a)

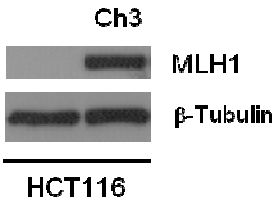
Ch3
MLH1
β-Tubulin
HCT116

b)

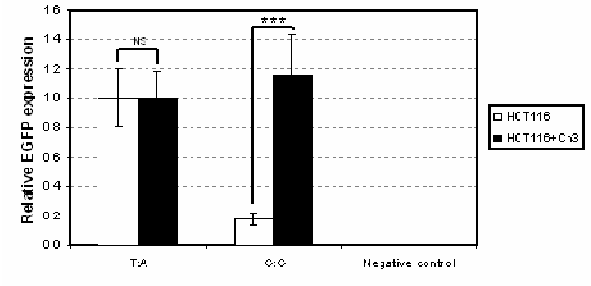
Relative EGFP expression
NS
***
HCT116
HCT116+Ch3
Negative control

c)

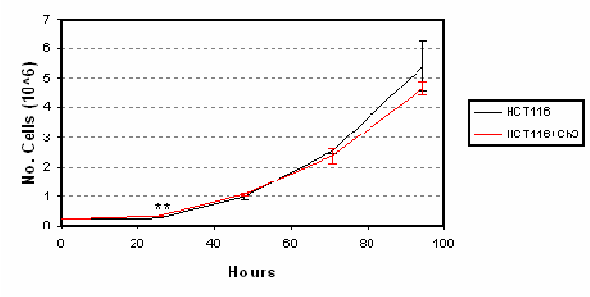
No. Cells (10^6)
**
Hours
HCT116
HCT116+Ch3

**Figure 3.1. Cell line characterisation.** (a) Whole cell lysates of wild-type HCT116 and chromosome 3 microinjected HCT116+Ch3 immunoblotted for MLH1 expression. β-tubulin was included as a loading control. (b) Restoration of a G:G mismatch-disrupted substrate encoding green fluorescent protein (EGFP) in live cells of differential MMR status. A wild-type substrate lacking any mismatched sites was included as a positive control with a mock transfection as a negative control. 10,000 events were counted per measurement. (c) Doubling times of HCT116 and HCT116+Ch3 cell lines. Data represents mean and standard error of three independent experiments (excluding western blot where n=1).

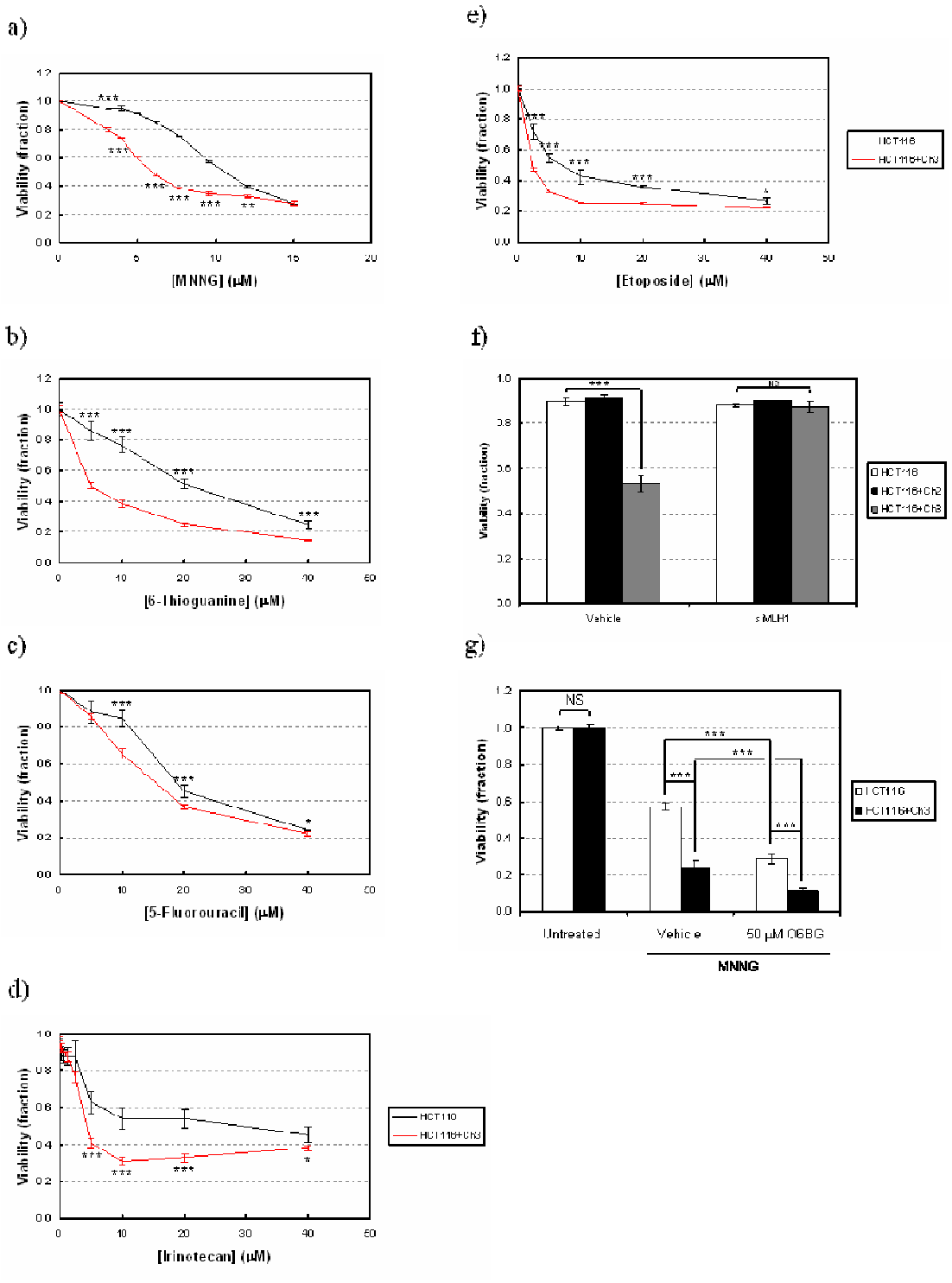
a)
Viability (fraction)
[MNNG] (μM)
e)
Viability (fraction)
[Etoposide] (μM)
HCT116
HCT116+CH2
b)
Viability (fraction)
[6-Thioguanine] (μM)
f)
Viability (fraction)
Vehicle
siMLH1
HCT116
HCT116+CH2
HCT116+CH3
c)
Viability (fraction)
[5-Fluorouracil] (μM)
g)
Viability (fraction)
NS
Untreated
Vehicle
50 μM O6BG
MNNG
HCT116
HCT116+CH3
d)
Viability (fraction)
[Irinotecan] (μM)
HCT116
HCT116+CH3

**Figure 3.2. Mismatch repair status and the response to cytotoxic drugs.** Measurement of HCT116 and HCT116+Ch3 cellular viability following a 24 hour exposure to increasing doses of (a) MNNG, (b) 6-thioguanine, (c) 5-fluorouracil, (d) irinotecan, and (e) etoposide. (f) Cellular viability of the indicated cell lines transfected with either Dharmacon DharmaFect transfection reagent together with siRNA targeting MLH1 expression or DharmaFect transfection reagent alone, following a 24 hour treatment with 7.5 μM MNNG. (g) Effect of methylguanine methyltransferase (MGMT) inhibition by 50 μM O6-benzylguanine on the differential response of HCT116 and HCT116+Ch3 cells to a 24 hour treatment with 7.5 μM MNNG. Measurement of cellular viability in all experiments was assessed after 120 hours of drug-free growth, and is expressed as a fraction of the untreated control. Data represents mean and standard error of three independent experiments.

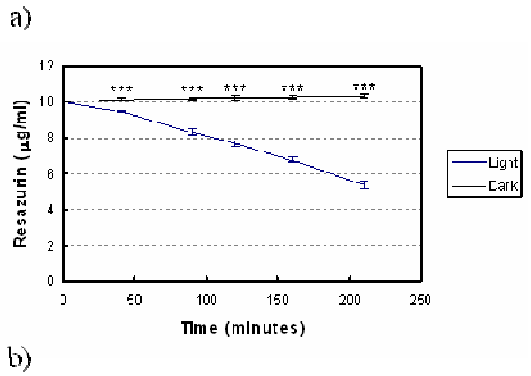
a)
Resazurin (µg/ml)
Time (minutes)
Light
Dark

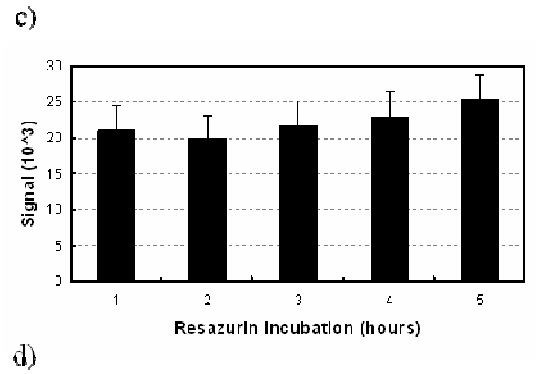
c)
Signal (10^3)
Resazurin Incubation (hours)

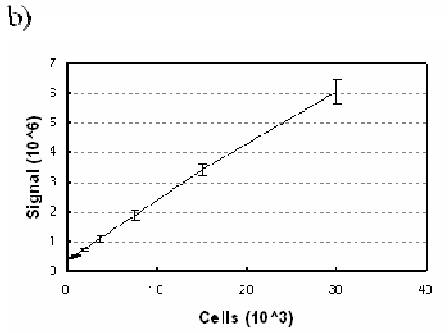
b)
Signal (10^6)
Cells (10^3)

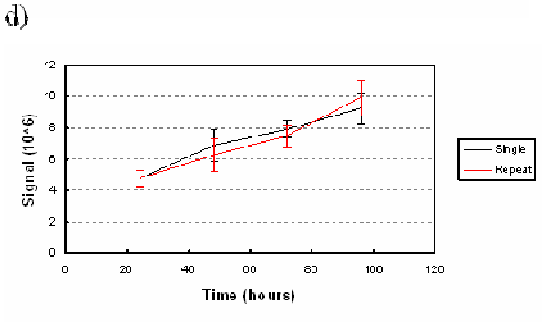
d)
Signal (10^6)
Time (hours)
Single
Repeat

**Figure 3.3. End-point optimisation.** (a) Photo-stability over time of a 10 μg/ml solution of resazurin dissolved in cell culture media, as measured by spectrophotometry. (b) Relationship of cell density to resorufin signal, measured 24 hours after cell seeding. (c) Effect of resazurin incubation time on resorufin signal, measured 24 hours after seeding 12,000 cells/well. (d) Comparison of cellular viability of the same set of plates every 24 hours compared the viability of plates that were measured once at the equivalent time point. Data represents mean and standard error of three independent experiments.

a)

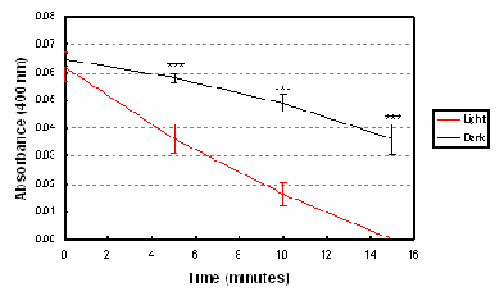
Absorbance (490 nm)
Time (minutes)
Light
Dark

d)

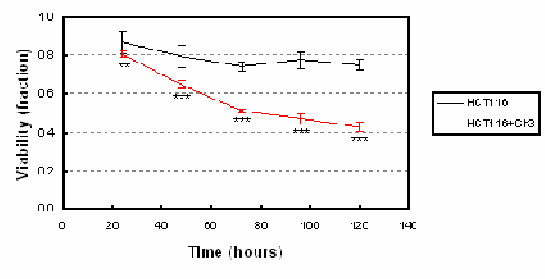
Viability (fraction)
Time (hours)
HCT116
HCT116+CH3

b)

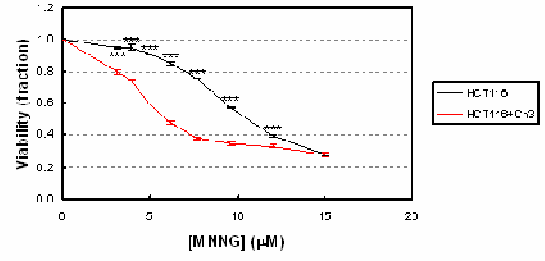
Viability (fraction)
[MNNG] (μM)
HCT116
HCT116+CH3

e)

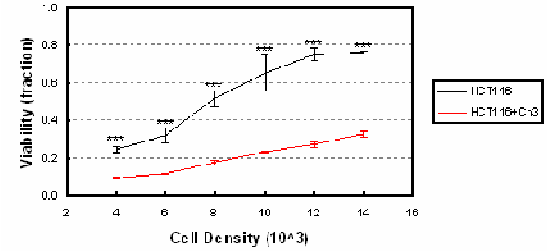
Viability (fraction)
Cell Density (10^3)
HCT116
HCT116+CH3

c)

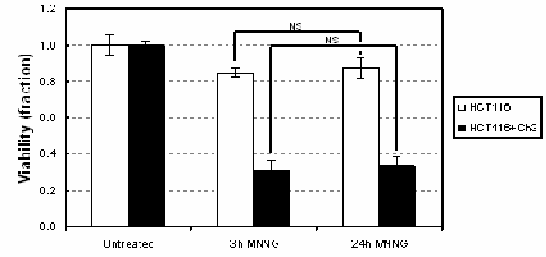
Viability (fraction)
NS
NS
Untreated
3h MNNG
24h MNNG
HCT116
HCT116+CH3

**Figure 3.4. Optimising the differential response of MMR-proficient and –deficient cells to MNNG.** (a) Photo-stability of a 1 mM MNNG dissolved in cell culture media over time, as assessed by spectrophotometry. (b) Optimisation of the differential cellular viability of HCT116/Ch3 cells following a 24 hour treatment with the indicated concentration of MNNG followed by 120 hours subsequent drug-free growth. (c) Comparison of the differential viability of HCT116/Ch3 cells resulting from a 3 hour or 24 hour treatment with 7.5 μM MNNG followed by 120 hours drug-free growth. Optimisation of the (d) drug-free growth period or (e) cell seeding density to maximise the differential viability of HCT116/Ch3 following a 24 hour treatment with 7.5 μM MNNG. Cellular viability is expressed as a fraction of the untreated control. Data represents mean and standard error of three independent experiments.

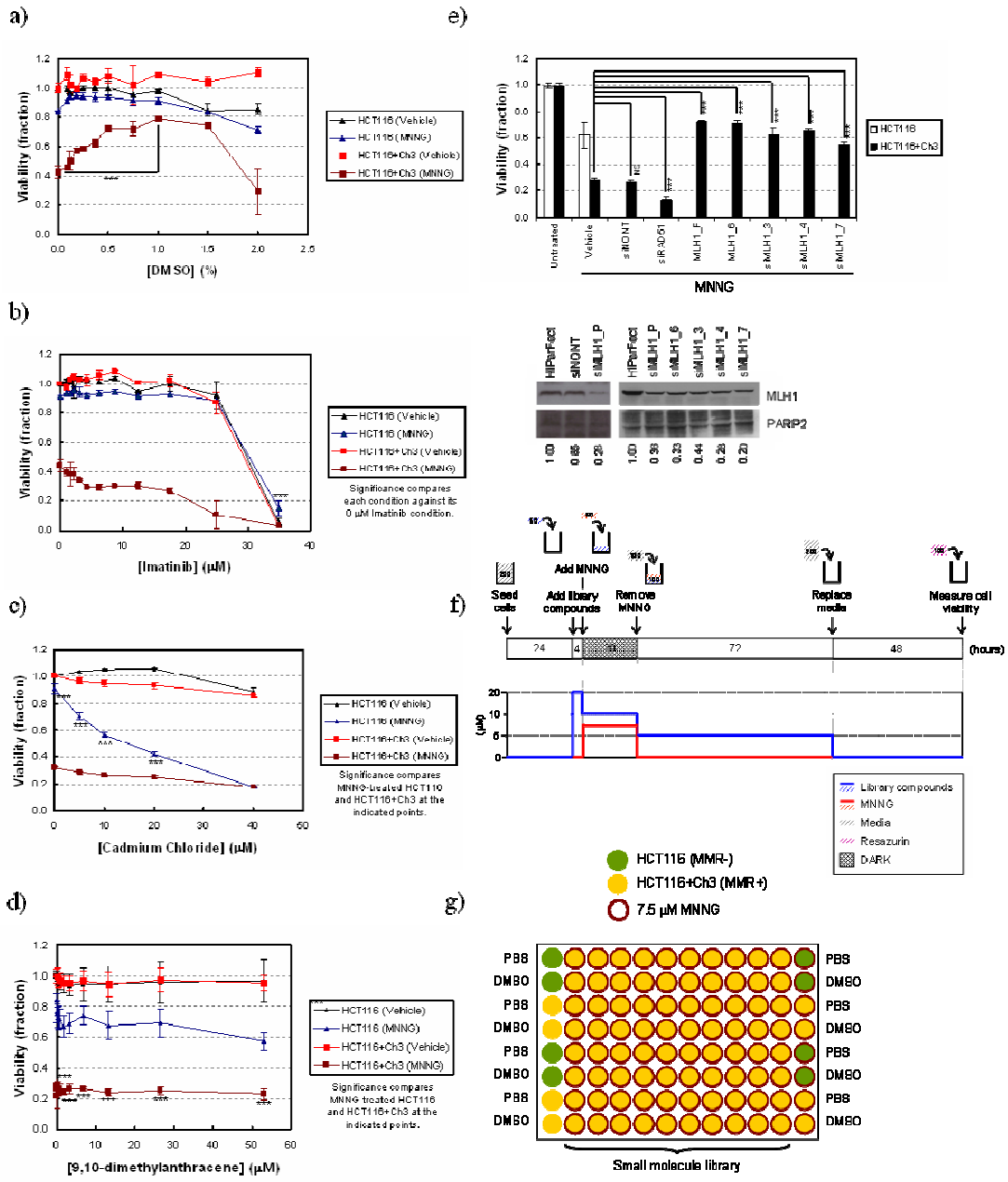
a)
Viability (fraction)
[DMSO] (%)
HCT116 (Vehicle)
HCT116 (MNNG)
HCT116+Ch3 (Vehicle)
HCT116+Ch3 (MNNG)
b)
Viability (fraction)
[Imatinib] (μM)
Significance compares each condition against its 0 μM Imatinib condition.
c)
Viability (fraction)
[Cadmium Chloride] (μM)
Significance compares MNNG-treated HCT116 and HCT116+Ch3 at the indicated points.
d)
Viability (fraction)
[9,10-dimethylanthracene] (μM)
Significance compares MNNG treated HCT116 and HCT116+Ch3 at the indicated points.
e)
Viability (fraction)
HCT116
HCT116+Ch3
Untreated
Vehicle
siNONT
siR3D51
MLH1_5
MLH1_6
siMLH1_3
siMLH1_4
siMLH1_7
MNNG
HiPerFect
siNONT
siMLH1_P
siMLH1_5
siMLH1_6
siMLH1_3
siMLH1_4
siMLH1_7
MLH1
PARP2
f)
Seed cells
Add library compounds
Add MNNG
Remove MNNG
Replace media
Measure cell viability
24
4
4
72
48
(hours)
(μM)
Library compounds
MNNG
Media
Resazurin
DARK
HCT116 (MMR-)
HCT116+Ch3 (MMR+)
7.5 μM MNNG
g)
PBS
DMSO
Small molecule library

**Figure 3.5. Optimisation of controls and design of the small molecule screen.** Dose-response of increasing concentrations of (a) DMSO, (b) imatinib, (c) cadmium chloride, or (d) 9,10-dimethylanthracene on the cellular viability of vehicle- and MNNG-treated HCT116/Ch3 cells. Significance shown in figure b compares each condition at 35 μM Imatinib against 0 μM Imatinib. (e) Effect on cellular viability of transfecting HCT116/Ch3 cells with either 0.75% (v/v) HiPerFect vehicle, non-targeting siRNA, or siRNA targeting RAD51 or MLH1 (individual and pooled) prior to treating with MNNG (top panel). Western blot showing the effect of each siRNA on the expression level of MLH1 (bottom panel). Blotting for PARP2 expression acted as a loading control, whilst numbers represent quantification of MLH1 expression for each condition. Schematics of the (f) overall assay design and (g) plate format used in the small molecule screen. All MNNG treatments used a concentration of 7.5 μM, whilst measurement of cellular viability was assessed after 120 hours of subsequent drug-free growth, and is expressed as a fraction of the untreated control. Data represents mean and standard error of three independent experiments (excluding western blots where n=1).

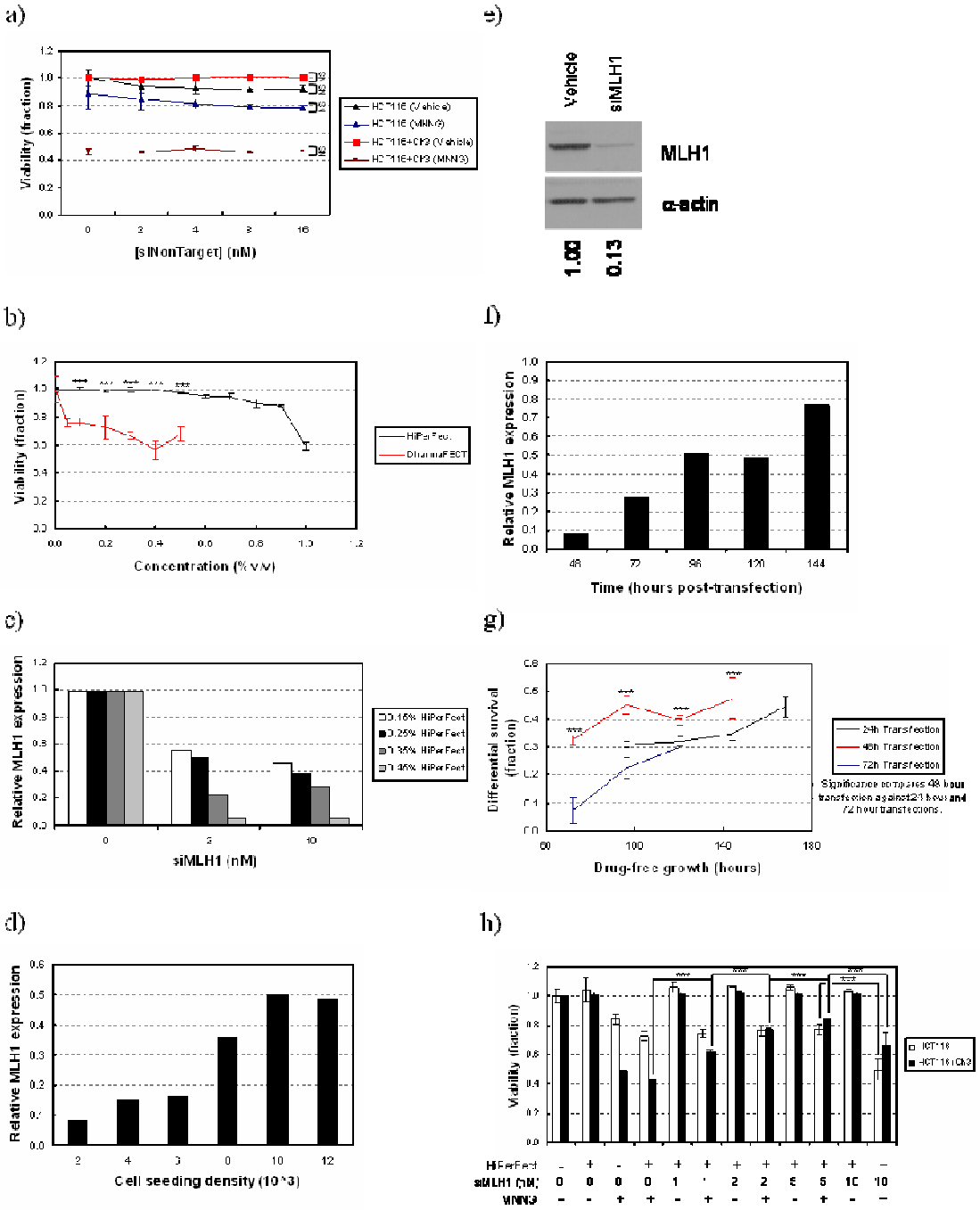
a)
Viability (fraction)
[siNonTarget] (nM)
HCT116 (Vehicle)
HCT116 (MNNG)
HCT116+Ch3 (Vehicle)
HCT116+Ch3 (MNNG)
e)
Vehicle
siMLH1
MLH1
α-actin
1.00
0.13
b)
Viability (fraction)
Concentration (% v/v)
HiPerFect
DharmaFECT
f)
Relative MLH1 expression
Time (hours post-transfection)
c)
Relative MLH1 expression
siMLH1 (nM)
0.15% HiPerFect
0.25% HiPerFect
0.35% HiPerFect
0.45% HiPerFect
g)
Differential survival (fraction)
Drug-free growth (hours)
24h Transfection
48h Transfection
72h Transfection
d)
Relative MLH1 expression
Cell seeding density (10^3)
h)
Viability (fraction)
HCT116
HCT116 Ch3
HiPerFect
siMLH1 (nM)
MNNG

i)

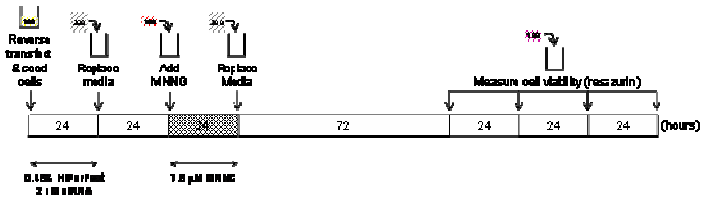
Reverse transfect & seed cells
Replace media
Add MNNG
Replace Media
Measure cell viability (resazurin)
24
24
24
72
24
24
24
(hours)

j)

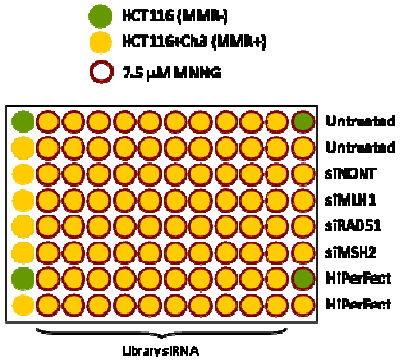
HCT116 (MMR-)
HCT116+Ch3 (MMR+)
7.5 µM MNNG
Untreated
Untreated
siNONT
siMLH1
siRAD51
siMSH2
H1PerFect
H1PerFect
LibrarysiRNA

k)

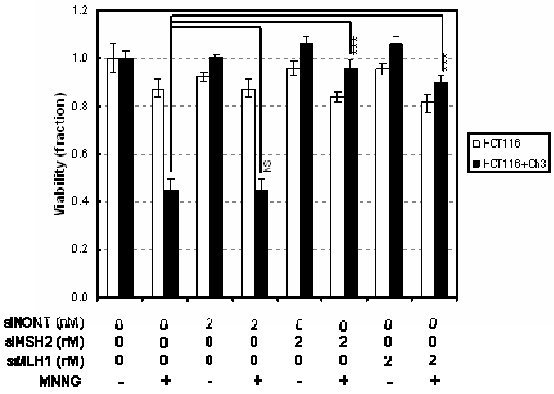
Viability (fraction)
1.2
1.0
0.8
0.6
0.4
0.2
0.0
HCT116
HCT116+Ch3
siNONT (nM) 0 0 2 2 0 2 0 2
siMSH2 (nM) 0 0 0 0 2 2 0 0
siMLH1 (nM) 0 0 0 0 0 0 2 2
MNNG - + - + - + - +

**Figure 3.6. Optimisation of siRNA-mediated knockdowns and design of the RNA interference screen.** (a) Effect of transfecting increasing concentrations of non-targeting siRNA on the cellular viability of vehicle- and MNNG-treated HCT116/Ch3 cells. (b) Cellular viability of HCT116+Ch3 cells following a 24 hour treatment with increasing concentrations of the transfection reagents HiPerFect and DharmaFECT. (c) Effect of a 48 hour transfection of HCT116/Ch3 cells with increasing concentrations of HiPerFect and siMLH on the knockdown efficiency of MLH1. (d) Relative MLH1 expression level resulting from a 48 hour transfection of HCT116+Ch3 cells at the indicated seeding density with 0.45% HiPerFect (v/v) and 2 nM siMLH1. (e) Western blot of HCT116+Ch3 whole cell lysates that were prior transfected with either 0.45% HiPerFect (v/v) alone, or HiPerFect together with 2 nM siMLH1 for 48 hours, and probed for MLH1 expression. Numbers represent quantification of relative MLH1 expression. (f) Quantification of the re-expression of depleted MLH1 at various time points following a 48 hour transfection with 0.45% HiPerFect and 2 nM siMLH1. (g) Optimisation of the transfection length and post-MNNG drug-free incubation length on the differential cellular viability of HCT116/Ch3 cells following a 24 hour treatment with MNNG. (h) Effect of transfection of increasing siMLH1 concentrations on the differential viability of HCT116/Ch3 cells following a 24 hour treatment with either vehicle or MNNG. Schematics of the (i) assay design and (j) plate format that was used in the RNA interference screen. (k) Effect of transfection with non-targeting siRNA or siRNA targeting MLH1 or MSH2 on the cellular viability of MNNG-treated HCT116/Ch3 cells. Unless otherwise stated, all MNNG treatments used a concentration of 7.5 μM, whilst measurement of cellular viability was assessed after 120 hours of subsequent drug-free

growth, and is expressed as a fraction of the untreated control. Data from (c), (d), and (e) represents quantification of a single western blot analysing whole cell lysates that was probed for MLH1 expression using actin as a loading control. MLH1 levels normalised against the actin loading control were expressed relative to MLH1 expression in transfection reagent controls. Data from (a), (g), and (h) represents mean and standard error of three independent experiments.

a)

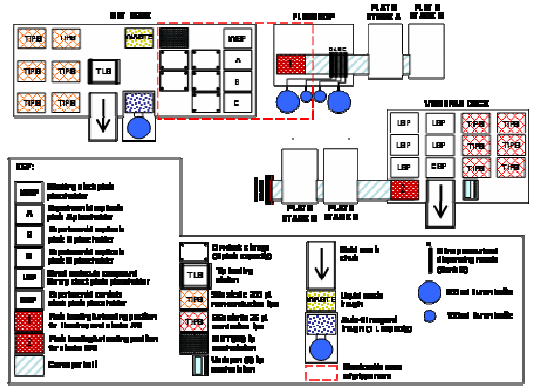

d)

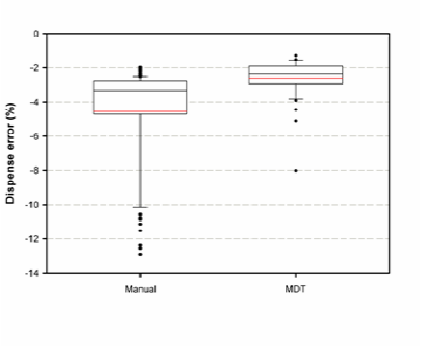
Dispense error (%)
Manual
MDT

b)

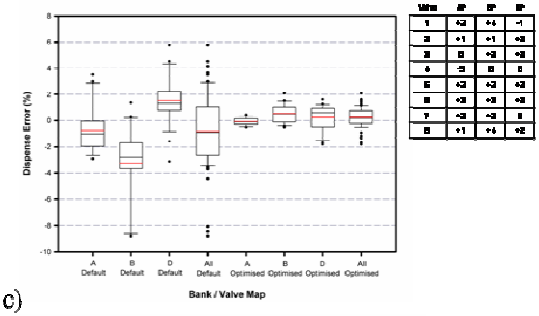
Dispense Error (%)
A Default
B Default
D Default
All Default
A Optimised
B Optimised
D Optimised
All Optimised
Bank / Valve Map

c)

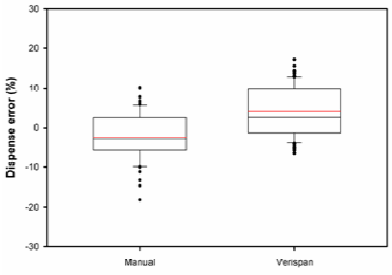
Dispense error (%)
Manual
Verispan

e)

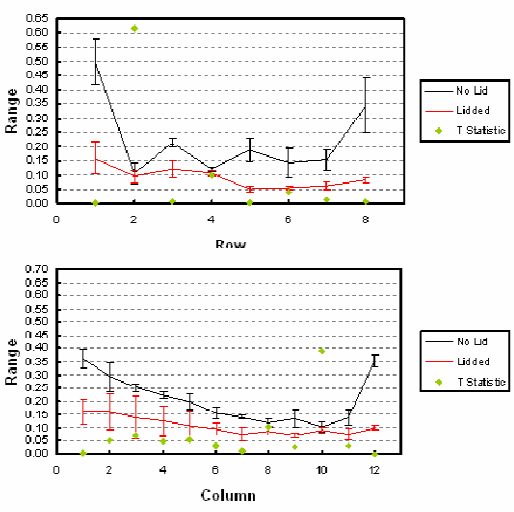
Range
Row
No Lid
Lidded
T Statistic
Range
Column
No Lid
Lidded
T Statistic

**Figure 3.7. Screen automation data.** (a) Schematic showing a top-down view of the robotics platform used to automate the high-throughput screens discussed in this study. (b) Boxplot showing the percentage error in dispensing 200 µl aliquots of cell culture medium by banks A, B and D, in addition to the overall dispense error, of the Perkin Elmer Flexdrop. Data is shown for the optimised valve settings. Comparison between manual pipetting and automated pipetting with the Perkin Elmer (c) Verispan and (d) MDT in terms of the percentage error in dispensing 200 µl aliquots of cell culture medium. (e) Range between the minimum and maximum cellular viability values for each row (top panel) and column (bottom panel) of either lidded or unlidded 96-well plates seeded with 12,000 cells/well and grown for 120 hours, and is expressed as a fraction of the untreated control. Data in figure (e) represents the mean and standard deviation of three replicates obtained from one independent experiment. Data from the remaining figures represent mean and standard error of three independent experiments.

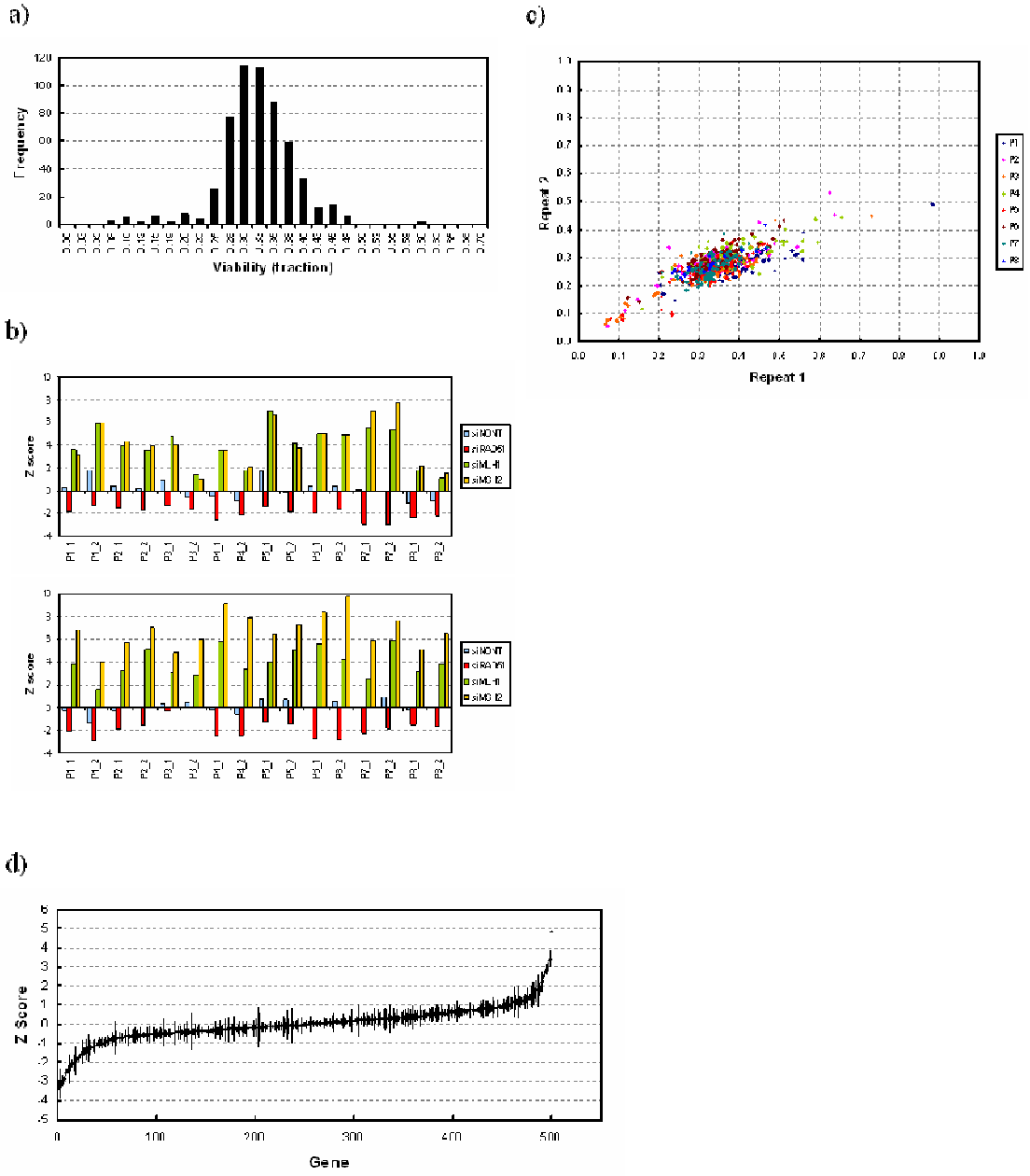
a)
Frequency
Viability (fraction)
c)
Repeat 2
Repeat 1
b)
Z score
siNONT
siRAD51
siMLH1
siMSH2
d)
Z Score
Gene

**Figure 4.1. High-throughput screen for the key genetic determinants of MNNG sensitivity.** (a) Histogram visualising the distribution of cellular viability data obtained from the RNA interference screen. (b) Z scores relating to the negative (RAD51), non-targeting, and positive (MSH2 & MLH1) controls on each plate involved in the first (top panel) and second (bottom panel) repeats of the RNA interference screen. The x axis is labelled with plate number followed by replicate number (e.g. P1_1 refers to plate 1 replicate 1). (c) Plot of replicate data points to reveal the level of correlation between the first and second repeats of the screen. Results for each plate of the library are colour-coded as shown. (d) Overview of the screen data, ordered from low to high by mean Z score with standard error.

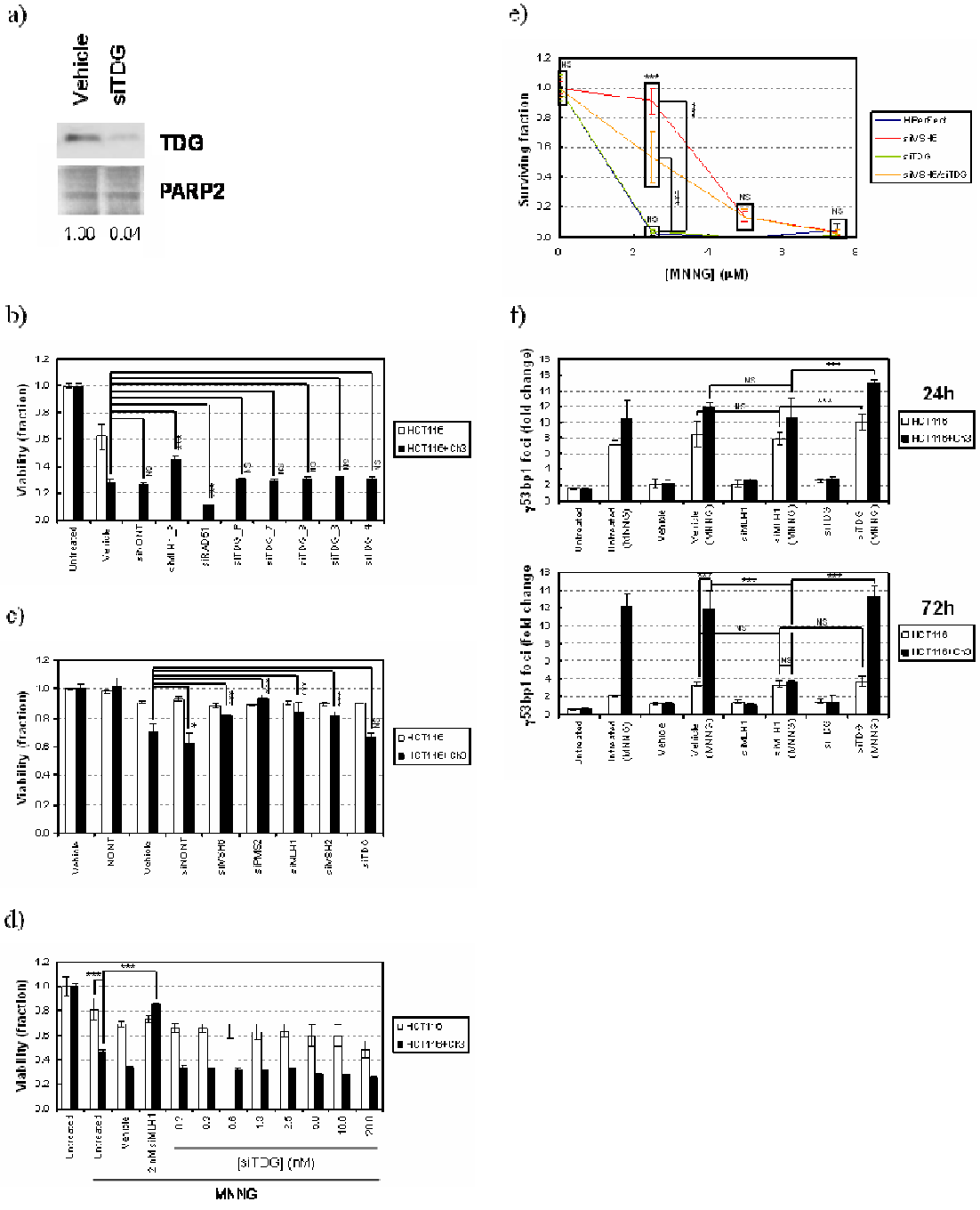
a)
Vehicle
siTDG
TDG
PARP2
1.00 0.04
b)
Viability (fraction)
HCT116
HCT116+CH3
c)
Viability (fraction)
d)
Viability (fraction)
[siTDG] (nM)
MMNG
e)
Surviving fraction
[MNNG] (μM)
f)
γ53bp1 foci (fold change)
24h
72h

**Figure 4.2. TDG validation data.** (a) Western blot showing whole cell lysates of vehicle- and siTDG-transfected HCT116+Ch3 cells. The blot was probed with antiTDG, whilst anti-PARP2 as a loading control. Quantification of loading control-adjusted TDG expression is shown. (b) Effect of transfection with pooled or individual siRNA targeting TDG expression on the cellular viability of MNNG-treated HCT116+Ch3. Untransfected and mock-transfected HCT116/Ch3 cells were included as controls, in addition to HCT116+Ch3 cells transfected with non-targeting siRNA, or siRNA that targets RAD51 (negative control) or MLH1 (positive control). (c) Use of Dharmacon siRNA to compare the effect of depleting known mismatch repair genes against depletion of TDG on the sensitivity of MNNG-treated HCT116/Ch3, as assessed by cellular viability. (d) Transfection of increasing concentrations of siRNA targeting TDG compared with an optimised depletion of MLH1 on the sensitivity of MNNG-treated HCT116/Ch3 cells. (e) Clonogenic survival of siRNA-transfected cells in which MSH6, TDG, or both MSH6/TDG were depleted and subjected to a 24 hour treatment with the indicated concentration of MNNG before allowing 14 days for colonies to form. (f) Fold-change in the numbers of nuclear γ53bp1 foci in either untransfected-, vehicle-, MLH1- or TDG-depleted cells immediately following a 24 hour (top panel) or 72 hour (bottom panel) treatment with MNNG. Unless otherwise stated, all MNNG treatments used a concentration of 7.5 μM, Qiagen siRNA were used in all experiments, and measurement of cellular viability was assessed after 120 hours of subsequent drug-free growth, and is expressed as a fraction of the untreated control. Vehicle refers to 0.75% (v/v) HiPerFect transfection reagent. Data represents mean and standard error of three independent experiments

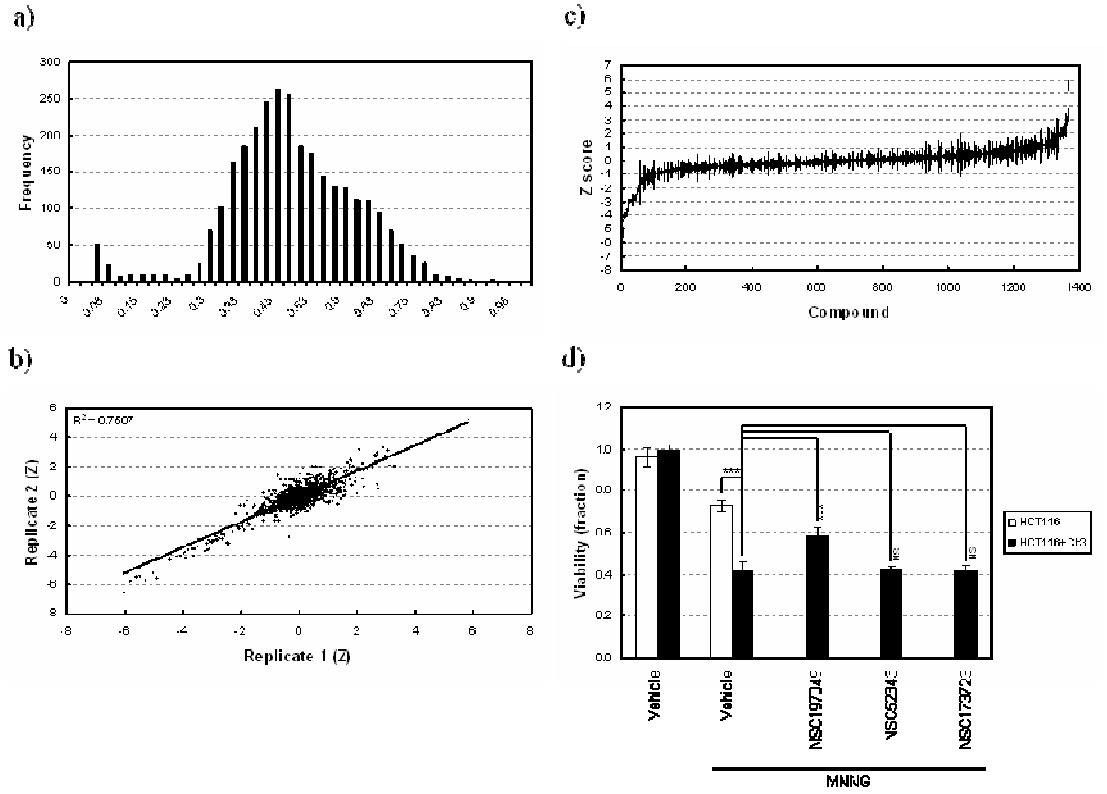
a)
Frequency
c)
Z score
Compound
b)
Replicate 2 (Z)
Replicate 1 (Z)
d)
Viability (fraction)
HCT116
HCT116+CR3
Vehicle
Vehicle
MNNG

**Figure 5.1. High-throughput screen for small molecule structures that decrease sensitivity to MNNG.** (a) Histogram visualising the distribution of cellular viability data obtained from the small molecule screen. (b) Scatter plot showing the level of correlation between the first and second replicate plates of the screen. (c) Overview of the screen data, ordered from low to high by mean Z score with standard error. (d) Repeat of the screening assay on the three hit compounds identified from the primary screen, all assayed at a final concentration of 10 μM. All MNNG treatments used a concentration of 7.5 μM, whilst measurement of cellular viability was assessed after 120 hours of subsequent drug-free growth, and is expressed as a fraction of the untreated control. Data from figure d represents mean and standard error of three independent experiments.

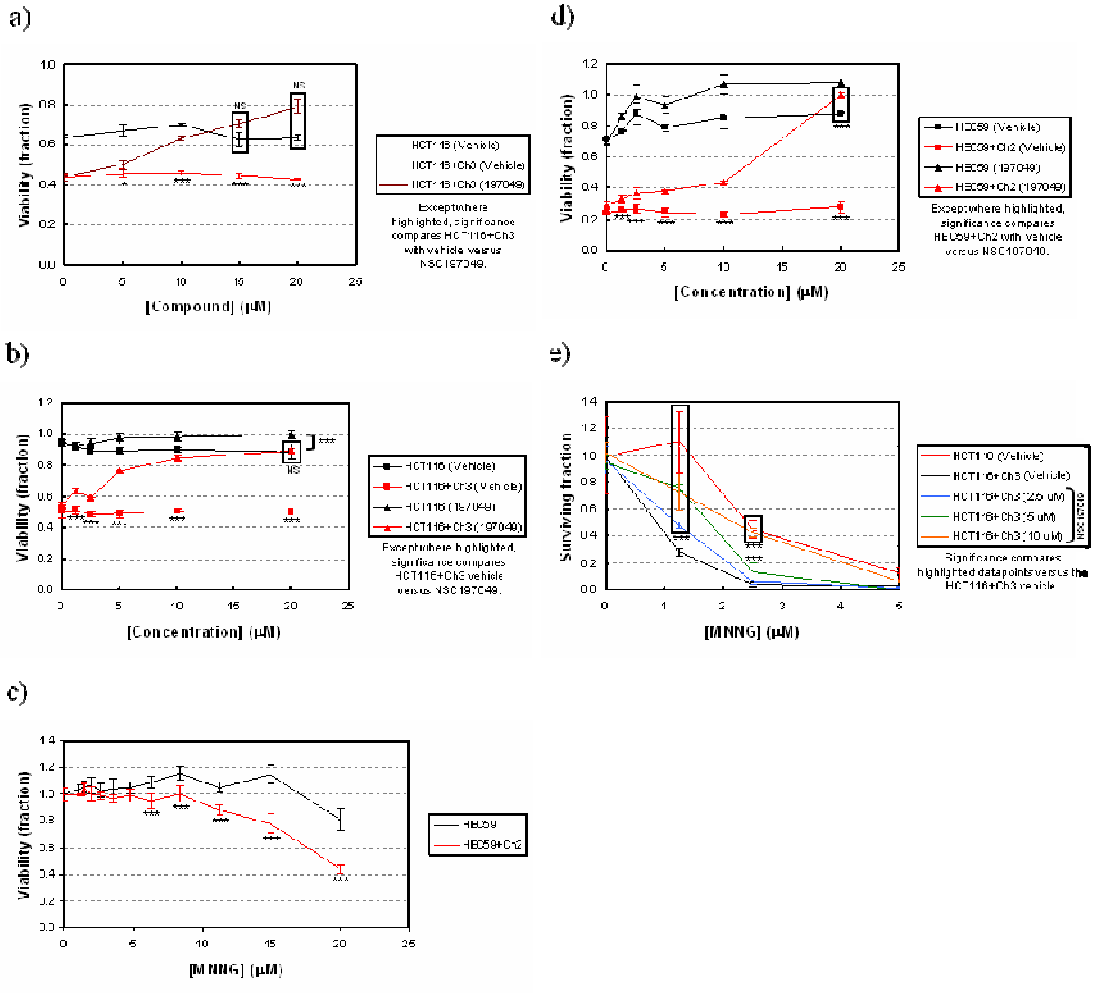
a)
Viability (fraction)
[Compound] (μM)
HCT-15 (Vehicle)
HCT-15+Ch3 (Vehicle)
HCT-15+Ch3 (197049)
Except where highlighted, significance compares HCT-15+Ch3 with vehicle versus NSC 197049.
d)
Viability (fraction)
[Concentration] (μM)
HEC59 (Vehicle)
HEC59+Ch2 (Vehicle)
HEC59 (197049)
HEC59+Ch2 (197049)
Except where highlighted, significance compares HEC59+Ch2 with vehicle versus NSC107040.
b)
Viability (fraction)
[Concentration] (μM)
HCT116 (Vehicle)
HCT116+Ch3 (Vehicle)
HCT116 (197049)
HCT116+Ch3 (197049)
Except where highlighted, significance compares HCT116+Ch3 vehicle versus NSC 197049.
e)
Surviving fraction
[MNNG] (μM)
HCT116 (Vehicle)
HCT116+Ch3 (Vehicle)
HCT116+Ch3 (2.5 uM)
HCT116+Ch3 (5 uM)
HCT116+Ch3 (10 uM)
NSC107040
Significance compares highlighted data points versus the HCT116+Ch3 vehicle
c)
Viability (fraction)
[MNNG] (μM)
HEC59
HEC59+Ch2

**Figure 5.2. Small molecule hit validation.** Cellular viability of MNNG-treated HCT116/Ch3 cells that were co-treated with increasing doses of DMSO vehicle or (a) library stocks of NSC197049 or (b) new stocks of NSC197049. (c) Differential survival of MMR-deficient HEC59 and MMR-proficient HEC59+Ch2 cells following a 24 hour treatment with increasing doses of MNNG (d) Cellular viability of HEC59/Ch2 cells treated with 20 μM MNNG together with increasing doses of either DMSO vehicle or 10 μM NSC197049. (e) Clonogenic survival of HCT116/Ch3 cells co-treated for 24 hours with the indicated concentration of MNNG and either 2.5 μM, 5 μM, or 10 μM NSC197049, and grown for 14 days before quantification of colonies. Unless otherwise stated, all MNNG treatments used a concentration of 7.5 μM, whilst measurement of cellular viability was assessed after 120 hours of subsequent drug-free growth, and is expressed as a fraction of the untreated control. Data represents mean and standard error of three independent experiments.

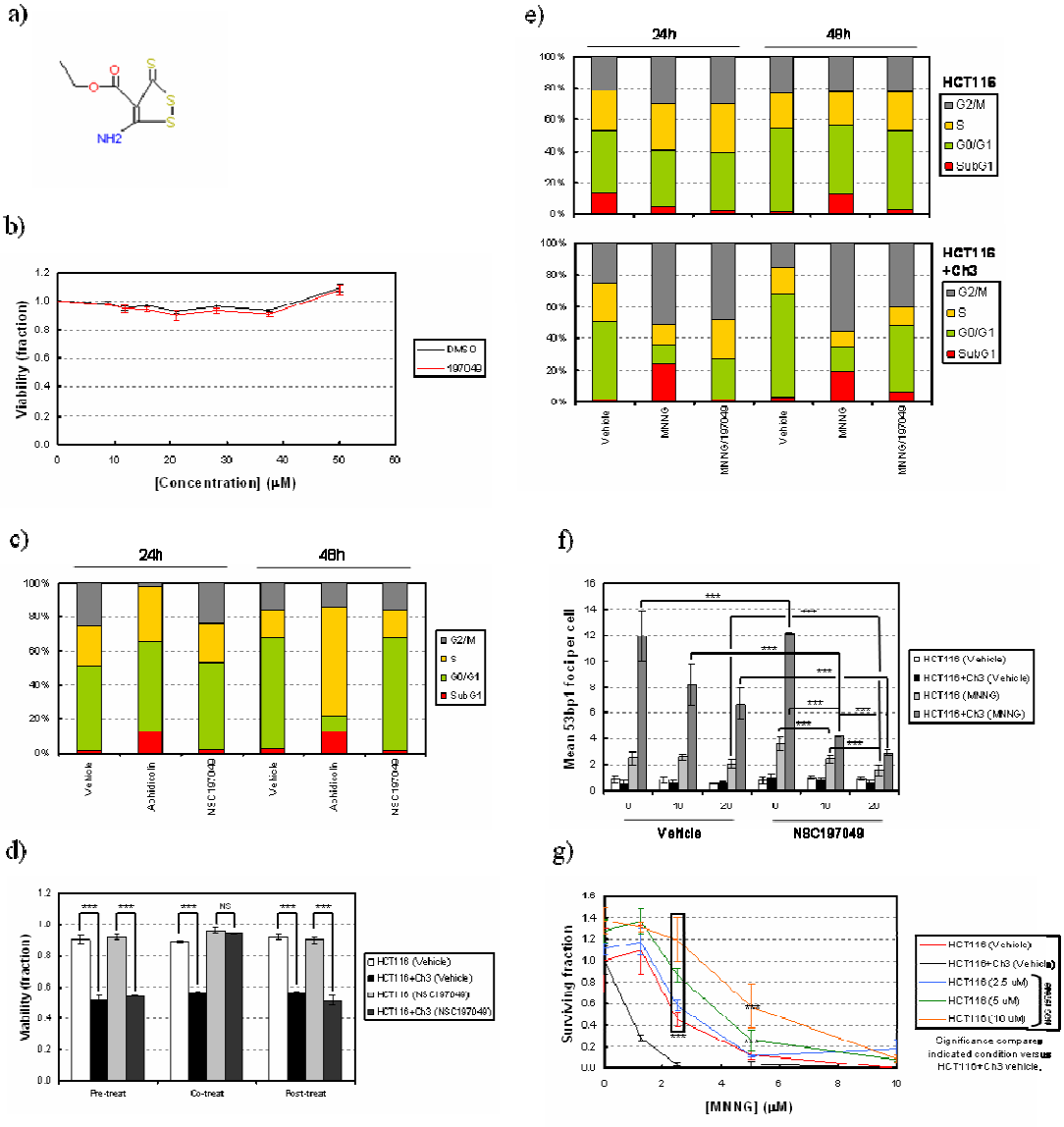
a)
NH2
b)
Viability (fraction)
[Concentration] (μM)
DMSO
197049
c)
24h
48h
G2/M
S
G0/G1
Sub G1
Vehicle
Acihdicolin
NSC197049
d)
Viability (fraction)
HCT116 (Vehicle)
HCT116+Ch3 (Vehicle)
HCT116 (NSC197049)
HCT116+Ch3 (NSC197049)
Pre-treat
Co-treat
Post-treat
NS
e)
24h
48h
HCT116
HCT116 +Ch3
G2/M
S
G0/G1
SubG1
Vehicle
MNNG
MNNG/197049
f)
Mean 53bp1 foci per cell
HCT116 (Vehicle)
HCT116+Ch3 (Vehicle)
HCT116 (MNNG)
HCT116+Ch3 (MNNG)
Vehicle
NSC197049
g)
Surviving fraction
[MNNG] (μM)
HCT116 (Vehicle)
HCT116+Ch3 (Vehicle)
HCT116 (2.5 uM)
HCT116 (5 uM)
HCT116 (10 uM)
Significance compares indicated condition versus HCT116+Ch3 Vehicle.

**Figure 5.3. Characterisation of NSC197049 chemoprotection.** (a) 2D molecular structure of NSC197049. (b) Cellular viability of HCT116+Ch3 cells following a 24 hour treatment with the indicated concentration of NSC197049. (c) Cell-cycle distribution of HCT116+Ch3 cells treated with either DMSO vehicle, 5 μM aphidicolin, or 10 μM NSC197049 for 24 hours and 48 hours. (d) Cellular viability of HCT116/Ch3 cells treated for 3 hours with 10 μM NSC197049 or DMSO vehicle either 3 hours prior to, during, or after a 3 hour treatment with MNNG. (e) Cell-cycle distribution of HCT116 (top panel) and HCT116+Ch3 (bottom panel) cells treated with either DMSO vehicle, MNNG alone, or MNNG and 10 μM NSC197049 for 24 hours. Cell-cycle profiles were obtained 24 hours and 48 hours after treatment addition. (f) Formation of nuclear p53bp1 foci in HCT116+Ch3 cells co-treated for 24 hours with MNNG or DMSO vehicle, together with the indicated concentration of NSC197049 or DMSO vehicle. (g) Clonogenic survival data of HCT116 cells co-treated for 24 hours with the indicated concentration of MNNG with either 2.5 μM, 5 μM, or 10 μM NSC197049, in which colonies were stained and counted after 14 days of subsequent growth. Unless otherwise stated, all MNNG treatments used a concentration of 7.5 μM, whilst measurement of cellular viability was assessed after 120 hours of subsequent drug-free growth, and is expressed as a fraction of the untreated control. Cell-cycle experiments represent the mean of 20,000 events from a single experiment. All data except cell cycle analyses represents mean and standard error of three independent experiments. Cell cycle analyses represent the mean of 10,000 events from a single independent experiment.

a)

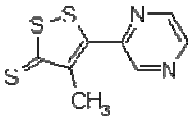
S
S
S
N
N
CH3

b)

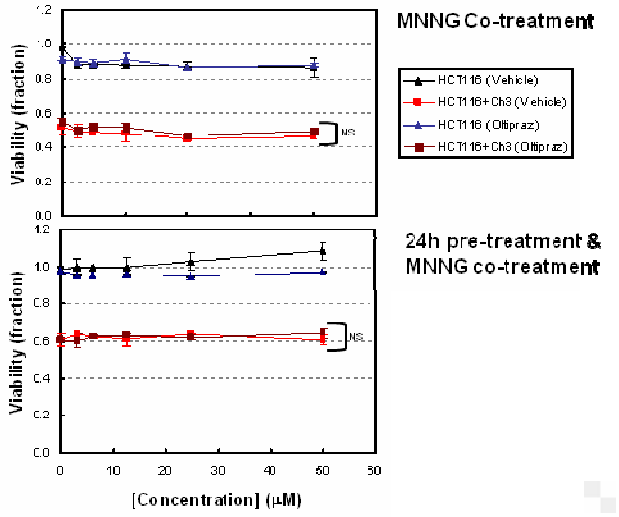
MNNG Co-treatment
HCT116 (Vehicle)
HCT116+Ch3 (Vehicle)
HCT116 (Olipraz)
HCT116+Ch3 (Olipraz)
NS
24h pre-treatment &
MNNG co-treatment
NS
Viability (fraction)
[Concentration] (μM)

c)

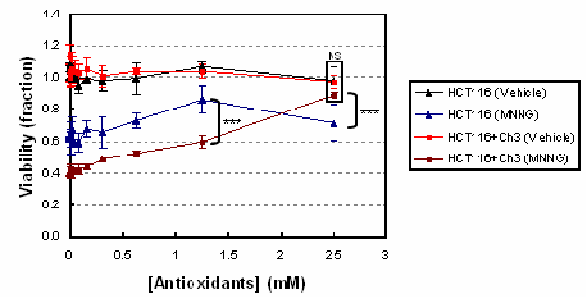
HCT 116 (Vehicle)
HCT 116 (MNNG)
HCT 116+Ch3 (Vehicle)
HCT 116+Ch3 (MNNG)
NS
***
***
Viability (fraction)
[Antioxidants] (mM)

d)

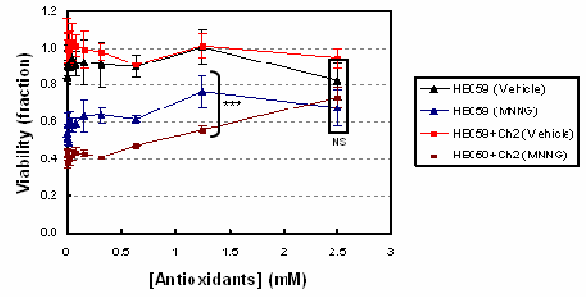
HEC59 (Vehicle)
HEC59 (MNNG)
HEC59+Ch2 (Vehicle)
HEC59+Ch2 (MNNG)
***
NS
Viability (fraction)
[Antioxidants] (mM)

**Figure 5.4. Effect of Oltipraz and antioxidants on MNNG sensitivity.** (a) 2D molecular structure of Oltipraz. (b) Cellular viability of HCT116/Ch3 cells co-treated with MNNG and the indicated concentration of Oltipraz for 24 hours, with (bottom panel) or without (top panel) a 24 hour Oltipraz pre-treatment. Effect of the indicated concentration of antioxidants on the cellular viability of (c) HCT116/Ch3 and (d) HEC59/Ch2 cells co-treated for 24 hours with MNNG. MNNG concentrations of 7.5 μM were used where stated, except for HEC59/Ch2 cells in which 20 μM was used. Measurement of cellular viability was assessed after 120 hours of subsequent drug-free growth, and is expressed as a fraction of the untreated control. DMSO vehicles were used throughout all experiments. Data represents mean and standard error of three independent experiments.

a)

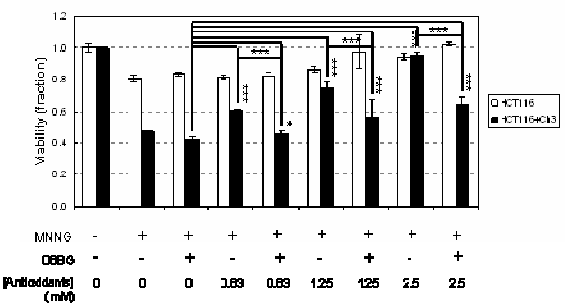
Viability (fraction)
HCT116
HCT116+Ch3
MNNG
DEBG
[Antioxidants] (mM)

b)

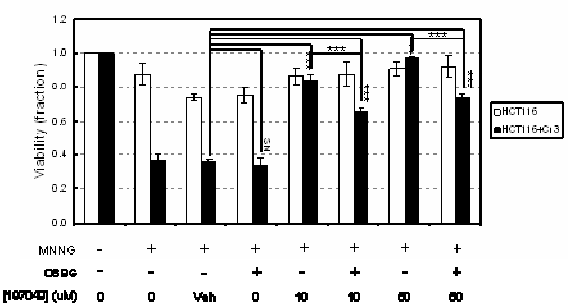
Viability (fraction)
HCT116
HCT116+Ch3
MNNG
cspc
[10074G2] (uM)
Veh

**Figure 5.5. Protection against $O^6$-methylguanine toxicity by antioxidants and NSC197049.** (a) Effect of increasing concentrations of (a) antioxidants or (b) NSC197049 on the cellular viability of HCT116/Ch3 cells treated for 24 hours with DMSO vehicle or 7.5 μM MNNG, plus or minus the addition of 50 μM $O^6$-benzylguanine. Measurement of cellular viability was assessed after 120 hours of subsequent drug-free growth, and is expressed as a fraction of the untreated control. Data represents mean and standard error of three independent experiments.

# CHAPTER EIGHT

*References*

**Aaltonen, P., Peltomaki, P., Leach, F. S., Sistonen, P., Pylkkanen, L., Mecklin, J. P., Jarvinen, H., Powell, S. M., Jen, J., Hamilton, S. R., *et al*.** (1993) Clues to the pathogenesis of familial colorectal cancer. *Science* **260**: 812-816.

**Acharya, S., Wilson, T., Gradia, S., Kane, M. F., Guerrette, S., Marsischky, G. T., Kolodner, R. & Fishel, R.** (1996) hMSH2 forms specific mispair-binding complexes with hMSH3 and hMSH6. *Proceedings of the National Academy of Sciences* **93**: 13629-13634.

**Acton, E. M., Narayanan, V. L., Risbood, P. A., Shoemaker, R. H., Vistica, D. T. & Boyd, M. R.** (1994) Anti-cancer specificity of some ellipticinium salts against human brain tumors *in vitro*. *Journal of Medicinal Chemistry* **37**: 2185-2189.

**Adamson, A. W., Beardsley, D. I., Kim, W. J., Gao, Y., Baskaran, R. & Brown, K. D.** (2005) Methylator-induced, mismatch repair-dependent G2 arrest is activated through Chk1 and Chk2. *Molecular Biology of the Cell* **16**: 1513-1526.

**Adhikari, S., Choudhury, S., Mitra, P. S., Dubash, J. J., Sajankila, S. P. & Roy, R.** (2008) Targeting base excision repair for chemosensitization. *Anti-cancer Agents in Medicinal Chemistry* **8**: 351-357.

**Aebi, S., Fink, D., Gordon, R., Kim, H. K., Zheng, H., Fink, J. L. & Howell, S. B.** (1997) Resistance to cytotoxic drugs in DNA mismatch repair-deficient cells. *Clinical Cancer Research* **3**: 1763-1767.

**Ahmed S. A., Gogal, R. M. & Walsh, J. E.** (1994) A new rapid and simple non-radioactive assay to monitor and determine the proliferation of lymphocytes: an alternative to [3H]thymidine incorporation assay. *Journal of Immunological Methods* **170**: 211-224.

**Alani, E., Sokolsky, T., Studamire, B., Miret, J. J. & Lahue, R. S.** (1997) Genetic and biochemical analysis of Msh2p-Msh6p: role of ATP hydrolysis and Msh2p-Msh6p subunit interactions in mismatch base pair recognition. *Molecular and Cellular Biology* **17**: 2436-2447.

**Alexander, J., Watanabe, T., Wu, T. T., Rashid, A., Li., S. & Hamilton, S. R.** (2001) Histopathological identification of colon cancer with microsatellite instability. *The American Journal of Pathology* **158**: 527-535.

**Almeida, K. H. & Sobol, R. W.** (2007) A unified view of base excision repair: lesion-dependent protein complexes regulated by post-translational modification. *DNA Repair* **6**: 695-711.

**Ansher, S. S., Dolan, P. & Bueding, E.** (1983) Chemoprotective effects of two dithiolethiones and of butylhydroxyanisole against carbon tetrachloride and acetaminophen toxicity. *Hepatology* **3**: 932-935.

**Ansher, S. S., Dolan, P. & Bueding, E.** (1986) Biochemical effects of dithiolthiones. *Food and Chemical Toxicology* **24**: 405-415.

**Arguello, F., Alexander, M. A., Greene, J. F., Stinson, S. F., Jorden, J. L., Smith, E. M., Kalavar, N. T., Alvord, W. G., Klabansky, R. L. & Sausville, E. A.** (1998) Preclinical evaluation of 9-chloro-2-methylellipticinium acetate alone and in combination with conventional anti-cancer drugs for the treatment of human brain tumor xenografts. *Journal of Cancer Research & Clinical Oncology* **124**: 19-26.

**Arora, S., Bisanz, K. M., Peralta, L. A., Basu, G. D., Choudhary, A., Tibes, R. & Azorsa, D. O.** (2010) RNAi screening of the kinome identifies modulators of cisplatin response in ovarian cancer cells. *Gynecologic Oncology* **118**: 220-227.

**Asagoshi, K., Liu, Y., Masaoka, A., Lan, L., Prasad, R., Horton, J. K., Brown, A. R., Wang, X. H., Bdour, H. M., Sobol, R. W., Taylor, J. S., Yasui, A. & Wilson, S. H.** (2010a) DNA polymerase beta-dependent long patch base excision repair in living cells. *DNA Repair* **9**: 109-119.

**Asagoshi, K., Tano, K., Chastain, P. D., Adachi, N., Sonoda, E., Kikuchi, K., Koyama, H., Nagata, K., Kaufman, D. G., Takeda, S., Wilson, S. H., Watanabe, M., Swenberg, J. A. & Nakamura, J.** (2010b) FEN1 functions in long patch base excision repair under conditions of oxidative stress in vertebrate cells. *Molecular Cancer Research* **8**: 204-215.

**Astsaturov, I., Ratushny, V., Sukhanova, A., Einarson, M. B., Bagnyukova, T., Zhou, Y., Devarajan, K., Silverman, J. S., Tikhmyanova, N., Skobeleva, N., Pecherskaya, A., Nasto, R. E., Sharma, C., Jablonski, S. A., Serebriiskii, I. G., Weiner, L. M. & Golemis, E. A.** (2010) Synthetic lethal screen of an EGFR-centered network to improve targeted therapies. *Science Signalling* **3**: ra67.

**Au, K. G., Welsh, K. & Modrich, P.** (1992) Initiation of methyl-directed mismatch repair. *The Journal of Biological Chemistry* **267**: 12142-12148.

**Bai, R., Paull, K. D., Herald, C. L., Malspeis, L., Pettit, G. R. & Hamel, E.** (1991) Halichondrin B and homohalichondrin B, marine natural products binding in the vinca domain of tubulin. *The Journal of Biological Chemistry* **266**: 15882-15889.

**Balansky, R. M., Blagoeva, P. M., Mircheva, Z. I., Stoitchev, I. & Chernozemski, I.** (1986) The effect of antioxidants on MNNG-induced stomach carcinogenesis in rats. *Journal of Cancer Research and Clinical Oncology* **112**: 272-275.

**Banerjee, S. & Flores-Rozas, H.** (2004) Cadmium inhibits mismatch repair by blocking the ATPase activity of the MSH2–MSH6 complex. *Nucleic Acids Research* **33**: 1410-1419.

**Baselga, J., Tripathy, D., Mendelsohn, J., Baughman, S., Benz, C. C., Dantis, L., Sklarin, N. T., Seidman, A. D., Hudis, C. A., Moore, J., Rosen, P. P., Twaddell, T., Henderson, I. C. & Norton, L.** (1996) Phase II study of weekly intravenous recombinant humanized anti-p185HER2 monoclonal antibody in patients with HER2/neu-overexpressing metastatic breast cancer. *Journal of Clinical Oncology* **14**: 737-744.

**Baudot, A., de la Torre, V. & Valencia, A.** (2010) Mutated genes, pathways and processes in tumours. *European Molecular Biology Organisation Reports* **11**: 805-810.

**Beardsley, D. I., Kim, W. J. & Brown, K.** (2005) *N*-Methyl-*N′*-nitro-*N*-nitrosoguanidine activates cell-cycle arrest through distinct mechanisms activated in a dose-dependent manner. *Molecular Pharmacology* **68**: 1049-1060.

**Beckman, R. A.** (2009) Mutator mutations enhance tumorigenic efficiency across fitness landscapes. *PLoS ONE* **4**: e5860.

**Beranek, D. T.** (1990) Distribution of methyl and ethyl adducts following alkylation with monofunctional alkylating agents. *Mutation Research* **231**: 11-30.

**Berns, K., Hijmans, E. M., Mullenders, J., Brummelkamp, T. R., Veids, A., Heimerikx, M., Kerkhoven, R. M., Madiredjo, M., Nijkamp, W., Weigelt, B., Agami, R., Ge, W., Cavet, G., Linsley, P. S., Beijersbergen, R. L. & Bernards, R.** (2004) A large-scale RNAi screen in human cells identifies new components of the p53 pathway. *Nature* **428**: 431-437.

**Bernstein, E., Caudy, A. A., Hammond, S. M. & Hannon, G. J.** (2001) Role for a bidentate ribonuclease in the initiation step of RNA interference. *Nature* **409**: 363-366.

**Biasiak, J., Trzeciak, A., Gasiorowska, A., Drzewoski, J. & Maiecka-Panas, E.** (2002) Vitamin C and quercetin modulate DNA-damaging effect of *N*-methyl-*N'*-nitro-*N*-nitrosoguanidine (MNNG). *Plant Foods for Human Nutrition* **57**: 53-61.

**Bignami, M., O'Driscoll, M., Aquilina, G. & Karran, P.** (2000) Unmasking a killer: DNA $O^6$-methylguanine and the cytotoxicity of methylating agents. *Mutation Research* **462**: 71-82.

**Birmingham, A., Anderson, E. M., Reynolds, A., Ilsley-Tyree, D., Leake, D., Fedorov, Y., Baskerville, S., Maksimova, E., Robinson, K., Karpilow, J., Marshall, W. S. & Khvorova, A.** (2006) 3' UTR seed matches, but not overall identity, are associated with RNAi off-targets. *Nature Methods* **3**: 199-204.

**Birmingham, A., Anderson, E., Sullivan, K., Reynolds, A., Boese, Q., Leake, D., Karpilow, J. & Khvorova, A.** (2007) A protocol for designing siRNAs with high functionality and specificity. *Nature Protocols* **2**: 2068-2078.

**Blackwell, L. J., Martik, D., Bjornson, K. P., Bjornson, E. S. & Modrich, P.** (1998) Nucleotide-promoted release of hMutSα from heteroduplex DNA is consistent with an ATP-dependent translocation mechanism. *The Journal of Biological Chemistry* **273**: 32055-32062.

**Boland, C. R., Thibodeau, S. N., Hamilton, S. R., Sidransky, D., Eshleman, J. R., Burt, R. W., Meltzer, S. J., Rodriguez-Bigas, M. A., Fodde, R., Ranzani, G. N. & Srivastava, S.** (1998) A national cancer institute workshop on microsatellite instability for cancer detection and familial predisposition: development of international criteria for the determination of microsatellite instability in colorectal cancer. *Cancer Research* **58**: 5248-5257.

**Boland, C. R. & Goel, A.** (2010) Microsatellite instability in colorectal cancer. *Gastroenterology* **138**: 2073-2087.

**Bolton, M. G., Muñoz, A., Jacobson, L. P., Groopman, J. D., Maxuitenko, Y. Y., Roebuck, B. D., Kensler, T. W.** (1993) Transient intervention with Oltipraz protects against aflatoxin-induced hepatic tumorigenesis. *Cancer Research* **53**: 3499-3504.

**Boyer, J. C. & Farber, R. A.** (1998) Mutation rate of a microsatellite sequence in normal human fibroblasts. *Cancer Research* **58**: 3946-3949.

**Brideau, C., Gunter, B., Pikounis, B. & Liaw, A.** (2003) Improved statistical methods for hit selection in high-throughput screening. *Journal of Biomolecular Screening* **8**: 634-647.

**Bronner, C. E., Baker, S. M., Morrison, P. T., Warren, G., Smith, L. G., Lescoe, M. K., Kane, M., Earabino, C., Lipford, J., Lindblom, A., Tannergård, P., Bollag, R. J., Godwin, A. R., Ward, D. C., Nordenskjøld, M., Fishel, R., Kolodner, R. & Liskay, R. M.** (1994) Mutation in the DNA mismatch repair gene homologue *hMLH1* is associated with hereditary non-polyposis colon cancer. *Nature* **368**: 258-261.

**Bryant, H. E., Schultz, N., Thomas, H. D., Parker, K. M., Flower, D., Lopez, E., Kyle, S., Meuth, M., Curtin, N. J. & Helleday, T.** (2005) Specific killing of BRCA2-deficient tumours with inhibitors of poly(ADP-ribose) polymerase. *Nature* **434**: 913-917.

**Buckowitz, A., Knaebel, H. P., Benner, A., Bläker, H., Gebert, J., Kienle, P., von Knebel Doeberitz, M. & Kloor, M.** (2005) Microsatellite instability in colorectal cancer is associated with local lymphocyte infiltration and low frequency of distant metastases. *British Journal of Cancer* **92**: 1746-1753.

**Buetler, T. M., Gallagher, E. P., Wang, C., Stahl, D. L., Hayes, J. D. & Eaton, D. L.** (1995) Induction of phase I and phase II drug-metabolizing enzyme mRNA, protein, and activity by BHA, ethoxyquin, and oltipraz. *Toxicology and Applied Pharmacology* **135**: 45-57.

**Burdett, V., Baitinger, C., Viswanathan, M., Lovett, S. T. & Modrich, P.** (2001) *In vivo* requirement for RecJ, ExoVII, ExoI, and ExoX in methyl-directed mismatch repair. *Proceedings for the National Academy of Sciences U.S.A.* **98**: 6765-6770.

**Burgers, P. M.** (2009) Polymerase dynamics at the eukaryotic DNA replication fork. *The Journal of Biological Chemistry* **284**: 4041-4045.

**Burt, S. M., Carter, T. J. & Kircka, L. J.** (1979) Thermal characteristics of microtitre plates used in immunological assays. *Journal of Immunological Methods* **31**: 231-236.

**Calabrese, E. J.** (1994) Biological effects of low level exposures: dose-response relationships. Boca Raton: CRC Press.

**Cannavo, E., Gerrits, B., Marra, G., Schlapbach, R. & Jiricny, J.** (2007) Characterisation of the interactome of the human MutL homologues, MLH1, PMS1, and PMS2. *The Journal of Biological Chemistry* **282**: 2976-2986.

**Capdeville, R., Buchdunger, E., Zimmermann, J. & Matter, A.** (2002) Glivec (STI571, Imatinib), a rationally developed, targeted anti-cancer drug. *Nature Reviews Drug Discovery* **1**: 493-502.

**Carelle, N., Piotto, E., Bellanger, A., Germanaud, J., Thuillier, A. & Khayat, D.** (2002) Changing patient perceptions of the side-effects of cancer chemotherapy. *Cancer* **95**: 155-163.

**Carethers, J. M., Chauhan, D. P., Fink, D., Nebel, S., Bresalier, R. S., Howell, S. B. & Boland, C. R.** (1999) Mismatch repair proficiency and in vitro response to 5-fluorouracil. *Gastroenterology* **117**: 123-131.

**Cascinu, S., Cordella, L., Del Ferro, E., Fronzoni, M. & Catalano, G.** (1995) Neuroprotective effect of reduced glutathione on cisplatin-based chemotherapy in advanced gastric cancer: a randomized double-blind placebo-controlled trial. *Journal of Clinical Oncology* **13**: 26-32.

**Cascinu, S., Catalano, V., Cordella, L., Labianca, R., Giordani, P., Baldelli, A. M., Beretta, G. D., Ubiali, E., Catalano, G.** (2002) Neuroprotective effect of reduced glutathione on oxaliplatin-based chemotherapy in advanced colorectal cancer: A randomized, double-blind, placebo-controlled trial. *Journal of Clinical Oncology* **20**: 3478-3483.

**Cejka, P., Stojic, L., Mojas, N., Russell, A. M., Heinimann, K., Cannavó, E., di Pietro, M., Marra, G. & Jiricny, J.** (2003) Methylation-induced G2/M arrest requires a full complement of the mismatch repair protein hMLH1. *European Molecular Biology Organisation Journal* **22**: 2245-2254.

**Cejka, P., Mojas, N., Gillet, L., Schar, P. & Jiricny, J.** (2005) Homologous recombination rescues mismatch-repair-dependent cytotoxicity of S(N)1-type methylating agents in *S. cerevisiae*. *Current Biology* **15**: 1395-1400.

**Cejka, P. & Jiricny, J.** (2008) Interplay of DNA repair pathways controls methylation damage toxicity in *Saccharomyces cerevisiae*. *Genetics* **179**: 1835-1844.

**Cerea, G., Vaghi, M., Ardizzoia, A., Villa, S., Bucovec, R., Mengo, S., Gardani, G., Tancini, G. & Lissoni, P.** (2003) Biomodulation of cancer chemotherapy for metastatic colorectal cancer: a randomized study of weekly low-dose irinotecan alone versus irinotecan plus the oncostatic pineal hormone melatonin in metastatic colorectal cancer patients progressing on 5-fluorouracil-containing combinations. *Anti-cancer Research* **23**: 1951-1954.

**Chi, N. W. & Kolodner, R. D.** (1994) The effect of DNA mismatches on the ATPase activity of MSH1, a protein in yeast mitochondria that recognises DNA mismatches. *The Journal of Biological Chemistry* **269**: 29993-29997.

**Citti, L., Mariani, L., Capecchi, B., Piras, A., Leuzzi, R. & Rainaldi, G.** (1998) The sensitisation of cells treated with $O^6$-methylguanine to alkylation damage is affected by the number of $O^6$-methylguanine-DNA-methyltransferase molecules escaped from inactivation. *Mutation Research / DNA Repair* **409**: 173-179.

**Claij, N. & te Riele, H.** (2002) Methylation tolerance in mismatch repair proficient cells with low MSH2 protein level. *Oncogene* **21**: 2873-2879.

**Clapper, M. L., Wood, M., Leahy, K., Lang, D., Miknyoczki, S. & Ruggeri, B. A.** (1995) Chemopreventive activity of Oltipraz against N-nitrosobis(2-oxopropyl)amine (BOP)-induced ductal pancreatic carcinoma development and effects on survival of Syrian goldern hamsters. *Carcinogenesis* **16**: 2159-2165.

**Clark, A. B. & Kunkel, T. A.** (2004) Cadmium inhibits the functions of eukaryotic MutS complexes. *The Journal of Biological Chemistry* **279**: 53903-53906.

**Clark, O., Engel, T., Clark, L., Paladini, L., Faleiros, E. & Pegoretti, B.** (2009) Efficacy of palonosetron (PAL) compared to other serotonin inhibitors (5-HT3R) in preventing chemotherapy-induced nausea and vomiting (CINV) in patients receiving moderately or highly emetogenic (MoHE) treatments: Systematic review and meta-analysis. *Journal of Clinical Oncology* **27**: e20620.

**Coates, A., Abraham, S., Kaye, S. B., Sowerbutts, T., Frewin, C., Fox, R. M. & Tattersall, M. H.** (1983) On the receiving end-patient perception of the side-effects of cancer chemotherapy. *European Journal of Cancer & Clinical Oncology* **19**: 203-208.

**Cobleigh, M. A., Vogel, C. L., Tripathy, D., Robert, N. J., Scholl, S., Fehrenbacher, L., Wolter, J. M., Paton, V., Shak, S., Lieberman, G. & Slamon, D. J.** (1999) Multinational study of the efficacy and safety of humanized anti-HER2 monoclonal antibody in women who have HER2-overexpressing metastatic breast cancer that has progressed after chemotherapy for metastatic disease. *Journal of Clinical Oncology* **17**: 2639-2648.

**Colella, G., Marchini, S., D'Incalci, M., Brown, R., & Broggini, M.** (1999). Mismatch repair deficiency is associated with resistance to DNA minor groove alkylating agents. *British Journal of Cancer* **80**: 338-343.

**Collins, A. R.** (2004) The comet assay for DNA damage and repair: principles, applications, and limitations. *Molecular Biotechnology* **26**: 249-261.

**Constantin, N., Dzantiev, L., Kadyrov, F. A. & Modrich, P.** (2005) Human mismatch repair: reconstitution of a nick-directed bi-directional reaction. *The Journal of Biological Chemistry* **280**: 39752-39761.

**Cortázar, D., Kunz, C., Saito, Y., Steinacher, R. & Schär, P.** (2007) The enigmatic thymine DNA glycosylase. *DNA Repair* **6**: 489-504.

**Crouse, G. F.** (2010) An end for mismatch repair. *Proceedings of the National Academy of Sciences* **107**: 20851-20852.

**Cunningham, J. M., Christensen, E. R., Tester, D. J., Kim, C. Y., Roche, P. C., Burgart, L. J. & Thibodeau, S. N.** (1998) Hypermethylation of the *hMLH1* promoter in colon cancer with microsatellite instability. *Cancer Research* **58**: 3455-3460.

**Curtin, N. J., Wang, L. Z., Yiakouvaki, A., Kyle, S., Arris, C. A., Canan-Koch, S., Webber, S. E., Durkacz, B. W., Calvert, H. A., Hostomsky, Z. & Newell, D. R.** (2004) Novel poly(ADP-ribose) polymerase-1 inhibitor, AG14361, restores sensitivity to temozolomide in mismatch repair-deficient cells. *Clinical Cancer Research* **10**: 881-889.

**D'Andrea, G. M.** (2005) Use of antioxidants during chemotherapy and radiotherapy should be avoided. *CA: A Cancer Journal for Clinicians* **55**: 319-321.

**Dao, V. & Modrich, P.** (1998) Mismatch-, MutS-, MutL-, and helicase II-dependent unwinding from the single-strand break of an incised heteroduplex. *The Journal of Biological Chemistry* **273**: 9202-9207.

**Daub, H., Specht, K., Ullrich, A.** (2004) Strategies to overcome resistance to targeted protein kinase inhibitors. *Nature Reviews Drug Discovery* **3**: 1001-1010.

**Demicheli, R., Pratesi, G. & Foroni, R.** (1991) The exponential-Gompertzian tumor growth model: data from six tumor cell lines *in vitro* and *in vivo*. Estimate of the transition point from exponential to Gompertzian growth and potential clinical implications. *Tumori* **77**: 189-195.

**Ding, S. W. & Voinnet, O.** (2007) Antiviral immunity directed by small RNAs. *Cell* **130**: 413-426.

**Dmitrieva, N. I. & Burg, M. B.** (2005) Hypertonic stress response. *Mutation Research* **569**: 65-74.

**Dolan, M. E., Pegg, A. E., Dumenco, L. L., Moschel, R. C. & Gerson, S. L.** (1991) Comparison of the inactivation of mammalian and bacterial $O^6$-alkylguanine-DNA alkyltransferases by $O^6$-benzylguanine and $O^6$-methylguanine. *Carcinogenesis* **12**: 2305-2309.

**Donson, A. M., Addo-Yobo, S. O., Handler, M. H., Gore, L. & Foreman, N. K.** (2007) MGMT promoter methylation correlates with survival benefit and sensitivity to temozolomide in pediatric glioblastoma. *Pediatric Blood & Cancer* **48**: 403-407.

**Drotschmann, K., Shcherbakova, P. V., Wang, H., Erie, D. A., Brownewell, F. R., Kool, E. T. & Kunkel, T. A.** (2002) DNA binding properties of the yeast Msh2-Msh6 and Mlh1-Pms1 heterodimers. *Biological Chemistry* **383**: 969-975.

**Drummond, J. T., Genschel, J., Wolf, E. & Modrich, P.** (1997) DHFR/MSH3 amplification in methotrexate-resistant cells alters the hMutSalpha/hMutSbeta ratio and reduces the efficiency of base-base mismatch repair. *Proceedings of the National Academy of Sciences* **94**: 10144-10149.

**Drummond, J. T. & Bellacosa, A.** (2001) Human DNA mismatch repair *in vitro* operates independently of methylation status at CpG sites. *Nucleic Acids Research* **29**: 2234-2243.

**Duan, Z., Choy, E. & Hornicek, F. J.** (2009) NSC23925, identified in a high-throughput cell-based screen, reverses multidrug resistance. *PLoS One* **4**: e7415.

**Duncan, B. K. & Miller, J. H.** (1980) Mutagenic deamination of cytosine residues in DNA. *Nature* **287**: 560-561.

**Dunkern, T., Roos, W. & Kaina, B.** (2003) Apoptosis induced by MNNG in human TK6 lymphoblastoid cells is p53 and Fas/CD95/Apo-1 related. *Mutation Research* **544**: 167-172.

**Dzantiev, L., Constantin, N., Genschel, J., Iyer, R. R., Burgers, P. M. & Modrich, P.** (2004) A defined human system that supports bi-directional mismatch-provoked excision. *Molecular Cell* **15**: 31-41.

**Edwards, S. L., Brough, R., Lord, C. J., Natrajan, R., Vatcheva, R., Levine, D. A., Boyd, J., Reis-Filho, J. S. & Ashworth, A.** (2008) Resistance to therapy caused by intragenic deletion in *BRCA2*. *Nature* **451**: 1111-1115.

**Ekambaram, G., Rajendran, P., Magesh, V. & Sakthisekaran, D.** (2008) Naringenin reduces tumor size and weight lost in *N*-methyl-*N'*-nitro-*N*-nitrosoguanidine-induced gastric carcinogenesis in rats. *Nutrition Research* **28**: 106-112.

**Elbashir, S. M., Harborth, J., Lendeckel, W., Yalcin, A., Weber, K. & Tuschl, T.** (2001) Duplexes of 21-nucleotide RNAs mediate RNA interference in cultured mammalian cells. *Nature* **411**: 494-498.

**Engelward, B. P., Boosalis, M. S., Chen, B. J., Deng, Z., Siciliano, M. J., Samson, L. D.** (1993) Cloning and characterization of a mouse 3-methyladenine/7-methylguanine/3-methylguanine DNA glycosylase cDNA whose gene maps to chromosome 11. *Carcinogenesis* **14**: 175-181.

**Fackenthal, J. D. & Olopade, O. I.** (2007) Breast cancer risk associated with *BRCA1* and *BRCA2* in diverse populations. *Nature Reviews Cancer* **7**: 937-948.

**Fahey, J. W., Haristoy, X., Dolan, P. M., Kensler, T. W., Scholtus, I., Stephenson, K. K., Talalay, P. & Lozniewski, A.** (2002) Sulforaphane inhibits extracellular, intracellular, and antibiotic-resistant strains of *Helicobacter pylori* and prevents benzo[a]pyrene-induced stomach tumours. *Proceedings of the National Academy of Sciences U.S.A.* **99**: 7610-7615.

**Falnes, P. Ø., Johansen, R. G. & Seeberg, E.** (2002) AlkB-mediated oxidative demethylation reverses DNA damage in *Escherichia coli*. **419**: 178-182.

**Falsaperta, M., Morgia, G., Tartarone, A., Ardito, R. & Romano, G.** (2005) Support ellagic acid therapy in patients with hormone refractory prostate cancer (HRPC) on standard chemotherapy using vinorelbine and estramustine phosphate. *European Urology* **47**: 449-455.

**Fang, W. & Modrich, P.** (1993) Human strand-specific mismatch repair occurs by a bi-directional mechanism similar to that of the bacterial reaction. *The Journal of Biological Chemistry* **268**: 11838-11844.

**Farmer, H., McCabe, N., Lord, C. J., Tutt, A. N. J., Johnson, D. A., Richardson, T. B., Santarosa, M., Dillon, K. J., Hickson, I., Knights, C., Martin, N. M. B., Jackson, S. P., Smith, G. C. M. & Ashworth, A.** (2005) Targeting the DNA repair defect in *BRCA* mutant cells as a therapeutic strategy. *Nature* **434**: 917-921.

**Fedier, A., Schwarz, V. A., Walt, H., Carpini, R. D., Haller, U. & Fink, D.** (2001) Resistance to topoisomerase poisons due to loss of DNA mismatch repair. *International Journal of Cancer* **93**: 571-576.

**Feng, Z., Scott, S. P., Bussen, W., Sharma, G. G., Guo, G., Pandita, T. K. & Powell, S. N.** (2011) Rad52 inactivation is synthetically lethal with BRCA2 deficiency. *Proceedings of the National Academy of Sciences U.S.A.* **108**: 686-691.

**Fink, D., Nebel, S., Aebi, S., Zheng, H., Cenni, B., Nehme, A., Christen, R. D. & Howell, S. B.** (1996). The role of DNA mismatch repair in platinum drug resistance. *Cancer Research* **56**: 4881-4886.

**Fire, A., Xu, S., Montgomery, M. K., Kostas, S. A., Driver, S. E. & Mello, C. C.** (1998) Potent and specific genetic interference by double-stranded RNA in *Caenorhabditis elegans*. *Nature* **391**: 806-811.

**Fishel, R., Lescoe, M. K., Rao, M. R., Copeland, N. G., Jenkins, N. A., Garber, J., Kane, M. & Kolodner, R.** (1993) The human mutator gene homolog MSH2 and its association with hereditary nonpolyposis colon cancer. *Cell* **75**: 1027-1038.

**Flores-Rozas, H. & Kolodner, R. D.** (1998) The *Saccharomyces cerevisiae* MLH3 gene functions in MSH3-dependent suppression of frameshift mutations. *Proceedings of the National Academy of Sciences U.S.A.* **95**: 12404-12409.

**Foltínová, P., Lahitová, N. & Ebringer, L.** (1994) Antimutagenicity in *Euglena gracilis*. *Mutation Research* **323**: 167-171.

**Foote, R. S., Mitra, S. & Pal, B. C.** (1980) Demethylation of $O^6$-methylguanine in a synthetic DNA polymer by an inducible activity in *Escherichia coli*. *Biochemical and Biophysical Research Communications* **97**: 654-659.

**Fry, R. C., Svensson, J. P., Valiathan, C., Wang, E., Hogan, B. J., Bhattacharya, S., Bugni, J. M., Whittaker, C. A. & Samson, L. D.** (2008) Genomic predictors of interindividual differences in response to DNA damaging agents. *Genes & Development* **22**: 2621-2626.

**Gafà, R., Maestri, I., Matteuzzi, M., Santini, A., Ferretti, S., Cavazzini, L. & Lanza, G.** (2000) Sporadic colorectal adenocarcinomas with high-frequency microsatellite instability. *Cancer* **89**: 2025-2037.

**Galloway, S. M. & Painter, R. B.** (1979) Vitamin C is positive in the DNA synthesis inhibition and sister-chromatid exchange tests. *Mutation Research* **60**: 321-327.

**Genschel, J., Littman, S. J., Drummond, J. T. & Modrich, P.** (1998) Isolation of MutSbeta from human cells and comparison of the mismatch repair specificities of MutSbeta and MutSalpha. *The Journal of Biological Chemistry* **273**: 19895-19901.

**Genschel, J., Bazemore, L. R. & Modrich, P.** (2002) Human exonuclease I is required for 5' and 3' mismatch repair. *The Journal of Biological Chemistry* **277**: 13302-13311.

**Genschel, J. & Modrich, P.** (2003) Mechanism of 5'-directed excision in human mismatch repair. *Molecular Cell* **12**: 1077-1086.

**Gerson, S. L., Berger, N. A., Arce, C., Petzold, S. J. & Willson, J. K. V.** (1992) Modulation of nitrosourea resistance in human colon cancer by $O^6$-methylguanine. *Biochemical Pharmacology* **43**: 1101-1107.

**Giaginis, C., Gatzidou, E. & Theocharis, S.** (2006) DNA repair systems as targets of cadmium toxicity. *Toxicology and Applied Pharmacology* **213**: 282-290.

**Gilad, O., Nabet, B. Y., Ragland, R. L., Schoppy, D. W., Smith, K. D., Durham, A. C., Brown, E. J.** (2010) Combining ATR suppression with oncogenic Ras synergistically increases genomic instability, causing synthetic lethality or tumorigenesis in a dosage-dependent manner. *Cancer Research* **70**: 9693-9702.

**Glaab, W. E. & Tindall, K. R.** (1997) Mutation rate at the *hprt* locus in human cancer cell lines with specific mismatch repair-gene defects. *Carcinogenesis* **18**: 1-8.

**Glickman, B. W. & Radman, M.** (1980) *Escherichia coli* mutator mutants deficient in methylation-instructed DNA mismatch correction. *Proceedings of the National Academy of Sciences U.S.A.* **77**: 1063-1067.

**Glintborg, B., Weimann, A., Kensler, T. W. & Poulsen, H. E.** (2006) Oltipraz chemoprevention trial in Qidong, People's Republic of China: unaltered oxidative biomarkers. *Free Radical Biology & Medicine* **41**: 1010-1014.

**Gorre, M. E., Mohammed, M., Ellwood, K., Hsu, N., Paquette, R., Rao, P. N. & Sawyers, C. L.** (2001) Clinical resistance to STI-571 cancer therapy caused by BCL-ABL gene mutation or amplification. *Science* **293**: 876-880.

**Gottipati, P., Vischioni, B., Schultz, N., Solomons, J., Bryant, H. E., Djureinovic, T., Issaeva, N., Sleeth, K., Sharma, R. A. & Helleday, T.** (2010) Poly(ADP-ribose) polymerase is hyperactivated in homologous recombination-defective cells. *Cancer Research* **70**: 5389-5398.

**Gradia, S., Acharya, S. & Fishel, R.** (1997) The human mismatch recognition complex hMSH2-hMSH6 functions as a novel molecular switch. *Cell* **91**: 995-1005.

**Gregory, R. I., Yan, K. P., Amuthan, G., Chendrimada, T., Doratotaj, B. Cooch, N. & Shiekhattar, R.** (2004) The microprocessor complex mediates genesis of microRNAs. *Nature* **432**: 235-240.

**Gregory, R. I., Chendrimada, T. P., Cooch, N. & Shiekhattar, R.** (2005) Human RISC couples microRNA biogenesis and posttranscriptional gene silencing. *Cell* **123**: 631-640.

**Grevelman, E. G. & Breed, W. P.** (2005) Prevention of chemotherapy-induced hair loss by scalp cooling. *Annals of Oncology* **16**: 352-358.

**Griffin, S., Branch, P., Xu, Y. Z. & Karran, P.** (1994) DNA mismatch binding and incision at modified guanine bases by extracts of mammalian cells: implications for tolerance to DNA methylation damage. *Biochemistry* **33**: 4787-4793.

**Gu, Y., Parker, A., Wilson, T. M., Bai, H., Chang, D. Y. & Lu, A. L.** (2002) Human MutY homolog, a DNA glycosylase involved in base excision repair, physically and functionally interacts with mismatch repair proteins human MutS homolog 2/human MutS homolog 6. *The Journal of Biological Chemistry* **277**: 11135-11142.

**Guarente, L.** (1993) Synthetic enhancement in gene interaction: a genetic tool come of age. *Trends in Genetics*. **9**: 362-366.

**Guarne, A., Ramon-Maiques, S., Wolff, E. M., Ghirlando, R., Hu, X., Miller, J. H. & Yang, W.** (2004) Structure of the MutL C-terminal domain: a model of intact MutL and its roles in mismatch repair. *European Molecular Biology Organisation Journal* **23**: 4134-4145.

**Guengerich, F. P., Johnson, W. W., Shimada, T., Ueng, Y. F., Yamazaki, H. & Langouët, S.** (1998) Activation and detoxication of aflatoxin $B_1$. *Mutation Research/Fundamental and Molecular Mechanisms of Mutagenesis* **402**: 121-128.

**Guidoboni, M., Gafà, R., Viel, A., Doglioni, C., Russo, A., Santini, A., Del Tin, L., Macri, E., Lanza, G., Boiocchi, M. & Dolcetti, R.** (2001) Microsatellite instability and high content of activated cytotoxic lymphocytes identify colon cancer patients with a favorable prognosis. *American Journal of Pathology* **159**: 297-304.

**Haber, L. T. & Walker, G. C.** (1991) Altering the conserved nucleotide binding motif in the *Salmonella typhimurium* MutS mismatch repair protein affects both its ATPase and mismatch binding activities. *European Molecular Biology Organisation Journal* **10**: 2707-2715.

**Hamilton, A. J., Baulcombe, D. C.** (1999) A species of small antisense RNA in posttranscriptional gene silencing in plants. *Science* **286**: 950-952.

**Hammond, S. M., Bernstein, E., Beach, D. & Hannon, G. J.** (2000) An RNA-directed nuclease mediates post-transcriptional gene silencing in *Drosophila* cells. *Nature* **404**: 293-296.

**Hampel, H., Frankel, W. I., Martin, E., Arnold, M., Khanduja, K., Kuebler, P., Clendenning, M., Sotamaa, K., Prior, T., Westman, J. A., Panescu, J., Fix, D.,**

**Lockman, J., LaJeunesse, J., Comeras, I. & de la Chapelle, A.** (2008) Feasibility of screening for Lynch Syndrome among patients with colorectal cancer. *Journal of Clinical Oncology* **26**: 5783-5788.

**Hanahan, D. & Weinberg, R. A.** (2000) The hallmarks of cancer. *Cell* **100**: 57-70.

**Hanford, M. G., Rushton, B. C., Gowen, L. C. & Farber, R. A.** (1998) Microsatellite mutation rates in cancer cell lines deficient or proficient in mismatch repair. *Oncogene* **16**: 2389-2393.

**Hardeland, U., Bentele, M., Lettieri, T., Steinacher, R., Jiricny, J. & Schär, P.** (2001) Thymine DNA glycosylase. *Progress in Nucleic Acid Research and Molecular Biology* **68**: 235-253.

**Hardeland, U., Steinacher, R., Jiricny, J. & Schär, P.** (2002) Modification of the human thymine-DNA glycosylase by ubiquitin-like proteins facilitates enzymatic turnover. *European Molecular Biology Organisation Journal* **21**: 1456-1464.

**Hardeland, U., Kunz, C., Focke, F., Szadkowski, M., Schär, P.** (2007) Cell-cycle regulation as a mechanism for functional separation of the apparently redundant uracil DNA glycosylases TDG and UNG2. *Nucleic Acids Research* **35**: 3859-3867.

**Hare, J. & Taylor, J. H.** (1985) Methylation directed strand discrimination in mismatch repair. *Progress in Clinical and Biological Research* **198**: 37-44.

**Harrington, J. M. & Kolodner, R. D.** (2007) *Saccharomyces cerevisiae* Msh2-Msh3 acts in repair of base-base mispairs. *Molecular and Cellular Biology* **27**: 6546-6554.

**Harris, A. L., Nicholson, S., Sainsbury, J. R., Farndon, J. & Wright, C.** (1989) Epidermal growth factor receptors in breast cancer: association with early relapse and death, poor response to hormones and interactions with neu. *Journal of Steroid Biochemistry* **34**: 123-131.

**Hart, C. P.** (2005) Finding the target after screening the phenotype. *Drug Discovery Today: Targets* **10**: 513-519.

**Hatch, S. B. & Farber, R. A.** (2004) Mutation rates in the complex microsatellite MYCL1 and related simple repeats in cultured human cells. *Mutation Research* **545**: 117-126.

**Haushalter, K. A., Todd, Stukenberg, M. W., Kirschner, M. W. & Verdine, G. L.** (1999) Identification of a new uracil-DNA glycosylase family by expression cloning using synthetic inhibitors. *Current Biology* **9**: 174-185.

**Helleday, T., Petermann, E., Lundin, C., Hodgson, B., Sharma, R. A.** (2008) DNA repair pathways as targets for cancer therapy. *Nature Reviews Cancer* **8**: 193-204.

**Hendrich, B., Hardeland, U., Ng, H. H., Jiricny, J. & Bird, A.** (1999) The thymine glycosylase MBD4 can bind to the product of deamination at methylated CpG sites. *Nature* **401**: 301-304.

**Hendriks, Y. M., Wagner, A., Morreau, H., Menko, F., Stormorken, A., Quehenberger, F., Sandkuijl, L., Møller, P., Genuardi, M., Van Houwelingen, H., Tops, C., Van Puijenbroek, M., Verkuijlen, P., Kenter, G., Van Mil, A., Meijers-Heijboer, H., Tan, G. B., Breuning, M. H., Fodde, R., Wijnen, J. T., Bröcker-Vriends, A. H. & Vasen, H.** (2004) Cancer risk in hereditary nonpolyposis colorectal cancer due to MSH6 mutations: impact on counselling and surveillance. *Gastroenterology* **127**: 17-25.

**Hickman, M. J. & Samson, L. D.** (1999) Role of DNA mismatch repair and p53 in signaling induction of apoptosis by alkylating agents. *Proceedings of the National Academy of Sciences U.S.A.* **96**: 10764-10769.

**Hinz, J. M. & Meuth, M.** (1999) MSH3 deficiency is not sufficient for a mutator phenotype in Chinese hamster ovary cells. *Carcinogenesis* **20**: 215-220.

**Hitchins, M., Williams, R., Cheong, K., Halani, N., Lin, V. A., Packham, D., Ku, S., Buckle, A., Hawkins, N., Burn, J., Gallinger, S., Goldblatt, J., Kirk, J., Tomlinson, I., Scott, R., Spigelman, A., Suter, C., Martin, D., Suthers, G. & Ward, R.** (2005)

MLH1 germline epimutations as a factor in hereditary nonpolyposis colorectal cancer. *Gastroenterology* **129**: 1392-1399.

**Hortobagyi, G. N.** (2000) Developments in chemotherapy of breast cancer. *Cancer* **88**: 3073-3079.

**Hsieh, P. & Yamane, K.** (2008) DNA mismatch repair: molecular mechanism, cancer, and ageing. *Mechanisms of Ageing and Development* **129**: 391-407.

**Hübscher, U., Maga, G. & Spadari, S.** (2002) Eukaryotic DNA polymerases. *Annual Reviews in Biochemistry* **71**: 133-163.

**Hutvágner, G., McLachlan, J., Pasquinelli, A. E., Bálint, E., Tuschl, T. & Zamore, P. D.** (2001) A cellular function for the RNA-interference enzyme Dicer in the maturation of the let-7 small temporal RNA. *Science* **293**: 834-838.

**Ikegami, S., Taguchi, T., Ohashi, M., Oguro, M., Nagano, H. & Mano, Y.** (1978) Aphidicolin prevents mitotic division by interfering with the activity of DNA polymerase α. *Nature* **275**: 458-460.

**Ionov, Y., Peinado, M. A., Malkhosyan, S., Shibata, D. & Perucho, M.** (1993) Ubiquitous somatic mutations in simple repeated sequences reveal a new mechanism for colonic carcinogenesis. *Nature* **363**: 558-561.

**Iop, A., Manfredi, A. M. & Bonura, S.** (2004) Fatgue in cancer patients receiving chemotherapy: an analysis of published studies. *Annals of Oncology* **15**: 712-720.

**Isaacs, R. J., Rayens, W. S. & Spielmann, H. P.** (2002) Structural diffferences in the NOE-derived structure of G-T mismatched DNA relative to normal DNA are correlated with differences in (13)C relaxation-based internal dynamics. *Journal of Molecular Biology* **319**: 191-207.

**Issaeva, N., Thomas, H. D., Djurenovic, T., Jaspers, J. E., Stoimenov, I., Kyle, S., Pedley, N., Gottipati, P., Zur, R., Sleeth, K., Chatzakos, V., Mulligan, E. A., Lundin, C., Gubanova, E., Kersbergen, A., Harris, A. L., Sharma, R. A., Rottenberg, S., Curtin, N. J. & Helleday, T.** (2010) 6-Thioguanine selectively kills BRCA2-defective tumours and overcomes PARP inhibitor resistance. *Cancer Research* **70**: 6268-6276.

**Itoh, K., Wakabayashi, N., Katoh, Y., Ischii, T., Igarashi, K., Engel, J. D. & Yamamoto, M.** (1999) Keap1 represses nuclear activation of antioxidant responsive elements by Nrf2 through binding to the amino-terminal Neh2 domain. *Genes & Development* **13**: 76-86.

**Iyer, R. R., Pluciennik, A., Burdett, V. & Modrich, P. L.** (2006) DNA mismatch repair : functions and mechanisms. *Chemical Reviews* **106**: 302-323.

**Jackson, A. L., Bartz, S. R., Schelter, J., Kobayashi, S. V., Burchard, J., Mao, M., Li, B., Cavet, G. & Linsley, P. S.** (2003) Expression profiling reveals off-target gene regulation by RNAi. *Nature Biotechnology* **21**: 635-637.

**Jackson, A. L., Burchard, J., Leake, D., Reynolds, A., Schelter, J., Guo, J., Johnson, J. M., Lim, L., Karpilow, J., Nichols, K., Marshall, W., Khvorova, A. & Linsley, P. S.** (2006) Position-specific chemical modification of siRNAs reduces "off-target" transcript silencing. *RNA* **12**: 1197-1205.

**Jain, A. K., Shimoi, K., Nakamura, Y., Kada, T., Hara, Y. & Tomita, I.** (1989) Crude tea extracts decrease the mutagenic activity of *N*-methyl-*N'*-nitro-*N*-nitrosoguanidine *in vitro* and in intragastric tract of rats. *Mutation Research* **210**: 1-8.

**Jia, Z., Zhu, H., Li, Y. & Misra, H. P.** (2010) Potent inhibition of peroxynitrite-induced DNA strand breakage and hydroxyl radical formation by dimethyl sulfoxide at very low concentrations. *Experimental Biology and Medicine* **235**: 614-622.

**Jiang, X. Y., Qian, L. P., Zheng, X. J., Xia, Y. Y., Jiang, Y. B. & Sun da, Y.** (2009) Interventional effect of Ginkgo biloba extract on the progression of gastric precancerous lesions in rats. *Journal of Digestive Diseases* **10**: 293-299.

**Jin Y. H., Clark, A. B., Slebos, R. J., Al-Refai, H., Taylor, J. A., Kunkel, T. A., Resnick, M. A. & Gordenin, D. A.** (2003) Cadmium is a mutagen that acts by inhibiting mismatch repair. *Nature Genetics* **34**: 326-329.

**Jiricny, J.** (2000) Mismatch repair: The praying hands of fidelity. *Current Biology* **10**: R788-R790.

**Jiricny, J.** (2006). The multifaceted mismatch-repair system. *Nature Reviews Molecular Cell Biology* **7**: 335-346.

**Junop, M. S., Obmolova, G., Rausch, K., Hsieh, P. & Yang, W.** (2001) Composite active site of an ABC ATPase: MutS uses ATP to verify mismatch recognition and authorize DNA repair. *Molecular Cell* **7**: 1-12.

**Kadyrov, F. A., Dzantiev, L., Constantin, N. & Modrich, P.** (2006) Endonucleolytic function of MutLα in human mismatch repair. *Cell* **126**: 297-308.

**Kaelin, W. G.** (2005) The concept of synthetic lethality in the context of anti-cancer therapy. *Nature Reviews Cancer* **5**: 689-698.

**Kane, M. F., Loda, M., Gaida, G. M., Lipman, J., Mishra, R., Goldman, H., Jessup, J. M. & Kolodner, R.** (1997) Methylation of the hMLH1 promoter correlates with lack

of expression of hMLH1 in sporadic colon tumors and mismatch repair-defective human tumor cell lines. *Cancer Research* **57**: 808-811.

**Kawasaki, H. & Taira, K.** (2004) Induction of DNA methylation and gene silencing by short interfering RNAs in human cells. *Nature* **431**: 211-217.

**Kawasaki, H., Taira, K. & Morris, K. V.** (2005) siRNA induced transcriptional gene silencing in mammalian cells. *Cell-cycle* **4**: 442-448.

**Kelley, M. J., Glaser, E. M., Herndon, J. E., Becker, F., Bhagat, R., Zhang, Y. J., Santella, R. M., Carmella, S. G., Hecht, S. S., Gallot, L., Schilder, L., Crowell, J. A., Perloff, M., Folz, R. J., Bergan, R. C.** (2005) Safety and efficacy of weekly oral Oltipraz in chronic smokers. *Cancer Epidemiology, Biomarkers, and Prevention* **14**: 892-899.

**Kensler, T. W., Egner, P. A., Trush, M. A., Bueding, E. & Groopman, J. D.** (1985) Modification of aflatoxin B1 binding to DNA *in vivo* in rats fed phenolic antioxidants, ethoxyquin and a dithiothione. *Carcinogenesis* **6**: 759-763.

**Kerns, E. H. & Di, L.** (2008) Drug-like properties: concepts, structure design and methods, 1st ed. U.S.A: Wyeth Research.

**Ketkar, M., Reznik, G. & Green, U.** (1978) Carcinogenic effect of *N*-methyl-*N'*-nitro-*N*-nitrosoguanidine (MNNG) in European hamsters. *Cancer Letters* **4**: 241-244.

**Kharbanda, S., Yuan, Z. M., Weichselbaum, R. & Kufe, D.** (1997) Functional role for the c-Abl protein tyrosine kinase in the cellular response to genotoxic stress. *Biochimica et Biophysica Acta* **1333**: 1-7.

**King, M. C., Marks, J. H. & Mandell, J. B.** (2003) Breast and ovarian cancer risks due to inherited mutations in *BRCA1* and *BRCA2*. *Science* **24**: 643-646.

**Klapacz, J., Meira, L. B., Luchetti, D. G., Calvo, J. A., Bronson, R. T., Edelmann, W. & Samson, L. D.** (2009) $O^6$-methylguanine-induced cell death involves exonuclease 1 as well as DNA mismatch recognition in vivo. *Proceedings for the National Academy of Sciences U.S.A* **106**: 576-581.

**Koi, M., Umar, A., Chauban, D. P., Cherian, S. P., Carethers, J. M., Kunkel, T. A. & Boland, C. R.** (1994) Human chromosome 3 corrects mismatch repair deficiency and microsatellite instability and reduces *N*-methyl-*N'*-nitro-*N*-nitrosoguanidine tolerance in colon tumor cells with homozygous *hMLH1* mutation. *Cancer Research* **54**: 4308-4312.

**Komarov, P. G., Komarova, E. A., Kondratov, R. V., Christov-Tselkov, K., Coon, J. S., Chernov, M. V. & Gudkov, A. V.** (1999) A chemical inhibitor of p53 that protects mice from the side-effects of cancer therapy. *Science* **285**: 1733-1737.

**Kondo, E., Horii, A. & Fukushige, S.** (2001) The interacting domains of three MutL heterodimers in man: hMLH1 interacts with 36 homologous amino acid residues with hMLH3, hPMS1, and hPMS2. *Nucleic Acids Research* **29**: 1695-1702.

**Konwinski, R. R., Haddad, R., Chun, J. A., Klenow, S., Larson, S. C., Haab, B. B. & Lowe Furge, L.** (2004) Oltipraz, 3*H*-1,2-dithiole-3-thione, and sulforaphane induce overlapping and protective antioxidant responses in murine microglial cells. *Toxicology Letters* **153**: 343-355.

**Kranz, D. & Dobbelstein, M.** (2006) Nongenotoxic p53 activation protects cells against S-phase-specific chemotherapy. *Cancer Research* **66**: 10274-10280.

**Kricka, L. J., Carter, T. J., Burt, S. M., Kennedy, J. H., Holder, R. L., Halliday, M. I., Telford, M. E. & Wisdom, G. B.** (1980) Variability in the adsorption properties of microtitre plates used as solid supports in enzyme immunoassay. *Clinical Chemistry* **26**: 741-744.

**Krokan, H. E., Standal, R. & Slupphaug, G.** (1997) DNA glycosylases in the base excision of DNA. *The Biochemical Journal* **325**: 1-16.

**Kunkel, T. A. & Erie, D. A.** (2005) DNA mismatch repair. *Annual Review of Biochemistry* **74**: 681-710.

**Lai, Y. & Sun, F.** (2003) The relationship between microsatellite slippage mutation rate and the number of repeat units. *Molecular Biology and Evolution* **20**: 2123-2131.

**Lamers, M. H., Perrakis, A., Enzlin, J. H., Winterwerp, H. H., de Wind, N. & Sixma, T. K.** (2000) The crystal structure of DNA mismatch repair protein MutS binding to a G x T mismatch. *Nature* **407**: 711-717.

**Lamers, M. H., Georgijevic, D., Lebbink, J. H., Winterwerp, H. H. K., Agianian, B., de Wind, N. & Sixma, T. K.** (2004) ATP increases the affinity between MutS ATPase domains: implications for ATP hydrolysis and conformational changes. *The Journal of Biological Chemistry* **279**: 43879-43885.

**Längle-Rouault, F., Maenhaut-Michel, G. & Radman, M.** (1987) GATC sequences, DNA nicks and the MutH function in *Escherichia coli* mismatch repair. *European Molecular Biology Organisation Journal* **6**: 1121-1127.

**Lari, S. U., Day III, R. S., Dobler, K. & Paterson, M. C.** (2001) Intiation of strand excision at G:T and $O^6$-methylguanine:T base mismatches in DNA by human cell extracts. *Nucleic Acids Research* **29**: 2409-2417.

**Lari, S. U., Al-Khodairy, F. & Paterson, M. S.** (2002) Substrate specificity and sequence preference of G:T mismatch repair: incision at G:T, $O^6$-methylguanine:T, and G:U mispairs in DNA by human cell extracts. *Biochemistry* **41**: 9248-9255.

**Lawenda, B. D., Kelly, K. M., Ladas, E. J., Sagar, S. M., Vickers, A. & Blumberg, J. B.** (2008) Should supplemental antioxidant administration be avoided during chemotherapy and radiation therapy? *Journal of the National Cancer Institute* **100**: 773-783.

**Leach, F. S., Nicolaides, N. C., Papadopoulos, N., Liu, B., Jen, J., Parsons, R., Peltomäki, P., Sistonen, P., Aaltonen, L. A., Nyström-Lahti, M., Guan, X. Y., Zhang, J., Meltzer, P. S., Yu, J. W., Kao, F. T., Chen, D. J., Cerosaletti, K. M., Fournier, R. E. K., Todd, S., Lewis, T., Leach, R. J., Naylor, S. L., Weissenbach, J., Mecklin, J. P., Järvinen, H., Petersen, G. M., Hamilton, S. R., Green, J., Jass, J., Watson, P., Lynch, H. T., Trent, J. M., de la Chapelle, A., Kinzler, K. W. & Vogelstein, B.** (1993) Mutations of a *mutS* homolog in hereditary nonpolyposis colorectal cancer. *Cell* **75**: 1215-1225.

**Lebofsky, R.** (2003) Single DNA molecule analysis: applications of molecular combing. *Briefings in Functional Genomics* **1**: 385-396.

**Lee, Y., Ahn, C., Han, J., Choi, H., Kim, J., Yim, J., Lee, J., Provost, P., Rådmark, O., Kim, S. & Kim, N.** (2003) The nuclear RNase III Drosha initiates microRNA processing. *Nature* **425**: 415-419.

**Lei, X., Zhu, Y., Tomkinson, A. & Sun, L.** (2004) Measurement of DNA repair activity in live cells. *Nucleic Acids Research* **32**: e100.

**Lettieri, T., Marra, G., Aquilina, G., Bignami, M., Crompton, N. E., Palombo, F. & Jiricny, J.** (1999) Effect of hMSH6 cDNA expression on the phenotype of mismatch repair-deficient colon cancer cell line HCT15. *Carcinogenesis* **20**: 373-382.

**Li, C. Q., Kim, M. Y., Godoy, L. C., Thiantanawat, A., Trudel, L. J. & Wogan, G. N.** (2009) Nitric oxide activation of Keap1/Nrf2 signaling in human colon carcinoma cells. *Proceedings of the National Academy of Sciences U.S.A.* **106**: 14547-14551.

**Li, G. M.** (1999) The role of mismatch repair in DNA damage-induced apoptosis. *Oncology Research* **11**: 393-400.

**Li, G. M.** (2008) Mechanisms and functions of DNA mismatch repair. *Cell Research* **18**: 85-98.

**Li, L. S., Morales, J. C., Hwang, A., Wagner, M. W. & Boothman, D. A.** (2008) DNA mismatch repair-dependent activation of c-Abl/p73α/GADD45α-mediated apoptosis. *The Journal of Biological Chemistry* **283**: 21394-21402.

**Licciulli, S. & Kissil, J. L.** (2010) WT1: a weak spot in KRAS-induced transformation. *Journal of Clinical Investigation* **120**: 3804-3807.

**Lida, K., Itoh, K., Kumagai, Y., Oyasu, R., Hattori, K., Kawai, K., Shimazui, T., Akaza, H. & Yamamoto, M.** (2004) Nrf2 is essential for the chemopreventative efficacy of Oltipraz against urinary bladder carcinogenesis. *Cancer Research* **64**: 6424-6431.

**Lim, A. & Li, B. F.** (1996) The nuclear targeting and nuclear retention properties of a human DNA repair protein $O^6$-methylguanine-DNA-methyltransferase are both required for its nuclear localization: the possible implications. *The European Molecular Biology Organisation* **15**: 4050-4060.

**Lin, D. P., Wang, Y., Scherer, S. J., Clark, A. B., Yang, K., Avdievich, E., Jin, B., Werling, U., Parris, T., Kurihara, N., Umar, A., Kucherlapati, R., Lipkin, M., Kunkel, T. A. & Edelmann, W.** (2004) An Msh2 point mutation uncouples DNA mismatch repair and apoptosis. *Cancer Research* **64**: 517-522.

**Lin, X., Ruan, X., Anderson, M. G., McDowell, J. A., Kroeger, P. E., Fesik S. W. & Shen, Y.** (2005) siRNA-mediated off-target gene silencing triggered by a 7 nt complementation. *Nucleic Acids Research* **33**: 4527-4535.

**Lindblom, A., Tannergard, P., Werelius, B. & Nordenskjöld, M.** (1993) Genetic mapping of a second locus predisposing to hereditary non-polyposis colon cancer. *Nature Genetics* **5**: 279-282.

**Lindley, C., Vasa, S., Sawyer, WT. & Winer, EP.** (1998) Quality of life and preferences for treatment following systemic adjuvant therapy for early-stage breast cancer. *Journal of Clinical Oncology* **16**: 1380-1387.

**Ling-Ling, C., Nakamura, T., Nakatsu, Y., Sakumi, K., Hayakawa, H. & Sekiguchi, M.** (1992) Specific amino acid sequences required for $O^6$-methylguanine-DNA methyltransferase: analyses of three residues at or near the methyl acceptor site. *Carcinogenesis* **13**: 837-843.

**Linnebacher, M., Gebert, J., Rudy, W., Woerner, S., Yuan, Y. P., Bork, P. & von Knebel Doeberitz, M.** (2001) Frameshift peptide-derived T-cell epitopes: a source of novel tumor-specific antigens. *International Journal of Cancer* **93**: 6-11.

**Lipkin, S. M., Wang, V., Jacoby, R., Banerjee-Basu, S., Baxevanis, A. D., Lynch, H. T., Elliot, R. M. & Collins, F. S.** (2000) MLH3: a DNA mismatch repair gene associated with mammalian microsatellite instability. *Nature Genetics* **24**: 27-35.

**Lissoni, P., Barni, S., Mandalá, M., Ardizzoia, A., Paolorossi, F., Vaghi, M., Longarini, R., Malugani, F. & Tancini, G.** (1999) Decreased toxicity and increased efficacy of cancer chemotherapy using the pineal hormone melatonin in metastatic solid tumour patients with poor clinical status. *European Journal of Cancer* **35**: 1688-1692.

**Liu, J., Carmell, M. A., Rivas, F. V., Marsden, C. G., Thomson, J. M., Song, J. J., Hammond, S. M., Joshua-Tor, L. & Hannon, G. J.** (2004) Argonaute 2 is the catalytic engine of mammalian RNAi. *Science* **305**: 1437-1441.

**Liu, L., Taverna, P., Whitacre, C. M., Chatterjee, S. & Gerson, S. L.** (1999) Pharmacologic disruption of base excision repair sensitizes mismatch repair-deficient and –proficient colon cancer cells to methylating agents. *Clinical Cancer Research* **5**: 2908-2917.

**Liu, T., Mokuolu, A. O., Rao, C. V., Reddy, B. S. & Holt, P. R.** (1995) Regional chemoprevention of carcinogen-induced tumors in rat colon. *Gastroenterology* **109**: 1167-1172.

**Loeb, L. A., Springgate, C. F. & Battula, N.** (1974) Errors in DNA replication as a basis of malignant changes. *Cancer Research* **34**: 2311-2321.

**Loeb, L. A., Loeb, K. R. & Anderson, J. P.** (2003) Multiple mutations and cancer. *Proceedings for the National Academy of Sciences U.S.A.* **100**: 776-781.

**Loechler, E. L., Green, C. L. & Essigmann, J. M.** (1984) *In vivo* mutagenesis by $O^6$-methylguanine built into a unique site in a viral genome. *Proceedings of the National Academy of Science U.S.A.* **81**: 6271-6275.

**Longley, M. J., Pierce, A. J. & Modrich, P.** (1997) DNA polymerase delta is required for human mismatch repair *in vitro*. *The Journal of Biological Chemistry* **272**: 10917-10921.

**López de Saro, F. J. & O'Donnell, M.** (2001) Interaction of the beta sliding clamp with MutS, ligase, and DNA polymerase I. *Proceedings of the National Academy of Sciences U.S.A.* **98**: 8376-8380.

**Lord, C. J., Martin, S. A. & Ashworth, A.** (2009) RNA interference screening demystified. *Journal of Clinical Pathology* **62**: 195-200.

**Los, M., Herr, I., Friesen, C., Fulda, S., Schulze-Osthoff, K. & Debatin, K. M.** (1997) Cross-resistance of CD95- and drug-induced Apoptosis as a consequence of deficient activation of caspases (ICE/Ced-3 proteases). *Blood* **90**: 3118-3129.

**Lowe, S. W., Ruley, H. E., Jacks, T. & Housman, D. E.** (1993) p53-dependent apoptosis modulates the cytotoxicity of anti-cancer agents. *Cell* **74**: 957-967.

**Lu, A. L., Clark, S. & Modrich, P.** (1983) Methyl-directed repair of DNA base-pair mismatches *in vitro*. *Proceedings of the National Academy of Science U.S.A* **80**: 4639-4643.

**Lundholt, B. K., Scudder, K. M. & Pagliaro, L.** (2003) A simple technique for reducing edge-effect in cell-based assays. *Journal of Biomolecular Screening* **8**: 566-570.

**Luo, J., Emanuele, M. J., Creighton, C. J., Schlabach, M. R., Westbrook, T. F., Wong, K. K. & Elledge, S. J.** (2009a) A genome-wide RNAi screen identifies multiple synthetic lethal interactions with the Ras oncogene. *Cell* **137**: 835-848.

**Luo, J., Solimini, N. L. & Elledge, S. J.** (2009b) Principles of cancer therapy: oncogene and non-oncogene addition. *Cell* **136**: 823-837.

**Lützen, A., Liberti, S. E. & Rasmussen, L. J.** (2004) Cadmium inhibits human DNA mismatch repair *in vivo*. *Biochemical and Biophysical Research Communications* **321**: 21-25.

**Lynch, H. T., Lynch, P. M., Lanspa, S. J., Snyder, C. L., Lynch, J. F. & Boland, C. R.** (2009) Review of the lynch syndrome: history, molecular genetics, screening, differential diagnosis, and medicolegal ramifications. *Clinical Genetics* **76**: 1-18.

**Malhotra, V. & Perry, M. C.** (2003) Classical chemotherapy: mechanisms, toxicities and the therapeutic window. *Cancer Biology & Therapy* **2**: S2-S4.

**Malo, N., Hanley, J. A., Cerquozzi, S., Pelletier, J. & Nadon, R.** (2006) Statistical practice in high-throughput screening data analysis. *Nature Biotechnology* **24**: 167-175.

**Manikandan, P., Vidjaya Letchoumy, P., Prathiba, D. & Nagini, S.** (2008) Combinatorial chemopreventive effect of Azadirachta indica and Ocimum sanctum on oxidant-antioxidant status, cell proliferation, apoptosis and angiogenesis in a rat forestomach carcinogenesis model. *Singapore Medical Journal* **49**: 814-822.

**Marra, G., Iaccarino, I., Lettieri, T., Roschilli, G., Delmastro, P. & Jiricny, J.** (1998) Mismatch repair deficiency associated with overexpression of the MSH3 gene. *Proceedings of the National Academy of Sciences U.S.A.* **95**: 8568-8573.

**Martik, D., Baitinger, C. & Modrich, P.** (2004) Differential specificities and simultaneous occupancy of human MutSα nucleotide binding sites. *The Journal of Biological Chemistry* **279**: 28402-28410.

**Martin, S. A., McCabe, N., Mullarkey, M., Cummins, R., Burgess, D. J., Nakabeppu, Y., Oka, S., Kay, E., Lord, C. J. & Ashworth, A.** (2010) DNA polymerases as potential therapeutic targets for cancers deficient in the DNA mismatch repair proteins MSH2 or MLH1. *Cancer Cell* **17**: 235-248.

**Martin, S. A., Hewish, M., Sims, D., Lord, C. J. & Ashworth, A.** (2011) Parallel high throughput RNA interference screens identify PINK1 as a potential therapeutic target for the treatment of DNA mismatch repair deficient cancers. *Cancer Research* **Epub**.

**Martinez, J., Patkaniowska, A., Urlaub, H., Luhrmann, R. & Tuschl, T.** (2002) Single-stranded antisense siRNAs guide target RNA cleavage in RNAi. *Cell* **110**: 563-574.

**Mattila, J. & Puig, O.** (2010) Insights into transcriptional networks by using high throughput RNAi strategies. *Briefings in Functional Genomics*. **9**: 43-52.

**Mayr, L. M. & Bojanic, D.** (2009) Novel trends in high-throughput screening. *Current Opinion in Pharmacology* **9**: 580-588.

**Meister, G., Landthaler, M., Patkaniowska, A., Dorsett, Y., Teng, G. & Tuschl, T.** (2004) Human Argonaute2 mediates RNA cleavage targeted by miRNAs and siRNAs. *Molecular Cell* **15**: 185-19

**Mendillo, M. L., Hargreaves, V. V., Jamison, J. W., Mo, A. O., Li, S., Putnam, C. D., Woods, V. L., Kolodner, R. D.** (2009) A conserved MutS homolog connector domain interface interacts with MutL homologs. *Proceedings for the National Academy of Sciences* **106**: 22223-22228.

**Méplan, C., Mann, K. & Hainaut, P.** (1999) Cadmium induces conformational modifications of wild-type p53 and suppresses p53 response to DNA damage in cultured cells. *The Journal of Biological Chemistry* **274**: 31663-31670.

**Merlo, L. M. F., Pepper, J. W., Reid, B. J. & Maley, C. C.** (2006) Cancer as an evolutionary and ecological process. *Nature Reviews Cancer* **6**: 924-935.

**Middlemas, D. S., Stewart, C. F., Kirstein, M. N., Poquette, C., Friedman, H. S., Houghton, P. J. & Brent, T. P.** (2000) Biochemical correlates of temozolomide sensitivity in pediatric solid tumour xenograft models. *Clinical Cancer Research* **6**: 998-1007.

**Mikuni, T., Tatsuta, M. & Kamachi, M.** (1985) Production of hydroxyl-free radical by reaction of hydrogen peroxide with *N*-methyl-*N'*-nitro-*N*-nitrosoguanidine. *Cancer Research* **45**: 6442-6445.

**Mikuni, T. & Tatsuta, M.** (1994) Production of hydroxyl free radical by exposure of *N*-methyl-*N'*-nitro-*N*-nitrosoguanidine to visible light in the absence of hydrogen peroxide. *Radiation Research* **138**: 320-325.

**Mikuni, T. & Tatsuta, M.** (2002) Production of hydroxyl radical in the xanthine oxidase system with addition of 1-methyl-3-nitro-1-nitrosoguanidine. *Free Radical Research* **36**: 641-647.

**Mills, E. E.** (1988) The modifying effect of beta-carotene on radiation and chemotherapy induced oral mucositis. *British Journal of Cancer* **57**: 416-417.

**Misra, U. K., Gawdi, G., Akabani, G. & Pizzo, S. V.** (2002) Cadmium-induced DNA synthesis and cell proliferation in macrophages: The role of intracellular calcium and signal transduction mechanisms. *Cellular Signalling* **14**: 327-340.

**Miyachi, M., Kakazu, N., Yagyu, S., Katsumi, Y., Tsubai-Shimizu, S., Kikuchi, K., Tsuchiya, K., Lehara, T. & Hosoi H.** (2009) Restoration of p53 pathway by nutlin-3 induces cell-cycle arrest and apoptosis in human rhabdomyosarcoma cells. *Clinical Cancer Research* **15**: 4077-4084.

**Mojas, N., Lopes, M. & Jiricny, J.** (2007) Mismatch repair-dependent processing of methylation damage gives rise to persistent single-stranded gaps in newly replicated DNA. *Genes & Development* **21**: 3342-3355.

**Mol, C. D., Izumi, T., Mitra, S., Tainer, J. A.** (2000) DNA-bound structures and mutants reveal abasic DNA binding by APE1 and DNA repair coordination. *Nature* **403**: 451-456.

**Monks, A., Scudiero, D. A., Johnson, G. S., Paull, K. D. & Sausville, E. A.** (1997) The NCI anti-cancer drug screen: a smart screen to identify effectors of novel targets. *Anti-Cancer Drug Design* **12**: 533-541.

**Motohashi, H. & Yamamoto, M.** (2004) Nrf2-Keap1 defines a physiologically important stress response mechanism. *Trends in Molecular Medicine* **10**: 549-557.

**Mukherjee, B., Basu, M. & Chatterjee, M.** (2001) Effect of selenomethionine on *N*-methylnitronitrosoguanidine-induced colonic aberrant crypt foci in rats. *European Journal of Cancer Prevention* **10**: 347-355.

**Murugan, R. S., Mohan, K. V., Uchida, K., Hara, Y., Prathiba, D. & Nagini, S.** (2007) Modulatory effects of black tea polyphenols on oxidant-antioxidant profile and expression of proliferation, apoptosis, and angiogenesis-associated proteins in the rat forestomach carcinogenesis model. *Journal of Gastroenterology* **42**: 352-361.

**Neddermann, P. & Jiricny, J.** (1993) The purification of a mismatch-specific thymine-DNA glycosylase from HeLa cells. *The Journal of Biological Chemistry* **268**: 21218-21224.

**Neddermann, P., Gallinari, P., Lettieri, T., Schmid, D., Truong, O., Hsuan, J. J., Wiebauer, K. & Jiricny, J.** (1996) Cloning and expression of human G/T mismatch-specific thymine-DNA glycosylase. *The Journal of Biological Chemistry* **271**: 12767-12774.

**Negrini, S., Gorgoulis, V. G. & Halazonetis, T. D.** (2010) Genomic instability – an evolving hallmark of cancer. *Nature Reviews Molecular Cell Biology* **11**: 220-228.

**Nelson, D. L. & Cox, M. M.** (2004) Lehninger Principles of Biochemistry, Fourth Edition. W. H. Freeman.

**Nick McElhinny, S. A., Kissling, G. E. & Kunkel, T. A.** (2010) Differential correction of lagging-strand replication errors made by DNA polymerases α and δ. *Proceedings of the National Academy of Sciences U.S.A.* **107**: 21070-21075.

**Nicolaides, N. C., Papadopoulos, N., Liu, B., Wei, Y. F., Carter, K. C., Ruben, S. M., Rosen, C. A., Haseltine, W. A., Fleischmann, R. D., Fraser, C. M., Adams, M. D., Venter, J. C., Dunlop, M. G., Hamilton, S. R., Petersen, G. M., de la Chapelle, A., Vogelstein, B. & Kinzler, K. W.** (1994) Mutations of two PMS homologues in hereditary nonpolyposis colon cancer. *Nature* **371**: 75-80.

**Nicolaides, N. C., Grasso, L. & Sass, P. M.,** Morphotek Inc. (2006) Chemical inhibitors of DNA mismatch repair, U.S. Pat. 09760285.

**Nijman, S. M. B.** (2010) Synthetic lethality: general principles, utility and detection using genetic screens in human cells. *FEBS Letters* **585**: 1-6.

**Nino, M., Calabrò, G. & Santoianni, P.** (2010) Topical delivery of active principles: The field of dermatological research. *Dermatology Online Journal* **16**: 4.

**Nishijima, H., Yasunari, T., Nakayama, T., Adachi, N. & Shibahara, K.** (2009) Improved applications of the tetracycline-regulated gene depletion system. *Bioscience Trends* **3**: 161-167.

**Nishikawa, A., Tanakamaru, Z. Y., Furukawa, F., Lee, I. S., Kasahaea, K. I., Ikezaki, S. & Takahashi, M.** (1998) Chemopreventive activity of Oltipraz against induction of glandular stomach carcinogenesis in rats by *N*-methyl-*N'*-nitro-*N*-nitrosoguanidine. *Carcinogenesis* **19**: 365-368.

**Nowosielska, A. & Marinus, M. G.** (2008) DNA mismatch repair-induced double-strand breaks. *DNA Repair* **7**: 48-56.

**O'Connell, J. F., Nesnow, S. & Slaga, T. J.** (1987) Initiation, promotion and complete carcinogenesis by *N*-methyl-*N'*-nitro-*N*-nitrosoguanidine or ethylnitrosourea in the Sencar mouse skin tumorigenesis model. *Cancer Letters* **37**: 301-310.

**Obmolova, G., Ban, C., Hsieh, P. & Yang, W.** (2000) Crystal structures of mismatch repair protein MutS and its complex with a substrate DNA. *Nature* **407**: 703-710.

**Ochs, K. & Kaina, B.** (2000) Apoptosis induced by DNA damage $O^6$-methylguanine is Bcl-2 and caspase-9/3 regulated and Fas/caspase-8 independent. *Cancer Research* **60**: 5815-5824.

**Oliver, D. G., Sanders, A. H., Hogg, R. D. & Hellman, J. W.** (1981) Thermal gradients in microtitration plates. Effects on enzyme-linked immunoassay. *Journal of Immunological Methods* **42**: 195-201.

**Olsson, M. & Lindahl, T.** (1980) Repair of alkylated DNA in *Escherichia coli*. Methyl group transfer from $O^6$-methylguanine to a protein cysteine residue. *The Journal of Biological Chemistry* **255**: 10569-10571.

**Papadopoulos, N., Nicolaides, N. C., Wei, Y. F., Ruben, S. M., Carter, K. C., Rosen, C. A., Haseltine, W. A., Fleischmann, R. D., Fraser, C. M., Adams, M. D. *et al*.** (1994) Mutation of a mutL homolog in hereditary colon cancer. *Science* **263**: 1625-1629.

**Papouli, E., Cejka, P. & Jiricny, J.** (2004). Dependence of the cytotoxicity of DNA-damaging agents on the mismatch repair status of human cells. *Cancer Research* **64**: 3391-3394.

**Parsons, B. D., Schindler, A., Evans, D. H. & Foley, E.** (2009) A direct phenotypic comparison of siRNA pools and multiple individual duplexes in a functional assay. *PLoS ONE* **4**: e8471.

**Pavlov, Y. I., Mian, I. M. & Kunkel, T. A.** (2003) Evidence for preferential mismatch repair of lagging strand DNA replication errors in yeast. *Current Biology* **13**: 744-748.

**Paz, M. F., Fraga, M. F., Avila, S., Guo, M., Pollan, M., Herman, J. G. & Esteller, M.** (2003) A systematic profile of DNA methylation in human cancer cell lines. *Cancer Research* **63**: 1114-1121.

**Pedrali-Noy, G., Spadari, S., Miller-Faurès, A., Miller, A. O. A., Kruppa, J. & Koch, G.** (1980) Synchronisation of HeLa cell cultures by inhibition of DNA polymerase α with aphidicolin. *Nucleic Acids Research* **8**: 377-387.

**Pellicciari, C., Filippini, C., De Grada, L., Fuhrman Conti, A. M., Manfredi Romanini, M. G.** (1995) Cell-cycle effects of hypertonic stress on various human cells in culture. *Cell Biochemistry and Function* **13**: 1-8.

**Peltomäki, P., Aaltonen, L. & Sistonen, P.** (1993) Genetic mapping of a locus predisposing to human colorectal cancer. *Science* **260**: 810-812.

**Peltomäki, P.** (2003) Role of DNA mismatch repair defects in the pathogenesis of human cancer. *Journal of Clinical Oncology* **21**: 1174-1179.

**Peng, J. B., Chen, X. Z., Berger, U. V., Vassilev, P. M., Tsukaguchi, H., Brown, E. M. & Hediger, M. A.** (1999) Molecular cloning and characterization of a channel-like transporter mediating intestinal calcium absorption. *The Journal of Biological Chemistry* **274**: 22739-22746.

**Petzer, J. P., Navamal, M., Johnson, J. K., Kwak, M. K., Kensler, T. W. & Fishbein, J. C.** (2003) Phase 2 enzyme induction by the major metabolite of Oltipraz. *Chemical Research in Toxicology* **16**: 1463-1469.

**Pierce, J. H., Arnstein, P., DiMarco, E., Artrip, J., Kraus, M. H., Lonardo, F., Di Fiore, P. P. & Aaronson, S. A.** (1991) Oncogenic potential of erbB-2 in human mammary epithelial cells. *Oncogene* **6**: 1189-1194.

**Pillai, R. S., Bhattacharyya, S. N. & Filipowicz, W.** (2007) Repression of protein synthesis by miRNAs: how many mechanisms? *Trends in Cell Biology* **17**: 118-126.

**Pluciennik, A. & Modrich, P.** (2007) Protein roadblocks and helix discontinuities are barriers to the initiation of mismatch repair. *Proceedings of the National Academy of Sciences U.S.A.* **104**: 12709-12713.

**Pluciennik, A., Dzantiev, L., Iyer, R. R., Constantin, N., Kadyrov, F. A. & Modrich, P.** (2010) PCNA function in the activation and strand direction of MutLα endonuclease in mismatch repair. *Proceedings of the National Academy of Sciences U. S. A.* **107**: 16066-16071.

**Plumb, J. A.** (2004) Cell sensitivity assays: clonogenic assay. *Methods in Molecular Medicine* **88**: 159-164.

**Popat, S., Hubner, R. & Houlston, R. S.** (2005) Systematic review of microsatellite instability and colorectal cancer prognosis. *Journal of Clinical Oncology* **23**: 609-618.

**Powell, S. M. & Kachnic, L. A.** (2003) Roles of BRCA1 and BRCA2 in homologous recombination, DNA replication fidelity and the cellular response to ionising radiation. *Oncogene* **22**: 5784-5791.

**Prasad, R., Batra, V. K., Xiao-Ping, Y., Krahn, J. M., Pedersen, L. C., Beard, W. A. & Wilson, S. H.** (2005) Structural insight into the DNA polymerase β deoxyribose phosphate lyase mechanism. *DNA Repair* **4**: 1347-1357.

**Prolla, T. A., Baker, S. M., Harris, A. C., Tsao, J. L., Yao, X., Bronner, C. E., Zheng, B., Gordon, M., Reneker, J., Arnheim, N., Shibata, D., Bradley, A. & Liskay, M.** (1998) Tumour susceptibility and spontaneous mutation in mice deficient in Mlh1, Pms1 and Pms2 DNA mismatch repair. *Nature Genetics* **18**: 276-279.

**Prozialeck, W. C., Lamar, P. C. & Lynch, S. M.** (2003) Cadmium alters the localization of N-cadherin, E-cadherin, and beta-catenin in the proximal tubule epithelium. *Toxicology and Applied Pharmacology* **189**: 180-195.

**Pukkila, P. J., Peterson, J., Herman, G., Modrich, P. & Meselson, M.** (1983) Effects of high levels of DNA adenine methylation on methyl-directed mismatch repair in *Escherichia coli*. *Genetics* **104**: 571-582.

**Puyol, M., Martin, A., Dubus, P., Mulero, F., Pizcueta, P., Khan, G., Guerra, C., Santamaria, D. & Barbacid, M.** (2010) A synthetic lethal inteaction between K-Ras

oncogenes and Cdk4 unviels a therapeutic strategy for non-small cell lung carcinoma. *Cancer Cell* **18**: 63-73.

**Ramos-Gomez, M., Kwak, M. K., Dolan, P. M., Itoh, K., Yamamoto, M., Talalay, P. & Kensler, T. W.** (2001) Sensitivity to carcinogenesis is increased and chemoprotective efficacy of enzyme inducers is lost in *nrf2* transcription factor-deficient mice. *Proceedings for the National Academy of Sciences U.S.A.* **98**: 3410-3415.

**Rangarajan, A., Hong, S. J., Gifford, A. & Weinberg, R. A.** (2004) Species- and cell type-specific requirements for cellular transformation. *Cancer Cell* **6**: 171-183.

**Räschle, M., Marra, G., Nyström-Lahti, Schär, P. & Jiricny, J.** (1999) Identification of hMutLb, a Heterodimer of hMLH1 and hPMS1. *The Journal of Biological Chemistry* **274**: 32368-32375.

**Remvikos, Y., Beuzeboc, P., Zajdela, A., Voillemot, N., Magdelénat, H. & Pouillart, P.** (1989) Correlation of pretreatment proliferative activity of breast cancer with the response to cytotoxic chemotherapy. *Journal of the National Cancer Institute* **81**: 1383-1387.

**Renshaw, M. W., Capozza, M. A. & Wang, J. Y. J.** (1988) Differential expression of type-specific c-abl mRNAs in mouse tissues and cell lines. *Molecular and Cellular Biology* **8**: 4547-4551.

**Reynolds, A., Leake, D., Boese, Q., Scaringe, S., Marshall, W. S., Khvorova, A.** (2004) Rational siRNA design for RNA interference. *Nature Biotechnology* **22**: 326-330.

**Roebuck, B. D., Liu, Y. L., Rogers, A. E., Groopman, J. D. & Kensler, T. W.** (1991) Protection against aflatoxin B1-induced hepatocarcinogenesis in F344 rats by 5-(2-pyrazinyl)-4-methyl-1,2-dithiole-3-thione (Oltipraz): predictive role for short-term molecular dosimetry. *Cancer Research* **51**: 5501-5506.

**Roos, W., Baumgartner, M. & Kaina, B.** (2004) Apoptosis triggered by DNA damage $O^6$-methylguanine in human lymphocytes requires DNA replication and is mediated by p53 and Fas/CD95/Apo-1. *Oncogene* **23**: 359-367.

**Roos, W. P., Nikolova, T., Quiros, S., Naumann, S. C., Kiedron, O., Zdzienicka, M. Z. & Kaina, B.** (2009) Brca2/Xrcc2 dependent HR, but not NHEJ, is required for protection against O(6)-methylguanine triggered apoptosis, DSBs and chromosomal aberrations by a process leading to SCEs. *DNA Repair* **8**: 72-86.

**Sanmartin-Suárez, C., Soto-Otero, R., Sánchez-Sellero, I. & Méndez-Álvarez, E.** (2010) Antioxidant properties of dimethyl sulfoxide and its viability as a solvent in the evaluation of neuroprotective antioxidants. *Journal of Pharmacological and Toxicological Methods* Epub.

**Schmutte, C., Marinescu, R. C., Sadoff, M. M., Guerrette, S., Overhauser, J. & Fishel, R.** (1998) Human exonuclease I interacts with the mismatch repair protein hMSH2. *Cancer Research* **58**: 4537-4542.

**Schnell, FM.** (2003) Chemotherapy-induced nausea and vomiting: the importance of acute antiemetic control. *Oncologist* **8**: 187-198.

**Schultz, L. B., Chehab, N. H., Malikzay, A. & Halazonetis, T. D.** (2000) p53 binding protein 1 (53bp1) is an early participant in the cellular response to DNA double-strand breaks. *The Journal of Chemical Biology* **151**: 1381-1390.

**Semizarov, D., Frost, L., Sarthy, A., Kroeger, P., Halbert, D. N. & Fesik, S. W.** (2003) Specificity of short interfering RNA determined through gene expression signatures. *Proceedings of the National Academy of Sciences U.S.A.* **100**: 6347-6352.

**Shackelford, R. E., Kaufmann, W. K. & Paules, R. S.** (1999) Cell-cycle control, checkpoint mechanisms, and genotoxic stress. *Environmental Health Perspectives* **107**: 5-24.

**Shan Li, L., Morales, J. C., Hwang, A., Wagner, M. W. & Boothman, D. A.** (2008) DNA mismatch repair-dependent activation of c-Abl/p73α/GADD45α-mediated apoptosis. *The Journal of Biological Chemistry* **283**: 21394-21403.

**Sharma, R., Tobin, P. & Clarke, S. J.** (2005) Management of chemotherapy-induced nausea, vomiting, oral mucositis, and diarrhoea. *Lancet Oncology* **6**: 93-102.

**Sharma, S., Gao, P. & Steele, V. E.** (2006) The chemopreventive efficacy of inhaled Oltipraz particulates in the B[α]P-induced A/J mouse lung adenoma model. *Carcinogenesis* **27**: 1721-1727.

**Shen, S. X., Weaver, Z., Xu, X., Li, C., Weinstein, M., Chen, L., Guan, X. Y., Ried, T. & Deng, C. X.** (1998) A targeted disruption of the murine Brca1 gene causes γ-irradiation hypersensitivity and genetic instability. *Oncogene* **17**: 3115-3124.

**Shoemaker, R. H., Balaschak, M. S., Alexander, M. R. & Boyd, M. R.** (1995) Therapeutic activity of 9-chloro-2-methylellipticinium acetate in an orthotopic model of human brain cancer. *Oncology Reports* **2**: 663-667.

**Shoemaker, R. H.** (2006) The NCI60 human tumour cell line anti-cancer drug screen. *Nature Reviews Cancer* **6**: 813-823.

**Skeel, R. T.** (2007) Handbook of cancer chemotherapy, 7th ed., Philadelphia: *Lippincott Williams & Wilkins.*

**Slamon, D. J., Clark, G. M., Wong, S. G., Levin, W. J., Ullrich, A. & McGuire, W. L.** (1987) Human breast cancer: correlation of relapse and survival with amplification of the HER-2/neu oncogene. *Science* **235**: 177-182.

**Slupphaug, G., Eftedal, I., Kavli, B., Bharati, S., Helle, N. M., Haug, T., Levine, D. W. & Krokan, H. E.** (1995) Properties of a recombinant human uracil-DNA glycosylase from the UNG gene and evidence that UNG encodes the major uracil-DNA glycosylase. *Biochemistry* **34**: 128-138.

**Smyrk, T. C., Watson, P., Kaul, K. & Lynch, H. T.** (2001) Tumor-infiltrating lymphocytes are a marker for microsatellite instability in colorectal carcinoma. *Cancer* **91**: 2417-2422.

**Sobol, R. W., Horton, J. K., Kühn, R., Gu, H., Singhal, R. K., Prasad, R., Rajewsky, K., Wilson, S. H.** (1996) Requirement of mammalian DNA polymerase-beta in base-excision repair. *Nature* **379**: 183-186.

**Soengas, M. S., Capodieci, P., Polsky, D., Mora, J., Esteller, M., Opitz-Araya, X., McCombie, R., Herman, J. G., Gerald, W. L., Lazebnik, Y. A., Cordón-Cardó, C. & Lowe, S. W.** (2001) Inactivation of the apoptosis effector Apaf-1 in malignant melanoma. *Nature* **409**: 207-211.

**Son, H. Y., Nishikawa, A., Furukawa, F., Kasahara, K., Miyauchi, M., Nakamura, H., Ikeda, T. & Hirose, M.** (2000) Organ-dependent modifying effects of Oltipraz on *N*-nitrosobis(2-oxopropyl)amine (BOP)-initiation of tumorigenesis in hamsters. *Cancer Letters* **153**: 211-218.

**Stojic, L., Mojas, N., Cejka, P., di Peitro, M., Ferrari, S., Marra, G. & Jiricny, J.** (2004) Mismatch repair-dependent G2 checkpoint induced by low doses of SN1 type methylating agents requires ATR kinase. *Genes & Development* **18**: 1331-1344.

**Stoler, D. L., Chen, N., Basik, M., Kahlenberg, M. S., Rodriguez-Bigas, M. A., Pentrelli, N. J. & Anderson, G. R.** (1999) The onset and extent of genomic instability in sporadic colorectal tumor progression. *Proceedings for the National Academy of Sciences U.S.A.* **96**: 15121-15126.

**Strand, M., Prolla, T. A., Liskay, R. M. & Petes, T. D.** (1993) Destabilization of tracts of simple repetitive DNA in yeast by mutations affecting DNA mismatch repair. *Nature* **365**: 274-276.

**Stucki, M., Pascucci, B., Parlanti, E., Fortini, P., Wilson, S. H., Hübscher, U. & Dogliotti, E.** (1998) Mammalian base excision repair by DNA polymerases delta and epsilon. *Oncogene* **17**: 835-843.

**Su, S. S. & Modrich, P.** (1986) Escherichia coli mutS-encoded protein binds to mismatched DNA base pairs. *Proceedings of the National Academy of Sciences U.S.A.* **83**: 5057-5061.

**Subapriya, R. & Nagini, S.** (2003) Ethanolic neem leaf extract protects against *N*-methyl-*N'*-nitro-*N*-nitrosoguanidine-induced gastric carcinogenesis in Wistar rats. *Asian Pacific Journal of Cancer Prevention* **4**: 215-223.

**Suntharalingam, G., Perry, M. R., Ward, S., Brett, S. J., Castello-Cortes, A., Brunner, M. D. & Panoskaltsis, N.** (2006) Cytokine storm in a phase 1 trial of anti-CD28 monoclonal antibody TGN1412. *The New England Journal of Medicine* **355**: 1018-1028.

**Suter, C. M., Martin, D. I. K., Ward, R. L.** (2004) Germline epimutation of *MLH1* in individuals with multiple cancers. *Nature Genetics* **36**: 497-501.

**Svetlanov, A. & Cohen, P. E.** (2004) Mismatch repair proteins, meiosis, and mice: understanding the complexities of mammalian meiosis. *Experimental Cell Research* **296**: 71-79.

**Symth, J. F., Bowman, A., Perren, T., Wilkinson, P., Prescott, R. J., Quinn, K. J. & Tedeschi, M.** (1997) Glutathione reduces the toxicity and improves quality of life of

women diagnosed with ovarian cancer treated with cisplatin: Results of a double-blind, randomised trial. *Annals of Oncology* **8**: 569-573.

**Thomas, D. C., Roberts, J. D. & Kunkel, T. A.** (1991) Heteroduplex repair in extracts of human HeLa cells. *The Journal of Biological Chemistry* **266**: 3744-3751.

**Thompson, L. A. & Ellman, J. A.** (1996) Synthesis and applications of small molecule libraries. *Chemical Reviews* **96**: 555-600.

**Tokalov, S. V. & Abolmaali, N. D.** (2010) Protection of p53 wild type cells from taxol by nutlin-3 in the combined lung cancer treatment. *BMC Cancer* **10**: 57.

**Tomkinson, A. E., Chen, L., Dong, Z., Leppard, J. B., Levin, D. S., Mackey, Z. B., Motycka, T. A.** (2001) Completion of base excision repair by mammalian DNA ligases. *Progress in Nucleic Acid Research and Molecular Biology* **68**: 151-164.

**Tong, A. H. Y., Evangelista, M., Parsons, A. B., Xu, H., Bader, G. D., Page, N., Robinson, M., Raghibizadeh, S., Hogue, C. W. V., Bussey, H., Andrews, B., Tyers, M. & Boone, C.** (2001) Systematic genetic analysis with ordered arrays of yeast deletion mutations. *Science* **294**: 2364-2368.

**Tong, A. H. Y., Lesage, G., Bader, G. D., Ding, H., Xu., H., Xin, X., Young, J., Berriz, G. F., Brost, R. L., Chang, M., Chen, Y., Cheng, X., Chua, G., Friesen, H.,**

**Goldberg, D., Haynes, J., Humphries, C., Hussein, G. H. S., Ke, L., Krogan, N., Li, Z., Levinson, J. N., Lu, H., Menard, P., Munyana, C., Parsons, A. B., Ryan, O., Tonikian, R., Roberts, T., Sdicu, A. M., Shapiro, J., Sheikh, B., Suter, B., Wong, S. L., Zhang, L. V., Zhu, H., Burd, C. G., Munro, S., Sander, C., Rine, J., Greenblatt, J., Peter, M., Bretscher, A., Bell, G., Roth, F. P., Brown, G. W., Andrews, B., Bussey, H. & Boone, C.** (2004) Global mapping of the yeast genetic interaction network. *Science* **303**: 808-813.

**Trewick, S. C., Henshaw, T. F., Hausinger, R. P., Lindahl, T., Sedgwick, B.** (2002) Oxidative demethylation by *Escherichia coli* AlkB directly reverts DNA base damage. *Nature* **419**: 174-178.

**Trojan, J., Zeuzem, S., Randolph, A., Hemmerle, C., Brieger, A., Raedle, J., Plotz, G., Jiricny, J., Marra, G.** (2002) Functional analysis of hMLH1 variants and HNPCC-related mutations using a human expression system. *Gastroenterology* **122**: 211-219.

**Tsaryk, R., Fabian, K., Thacker, J. & Kaina, B.** (2006) Xrcc2 deficiency sensitizes cells to apoptosis by MNNG and the alkylating anti-cancer drugs temozolomide, fotemustine and mafosfamide. *Cancer Letters* **239**: 305-313.

**Turner, N. C., Tutt, A. & Ashworth, A.** (2004) Hallmarks of 'BRCAness' in sporadic cancers. *Nature Reviews Cancer* **4**:1-6.

**Turner, N. C., Lord, C. J., Iorns, E., Brough, R., Swift, S., Elliott, R., Rayter, S., Tutt, A., N. & Ashworth, A.** (2008) A synthetic lethal siRNA screen identifying genes mediating sensitivity to a PARP inhibitor. *European Molecular Biology Organisation Journal* **27**: 1368-1377.

**Tutt, A., Gabriel, A., Bertwistle, D., Connor, F., Paterson, H., Peacock, J., Ross, G. & Ashworth, A.** (1999) Absence of Brca2 causes genome instability by chromosome breakage and loss associated with centrosome amplification. *Current Biology* **9**: 1107-1110.

**Umar, A., Koi, M., Risinger, J. I., Glaab, W. E., Tindall, K. R., Kolodner, R. D., Boland, C. R., Barrett, J. C. & Kunkel, T. A.** (1997) Correction of hypermutability, *N*-methyl-*N'*-nitro-*N*-nitrosoguanidine resistance, and defective DNA mismatch repair by introducing chromosome 2 into human tumor cells with mutations in MSH2 and MSH6. *Cancer Research* **57**: 3949-3955.

**van Haaften, G., Vastenhouw, N. L., Nollen, E. A. A., Plasterk, R. H. A. & Tijsterman, M.** (2004) Gene interactions in the DNA damage-response pathway identified by genome-wide RNA-interference analysis of synthetic lethality. *Proceedings of the National Academy of Sciences U.S.A.* **101**: 12992-12996.

**Vankoningsloo, S., de Longueville, F., Evrard, S., Rahier, P., Houbion, A., Fattaccioli, A., Gastellier, M., Remacle, J., Raes M., Renard, P. & Arnould, T.**

(2008) Gene expression silencing with 'specific' small interfering RNA goes beyond specificity – a study of key parameters to take into account in the onset of small interfering RNA off-target effects. *Federation of European Biochemical Societies Journal* **275**: 2738-2753.

**Velayutham, M., Villamena, F. A., Fishbein, J. C. & Zweier, J. L.** (2005) Cancer chemopreventive Oltipraz generates superoxide anion radical. *Archives of Biochemistry and Biophysics* **435**: 83-88.

**Velmurugan, B. & Nagini, S.** (2005) Combination chemoprevention of experimental gastric carcinogenesis by s-allylcysteine and lycopene: modulatory effects on glutathione redox cycle antioxidants. *Journal of Medicinal Food* **8**: 494-501.

**Vermes, I., Haanen, C., Steffens-Nakken, H. & Reutelingsperger, C.** (1995) A novel assay for apoptosis. Flow cytometric detection of phosphatidylserine expression on early apoptotic cells using fluorescein labelled Annexin V. *Journal of Immunological Methods* **184**: 39-51.

**Vilenchik, M. M. & Knudson, A. G.** (2000) Inverse radiation dose-rate effects on somatic and germ-line mutations and DNA damage rates. *Proceedings of the National Academy of Sciences U.S.A.* **97**: 5381-5386.

**Vistica, D. T., Kenney, S., Hursey, M. & Boyd, M. R.** (1996) Role of membrane potential in the accumulation of quaternized ellipticines by human tumor cell lines. *The Journal of Pharmacology and Experimental Therapeutics* **279**: 1018-1025.

**Vogelstein, B. & Kinzler, W.** (1994) Mutations of two PMS homologues in hereditary nonpolyposis colon cancer. *Nature* **371**: 75-80.

**Voigt, W.** (2005) Sulforhodamine B assay and chemosensitivity. *Methods in Molecular Medicine* **110**: 39-48.

**Vojteková, H. & Miertus, S.** (1986) Influence of ascorbic acid on the mutagenicity of *N*-methyl-*N*-nitrosoguanidine and nitrofurans studied by SOS chromotest. *Neoplasma* **33**: 691-698.

**Wadleigh, R. G., Redman, R. S., Graham, M. L., Krasnow, S. H., Anderson, A. & Cohen, M. H.** (1992) Vitamin E in the treatment of chemotherapy-induced mucositis. *The American Journal of Medicine* **92**: 481-484.

**Waga, S. & Stillman, B.** (1998) The DNA replication fork in eukaryotic cells. *Annual Review of Biochemistry* **67**: 721-751.

**Wagdi, P., Fluri, M., Aeschbacher, B., Fikrle, A. & Meier, B.** (1996) Cardioprotection in patients undergoing chemo- and/or radiotherapy for neoplastic disease. A pilot study. *Japanese Heart Journal* **37**: 353-359.

**Wagner, M. A., Li, L. S., Morales, J. C., Galindo, C. L., Garner, H. R., Bornmann, W. G. & Boothman, D. A.** (2008) Role of c-Abl kinase in DNA mismatch repair-dependent G2 cell-cycle checkpoint arrest responses. *The Journal of Biological Chemistry* **283**: 21382-21393.

**Wagner, R. & Meselson, M.** (1976). MMR may have a special relation to the replication complex. *Proceedings of the National Academy of Sciences* **73**: 4135-4139.

**Walton, S. M.** (2000) Advances in use of the 5-HT3 receptor antagonists. *Expert Opinion on Pharmacotherapy* **1**: 207-223.

**Wang, H. & Joseph, J. A.** (1999) Quantifying cellular oxidative stress by dichlorofluorescin assay using microplate reader. *Free Radical Biology and Medicine* **27**: 612-616.

**Wang, H. & Hays, J. B.** (2000) Preparation of DNA substrates for *in vitro* mismatch repair. *Molecular Biotechnology* **15**: 97-104.

**Wang, H. & Hays, J. B.** (2002) Mismatch repair in human nuclear extracts. Time courses and ATP requirements for kinetically distinguishable steps leading to tightly controlled 5' to 3' and aphidicolin-sensitive 3' to 5' mispair-provoked excision. *The Journal of Biological Chemistry* **277**: 26143-26148.

**Wang, H., Yang, Y., Schofield, M. J., Du, C., Fridman, Y., Lee, S. D., Larson, E. D., Drummond, J. T., Alani, E., Hsieh, P. & Erie, D. A.** (2003) DNA bending and unbending by MutS govern mismatch recognition and specificity. *Proceedings of the National Academy of Sciences* **100**: 14822-14827.

**Wang, H. & Hays, J. B.** (2004) Signaling from DNA mispairs to mismatch-repair excision sites despite intervening blockades. *European Molecular Biology Organisation Journal* **23**: 2126-2133.

**Wang, J. S., Shen, X., He, X., Zhu, Y. R., Zhang, B. C., Wang, J. B., Qian, G. S., Kuang, S. Y., Zarba, A., Egner, P. A., Jacobson, L. P., Muňoz, A., Helzlsouer, K. J., Groopman, J. D. & Kensler, T. W.** (1999) Protective alterations in phase 1 and 2 metabolism of aflatoxin B1 by Oltipraz in residents of Qidong, People's Republic of China. *Journal of the National Cancer Institute* **91**: 347-354.

**Wang, T. L., Diaz, L. A., Romans, K., Bardelli, A., Saha, S., Galizia, G., Choti, M., Donehower, R., Parmigiani, G., Shih, I. M., Lacobuzio-Donahue, C., Kinzler, K. W., Vogelstein, B., Lengauer, C. & Velculescu, V. E.** (2004) Digital karyotyping identifies

thymidylate synthase amplification as a mechanism of resistance to 5-fluorouracil in metastatic colorectal cancer patients. *Proceedings of the National Academy of Sciences U.S.A.* **101**: 3089-3094.

**Wargovich, M. J., Chen, C. D., Jimenez, A., Steele, V. E., Velasco, M., Clifton Stephens, L., Price, R., Gray, K. & Kelloff, G. J.** (1996) Aberrant crypts as a biomarker for colon cancer: evaluation of potential chemopreventive agents in the rat. *Cancer Epidemiology, Biomarkers & Prevention* **5**: 355-360.

**Waters, T. R., Gallinari, P., Jiricny, J. & Swann, P. F.** (1999) Human thymine DNA glycosylase binds to apurinic sites in DNA but is displaced by human apurinic endonuclease 1. *The Journal of Biological Chemistry* **274**: 67-74.

**Wattenberg, L. W. & Bueding, E.** (1986) Inhibitory effects of 5-(2-pyrazinyl)-4-methyl-1,2-dithiol-3-thione (Oltipraz) on carcinogenesis induced by benzo[a]pyrene, diethylnitrosamine uracil mustard. *Carcinogenesis* **7**: 1379-1381.

**Wei, K., Clark, A. B., Wong, E., Kane, M. F., Mazur, D. J., Parris, T., Kolas, N. K., Russell, R., Hou, H., Kneitz, B., Yang, G., Kunkel, T. A., Kolodner, R. D., Cohen, P. E. & Edelmann, W.** (2003) Inactivation of exonuclease 1 in mice results in DNA mismatch repair defects, increased cancer susceptibility, and male and female sterility. *Genes & Development* **17**: 603-614.

**Whittemore, A. S., Gong, G. & Itnyre, J.** (1997) Prevalence and contribution of BRCA1 mutations in breast cancer and ovarian cancer: results from three U.S. population-based case-control studies of ovarian cancer. *American Journal of Human Genetics* **60**: 496-504.

**Wieland, M., Levin, M. K., Hingorani, K. S., Biro, F. N. & Hingorani, M. M.** (2009) Mechanism of Cadmium-mediated inhibition of Msh2-Msh6 function in DNA mismatch repair. *Biochemistry* **48**: 9492-9502.

**Wiles, A. M., Ravi, D., Bhavani, S. & Bishop, A. J. R.** (2008) An analysis of normalization methods for *Drosophila* RNAi genomic screens and development of a robust validation scheme. *Journal of Biomolecular Screening* **13**: 777-784.

**Wimmer, K. & Etzler, J.** (2008) Constitutional mismatch repair-deficiency syndrome: have we so far seen only the tip of an iceberg? *Human Genetics* **124**: 105-122.

**Witkiewicz-Kucharczyk, A. & Bal, W.** (2006) Damage of zinc fingers in DNA repair proteins, a novel molecular mechanism in carcinogenesis. *Toxicology Letters* **162**: 29-42.

**Wu, T. H. & Marinus, M. G.** (1994) Dominant negative mutator mutations in the mutS gene of *Escherichia coli*. *Journal of Bacteriology* **176**: 5393-5400.

**Wyatt, M. D. & Pittman, D. L.** (2006) Methylating agents and DNA repair responses: methylated bases and sources of strand breaks. *Chemical Research in Toxicology* **19**: 1580-1594.

**Yamada, H., Vijayachandra, K., Penner, C. & Glick, A.** (2001) Increased sensitivity of transforming growth factor (TGF) β1 null cells to alkylating agents reveals a novel link between TGFβ signaling and $O^6$-methylguanine methyltransferase. *The Journal of Biological Chemistry* **276**: 19052-19058.

**Yamane, T., Takahashi, T., Kuwata, K., Oya, K., Inagake, M., Kitao, Y., Suganuma, M. & Fujiki, H.** (1995) Inhibition of *N*-methyl-*N'*-nitro-*N*-nitrosoguanidine-induced carcinogenesis by (-)-epigallocatechin gallate in the rat glandular stomach. *Cancer Research* **55**: 2081-2084.

**Yanamadala, S. & Ljungman, M.** (2003) Potential role of MLH1 in the induction of p53 and apoptosis by blocking transcription on damaged DNA templates. *Molecular Cancer Research* **1**: 747-754.

**Ye, N., Holmquist, G. P. & O'Connor, T. R.** (1998) Heterogeneous repair of *N*-methylpurines at the nucleotide level in normal human cells. *Journal of Molecular Biology* **284**: 269-285.

**York, S. J. & York, P.** (2006) Mismatch repair-dependent iterative excision at irreparable $O^6$-methylguanine lesions in human nuclear extracts. *The Journal of Biological Chemistry* **281**: 22674-22683.

**Yoshioka, K., Yoshioka, Y. & Hsieh, P.** (2006) ATR kinase activation mediated by MutSalpha and MutLalpha in response to cytotoxic $O^6$-methylguanine adducts. *Molecular Cell* **22**: 501-510.

**Zachariae, R., Paulsen, K., Mehlsen, M., Jensen, A. B., Johansson, A. & von der Maase, H.** (2007) Chemotherapy-induced nausea, vomiting, and fatigue – the role of individual differences related to sensory perception and autonomic reactivity. *Psychotherapy and Psychomatics* **76**: 376-384.

**Zhang, J. H., Chung, T. D. Y. & Oldenburg, K. R.** (1999) A simple statistical parameter for use in evaluation and validation of high throughput screening assays. *Journal of Biomolecular Screening* **4**: 67-73.

**Zhang, Y., Yuan, F., Presnell, S. R., Tian, K., Gao, Y., Tomkinson, A. E., Gu, L. & Li, G.** (2005) Reconstitution of 5'-directed human mismatch repair in a purified system. *Cell* **122**: 693-705.

**Zhang, Y. & Munday, R.** (2008) Dithiolethiones for cancer chemoprevention: where do we stand? *Molecular Cancer Therapy* **7**: 3470-3479.

**Zharkov, D. O.** (2008) Base excision DNA repair. *Cellular and Molecular Life Sciences* **65**: 1544-1565.

# CHAPTER NINE

*Appendix*

**Table A1.** Table of genes targeted by the custom siRNA library. Those highlighted in gray were screened but excluded from subsequent analysis after failing data quality checks, whilst those in green represent gene depletions that decreased sensitivity to MNNG by greater than two population standard deviations.

| | | | | | |
|---|---|---|---|---|---|
| ABL1 | CHD9 | HIST1H2BD | MLLT3 | POLG | SND1 |
| ACD | CHEK1 | HIST2H2AA3 | MMP9 | POLH | SNRPE |
| ACLY | CHEK2 | HIST2H3C | MMP9 | POLI | SNRPF |
| ADI1 | CHRAC1 | HIST2H4A | MNAT1 | POLK | SOD1 |
| ADO | CHTF18 | HIST3H2A | MPG | POLL | SOX4 |
| AHCY | CITED1 | HLTF | MRC1 | POLM | SPO11 |
| AKT1 | CITED2 | HMGA1 | MRE11A | POLN | SRCAP |
| AKT2 | CITED4 | HMGB1 | MRPL3 | POLQ | SSBP1 |
| ALKBH1 | CKS2 | HMGB2 | MRPS12 | POLS | SSR1 |
| ALKBH2 | CLK2 | HMGN1 | MSH2 | POT1 | SSX1 |
| ALKBH3 | CLSPN | HMGXB4 | MSH3 | PPARG | STK11 |
| ALKBH4 | COL1A2 | HNRNPA2B1 | MSH4 | PPP1R14C | SUPV3L1 |
| ALKBH5 | COPB2 | HNRNPK | MSH5 | PPP1R1B | SUV39H1 |
| ALKBH6 | CRIP2 | HP1BP3 | MSH6 | PPP2R1B | SUV39H2 |
| ALKBH7 | CSNK2A1 | HPRT1 | MTHFD2 | PPP2R5C | SUZ12 |
| ALKBH8 | CUL1 | HR | MUC1 | PPP3CA | TAL1 |
| APEX1 | CUL3 | HRAS | MUS81 | PRDX2 | TAPBP |
| APEX2 | CUL4A | HSP90B1 | MUTYH | PRDX4 | TARS |
| APTX | CUL4B | HSPBAP1 | MYL4 | PRKDC | TDG |
| ARID1A | DCLRE1A | HSPD1 | MYST1 | PRMT1 | TDP1 |
| ARID1B | DCLRE1B | HSPE1 | NAPRT1 | PSMA1 | TERF2 |
| ARID3A | DCLRE1C | HUS1 | NBN | PSMC4 | TERF2IP |
| ARID3B | DDB1 | IARS | NCBP2 | PSME2 | TET1 |
| ARID4A | DDB2 | IFNGR2 | NDC80 | PTCH1 | TET2 |
| ARID4B | DHX58 | IGF1 | NEIL1 | PTEN | TET3 |
| ARID5A | DMC1 | IGF1R | NEIL2 | PTMA | TGIF1 |
| ARID5B | DNMT1 | IGF2 | NEIL3 | PTTG1 | TIMELESS |
| ASF1A | DNMT3A | ILF2 | NEK2 | RAD1 | TINF2 |
| ASF1B | DNMT3B | ILK | NHEJ1 | RAD17 | TIPIN |
| ASPH | DOT1L | INCENP | NME1 | RAD18 | TLK1 |
| ASPHD1 | DSCC1 | INO80 | NONO | RAD21 | TLK2 |
| ASPHD2 | DUT | INO80C | NRAS | RAD23A | TMEM30A |
| ATAD5 | DVL3 | INSR | NTHL1 | RAD23B | TMLHE |

| | | | | | |
|---|---|---|---|---|---|
| ATF4 | E2F5 | IRS1 | NUDT1 | RAD50 | TNKS2 |
| ATM | ECT2 | JARID2 | NUDT10 | RAD51 | TOP1 |
| ATR | EGFR | JHDM1D | NUDT11 | RAD51AP1 | TOP2A |
| ATRIP | EGLN1 | JMJD1C | NUDT12 | RAD51C | TOP2B |
| BAZ1A | EGLN2 | JMJD4 | NUDT14 | RAD51L1 | TOP3A |
| BAZ1B | EGLN3 | JMJD5 | NUDT15 | RAD51L3 | TOP3B |
| BAZ2A | EHMT1 | JMJD6 | NUDT17 | RAD52 | TOPBP1 |
| BAZ2B | EIF4A3 | JMJD7 | NUDT18 | RAD54B | TOX2 |
| BBOX1 | EME1 | JMJD7-PLA2G4B | NUDT19 | RAD54L | TP53 |
| BLM | EME2 | JMJD8 | NUDT2 | RAD54L2 | TP53BP1 |
| BRCA1 | EP400 | KAT2B | NUDT22 | RAD9A | TP73 |
| BRCA2 | ERCC1 | KDELR2 | NUDT3 | RARA | TPX2 |
| BRD1 | ERCC2 | KDM2A | NUDT4 | RBBP8 | TRAF4 |
| BRD2 | ERCC3 | KDM2B | NUDT5 | RBM4 | TRDMT1 |
| BRD3 | ERCC4 | KDM3A | NUDT7 | RDM1 | TREX1 |
| BRD4 | ERCC5 | KDM3B | NUDT8 | RECQL | TREX2 |
| BRD7 | ERCC6 | KDM4A | NUDT9 | RECQL4 | TRIM28 |
| BRD8 | ERCC8 | KDM4B | NUP205 | RECQL5 | TSC1 |
| BRD9 | EXO1 | KDM4C | OBFC2B | REV1 | TSTA3 |
| BRDT | EZH2 | KDM4D | OGFOD1 | REV3L | TTF2 |
| BRIP1 | FANCA | KDM5A | OGFOD2 | RFC1 | TTRAP |
| BTAF1 | FANCB | KDM5B | OGG1 | RFC4 | TUBB |
| BTBD12 | FANCC | KDM5C | OGT | RFX1 | UBA52 |
| BUB3 | FANCD2 | KDM5D | ORC1L | RFX2 | UBE2A |
| C14orf169 | FANCE | KDM6A | ORC2L | RFX3 | UBE2B |
| C17orf101 | FANCF | KDM6B | ORC3L | RFX4 | UBE2I |
| C19orf40 | FANCG | KIAA0101 | ORC4L | RFX5 | UBE2N |
| C2orf60 | FANCI | KIF11 | ORC5L | RFX6 | UBE2S |
| C9orf102 | FANCL | KIF2C | ORC6L | RFX7 | UBE2V2 |
| CANX | FANCM | KIN | P4HA1 | RIF1 | UNG |
| CARM1 | FAP | KPNA2 | P4HA2 | RMI1 | UTY |
| CBX3 | FBXO18 | LDHA | P4HA3 | RNF40 | VHL |
| CCNA1 | FEN1 | LEPRE1 | P4HTM | RPA1 | WDHD1 |
| CCNA2 | FLJ35220 | LEPREL1 | PAFAH1B3 | RPA2 | WRN |
| CCNB1 | FOXO1 | LEPREL2 | PAICS | RPA3 | XAB2 |
| CCNB2 | FOXO3 | LIG1 | PALB2 | RPA4 | XPA |
| CCNB3 | FTO | LIG3 | PARP1 | RPL13 | XPC |
| CCND1 | G3BP1 | LIG4 | PARP2 | RPL27 | XRCC1 |
| CCND2 | GADD45A | LOC642846 | PCNA | RPL35 | XRCC2 |

| | | | | | |
|---|---|---|---|---|---|
| CCND3 | GEN1 | LOC730323 | PDS5A | RPN1 | XRCC3 |
| CCNE1 | GINS2 | MAD1L1 | PDS5B | RPS27A | XRCC4 |
| CCNE2 | GIYD2 | MAD2L2 | PER1 | RRM2B | XRCC5 |
| CCNH | GTF2H1 | MANF | PES1 | RTEL1 | XRCC6 |
| CCRN4L | GTF2H2 | MAP2K2 | PHB | RUVBL2 | ZBTB16 |
| CCT4 | GTF2H3 | MAPK1 | PHF1 | SDHC | ZDHHC17 |
| CCT5 | GTF2H4 | MBD1 | PHF2 | SETD7 | ZSWIM7 |
| CDC2 | GTF2H5 | MBD2 | PHF8 | SETD8 | |
| CDK2 | H2AFX | MBD3 | PHYH | SHFM1 | |
| CDK4 | H2AFZ | MBD4 | PHYHD1 | SHPRH | |
| CDK6 | HAAO | MCM10 | PIF1 | SIRT1 | |
| CDK7 | HAT1 | MCM2 | PIR | SIRT5 | |
| CDKN3 | HDAC1 | MCM3 | PLK1 | SMARCA1 | |
| CDO1 | HDAC10 | MCM4 | PLK2 | SMARCA2 | |
| CDYL | HDAC11 | MCM5 | PLK3 | SMARCA4 | |
| CENPA | HDAC2 | MCM6 | PLK4 | SMARCA5 | |
| CETN2 | HDAC3 | MCM7 | PLOD1 | SMARCAD1 | |
| CFDP1 | HDAC4 | MCM8 | PLOD2 | SMARCAL1 | |
| CHAF1A | HDAC5 | MCM9 | PLOD3 | SMARCB1 | |
| CHAF1B | HDAC6 | MDC1 | PMS1 | SMARCC1 | |
| CHD1 | HDAC7 | MECP2 | PMS2 | SMARCC2 | |
| CHD2 | HDAC8 | MEN1 | PMS2L3 | SMARCD1 | |
| CHD3 | HDAC9 | MGMT | PNKP | SMARCD2 | |
| CHD4 | HELLS | MINA | POLB | SMARCD3 | |
| CHD5 | HELQ | MLH1 | POLD1 | SMARCE1 | |
| CHD6 | HFM1 | MLH3 | POLE | SMC5 | |
| CHD7 | HGD | MLL | POLE3 | SMC6 | |
| CHD8 | HIF1AN | MLLT1 | POLE4 | SMUG1 | |